

REAL-TIME STUDIES OF CHEMICAL
REACTIONS IN LAB-ON-A-CHIP DEVICES

Real-time Studies of Chemical Reactions in Lab-on-a-chip Devices

Monica Brivio

Thesis University of Twente, Enschede, The Netherlands

ISBN 90-365-2148-3

This research has been financially supported by the Micro Chemical Systems (MiCS) scientific program of the MESA⁺ Institute for Nanotechnology and the University of Twente.

Publisher:

Print Partners Ipskamp, Postbus 33, 7500 AH Enschede, The Netherlands,

<http://www.ppi.nl>

© Monica Brivio, Enschede, 2005

Cover Design Monica Brivio

Cover Photograph: Hot spring at Yellowstone National Park, WY, USA, 2003.

The different colors in the water stream arise from thermophilic bacteria and algae mats that grow and live at different water temperatures.

No part of this work may be reproduced by print, photocopy or any other means without the permission in writing from the publisher.

REAL-TIME STUDIES OF CHEMICAL REACTIONS IN LAB-ON-A-CHIP DEVICES

PROEFSCHRIFT

ter verkrijging van
de graad van doctor aan de Universiteit Twente,
op gezag van de rector magnificus,
prof.dr.W.H.M. Zijm,
volgens besluit van het College voor Promoties
in het openbaar te verdedigen
op vrijdag 25 februari 2005 om 15.00 uur

door

Monica Brivio

geboren op 8 juni 1973

te Monza, Italië

Dit proefschrift is goedgekeurd door:

Promotor: Prof. dr. ir. D. N. Reinhoudt

Assistent-promotor: Dr. W. Verboom

*Considerate la vostra semenza:
fatti non foste a viver come bruti,
ma per seguir virtute e conoscenza.*

Dante Alighieri, La Divina Commedia,
Inf. XXVI 117-119

A mio padre

Contents

Chapter 1	General Introduction	1
1.1	Miniaturization and integration	1
1.2	References	4
Chapter 2	Miniaturization of the Reaction Vessel: High-Control, Information-Rich Chemical Reactions	5
2.1	Microfluidics	6
2.2	Analytical chemistry at the microscale; the μ -TAS	7
2.3	Synthetic chemistry at the microscale; the lab-on-a-chip	8
2.3.1	Introduction	8
2.3.2	Microreactors	9
2.3.3	Microfluidics handling	11
2.3.3.1	Electrokinetic pumping	11
2.3.3.2	Pressure-driven pumping	13
2.3.3.3	Flow-driven pumping	14
2.3.3.4	Alternative pumping methods	15
2.3.4	Synthesis in microreactors: an overview	15
2.3.5	Effects of downsizing the reaction vessel	16
2.4	Detection: a key issue in lab-on-a-chip	39
2.5	Conclusions and outlook	40
2.6	References	42

Chapter 3	Rate Enhancement of an Acid-catalyzed Esterification	
	Reaction within a Glass Microreactor	55
3.1	Introduction	56
3.2	Microreactor and chip holders	57
3.2.1	Microreactor	57
3.2.2	Chip holders	58
3.2.2.1	Initial holder	58
3.2.2.2	Improved chip holder	60
3.3	On-chip esterification reaction	60
3.4	Influence of surface phenomena	63
3.5	Conclusions	65
3.6	Experimental	65
3.7	References and notes	68
Chapter 4	Simple Chip-based Interfaces for On-line Nanospray-Chip	
	Mass Spectrometry	71
4.1	Introduction	72
4.2	Electrospray ionization mechanism	74
4.3	Nanospray ionization	74
4.4	Monolithically integrated NESIC-MS interface	75
4.5	Modular NESIC-MS interface	77
4.6	Chip design and fabrication	80

4.7	Continuous flow microreactors	81
4.8	Microreactor mixing evaluation	82
4.9	Conclusions	86
4.10	Experimental	86
4.11	References	89
Chapter 5	Supramolecular Interactions On-line Studied by Mass Spectrometry in a Nanoflow Electrospray Chip	93
5.1	Introduction	94
5.2	Microreactors	95
5.3	On-chip complexation studies	95
5.4	Conclusions	106
5.5	Experimental	107
5.6	References	111
Chapter 6	Kinetic Study of an On-chip Isocyanate Derivatization Reaction by On-line Picospray Mass Spectrometry	113
6.1	Introduction	114
6.2	Continuous flow microreactors	115
6.3	Background of the reaction of NBDPZ with isocyanates	117
6.4	On-chip experiments	118

6.4.1	Influence of the sample infusion flow rates on the NBDPZ ionization	119
6.4.2	Influence of co-solutes on the NBDPZ ionization	120
6.4.3	Ion suppression phenomena	121
6.4.4	On-chip reaction kinetics	122
6.5	Laboratory-scale reaction kinetics	125
6.6	Conclusions	126
6.7	Experimental	127
6.8	References	130
Chapter 7	Lab-on-a-chip Device Enabling (Bio)chemical Reactions with On-line MALDI-TOF Mass Spectrometry	133
7.1	Introduction	134
7.2	MALDI principle	135
7.3	MALDI instrument	136
7.4	Microreactor fabrication process and design	137
7.5	Inlets filling procedure	138
7.6	Chip-MALDI sample plate integration	138
7.7	Activation method	139
7.8	On-chip reactions	140
7.8.1	Schiff base formation	140
7.8.2	Polymers	142
7.8.3	Oligonucleotides	143

7.8.4	Peptide-sequencing	144
7.9	Conclusions	145
7.10	Experimental	146
7.11	References	150
Chapter 8	Towards a MALDI-Chip Integrated Device for the Study of Reaction Kinetics	153
8.1	Introduction	154
8.2	Fluid dynamics	155
8.3	Microreactor optimization	156
8.3.1	Microreactor design and fluid dynamics	156
8.3.2	“Monitoring window” description	158
8.3.3	Inlet loading system	159
8.4	“Monitoring window” testing	160
8.4.1	Inlet filling procedure	160
8.4.2	On-chip reaction and analysis	160
8.5	Conclusions	161
8.6	Outlook	162
8.7	Experimental	162
8.8	References	164
	Summary	165

Samenvatting 169

Acknowledgments 173

Chapter 1

General Introduction

1.1. Miniaturization and integration

Miniaturization is a leading development strategy in many research areas of both science and technology. Regardless of the field of application, general advantages of miniaturization are the ability of saving time, space, costs and materials and increasing performances by integrating miniaturized components.¹ This concept is clearly demonstrated by the tremendous progress made over the past fifty years within the field of electronics.² With the development of the first transistor at Bell Laboratories in 1947^{3,4} and the introduction of the first integrated circuit (IC) in 1958 by Kilby and Noyce, it became clear that IC technology would provide the tools to fabricate devices in which a huge number of functionalities per square mm could be packed. By the mid-seventies the large-scale integration (LSI) concept became reality, resulting in the development of complex integrated circuits containing large numbers of individual components. The consequences of the “electronic revolution” over the past decades are evident in a large number of microelectronic integrated circuit chips ruling our everyday life as parts of computers or other electronic devices (Figure 1.1). Since then, the tendency to reduce the size of a device in order to increase the density of stored information and to speed up the response time has spread in many other research areas, such as microoptics,⁵ microacoustics,^{6,7} micromechanics,⁸ and microfluidics.⁹

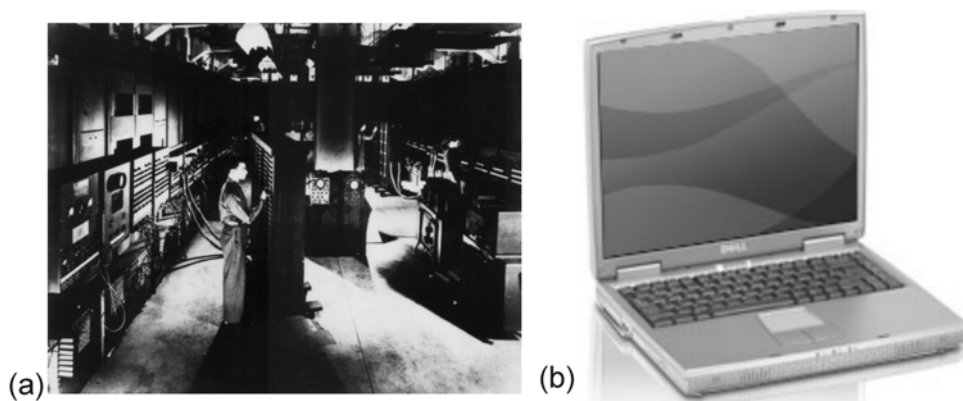


Figure 1.1. Picture of (a) the electronic numerical integrator and computer (ENIAC) as it was installed at the Moor School of Engineering (Pennsylvania University, 1946)¹⁰ and (b) a modern laptop.

Over the past two decades miniaturization has also been applied to the research areas of chemistry and life sciences.¹¹ Since the introduction of microfluidics technologies and the corresponding design strategies, microfluidics devices have been extensively used for research in the field of (bio)chemistry, mainly for analytical applications, resulting in the analytical equivalent of the “electronic revolution”. Based on the achievement of the micro total analysis systems (μ -TAS)¹²⁻¹⁴ the concept of miniaturization has been very recently extended to organic chemistry.¹⁵ Fundamental and practical advantages of microfluidics systems have been demonstrated for a number of catalytic and non-catalytic gas and liquid phase reactions carried out in microreactors, as reported in some recent reviews.^{15,16} A few studies¹⁷⁻¹⁹ have also demonstrated the high-throughput potential of the integration of microreactors with an analytical unit, resulting in continuous flow synthetic lab-on-a-chip systems (LOC) allowing on-line reaction monitoring. However, understanding the effects of downscaling the reaction vessel on chemical reactions is a prerequisite for the realization of the lab-on-a-chip potential for synthetic applications. Downscaling implies an increase of the gradient of physical properties, such as temperature, concentration, pressure, and density, which influences the reaction outcome.²⁰

This thesis aims to investigate some of the fundamental aspects of miniaturized chemical systems, such as the high surface-to-volume ratio and the fast diffusive mixing under laminar flow conditions in microchannels. The practical advantages of

the continuous flow microfluidics-based approach compared to conventional batch methodologies are also discussed. Furthermore, a key issue of lab-on-a-chip is addressed, *viz.* the realization of a hyphenated interface between a microreactor and an analytical unit for on-line reactions monitoring.

In Chapter 2 the lab-on-a-chip concept is introduced. The effects of decreasing the reaction vessel size will be discussed and illustrated with a number of examples reported in the recent literature.

Chapter 3 deals with surface phenomena, which play an important role in microfluidics systems, leading to higher yields and shorter reaction times. The large active surface inherent to microchannels is beneficial for the acid-catalyzed esterification of 9-pyrenebutyric acid with ethanol within a glass microreactor.

In Chapter 4 two approaches are discussed for coupling continuous flow glass microreactors to electrospray ionization (ESI) mass spectrometry (MS), based on a monolithic and a modular integration concept.

In Chapter 5 the high-throughput potential of the chip-MS integrated device described in Chapter 4 is demonstrated for a mass spectrometric qualitative and quantitative study of supramolecular systems based on metal-ligand and hydrophobic host-guest interactions.

In Chapter 6 the same chip-MS interface is used for a kinetic study of the derivatization reaction of mono- and diisocyanates with 4-nitro-7-piperazino-2,1,3-benzoxadiazole (NBDPZ) to yield the corresponding urea derivatives.

In Chapter 7 the first example of a lab-on-a-chip system enabling real-time analysis of on-chip reactions by matrix-assisted laser desorption ionization (MALDI) mass spectrometry (MS) is described. A unique passive pumping mechanism is used to drive reagent solutions through the microchannels, using the vacuum of the MALDI instrument.

In Chapter 8 a few ideas are presented for the optimization of the MALDI chip described in Chapter 7. Aiming to realize a lab-on-a-chip design enabling kinetic studies of on-chip (bio)chemical reactions by MALDI-MS, the concept of “monitoring window” is described. The feasibility of extracting ions through a sampling port (“monitoring window”) along the fluidic path is demonstrated.

1.2. References

- 1 Thorsen, T.; Maerkl, S. J.; Quake, S. R. *Science* **2002**, *298*, 580.
- 2 http://www-1.ibm.com/ibm/history/history/history_intro.html.
- 3 Bardeen, J.; Brattain, W. H. *Phys. Rev.* **1948**, *74*, 230.
- 4 Shockley, W.; Bardeen, J.; Brattain, W. H. *Science* **1948**, *108*, 678.
- 5 Jahns, J.; Sinzinger, S. *Microoptics*, Wiley-VCH: Weinheim, **1998**.
- 6 Fischeraurer, G.; Mauder, A.; Müller, R. in: Göpel, W.; Hesse, T.; Zemel, T. N. (eds) *Sensors: a Comprehensive Series*, VCH: Weinheim, **1995**, 8.
- 7 Grate, J. V.; Frye, G. C. in: Baltes, H.; Göpel, W.; Hesse, T. (eds) *Sensors Update*, VCH: Weinheim, **1996**, 2.
- 8 Timmer, W. S. (ed) *Micromechanics and MEMS: Classical and Seminal Papers to 1990*, Wiley-IEEE Press, **1997**.
- 9 Van den Berg, A.; Lammerink, T. S. J. *Top. Curr. Chem.* **1997**, *194*, 21.
- 10 <http://ftp.arl.army.mil/~mike/comphist/hist.html>.
- 11 Manz, A.; Becker, H. (eds) *Microsystem Technology in Chemistry and Life Science*, Springer-Verlag: Berlin, **1998**.
- 12 Reyes, D. R.; Iossifidis, D.; Auroux, P.-A.; Manz, A. *Anal. Chem.* **2002**, *74*, 2623.
- 13 Auroux, P.-A.; Iossifidis, D.; Reyes, D. R.; Manz, A. *Anal. Chem.* **2002**, *74*, 2637.
- 14 Vilkner, T.; Janasek, D.; Manz, A. *Anal. Chem.* **2004**, *76*, 3373.
- 15 Jähnisch, K.; Hessel, V.; Löwe, H.; Baerns, M. *Angew. Chem. Int. Ed.* **2004**, *43*, 406.
- 16 Fletcher, P. D. I.; Haswell, S. J.; Pombo-Villar, E.; Warrington, B. H.; Watts, P.; Wong, S. Z. F.; Yhang, X. *Tetrahedron* **2002**, *58*, 4735.
- 17 Mitchell, M. C.; Spikmans, V.; Manz, A.; De Mello, A. J. *J. Chem. Soc., Perkin Trans. 1* **2001**, 514.
- 18 Mitchell, M. C.; Spikmans, V.; De Mello, A. J. *Analyst* **2001**, *126*, 24.
- 19 Garcia-Egido, E.; Spikmans, V.; Wong, S. Y. F.; Warrington, B. H. *Lab Chip* **2003**, *3*, 73.
- 20 Ehrfeld, W.; Hessel, V.; Löwe, H. *Microreactors: New Technology for Modern Chemistry*, Wiley-VCH: Weinheim, Germany, **2000**.

Chapter 2

Miniaturization of the Reaction Vessel: High-Control, Information-Rich Chemical Reactions

This Chapter offers an overview of the relatively young research area of lab-on-a-chip for synthetic applications. An introduction of microfluidics and its earlier application to the field of analytical chemistry is given in the first part of the Chapter. Subsequently, the effects of downscaling reaction vessels as well as the advantages of the continuous flow microfluidics approach over conventional chemical laboratory methodologies in the field of organic chemistry are described and illustrated by a number of examples of organic reactions carried out on-chip. The last part deals with one key issue of the lab-on-a-chip approach, viz. the integration of the microreactor with the analytical instrumentation.

2.1. Microfluidics

The modern concept of microfluidics¹ can be traced back to the seventies when the first integrated microfluidics system was first reported at Stanford University.^{2,3} The device was a silicon-based miniaturized gas chromatographic analyzer capable of separating a simple mixture of compounds within a few seconds. In the same period another revolutionary microfluidics concept was developed at IBM, resulting in the ink jet printer.^{4,5} Despite the remarkable properties of these two devices, research towards integrated microfluidics systems remained practically dormant for more than a decade. At this early stage, microfluidics was a branch of microelectromechanical systems (MEMS)⁶ technology rather than an independent discipline. For a few more years the application of MEMS technology to microfluidics gave very modest results.¹ It was only in the second half of the eighties when research activities in this area increased considerably and microfluidics became a “hot” topic.⁷ However, until the early nineties microfluidics mainly focused on the development of single components such as valves,^{8,9} pumps,¹⁰⁻¹⁴ and sensors,¹⁵ rather than exploiting the possibility of integrating them in a single device. A few examples of microfluidics components are depicted in Figure 2.1.

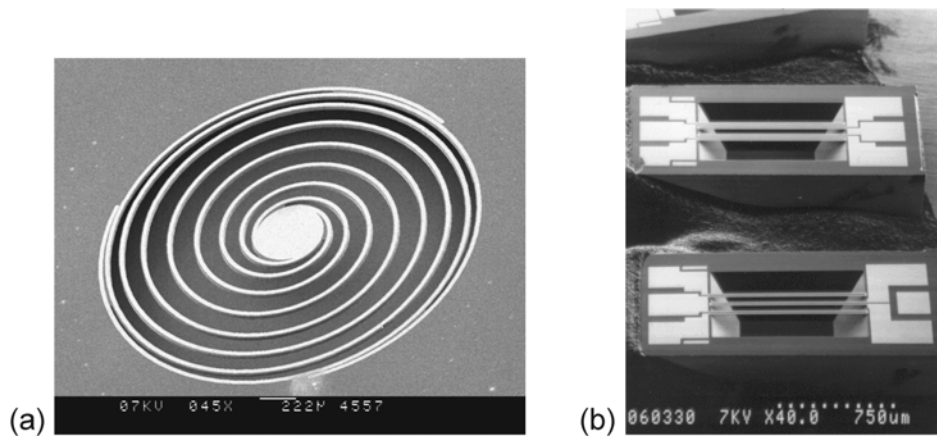


Figure 2.1. Examples of microfluidics components: (a) check valve¹⁶ and (b) thermal sensor.¹⁷

2.2. Analytical chemistry at the microscale; the μ -TAS

For the past two decades, the demand for continuous flow and fast-response measurements of small volume, low concentration samples has been the driving force for research in many areas of analytical chemistry.¹⁸⁻²¹ Two solutions have been proposed in order to satisfy these needs: the first is based on the use of selective chemical sensors²² and the second on the so-called total analysis system (TAS) approach.¹⁸ Although sensors have the advantages of *in-situ* analysis and fast response, the main limitations are the high sensitivity and selectivity required for the detection of tiny amounts of analytes in complex sample mixtures. TAS on the other hand is based on the lab-scale integration of a number of functions, such as sample collection, pretreatment, separation, analysis, and detection, and offers a reliable alternative. Nevertheless, TAS suffers from the limitations of bulky systems, such as large reagents consumption and slow response, and the lack of an efficient interface between units. The main idea behind TAS was to offer a valuable alternative to the existing (bio)chemical sensors rather than to reduce the size of analytical devices.²³

About fifteen years after the first silicon-based miniaturized gas chromatograph was presented,^{2,3} a new microfluidics integrated system appeared in the literature in 1990,²⁴ initiating a real “microfluidics revolution”. The device reported by Manz *et al.* consisted of an on-chip open-tubular column (1.5 nL volume) and a conductometric detector with a 1.2 pL volume detection cell. At the same time, Widmer and Manz²⁵ proposed the micro total analysis system (μ -TAS) concept, opening a new era in the field of analytical chemistry. The main aim of μ -TAS was to fabricate integrated systems ideally able to perform a number of functions in an automated way, in a miniaturized system.²⁶⁻³⁰ The smaller size was expected to provide shorter response times, reduce the sample consumption and enhance reagents mixing due to the fast molecular diffusion. During the first half of the nineties, the fundamental and practical advantages of miniaturized analysis systems compared to lab-scale instrumentation were demonstrated for a large number of applications.³¹⁻³⁵ Miniaturization has become a dominant trend in the field of analytical chemistry, providing chip-based methods for separation,³⁶⁻³⁸ clinical applications,³⁹ and biochemistry,¹⁸ producing most impressive results in the area of DNA analysis.⁴⁰⁻⁴⁶

The field of microfluidics has rapidly and progressively diverged from MEMS,⁴⁷ resulting in the diversification of the μ -TAS field in many application areas, as illustrated by the number of excellent reviews that appeared in the recent literature, covering fields such as (bio)chemical analysis,^{23,48,49} clinical and forensic analysis,⁵⁰ molecular⁵¹ and medical diagnostic,⁵² and point-of-care testing.⁵³

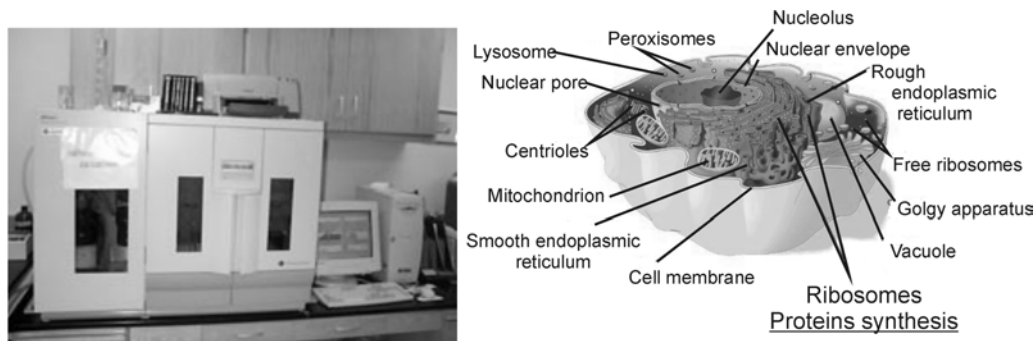
2.3. Synthetic chemistry at the microscale; the lab-on-a-chip

2.3.1. Introduction

Unlike their analytical colleagues, synthetic chemists are used to manipulate relatively large volumes of chemicals. In the conventional laboratory practice reactions are carried out in volumes ranging between a few and a few hundreds of milliliters. Reactions are subsequently monitored off-line by withdrawing aliquots from the reaction mixture to be analyzed batchwise with various analytical techniques. A main drawback of this approach is the reaction to analysis delay time, which is inherent to batch processes. The extension of chemical synthesis from the laboratory to the industrial scale adds further problems, mainly related to the poor reaction control achievable in large-scale batch reaction vessels. In particular, temperature control and mixing efficiency are important issues because the non-homogeneous temperature and concentration distribution may give rise to side-reactions as well as product decomposition, resulting in lower yields and process selectivity.

In living organisms Nature controls chemical and biochemical processes in an impressive way with extremely efficient (bio)chemical reactions in the micrometer-size compartments of cells. The impressively high degree of efficiency, selectivity, process speed and control is achieved without making use of laborious reagents preparation, synthesis, and product work-up steps that chemists are so familiar with. Cells and bacteria exploit chemistry in very small volumes (Figure 2.2a), where reaction products are provided at the point of use and in the required amount. On the contrary, chemists carry out chemistry in relatively large volumes (Figure 2.2b), which is dominated by bulk effects. The question arises whether performing organic

chemistry in nano- to picoliter reaction vessels would lead to such an efficiency and how chemists could take advantage of such knowledge to perform chemistry in a cell-size reaction vessel, in which surface rather than bulk phenomena are dominant.



(a) Laboratory robot: order of magnitude = 1 m; V ~ mL
 (b) Cell: order of magnitude: = 10^{-6} m; V ~ pL

Figure 2.2. (a) Photograph of a laboratory-scale peptide synthesizer⁵⁴ and (b) schematic representation of a cell with the functional organelles.⁵⁵

A few years ago microreactor technology was developed as a versatile and more efficient alternative to the faithfully working but limited batch chemical procedure. The idea of using microfluidics systems to perform chemical and biochemical syntheses has first been discussed in 1995 at a workshop in Mainz.⁵⁶ Since then research in the field of miniaturized (bio)chemical systems has focused on the application of miniaturization to synthetic chemistry.^{57,58} This resulted in the synthetic counterpart of μ -TAS, also known as lab-on-a-chip concept. However, this development has been much slower than μ -TAS.⁵⁹

2.3.2. Microreactors

Making use of MEMS technologies (already successfully used over the past decade to fabricate devices for μ -TAS applications⁶⁰⁻⁷⁰) microreactors can nowadays be fabricated and used to study chemical syntheses at the microscale.⁷¹ Microreactors are defined as miniaturized reaction systems fabricated by using, at least partially, methods of microtechnology and precision engineering.⁷² Microreactors consist of

three-dimensional structures (microchannels) with dimensions typically ranging between tens and a few hundreds of μm , which are used to manipulate reagent solutions. Some examples of liquid microreactors are given in Figure 2.3. A wide variety of materials such as glass, quartz, silicon, polymers, and metals can be used to fabricate microreactors.^{28,73} For synthetic applications glass is the most popular choice⁷⁴⁻⁸³ due to the availability of the fabrication equipment as acquired from MEMS and μ -TAS technologies, its transparency and its chemical inertness as well as its compatibility with a wide range of solvents and its suitability for electrokinetic fluidics pumping.^{84,85} Nevertheless, alternative materials such as polymers,^{86,87} combinations of polymers and glass,⁸⁸⁻⁹⁰ glass and silicon,⁹¹ silicon and quartz,⁹² metals⁹³⁻⁹⁵ and plastic⁶⁷ are being implemented more frequently in microreactor technology (MRT). Based on the material of choice a number of microfabrication methods can be used, ranging from photolithography, powderblasting, hot embossing and injection moulding to laser microforming. For an extensive coverage of microfabrication and microengineering one is referred to the books of Maddou⁹⁶ and Geschke.⁹⁷

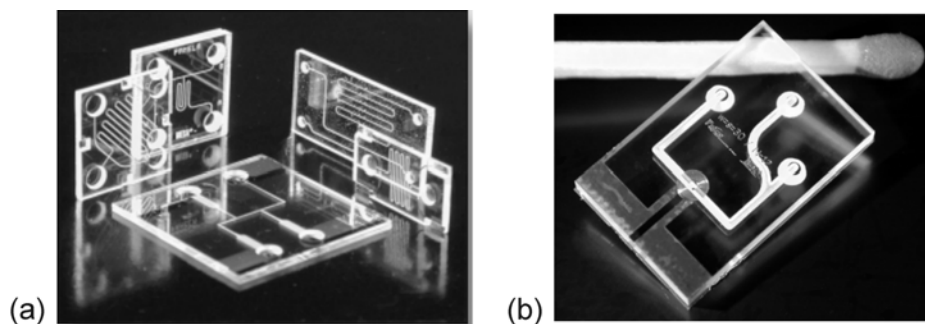


Figure 2.3. Photographs of microfluidics devices fabricated at the MESA⁺ Institute for Nanotechnology, University of Twente, The Netherlands. (a) Microreactors for electroosmotically driven fluidics chemical systems and (b) NMR microchip.

2.3.3. Microfluidics handling

The manufacturing of microfluidics devices involves the fabrication of an interconnected channels network. Handling of microfluidics within the channels in a controlled way is one of the main issues in lab-on-a-chip.^{98,99} In order to provide a precise and controlled output of chemical reactions, microfluidics systems need to receive precise and controlled inputs. For liquid phase chemistry a variety of both mechanical and non-mechanical pumping methods have been used, as reported recently by Manz.¹⁰⁰⁻¹⁰² and Van den Berg.¹⁰³ Main issues are the dead volumes, complexity, and bubble formation. The latter gives rise to backpressure and capacitance that blocks or even reverses the fluid flow. To drive liquids in the microchannels network of a microreactor three main methods are commonly used: electrokinetics, including electroosmosis and electrophoresis, pressure, and flow by pumps. A number of alternative pumping methods are currently under investigation.

2.3.3.1. Electrokinetic pumping

Electrokinetic pumping of a liquid is widely used in microfluidics applications. Electrophoresis, which involves ion transport by an electric field, is mainly used for separation purposes in μ -TAS applications.^{36,104} Electroosmosis, which is widely used in lab-on-a-chip technology for synthetic applications,¹⁰⁵ is the transport of fluid resulting from the drag of a moving, charged electric double layer (Figure 2.4). The electroosmotic flow (EOF) principle can be explained considering a wall of a glass microchannel having negatively charged groups at the surface. If the channel is filled with a liquid having ionic species in solution, the positive counterions form a double layer at the channel wall. Upon application of an electric field the positive counterions migrate towards the negative electrode dragging the bulk liquid through the channel. In an aqueous buffered system (pH 3-9) the solutions flow with a velocity up to a few mm s^{-1} , generating in microchannels flow with velocities typically up to min s^{-1} , depending on the channel geometry and the applied field.^{71d} The flow velocity v_{EOF} [m s^{-1}] is given by equation 2.1.

$$v_{EOF} = \frac{V}{L} \cdot \mu \quad (2.1)$$

where V [V] is the applied voltage, L [m] is the length of the channel and μ [$\text{m}^2\text{V}^{-1}\text{s}^{-1}$] is the electroosmotic mobility, which depends on parameters such as ionic strength, pH, and zeta potential (the charged double layer).¹⁰⁵

In principle, EOF is very simple to use for flow control of liquids in microchannels.^{71d} This pumping mechanism can be integrated in microchips relatively easily, as it only requires contact electrodes to apply an electric field. The ease of fabrication allows the manufacturing of relatively complex switchable fluidic networks.¹⁰⁶ A number of publications appeared in the early nineties demonstrating the potential of electrokinetic pumping to move aqueous solutions at the microscale.^{27,29,43,60,62,107-110} More recently, Harrison *et al.*⁸² extended the use of EOF to drive organic solvents. Similarly, Haswell *c.s.*⁷⁵ used EOF to transport a multiphase system (microemulsion) containing a non-polar liquid (benzene).

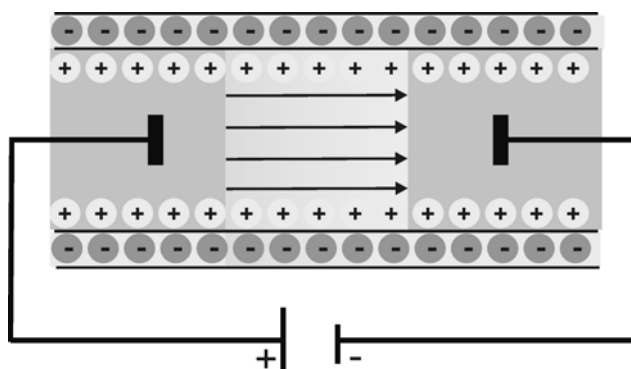


Figure 2.4. Schematic representation of the EOF principle: in microchannels with a negative surface charge, the channel walls attract positively charged ions. If a voltage is applied, ions move along the channel walls towards the negative electrode and drag the liquid with them making use of the liquid viscosity.¹¹¹

However, the practical use of EOF-based chips for the study of organic reactions, in particular for time-dependent studies, is still limited. For obvious reasons, the flow that is delivered by electroosmotic pumping is dependent on the channel material as well as on the nature of the solution to be transported (see

equation 2.1). Changes in the liquid conductivity, for example, will induce changes in the electric fields and, consequently, will influence the flow. The ionic strength of the solution being transported is also relevant; liquids with a high ionic strength cannot be transported by EOF because of excessive Joule heating.¹¹²

Oosterbroek *et al.*¹¹³ have recently reported a theoretical study based on computational simulations demonstrating that backflow from the channel outlet is one of the main drawbacks of EOF pumping. Poor control over the flow is clearly a drawback when a high temporal reaction control is required (*e.g.* to study reaction dynamics). Backpressure may arise from pressure effects related to different liquid volume heights at the inlet and outlet reservoirs or even from fluctuations in the EOF in different zones of the channels. These factors may eventually lead to variations in the reaction mixture composition caused by unwanted mixing of samples at different positions in the channel (also resulting in different reaction times) due to pressure-induced circulation. The overall result is a limited reaction control and fluctuating volume flows in time.

The electric field, which is used to move the liquid, may also influence the chemistry that is being investigated on-chip.^{114,115} The presence of electrodes in contact with solutions of reagents and products at the inlet and outlet reservoirs may induce electrochemical reactions, since typical voltages used in EOF are over the redox potential.¹¹⁶ The resulting pH changes will not only lead to the formation of side products, but also to an overall variation of the EOF magnitude.¹¹⁷ This problem is recognized and much work is currently carried out to overcome these drawbacks by separating the electrode-reservoirs from the main channels either by microfabrication¹¹⁸ or by using salt bridges.¹¹⁹

2.3.3.2. Pressure-driven pumping

In μ -TAS applications electroosmosis has been preferred to pressure-driven flow,⁹⁹ not only because of the ease of integration with microfluidics systems, but also because it is less affected by dispersion phenomena. However, Caliper Technologies Corp. (Mountain View, California, U.S.A.) has recently reported that at the length scales and flow rates in microfluidics devices “dispersion is much slower than

normal” in pressure-driven flows.^{120,121} They have therefore changed their strategy to drive fluids from electroosmosis to pressure-driven in order to avoid problems related to the fluidics control by EOF.

In pressure-driven flow systems pressure is applied to the liquid reservoirs, which drives the flow through the microchannel network. Pressure can be generated by piezoelectric elements,¹²² centrifugal force pumps,¹²³ on-chip pneumatic pumps,¹²⁴ and off-chip reservoirs or pneumatic devices.^{125,126} Fernandez-Suarez *et al.*¹²⁷ have used an eight-peristaltic pump system to move solutions in a glass microreactor.¹²⁸ This system works efficiently for biological applications, but is less suitable for driving organic solvents.¹²⁷ During a chemical reaction changes in the reaction mixture (upon mixing of reagents and products formation) may result in viscosity changes. As a consequence, the channel resistance, which is related to the liquid viscosity, will also vary, causing the relation between the applied pressure and the resulting flow rates to be hard to predict. A main advantage of pressure-driven flows is the possibility to use large, pressurized reservoirs to deliver flows for a long time without the need of re-filling.

2.3.3.3. *Flow-driven pumping*

Flow-driven pumping makes use of syringe pumps, HPLC pumps, or peristaltic pumps to drive solutions through microchannels. As a relatively simple and quick means for moving reagent solutions within a microreactor in a controlled way, this method is very suitable for carrying out time-resolved chemical reactions on-chip, without the need of flow sensors. The high degree of control is given by the fact that as long as the fluid is incompressible the flow rate through the chip is constant and equals the flow rate delivered by the pump. However, flow-driven systems cannot be easily integrated into complex fluidic channel networks.

Due to the remarkable stability as well as the high reproducibility of the generated flow, this method has been widely used in microfluidics, starting from the earlier μ -TAS applications^{1,129-131} to the most recent studies.^{78,79,87-89,93,132-134}

2.3.3.4. Alternative pumping methods

Although electrokinetic-, pressure-, and flow-driven methods have been extensively used to move liquids within microchannels, a number of other creative solutions have been proposed as well. Electrodynamic pumping, as demonstrated by McBride *et al.*¹³⁵ for various organic solvents including chloroform, tetrahydrofuran and *N,N*-dimethylformamide, can be used to transport either conductive or non-conductive fluids. A related method has been proposed by Gallardo *c.s.*¹³⁶ for the active control of organic or aqueous liquids. The method relies on the formation of gradients in the surface pressure induced by applying very low voltages (<1 V). The gradients are generated by the use of surface-active molecules, with redox-active groups. Upon application of a voltage a chemical reduction occurs, which induces a potential difference between the electrodes, resulting in a concentration differential. The control over the concentration is used to actively adjust the surface pressure and, hence, the fluid movement. Another very appealing method for the actuation of liquids has been reported by Gau *et al.*¹³⁷ They used surface wetting techniques to create hydrophobic / hydrophilic barriers on surfaces. Parallel liquid channels were formed on the structured surfaces. Zhao *et al.*¹³⁸ controlled the boundary between immiscible liquids by patterning the channel surface. More examples of surface tension-driven flows, the so-called “Marangoni effects”, used in microchannels are reported in a recent review.¹³⁹ A creative method to guide the movement of cells using sound waves has been published very recently by Marmottant and Hilgenfeldt.¹⁴⁰ More fluidics handling methods can be found in the reviews of Manz *et al.* on μ -TAS.¹⁰⁰⁻¹⁰²

2.3.4. Synthesis in microreactors: an overview

Lab-on-a-chip technology for synthetic applications is still a young research field as compared to the more mature μ -TAS arena. Nevertheless, after the first example of organic chemistry in a microreactor by Harrison,⁸² the number of gas and liquid phase reactions carried out in microfluidics systems have increased tremendously.^{57,85} The spectrum of reactions performed using microreactors includes many well-known reaction types: nucleophilic¹⁴¹ and electrophilic¹⁴²⁻¹⁴⁴ substitutions,

elimination reactions,^{145,146} additions,^{147,148} and radical polymerizations.¹⁴⁹ Many of these reactions provide improved yield and selectivity when performed in a continuous flow manner at the microscale as compared to the conventional lab-scale equipment.^{79,85,184} Microreactors have also been successfully used to synthesize peptides,^{114,150} to separate them after synthesis from the unreacted amines,¹⁵¹ and to investigate peptide racemization during synthesis.¹¹⁵ Several papers describe that microfluidics systems offer a suitable platform to carry out combinatorial chemistry and high-throughput drug discovery.^{76,81,83,90,152-154} They give high yields, high purity products in short times and a high chemical diversity. A few papers have also reported the feasibility of using microfluidics chips for large-scale chemical production.^{76,155} Other examples include reactions that require special safety regulations when carried out at the macroscale, involving explosive, highly toxic or flammable chemicals such as fluorinations,^{93,94,142,156,157} chlorinations,⁵⁷ nitrations,^{75,143,144} hydrogenations,^{145,158} and oxygenations.^{159,160} Because microreactors are inherently safe,^{71b,161} early studies on synthesis at the microscale focused on gas-phase reactions.⁵⁸ Recently published reactions include the hydrogenation of polyenes,^{158,162} the hydrogenation of cyclohexene,⁹¹ the dehydration of 2-propanol to propene,¹⁶³ the dehydrogenation of propane to propene,¹⁶⁴ and the fluorination of organic compounds.^{93,94} The oxidation of ammonia,^{165,166} of ethylene to ethyleneoxide,¹⁴⁸ of alcohols to aldehydes,¹⁶⁷ and of methane¹⁶⁸ for the manufacturing of syngas (a mixture of carbon monoxide and hydrogen) have also been reported. Though a few examples of gas and gas / liquid reactions are given, This Chapter mainly focuses on liquid-phase lab-on-a-chip systems.

2.3.5. Effects of downsizing the reaction vessel

As already demonstrated for miniaturized analysis systems,¹⁰⁰⁻¹⁰² the reduction in size of the reaction vessel provides a number of fundamental and practical advantages over the conventional lab-scale practice.⁷¹ Smaller devices need less space, use less energy and reagents, produce less waste, and often have much shorter response times.^{31,72} Miniaturized reaction vessels are expected to provide the degree of control which is necessary to increase process safety and to optimize either chemical production, in terms of product purity and yield, and of chemical screening,

in terms of high-throughput.^{57,58,85,169} Moreover, enhancement of the system performances can be obtained by integration of components as illustrated by Quake *et al.*¹⁰⁶ Parallel fabrication of identical miniaturized devices is also expected to reduce production costs.^{71e}

The most striking feature of microreactors is the large surface-to-volume ratio, which directly results from the downscaling process. Reducing the linear dimension causes in fact the surface area to decrease to the power two and the volume to the power three. As a consequence of the increased surface to volume ratio, the driving force for diffusion-based phenomena, such as mass and heat transfer, is much higher in microreactors as compared to conventional lab glassware and, even more, when compared to industrial reactors.⁷² The high heat exchange efficiency of microreactors (heat-transfer coefficient values in the order of $10 \text{ kW m}^{-2} \text{ K}^{-1}$)^{170,171} allows fast heating and cooling of the reaction mixture at the microscale, offering the possibility of carrying out reactions under isothermal conditions with a well-defined residence time distribution.¹⁷² Another implication is the higher safety when carrying out potentially explosive reactions.^{71b,159} The ease of process optimization has been clearly demonstrated by Wörz *et al.*^{72,167} The authors investigated a very fast, highly exothermic, homogeneously catalyzed reaction, which yields a vitamin precursor.¹⁷³

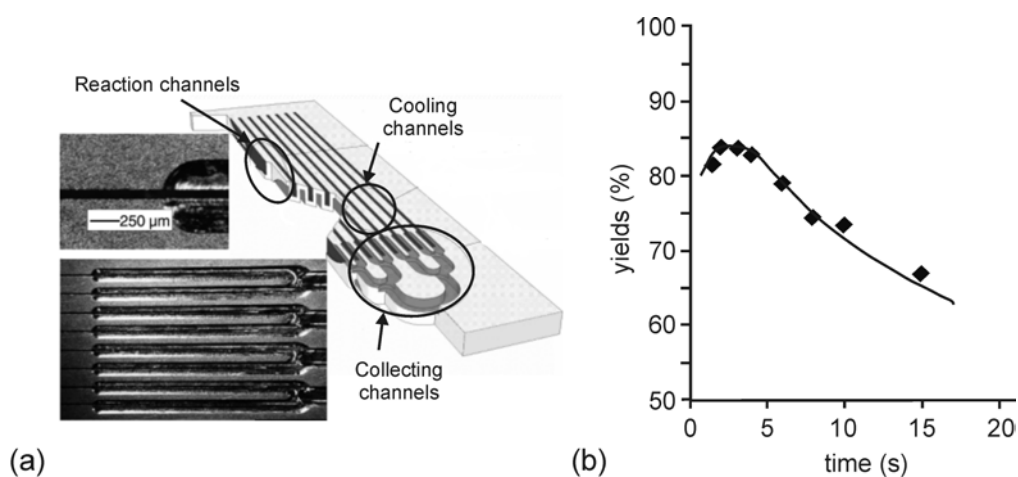
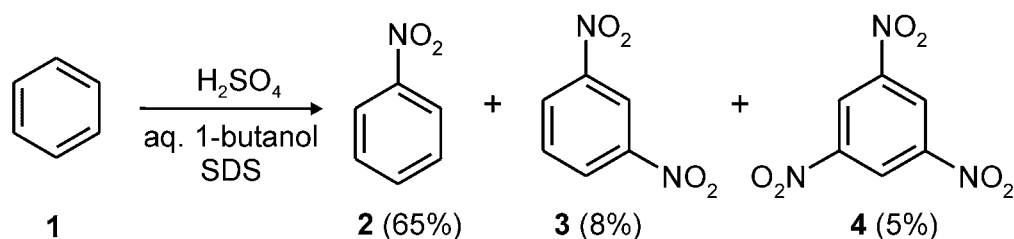


Figure 2.5. (a) Microreactor used in the synthesis of a vitamin precursor; (b) dependence of the product yield on the reaction time.⁵⁷

During this reaction a side-product was formed, causing a considerable decrease in the yield. Optimization of the industrial procedure had already been accomplished by replacing the semi-batch process (70% yield) with a continuous mixer / heat exchanger reactor (80-85% yield). The reaction has recently been investigated in a thirty-two channels ($900 \times 62 \mu\text{m}^2$) microreactor (Figure 2.5a) under isothermal conditions, leading to a better understanding of the dependence of the reaction yield on the residence times (Figure 2.5b). Consistent with the industrial process, yields of about 85% were obtained at a residence time of 4 s and a temperature of 50 °C. By decreasing the temperature to 20 °C, higher yields (90-95%) could be obtained at a residence time of 30 s, which allowed for optimization of the industrial scale production.

Making use of relatively large quantities of concentrated nitric and sulfuric acid, nitration reactions in organic synthesis are rather hazardous. Being highly exothermic, these reactions are difficult to handle, especially at the macroscale where the temperature is difficult to control. Due to the high heat transfer coefficient, microreactors are able to dissipate the heat generated during the reaction much better, offering a valuable alternative to the lab-scale equipment.

Doku *et al.*⁷⁵ have reported the nitration of benzene (**1**) in a glass microreactor to give 65% of nitrobenzene (**2**), about 8% of 1,3-dinitrobenzene (**3**), and about 5% of 1,3,5-trinitrobenzene (**4**) (Scheme 2.1). Relative reaction yields could be controlled by tuning parameters such as residence time, applied voltage, solution pH, amount of surfactant, and feed rate of the reagents. These results demonstrate the higher reaction control at the microscale.

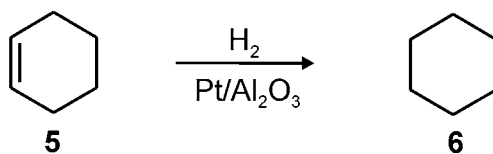


Scheme 2.1. Nitration of benzene.

Burns and Ramshaw have reported the nitration of benzene and toluene in stainless steel and polytetrafluoroethylene (PTFE) microreactors.^{85,144} They successfully demonstrated that the inherent safety character of microreactors make them suitable to carry out hazardous reactions. They found a linear relationship of the conversion with the temperature. Furthermore, the conversion could be considerably increased by reducing the microchannel diameter as well as by increasing the flow rates. The authors attributed the effect of the flow rate on the conversion to the mixing, which would be more efficient at higher flow rates. This study clearly demonstrated the possibility of optimizing reactions by studying the effect of independent parameters on reaction rates.

Beside the safety issue, the high degree of temperature control prevents side-reactions to occur in microreactors. In addition, thermal decomposition of the target product is reduced, resulting in overall increased product yield, selectivity, and purity, compared to the corresponding macroscale process.¹⁶⁷ An illustrative example was given by Hessel *et al.*,¹⁷⁴ who synthesized hydrogen cyanide *via* the Andrussow route and demonstrated that a microheat exchanger prevents the hydrolysis of the reaction product to ammonia.

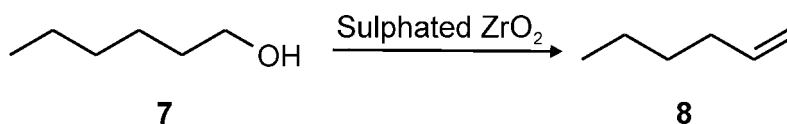
Mass transfer coefficients are also substantially increased as a consequence of downscaling. Due to the shorter diffusion lengths, mixing in microreactors is much faster¹⁷⁵ and consequently the influence of mass transport on the reaction rate is considerably reduced.¹⁷⁶ Moreover, the high mixing efficiency prevents the formation of concentration gradients and hence side reactions are minimized. Jensen and c.s.⁹¹ have recently found that mass transfer coefficients measured for the catalyzed hydrogenation of cyclohexene (**5**) to cyclohexane (**6**) (Scheme 2.2) in a silicon-glass microreactor exceed those reported in the literature for standard laboratory-scale reactors by two orders of magnitude.



Scheme 2.2. Catalyzed hydrogenation of cyclohexene.

Safety in microreactors is also related to the small reaction volumes involved. Furthermore, the opportunity exists for manufacturing at the point of use that could eliminate the hazard of transportation and storage of toxic or hazardous chemicals. This concept has been demonstrated by Jensen c.s.,¹⁷⁷ who used a microreactor for the synthesis of organic peroxides from acid chlorides and hydrogen peroxide. Accurate control of the temperature was possible due to fast heat transfer from the reaction, thus eliminating any explosion risk. The authors emphasized the “point-of-use production” of the exact amount of hazardous material needed.

Typical specific surface areas (surface [m²] / volume [m³]) in microreactors⁵⁷ range between 10 000 and 50 000 m⁻¹, while those of conventional lab-scale vessels are about 1000 m⁻¹. Such a large increase of active surface in microreactors is beneficial for surface-catalyzed reactions. An considerable increase in product yields has been reported for the heterogeneously catalyzed dehydration of alcohols in a glass / PDMS hybrid microreactor by McCreedy and Wilson.⁸⁸ The PDMS cover plate served both as heat source and as a catalyst (sulphated zirconia) support. The catalyst was introduced into the microreactor by dusting it over the surface of the PDMS plate before the top and bottom plates were joined together. This process not only immobilized the catalyst, but it also further increased the available catalytic surface area. As a result, the conversion of 1-hexanol (**7**) to 1-hexene (**8**) (Scheme 2.3) increased from 30% (batch process) to about 90%.



Scheme 2.3. Dehydration of 1-hexanol (**7**) to 1-hexene (**8**) carried out in a microreactor.

Kitamori c.s.¹⁷⁸ have very recently reported the use of a continuous flow glass microreactor to carry out three-phase hydrogenation reactions. The catalyst (microencapsulated palladium) was immobilized on the microchannel wall. A variety of substrates were reacted on-chip with hydrogen in a continuous flow fashion, giving pure reaction products in quantitative yield within two minutes (Figure 2.6).

Substrate	Product	Substrate	Product

Figure 2.6. Substrates reacted on-chip with H_2 and corresponding products.

Greenway *et al.*¹⁷⁹ have carried out a heterogeneously catalyzed Suzuki reaction in a borosilicate microreactor (Figure 2.7). Electroosmotic flow was used to transport the reagents through the channel network by periodic injections of the aryl cyanide **9** into the continuous flow of the phenylboronic acid **10**, to give 4-cyanobiphenyl **11** (Scheme 2.4). The on-chip continuous flow reaction gave 10% higher yields (67%) than the batch lab-scale process. The catalyst (1.8 wt% palladium on silica) was immobilized onto the channel surface and by heating a suspension at 100 °C for 1 h.

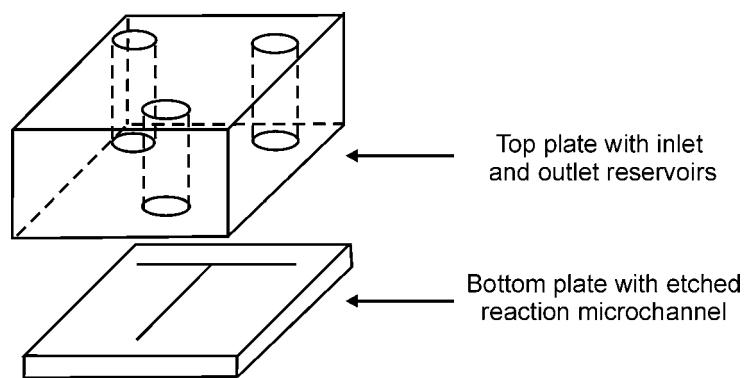
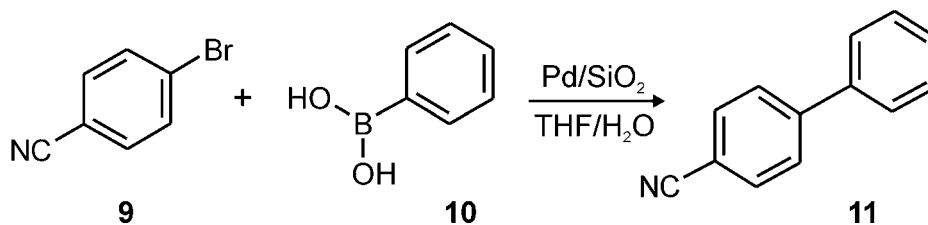
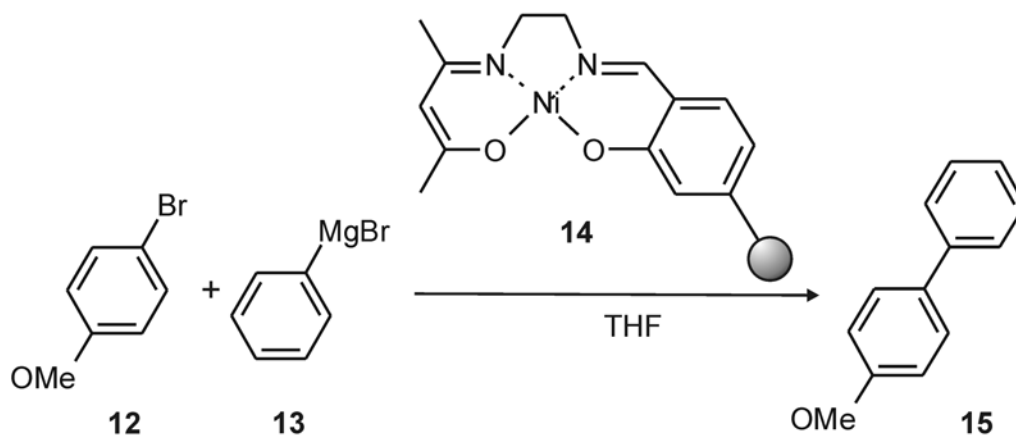


Figure 2.7. Schematic diagram of the EOF-based microreactor fabricated at the University of Hull and used to carry out many of the reactions described in this Chapter.⁸⁵



Scheme 2.4. Example of a heterogeneously catalyzed Suzuki reaction carried out in a borosilicate microreactor.

The group of Haswell¹³⁴ demonstrated that microreactors can also be used to carry out organometallic reactions with higher efficiency compared to the batch process. The reactor was constructed by placing a plug of catalyst into a polypropylene tube. The Kumada-Corriu reaction by reacting *p*-bromoanisole (**12**) with phenylmagnesium bromide (**13**) in the presence of a nickel catalyst supported on a Merrifield resin (**14**) to give 4-methoxybiphenyl (**15**) (Scheme 2.5) was investigated. In this case there is an enhancement of the reaction rate as well compared to the equivalent batch reaction.



Scheme 2.5. The Kumada-Corriu reaction carried out in a microflow reactor.

The high surface-to-volume ratio resulting from downscaling implies that inertance effects, which are related to the volume, become less important than viscous forces that result from frictional drag along the channel wall.¹⁸⁰ This property of microfluidics is well represented by the Reynolds number Re (equation 2.2).

$$Re = \frac{\rho \cdot v \cdot l}{\mu} \quad (2.2)$$

where ρ [kg m^{-3}] is the mass density, v [m s^{-1}] is the velocity, l [m] is the length, and μ [N s m^{-2}] is the dynamic viscosity. Typical Reynolds numbers encountered in microchannels lie well below the transition between laminar and turbulent regime ($Re \sim 2500$),¹⁸¹ being in most cases smaller than one.¹⁸⁰ Low Reynolds number flows are referred to as laminar and are characterized by a high degree of symmetry. In the laminar flow regime, mixing is accomplished through diffusion (random molecular motion along a concentration gradient),^{23,180} and it therefore depends on the nature of the chemical species to be mixed and on the channel geometry, as described in equation 2.3.

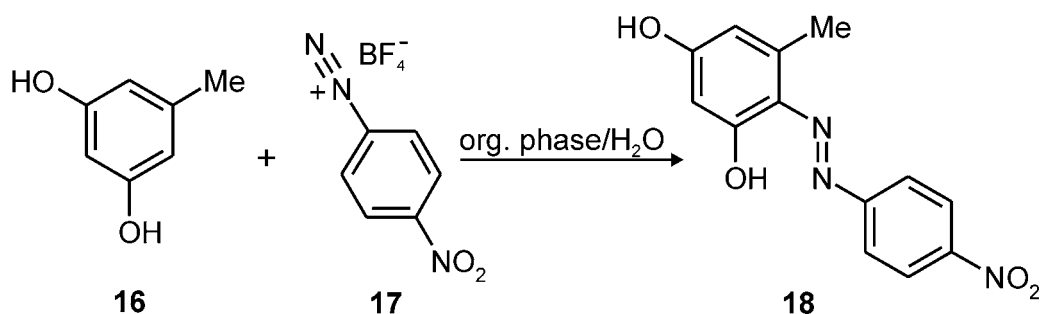
$$t_d = \frac{L^2}{D} \quad (2.3)$$

L [m] is the distance over which diffusion must take place and D [$\text{m}^2 \text{s}^{-1}$] is the diffusion coefficient that is described in equation 2.4 in which k is the Boltzmann constant ($1.38 \times 10^{-23} \text{ J K}^{-1}$), T [K] the absolute temperature, η [$\text{kg m}^{-1} \text{ s}^{-1}$] the absolute (solute) viscosity, and r the hydrodynamic radius [m].

$$D = \frac{k \cdot T}{6 \cdot \pi \cdot \eta \cdot r} \quad (2.4)$$

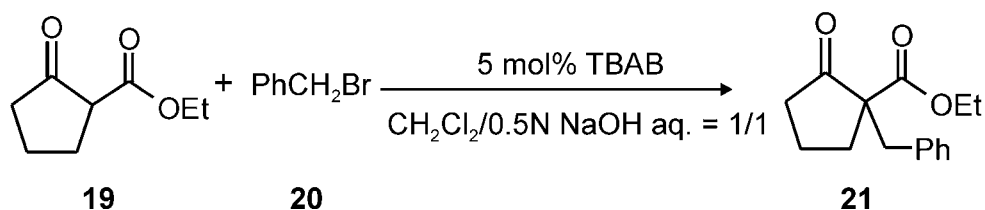
Assuming typical values of diffusion coefficient in the order of $1 \times 10^{-9} \text{ m}^2 \text{ s}^{-1}$ for small molecules or smaller for large molecules,¹⁸² under purely diffusive conditions the mixing time is typically in the order of seconds (with L in the order of 100 μm) to milliseconds (with L in the order of 10 μm).²³ Knight *et al.*¹⁸³ have developed a device that reduces the mixing time scale to less than 10 μs . The high symmetry of laminar flows (parallel, non-intersecting stream lines) allows for relatively simple system simulation and modeling,⁵⁷ as well as formation of very well defined interfaces between injected fluids. The group of Kitamori has demonstrated the use of this peculiar property of microfluidic systems to carry out liquid-liquid multi-phase reactions at the interface between the two phases, taking advantage of the large active surface area.^{79,184}

The first example is a phase-transfer diazo coupling reaction⁷⁹ (Scheme 2.6) in a pressure-driven glass microreactor. Solutions of 5-methylresorcinol (**16**) in ethyl acetate (organic phase) and 4-nitrobenzene diazonium tetrafluoroborate (**17**) in water were introduced on-chip under continuous flow conditions. The large active surface area at the interface and the short diffusion length allowed a high efficiency phase-transfer of reagents (**16** and **17**) and product (**18**) and suppressed undesirable side-reactions, resulting in higher yields (almost 100%) compared to the corresponding macroscale process.



Scheme 2.6. Phase-transfer diazo coupling reaction carried out in a microreactor.

Based on the same principle Ueno *et al.*¹⁸⁴ have carried out the phase-transfer benzylation reaction of ethyl 2-oxocyclopentanecarboxylate (**19**) with benzyl bromide (**20**) in the presence of tetrabutylammonium bromide as a phase-transfer catalyst to give the benzylated product (**21**) (Scheme 2.7) in a pressure-driven glass microreactor (Figure 2.8a).



Scheme 2.7. The phase-transfer benzylation reaction of ethyl 2-oxocyclopentanecarboxylate (**19**) with benzyl bromide (**20**).

Higher conversions were obtained in the microreactor as compared to the macroscale experiments carried out at different stirring speeds (Figure 2.8b). After proving the principle, the microreactor was used for the alkylation of a number of other β -keto esters.¹⁸⁴

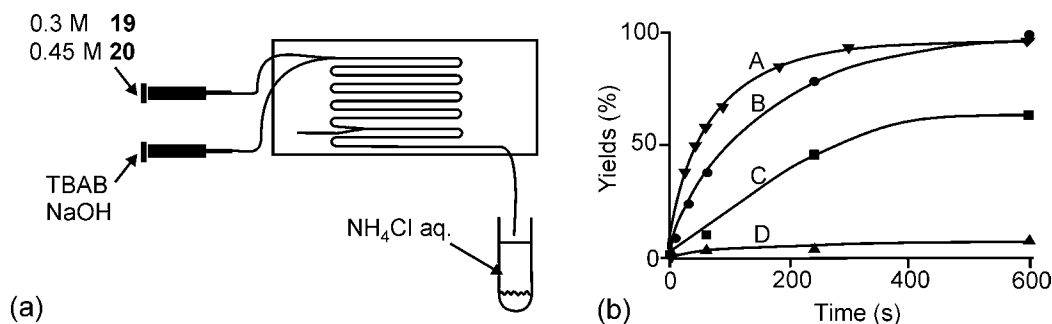
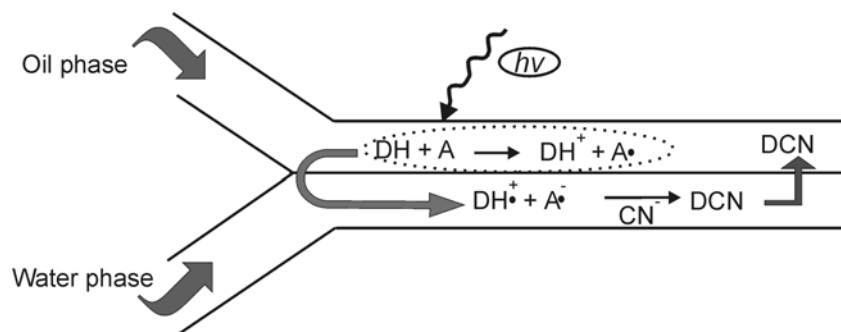


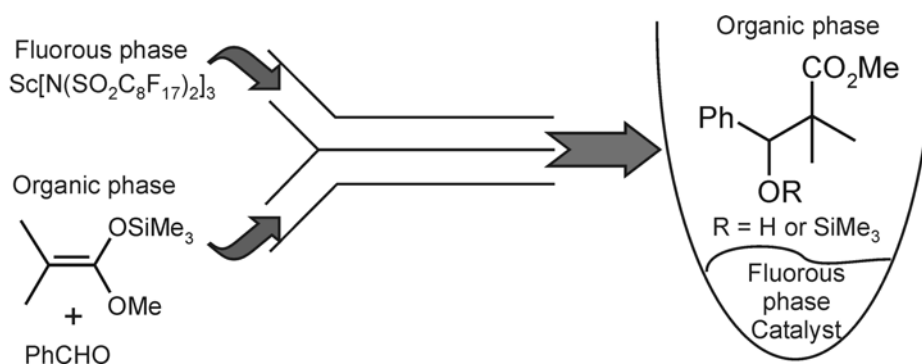
Figure 2.8. (a) Schematic representation of the microreactor and experimental set-up used in the phase-transfer alkylation experiments. (b) Profile of the alkylation of ethyl 2-oxocyclopentanecarboxylate (**19**) with benzyl bromide (**20**) (A) in a microreactor and in a conventional batch equipment at 1350 rpm (B), at 400 rpm (C), and at 0 rpm (D).¹⁸⁴

The group of Kitamura⁸⁷ has recently demonstrated the feasibility of the photocyanation of pyrene across an oil / water interface in two types of polymer microreactors under pressure-driven flow conditions. An aqueous NaCN solution and a propylene carbonate solution containing pyrene (DH) and 1,4-dicyanobenzene (A) were introduced into the polymer microreactor *via* two separate inlets and allowed to flow along each other under laminar flow conditions. Upon irradiation of the chip with a Hg lamp 1-cyanopyrene (DCN) was formed as the reaction product. The proposed reaction scheme (Scheme 2.8) showed that the reaction takes place either at the oil / water interface or by extracting reactants or products from one phase to another. The linear dependence of the yield on the contact time between the two phases demonstrated the possibility of influencing the reaction yield by tuning parameters such as flow rates and channel geometry.



Scheme 2.8. Photocyanation reaction of pyrene in a microchannel.⁸⁷

Recently, Mikami *et al.*¹⁸⁵ have reported a significantly increased reactivity of the Mukaiyama aldol reaction of benzaldehyde with trimethylsilyl enol ether, carried out in a microreactor controlled by a nano-feeder (Scheme 2.9). A solution of both reagents in toluene was injected in one inlet, while a solution of a fluorous catalyst, *viz.* $\text{Sc}[\text{N}(\text{SO}_2\text{C}_8\text{F}_{17})_2]_3$, in perfluoromethylcyclohexane was injected in a separate inlet. The aldol reaction was completed within seconds (yields up to 97%) even in the presence of a much smaller amount of the scandium complex (0.1 mole %) compared to the lab-scale experiment (1-10 mole %), in which the product was obtained in only 11% yield after vigorous stirring at 55 °C for 2 h.

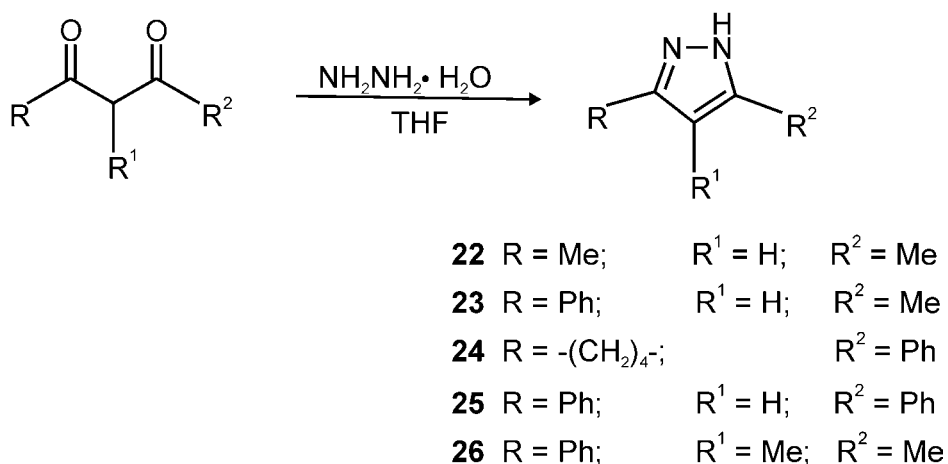


Scheme 2.9. Mukaiyama aldol reaction in a “fluorous nano flow” system.¹⁸⁵

Despite what the small dimensions would suggest, microreactors can be applied for large-scale chemical production. By increasing the number of functional units (1000 units of microreactors) it has been demonstrated^{71a} that large quantities of

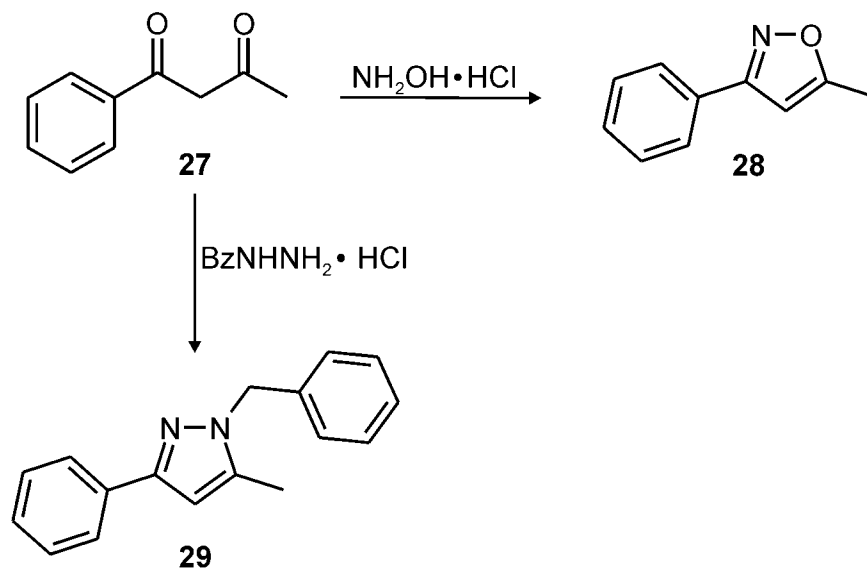
chemicals (up to 1 kg per day) can be produced. The numbering-up approach, also known as scaling-out, is expected to have obvious implications on costs and ease of process optimization.^{71d} However, mainly due to problems related to the liquid distribution through a large number of fluidic units,¹⁸⁶ only a few papers describing this approach have been published.

Wiles *et al.*⁷⁶ have reported the preparation of an array of pyrazoles (**22-26**, Scheme 2.10) in a microreactor (Figure 2.7) using electroosmosis to move reagent solutions within the microchannels. The authors extended the technique to the synthesis of isoxazole **28** and substituted pyrazole **29** (Scheme 2.11) starting from 1-phenylbutane-1,3-dione **27**. In all cases higher conversions have been obtained using the microreactor as compared to the lab-scale approach (Table 2.1).



Scheme 2.10. General reaction scheme for the preparation of 1,2-azoles.

The authors estimated that, based on the yield of one of the investigated reactions, 1000 microreactors working in parallel would produce 339 g of product per day. Based on this estimation and on the successful on-chip synthesis of the 1,4-azoles array, they envisioned that the EOF-based microreactor might be implemented in the large-scale production of fine chemicals and pharmaceuticals. It is interesting to notice that the same type of libraries have been earlier prepared by Garcia-Egido *et al.*⁸¹ using a pressure-driven device. In contrast to the EOF-based system described by Wiles *et al.*, the pressure-driven device can be employed for the rapid preparation of large libraries of compounds required in small amounts.⁷⁶



Scheme 2.11. Preparation of an isoxazole **28** and a substituted pyrazole **29**.

Table 2.1. Comparison of the conversions obtained for the preparation of 1,2-azoles **22-26**, **28**, and **29** on-chip and at the lab-scale.

Product no.	Conversion %	
	Lab-scale	Microreactor
22	62	100 ^a (100) ^b
23	63	100 ^a (100) ^b
24	72	100 ^a
25	64	100 ^a
26	71	98 ^a
28	52	98 ^a
29	76	42 ^a (100) ^c

^a Reaction performed using THF.

^b Reaction performed using DMF.

^c Reaction performed using stopped flow regime.

A different approach has been applied by the group of Kitamori,¹⁵⁵ who recently published the fabrication of a “pile-up” glass microreactor consisting of ten levels of microchannels (Figure 2.9a). Instead of gathering together a number of independent microfluidics units in a parallel configuration (numbering-up), in the “pile-up” approach one single unit is manufactured by bonding a number of piled-up glass plates on which microchannels are fabricated (Figure 2.9b).

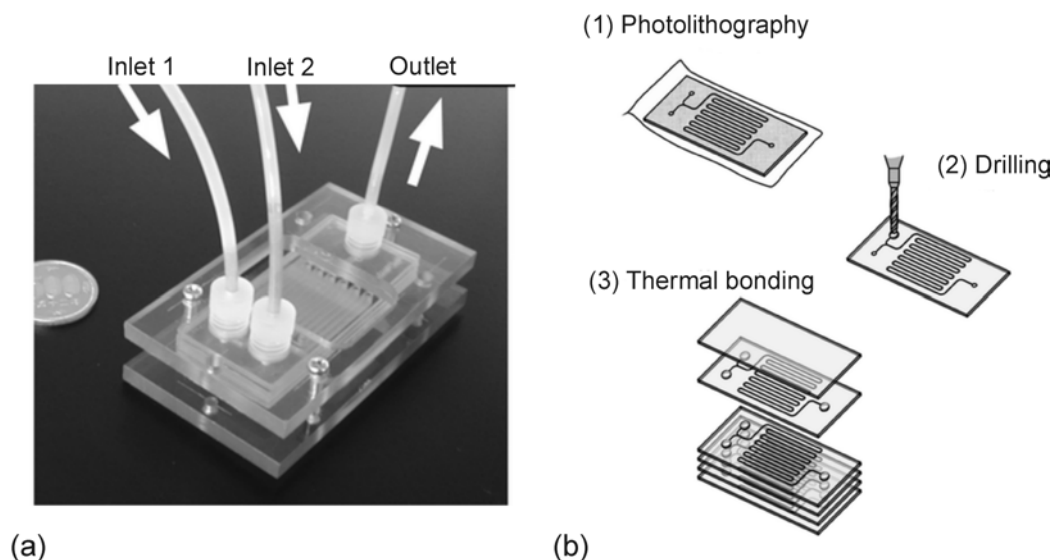


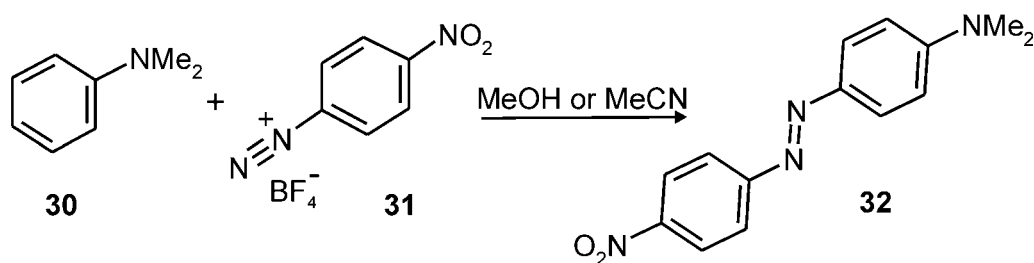
Figure 2.9. (a) Picture and (b) fabrication procedure scheme of the pile-up microreactor.¹⁵⁵

The two-phase (liquid / liquid) amide formation reaction between an amine in water and an acid chloride in ethyl acetate has been used as a model reaction to test the “pile-up” reactor. The maximum throughput of the “pile-up” microreactor was ten times higher than that of a single glass plate microreactor operated under the same conditions. A maximum production of 33 mg min^{-1} has been obtained for the “piled-up” device, from which the authors concluded the suitability of the approach to the industrial production of chemicals.

Due to the possibility of rapidly and efficiently varying reaction parameters guaranteeing a high level of chemical control and diversity, microreactors have a remarkable potential for application in high-throughput screening and the preparation of combinatorial chemical libraries. A few papers in the recent literature¹⁵³ indicate

the interest of the scientific community in demonstrating how the diversity offered by miniaturized chemical systems can be used to provide a low volume, well-controlled, and information-rich way of doing chemistry. Several examples demonstrating this concept have been published over the past four years by the group of Haswell, including the involvement of pharmaceutical industries like Glaxo SmithKline, and Novartis Pharma.⁸⁵

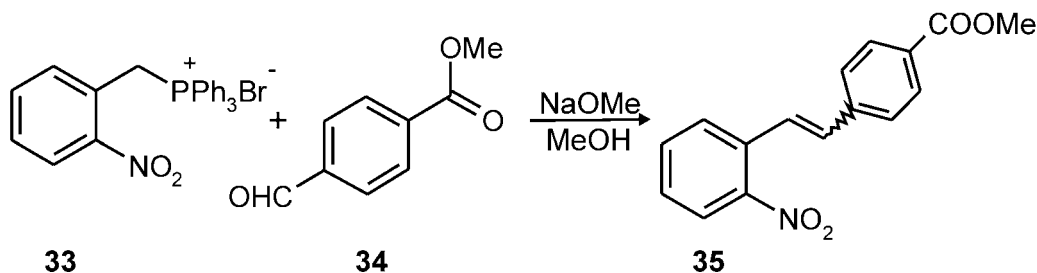
Salimi-Moosavi *et al.*⁸² have demonstrated the synthesis of diazo dyes in a glass microreactor, using EOF as a pumping mechanism. Reacting *N,N*-dimethylaniline (**30**) with *p*-nitrobenzenediazonium tetrafluoroborate (**31**) in both protic (methanol) and aprotic (acetonitrile) solvents gave diazo dye **32** (Scheme 2.12). Demonstrating the feasibility of valveless fluidic control at the microscale, this study has clearly proven the feasibility of a microfluidics-based integrated and automated platform for combinatorial applications.



Scheme 2.12. Synthesis of diazo dye **32** from *N,N*-dimethylaniline (**30**) and *p*-nitrobenzenediazonium tetrafluoroborate (**31**).

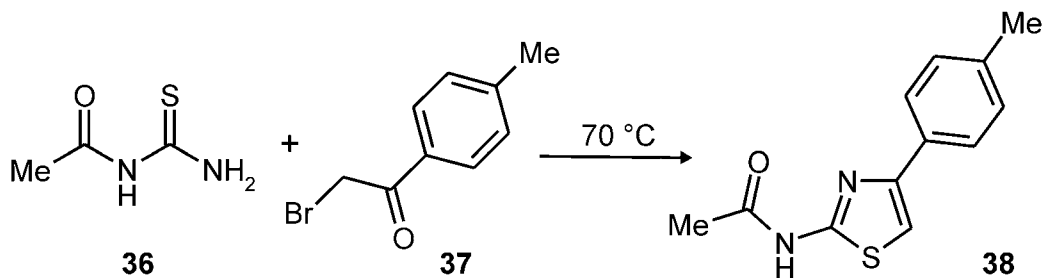
Skelton *et al.*^{154,187} have carried out the synthesis of *cis*- and *trans*-nitrostilbene esters **35** using a Wittig reaction (Scheme 2.13) in an EOF-based borosilicate microreactor (Figure 2.7). A 10% higher product yield (70%) compared to the conventional batch synthesis was obtained upon reacting 2 equivalents of aldehyde **34** with 1 equivalent of phosphonium salt **33** in methanol. Reaction of aldehyde **34** and phosphonium salt **33** in a 1:1 ratio gave lower yields (39%), which could be improved (59%) by replacing the continuous flow with a slug flow technique (plugs of phosphonium **33** salt were injected into a continuous flow of the solution of aldehyde **34**). In the microreactor a high stereochemical control was possible. The *E/Z* ratio of

olefin **35** could be varied by tuning the EOF potential and consequently varying relative reagents concentrations.



Scheme 2.13. The Wittig reaction between 2-nitrobenzyl triphenylphosphonium bromide (**33**) and 4-formyl methylbenzoate (**34**) to give olefin **35**.

Using the same type of chip (Figure 2.7) Garcia-Egido *et al.*^{188,189} carried out the synthesis of a series of 2-aminothiazoles *via* the Hantzsch reaction at 70°C under EOF control. The process was optimized by reacting 1-acetyl-2-thiourea (**36**) with 2-bromo-4'-methylacetophenone (**37**) to give 2-aminothiazol **38** as a product (Scheme 2.14).



Scheme 2.14. The Hantzsch synthesis of 2-aminothiazol **38** starting from 1-acetyl-2-thiourea (**36**) with 2-bromo-4'-methylacetophenone (**37**).

More recently, the synthesis of combinatorial pyrazole libraries using a single channel microreactor operating under pressure-driven flow (Figure 2.10a) was performed⁸¹. The pyrazoles **41** have been prepared *via* the Knorr reaction of 1,3-dicarbonyl compounds **39** with hydrazines **40** (Scheme 2.15) injecting 2.5 μ L slugs of reactants in a single channel microreactor (Figure 2.10b). On-line slug dilution was

carried out at the chip outlet, followed by UV detection. Besides being the first example of a completely automated on-chip reagents injection, syntheses, dilution, and analysis sequence, this study demonstrates the use of a single-channel microchip for the sequential synthesis of combinatorial libraries in a short time and with higher conversions as compared to the lab-scale approach.

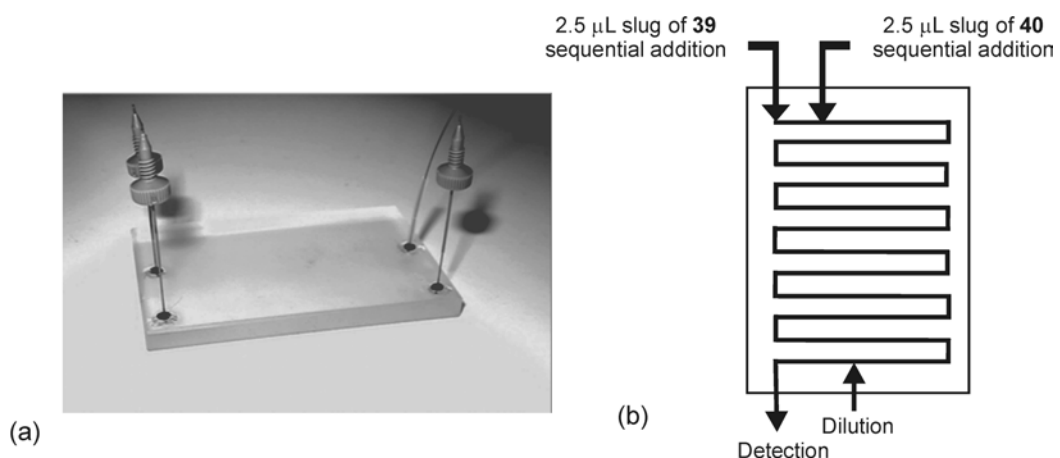
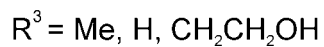
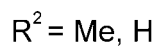
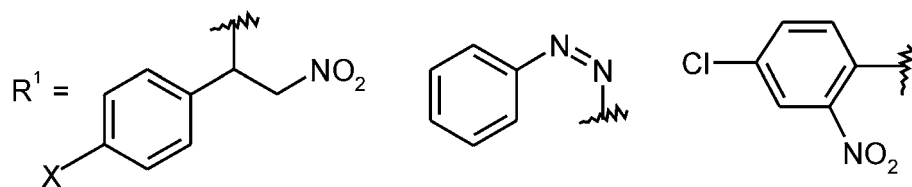
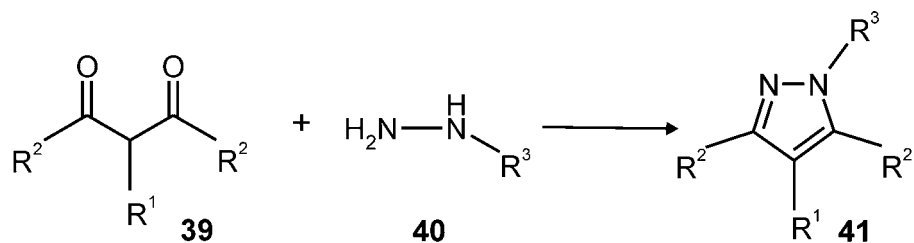
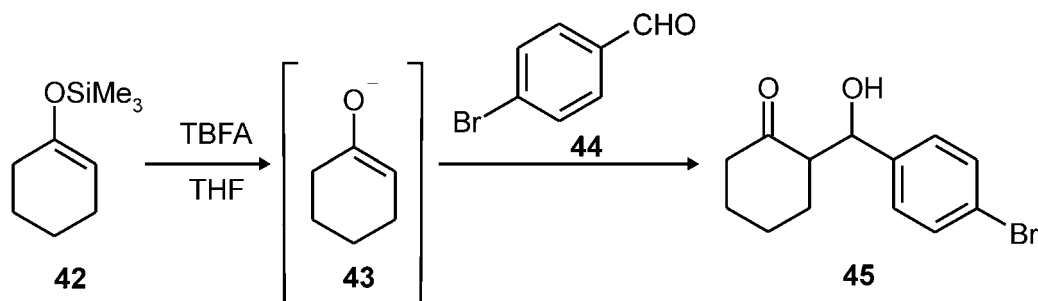


Figure 2.10. (a) Picture of the microreactor⁸¹ and (b) schematic representation of the injection system used to prepare a pyrazole library.



Scheme 2.15. Knorr's pyrazole synthesis.

Using four-channels chips (Figure 2.11) Wiles *et al.*^{190,191} described the reaction of trimethyl silyl enol ether **42** with *tetra-n*-butylammonium fluoride (TBAF) followed by an aldol condensation of the resulting phenolate **43** with 4-bromobenzaldehyde **44** to give β -hydroxyketone **45** (Scheme 2.16). Quantitative conversion of the silyl enol ether **42** to β -hydroxyketone **45** was observed within 20 min, which is a considerable enhancement of the reaction rate compared to the lab-scale procedure (100% conversion in 24 hours).



Scheme 2.16. Aldol reaction.

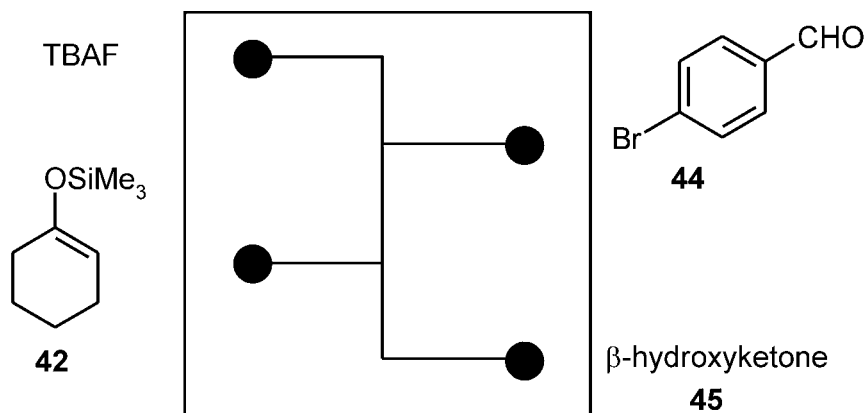
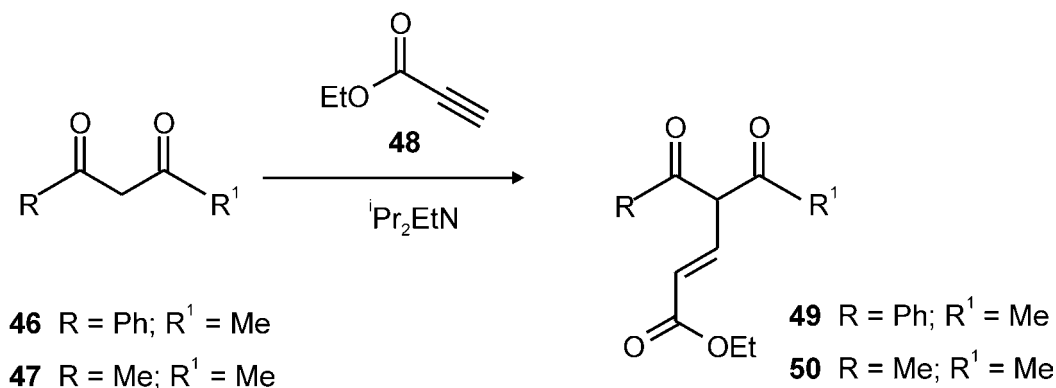


Figure 2.11. Layout of the four-channels microreactor.

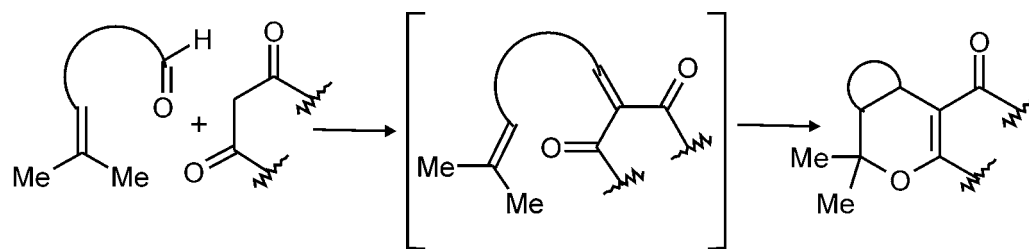
Likewise, Wiles and co-workers¹⁴⁷ reported the on-chip synthesis of Michael adducts **49** and **50** from *in-situ* formed enolates and α,β -unsaturated ester **48**. The enolates were prepared on-chip from 1,3-diketones **46** and **47**, using ethyldiisopropylamine as a base (Scheme 2.17). The authors used a stopped-flow

technique by applying discontinuous voltages (EOF pumping), which resulted in higher residence times and consequently higher product yields.



Scheme 2.17. Michael reaction.

Fernandez-Suarez *et al.*¹²⁷ used a pressure-driven glass microreactor to investigate a domino reaction consisting of a Knoevenagel condensation followed by an intramolecular hetero-Diels-Alder reaction (Scheme 2.18). Four different cycloadducts were individually prepared on-chip without any need for optimization, proving the reproducibility of the method. In a final multi-reaction experiment, a three-member array was prepared in a single run, demonstrating the combinatorial approach in a pressure-driven microchip.



Scheme 2.18. Domino reaction of a Knoevenagel condensation followed by an intramolecular hetero-Diels-Alder reaction. Ethylenediamine diacetate was used as a catalyst.

Kitamori c.s.¹⁵² recently reported the fabrication of an integrated multireactor system for 2×2 parallel organic syntheses, on a single glass microchip (Figure 2.12a.). Three glass plates were used to realize the three-dimensional channel network. It was pointed out that this methodology (Figure 2.12b) can in principle be extended to three-dimensional structures for much larger libraries.

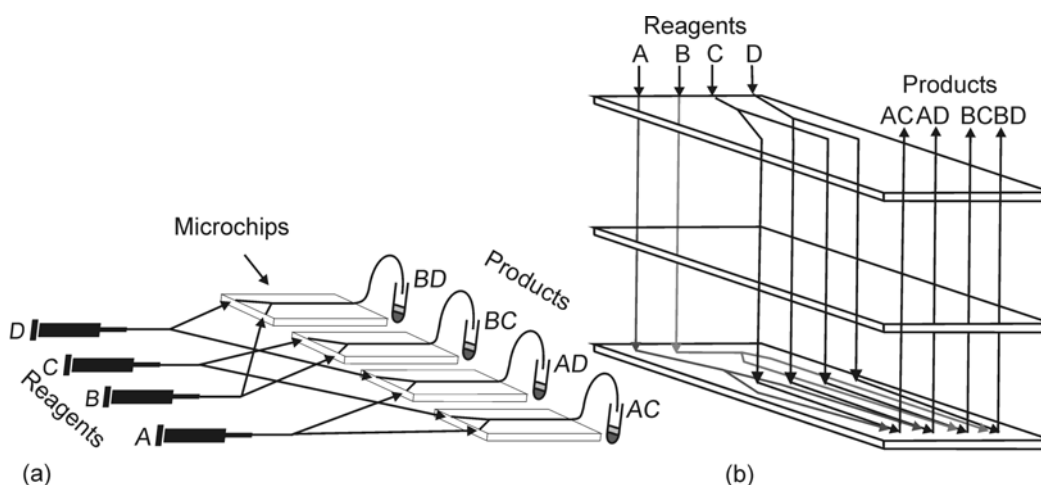
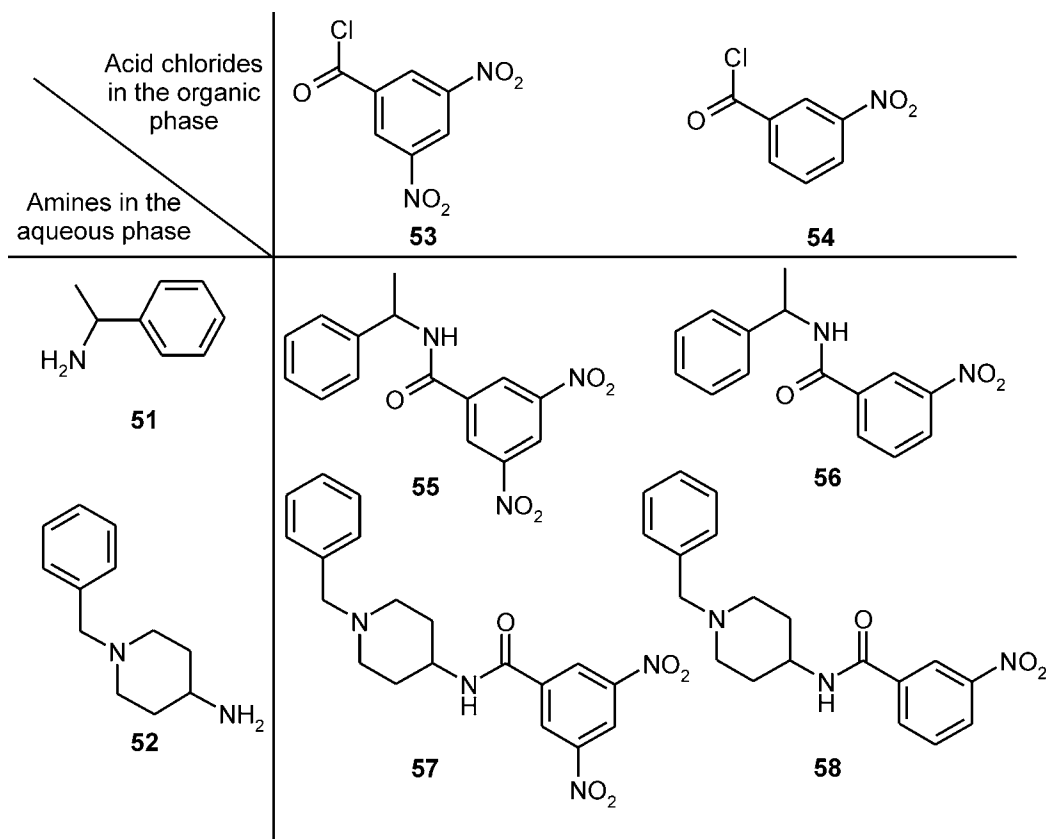


Figure 2.12. Schematic view of (a) the four-chips microreactor system used for the 2×2 combinatorial synthesis and (b) the three-dimensional microchannel circuit.¹⁵²

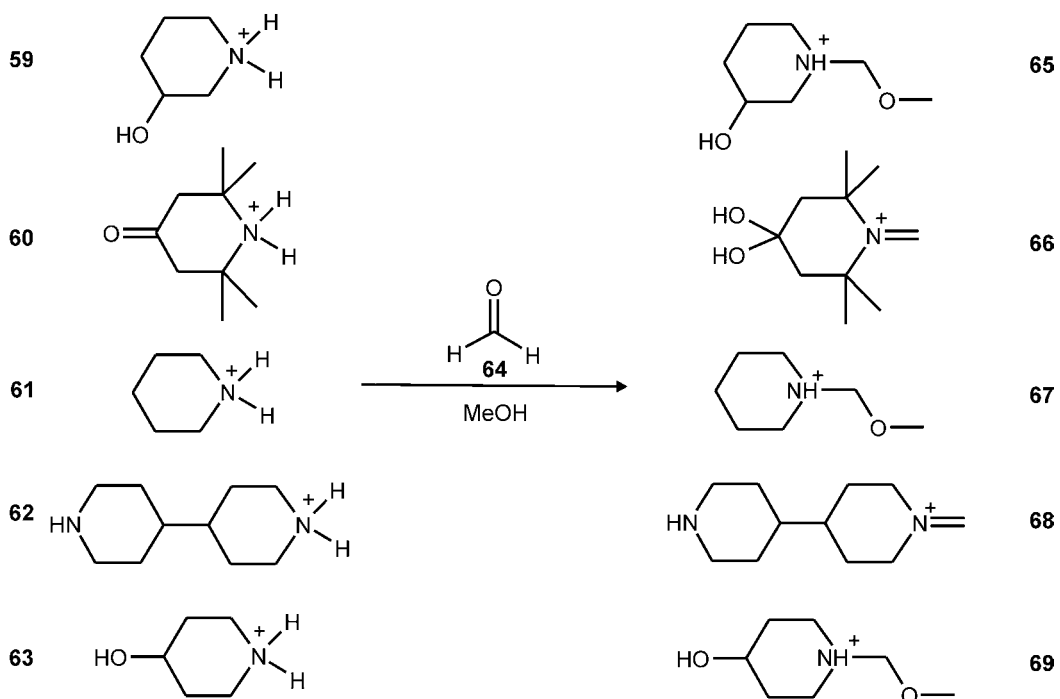
The liquid-liquid two-phase reaction between amines **51** and **52** in water and acid chlorides **53** and **54** in ethyl acetate to give amides **55-58** was used to test the novel microsystem. The 2×2 reagents system used as well as the proposed phase-transfer scheme for the amide formation are depicted in Scheme 2.19.

A problem that was encountered during the research described above is related to the distribution of equal volumes of solutions over the different microchannels. This problem is expected to become more important for combinatorial systems with larger libraries. However, the authors expect that the liquid distribution problems will be solved in the near future when system components with higher precision will become available.



Scheme 2.19. Phase-transfer 2×2 combinatorial amide formation reaction.

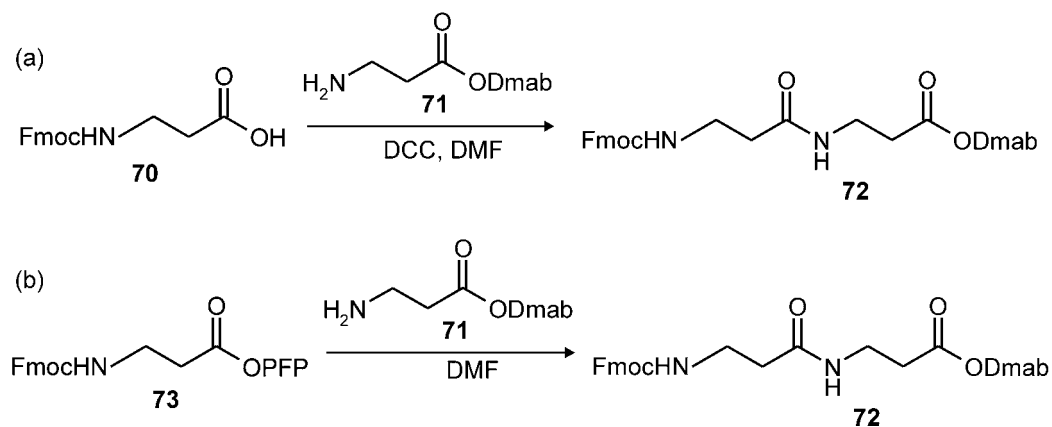
All the microreactor-based systems described in this section clearly demonstrate the potential of microfluidics devices for combinatorial applications. However, only a few⁸¹ contain an automated injection-reaction-analysis integrated system that is required for combinatorial applications. An interesting example of a chip device for combinatorial applications allowing on-line product analysis was described by Mitchell *et al.*^{83,192} The device consists of a silicon-based chemical microprocessor integrated with a time-of-flight (TOF) mass spectrometer. The integrated system (μ SYNTAS) was used for the preparation of compound libraries based on sub-reactions of an Ugi multicomponent reaction. Methanol solutions of piperidine hydrochlorides **59-63** were alternately injected into a stream of formaldehyde (**64**) in methanol to give compounds **65-69** (Scheme 2.20).



Scheme 2.20. Compound library synthesis: reaction of piperidine hydrochloride salts **59-63** with formaldehyde **64** to give products **65-69**.

Peptides are commonly prepared *via* solid support techniques. Watts *et al.*^{114,150} recently demonstrated that microreactors offer a valuable alternative to prepare peptides by multi-step synthesis in higher yield than using conventional batch methodologies. Dipeptide **72** was prepared using a carbodiimide coupling reaction of Fmoc-protected β -alanine **70** with amine **71** (Scheme 2.21a). Furthermore, they reported that by reacting on-chip the Fmoc-protected pentafluorophenylester of β -alanine **73** with amine **71** (Scheme 2.21b) dipeptide **72** could be prepared in quantitative yields in a reaction time of 20 min. The higher yield compared to that of the conventional batch process (50% in 24 h under the same conditions) has been explained by a combination of effects related to the fast mixing by diffusion in small channels and the electric field used to move solutions by EOF. The methodology was then extended to the multi-step synthesis of more complex peptides¹¹⁴ and to the investigation of racemization in the synthesis of optically active peptides starting from α -amino acids.¹¹⁵ In the latter case less racemization was found in the on-chip process compared to the batch methodology, which has been attributed to the shorter on-chip

residence time. Very recently the authors reported the first example of on-chip separation of peptides from unreacted amines using the reverse electrokinetic flow technique.¹⁵¹



Scheme 2.21. Peptide bond formation.

The results reported in these papers clearly demonstrate that microreactors are a powerful platform to perform rapid syntheses of peptides in higher yields and shorter times than conventional solid-phase batch methodologies, thereby allowing to control both peptide racemization and purification by on-chip separation.

2.4. Detection: a key issue in lab-on-a-chip

While synthetic chemistry traditionally deals with relatively large amounts of chemicals, analytical chemistry deals with tiny amounts of (often) complex samples. In these samples the compound of interest (*i.e.* which has to be detected) is sometimes only present in a very small quantity. By miniaturizing the reaction vessel the difference between organic and analytical chemistry tends to vanish. Organic reactions are in fact carried out in a micro- to picoliter volume reactor, employing lower reagent concentrations and, consequently, producing compounds in smaller amounts as compared to conventional reaction vessels.

Since the early nineties laser-induced fluorescence (LIF)¹⁹³⁻¹⁹⁵ has been the technique of choice for detection in μ -TAS devices, mainly due to its

sensitivity,^{25,196,197} simplicity, and suitability for the detection of biomolecules. However, the limited applicability of this technique to optically active species has stimulated research in other directions. A number of detection techniques for on-chip analysis have been exploited over the past decade, mainly for application in μ -TAS systems^{100-102,198} rather than synthetic applications. These include amongst others electrochemical methods,¹⁹⁹⁻²⁰³ UV-vis absorbance spectroscopy,²⁰⁴⁻²⁰⁶ refractive index measurements,^{207,208} and mass spectrometry.²⁰⁹

Most of the on-chip organic reactions that are reported in this Chapter have been monitored by off-line, off-chip detection. Reactions are conducted for a time long enough to collect a volume of product sufficiently large to be analyzed. The samples are then analyzed by HPLC,^{79,114,150,151,154,184,187} GC-MS,^{115,147,190,191} GC,^{152,155,185,210} or LC-MS.^{76,87,127,134,179,188} However, to be effectively used for screening and process development, analysis of on-chip reactions has to be done in real-time. Any delay time due to interfacing makes it more difficult to interpret the exact influence of the parameter settings on the reaction outcome. Since quenching of the reaction is not always easy and limits high-throughput screening, delay time reduction by direct on-line (either on- or off-chip) analysis is the best alternative. Only a few examples of on-line analysis of on-chip reactions have been reported, using off-chip mass spectrometry,^{81,83} on-chip UV detection,²¹¹ and, very powerful for organic chemistry, on-chip ¹H NMR detection.²¹²⁻²¹⁵

2.5. Conclusions and outlook

Lab-on-a-chip is a very young research field in which many scientists from the academic arena as well as from industry are currently active. As already occurred about fifty years ago in the field of electronics and, more recently, in the field of analytical chemistry, miniaturization is expected to revolutionize the way of doing organic chemistry. Beside the smaller space required, the lower costs of fabrication (in the ideal case of parallel fabrication) and the smaller amounts of reagents used, the use of microreactors for synthetic chemistry also has environmental implications due to the tiny amount of waste produced. The integration of a large number of microfluidics devices would also offer the advantage of creating high-speed, high-density information systems as in the field of electronics. However, it is clear that the

real benefits that synthetic chemistry will have as a result of downsizing the reaction vessels are related to the intrinsic properties of microfluidics. High surface-to-volume ratios, small volumes and laminar flow regimes imply faster and better controlled chemistry. In other words: the miniaturized reaction vessel offers a unique environment to carry out safer chemistry, faster and easier process optimization, with a high chemical diversity and a higher efficiency in terms of product yields, reaction times, and selectivity, compared to the conventional macroscale reaction vessels.

Beside investigations on the fundamental aspects of microscale chemistry, quite some effort is being devoted to the actual application of microreactors for process optimization and screening purposes. The real challenge in miniaturizing organic reactions is coupling of the microreactor to a suitable analytical instrument, which is the key requirement for realizing a breakthrough for the high-throughput potential of lab-on-a-chip.

Chapters 4 and 7 describe two lab-on-a-chip systems enabling on-line monitoring of organic reactions by means of nanoflow electrospray ionization (NESI) time-of-flight (TOF) and matrix assisted laser desorption ionization (MALDI) time-of-flight (TOF) mass spectrometry (MS), respectively. Chapters 5 and 6 demonstrate the use of a nanospray-based chip-MS interface for the study of supramolecular interactions and reaction kinetics, respectively. Chapter 3 deals with the effect of surface phenomena in glass microchannels on an acid-catalyzed esterification reaction.

2.6. References

- 1 Gravesen, P.; Branebjerg, J.; Jensen, O. S. *J. Micromech. Microeng.* **1993**, *3*, 168.
- 2 Terry, S. C. *PhD Thesis*, Stanford University, Stanford, USA, **1975**.
- 3 Terry, S. C.; Jerman, J. H.; Angell, J. B. *IEEE Trans. Electron. Devices* **1979**, *ED-26*, 1880.
- 4 Bassous, E.; Taub, H. H.; Kuhn, L. *Appl. Phys. Lett.* **1977**, *31*, 135.
- 5 Petersen, K. E. *IEEE Trans. Electron. Devices* **1979**, *ED-26*, 1918.
- 6 Wise, K. D. *Proc. IEEE* **1998**, *86*, 1531.
- 7 Van de Pol, F. C. M.; Branebjerg, J. *Proc. Micro System Technologies '90*, Berlin, **1990**, 799.
- 8 Shoji, S.; Esashi, M.; Matsuo, T. *Sens. Actuators* **1988**, *14*, 101.
- 9 Esashi, M. *Sens. Actuators A* **1990**, *21*, 161.
- 10 Van Lintel, H. T. G.; Van de Pol, F. C. M.; Bouwstra, S. *Sens. Actuators* **1988**, *15*, 153.
- 11 Esashi, M.; Shoji, S.; Nakano, A. *Sens. Actuators* **1989**, *20*, 163.
- 12 Van de Pol, F. C. M.; Van Lintel, H. T. G.; Elwenspoek, M.; Fluitman, J. H. J. *Sens. Actuators A* **1990**, *21*, 198.
- 13 Smith, J. G. *Sens. Actuators A* **1990**, *21*, 203.
- 14 Shoji, S.; Nakagawa, S.; Esashi, M. *Sens. Actuators A* **1990**, *21*, 189.
- 15 Göpel, W.; Jones, T. A.; Kleitz, M.; Lundstrom, I.; Seiyama T. *Chemical and biochemical sensors: Part I*, in: Göpel, W.; Hesse, J.; Zemel J. M. L. (eds.), *Sensors, A Comprehensive Survey 2*, Wiley-VCH: Weinheim, Germany, **1991**.
- 16 Oosterbroek, R. E., *PhD Thesis*, University of Twente, Enschede, The Netherlands, **1999**.
- 17 Lammerink, T. S. J.; Tas, N. R.; Elwenspoek, M.; Fluitman, J. H. J. *Sens. Actuators A* **1993**, *37*, 45.
- 18 Kopp, M. U.; Crabtree, H. J.; Manz, A. *Curr. Opin. Chem. Biol.* **1997**, *1*, 410.
- 19 Schult, K.; Katerkamp, A.; Trau, D.; Grawe, F.; Camman, K.; Meusel, M. *Anal. Chem.* **1999**, *71*, 5430.

- 20 Wang, J.; Rivas, G.; Cai, X.; Palecek, E.; Nielsen, P.; Shirashi, H.; Dontha, N.; Luo, D.; Parrado, C.; Chicharro, M.; Farias, P. A. M.; Valera, F. S.; Grant, D. H.; Ozsoz, M.; Flair, M. N. *Anal. Chim. Acta* **1997**, *347*, 1.
- 21 Chen, S. H.; Gallo, J. M. *Electrophoresis* **1998**, *19*, 2861.
- 22 Mallouk, T. E.; Harrison, D. J. (eds) *Interfacial design and chemical sensing*, American Chemical Society: Washinton, USA, **1994**.
- 23 Jakeway, S. C.; De Mello, A. J.; Russel, E. L. *Fresenius J. Anal. Chem.* **2000**, *366*, 525.
- 24 Manz, A.; Miyahara, Y.; Miura, J.; Watanabe, Y.; Miyagi, H.; Sato, K. *Sens. Actuators B* **1990**, *1*, 249.
- 25 Manz, A.; Graber, N.; Widmer, H. M. *Sens. Actuators B* **1990**, *1*, 244.
- 26 Manz, A.; Harrison, D. J.; Verpoorte, E.; Widmer, H. M. *Adv. Chromatogr.* **1993**, *33*, 1.
- 27 Jacobson, S. C.; Hergenroder, R.; Koutny, L. B.; Ramsey, J. M. *Anal. Chem.* **1994**, *66*, 1114.
- 28 Manz, A.; Harrison, D. J.; Verpoorte, E.; Fettinger, J. C.; Ludi, H.; Widmer, H. M. *Chimia* **1991**, *45*, 103.
- 29 Harrison, D. J.; Fluri, K.; Seiler, K.; Fan, Z. H.; Effenhauser, C. S.; Manz, A. *Science* **1993**, *261*, 895.
- 30 Manz, A.; Effenhauser, C. S.; Burggraf, N.; Verpoorte, E.; Raymond, D. E.; Widmer, H. M. *Anal. Mag.* **1994**, *22*, M25.
- 31 Widmer, H. M. in: Widmer, H. M.; Verpoorte, E. (eds) *Proc. μ TAS96–Special Issue of Analytical Methods and Instrumentation AMI*, Kluwer Academic Publishers: Dordrecht, The Netherlands **1996**, 3.
- 32 Van den Berg, A.; Bergveld, P. in: Widmer, H. M.; Verpoorte, E. (eds) *Proc. μ TAS96–Special Issue of Analytical Methods and Instrumentation AMI*, Kluwer Academic Publishers: Dordrecht, The Netherlands, **1996**, 9.
- 33 Ramsey, J. M. in: Widmer, H. M.; Verpoorte, E. (eds) *Proc. μ TAS96–Special Issue of Analytical Methods and Instrumentation AMI*, Kluwer Academic Publishers: Dordrecht, The Netherlands, **1996**, 24.
- 34 Northrup, M. A.; Benett, B.; Hadley, D.; Stratton, P.; Landre, P. in: Ehrfeld, W. (ed) *Proc. IMRETI*, Springer-Verlag: Berlin, Germany, **1997**, 278.

- 35 Van de Schoot, B. H.; Verpoorte, E. M. J.; Jeanneret, S.; Manz, A.; De Rooij, N. R. *Proc. μ TAS'94*, Kluwer Academic Publishers: Dordrecht, The Netherlands, **1994**, 181.
- 36 Effenhauser, C. S.; Bruin, G. J. M.; Paulus, A. *Electrophoresis*, **1997**, *18*, 2203.
- 37 Eijkel, J. C. T.; De Mello, A. J.; Manz, A. in: Masuhara, H.; Schryver, F. C. D. (eds) *Organic Mesoscopic Chemistry*, Blackwall Science, UK, **1999**, 185.
- 38 De Mello, A. J.; Manz, A. in: Meier, T.; Saluz, H. P. (eds) *Microsystem Technology: A Powerful Tool for Biomolecular Studies*, Birkhauser, Boston, USA, **1998**, 29.
- 39 Colyer, C. R.; Tang, T.; Chiem, N.; Harrison, D. J. *Electrophoresis* **1997**, *18*, 1733.
- 40 Service, R. F. *Science* **1998**, *282*, 399.
- 41 Woolley, A. T.; Mathies, R. A. *Anal. Chem.* **1995**, *67*, 3676.
- 42 Woolley, A. T.; Sensabaugh, G. F.; Mathies, R. A. *Anal. Chem.* **1997**, *69*, 2181.
- 43 Jacobson, S. C.; Ramsey, J. M. *Anal. Chem.* **1996**, *68*, 720.
- 44 Woolley, A. T.; Hadley, D.; Landre, P.; De Mello, A. J.; Mathies, R. A.; Northrup, M. A. *Anal. Chem.* **1996**, *68*, 4081.
- 45 Schmalzing, D.; Adourian, A.; Koutny, L.; Ziagura, L.; Matsudaria, P.; Ehrlich, D. *Anal. Chem.* **1998**, *70*, 2303.
- 46 Effenhauser, C. S.; Paulus, A.; Manz, A.; Widmer, H. M. *Anal. Chem.* **1994**, *66*, 2949.
- 47 Kamholz, A. *Lab Chip* **2004**, *4*, 16N.
- 48 Chovan, T.; Guttman, A. *Trends Biotechnolog.* **2002**, *20*, 116.
- 49 Beebe, D. J.; Mensing, G. A.; Walker, G. M. *Annu. Rev. Biomed. Eng.* **2002**, *4*, 261.
- 50 Verpoorte, E. *Electrophoresis* **2002**, *23*, 677.
- 51 Huang, Y.; Mather, E. L.; Bell, J. L.; Maddou, M. *Anal. Bioanal. Chem.* **2002**, *372*, 49.
- 52 Vo-Dinh, T.; Cullum, B. *Fresenius J. Anal. Chem.* **2000**, *366*, 540.
- 53 Tüdos, A. J.; Besselink, G. A. J.; Schasfoort, R. B. M. *Lab Chip* **2001**, *1*, 83.
- 54 <http://www.mcg.edu/Core/Labs/mbgcf/images/Peptide-Synthesis.jpg>
- 55 http://www.mhhe.com/biosci/esp/2001_saladin/folder_structure/le/m4/s3/asses/
- 56 Ehrfeld, W. (ed) *DECHEMA-Monographs*: Frankfurt, Germany, **1995**, 132.

- 57 Jähnisch, K.; Hessel, V.; Löwe, H.; Baerns, M. *Angew. Chem. Int. Ed.* **2004**, *43*, 406.
- 58 Schwalbe, T.; Autze, V.; Wolle, G. *Chimia* **2002**, *56*, 636.
- 59 Erickson, D.; Li, D. *Anal. Chim. Acta*, **2004**, *507*, 11.
- 60 Fan, Z. H.; Harrison, D. J. *Anal. Chem.* **1994**, *66*, 177.
- 61 Manz, A.; Verpoorte, E. J. M.; Effenhauser, C. S.; Burggraf, N.; Raymond, D. E.; Widmer, H. M. *Fresenius J. Anal. Chem.* **1994**, *348*, 567.
- 62 Harrison, D. J.; Fluri, K.; Chiem, N.; Tang, T.; Fang, Z. *Sens. Actuators B* **1996**, *3*, 105.
- 63 Wang, H. Y.; Foote, R. S.; Jacobson, F. C.; Schneibel, J. H.; Ramsey, J. M. *Sens. Actuators B* **1997**, *45*, 199.
- 64 Harrison, D. J.; Glavina, P. G.; Manz, A. *Sens. Actuators B* **1993**, *10*, 107.
- 65 Duffy, D. C.; McDonald, C. J.; Schueller, O. J. A.; Whitesides, G. M. *Anal. Chem.* **1998**, *70*, 4974.
- 66 Roberts, M. A.; Rossier, J. S.; Bercier, P.; Girault, H. *Anal. Chem.* **1997**, *69*, 2035.
- 67 Locascio, L. E. *Anal. Chem.* **1997**, *69*, 4783.
- 68 Ehrfeld, W.; Lehr, H. *Radiat. Phys. Chem.* **1995**, *45*, 349.
- 69 Anderson, J. R.; Chiu, D. T.; Jackman, R. J.; Cherniavskaya, O.; McDonald, J. C.; Wu, H.; Whitesides, S. J.; Whitesides, G. M. *Anal. Chem.* **2000**, *72*, 3158.
- 70 McDonald, J. C.; Chabinyk, M. L.; Metallo, S. J.; Anderson, J. R.; Stroock, A. D.; Whitesides, G. M. *Anal. Chem.* **2002**, *74*, 1537.
- 71 For introductory reviews on chemistry in microreactors: a) Fletcher, P. D. I.; Haswell, S. J. *Chem. Br.* **1999**, *1*, 17. b) McCreedy, T. *Chem. Ind.* **1999**, 588. c) Cowen, S. *Chem. Ind.* **1999**, 584. d) Haswell, S. J.; Middleton, R. J.; O'Sullivan, B.; Skelton, V.; Watts, P.; Styring, P. *Chem. Commun.* **2001**, 391. e) Jensen, K. F. *AIChE J.* **1999**, *45*, 2051. f) Barrow, D.; Cefai, J.; Taylor, S. *Chem. Ind.* **1999**, 591.
- 72 Ehrfeld, W.; Hessel, V.; Löwe, H. *Microreactors: New Technology for Modern Chemistry*, Wiley-VCH: Weinheim, Germany, **2000**.
- 73 For a review on fabrication techniques and materials used for the production of microreactors see: McCreedy, T. *TrAC* **2000**, *19*, 396.

- 74 Mikami, K.; Yamanaka, M.; Islam, Md. M.; Kudo, K.; Seino, N.; Shinoda, M. *Tetrahedron Lett.* **2003**, *44*, 7545.
- 75 Doku, G. N.; Haswell, S. J.; McCreedy, T.; Greenway, G. M. *Analyst* **2001**, *126*, 14.
- 76 Wiles, C.; Watts, P.; Haswell, S. J.; Pombo-Villar, E. *Org. Proc. Res. Dev.* **2004**, *8*, 28.
- 77 Sands, M.; Haswell, S. J.; Kelly, S. M.; Skelton, V.; Morgano, D. O.; Styring, P.; Warrington, B. H. *Lab Chip* **2001**, *1*, 64.
- 78 Wootton, R. C. R.; De Mello, A. J. *Lab Chip* **2002**, *2*, 5.
- 79 Hisamoto, H.; Saito, T.; Tokeshi, M.; Hibara, A.; Kitamori, T. *Chem. Commun.* **2001**, 2662.
- 80 Wootton, R. C. R.; Fortt, R.; De Mello, A. J. *Org. Proc. Res. Dev.* **2002**, *6*, 187.
- 81 Garcia-Egido, E.; Spikmans, V.; Wong, S. Y. F.; Warrington, B. H. *Lab Chip* **2003**, *3*, 73.
- 82 Salimi-Moosavi, H.; Tang, T.; Harrison, D. J. *J. Am. Chem. Soc.* **1997**, *119*, 8716.
- 83 Mitchell, M. C.; Spikmans, V.; Manz, A.; De Mello, A. J. *J. Chem. Soc., Perkin Trans.* **2001**, 514.
- 84 Fletcher, P. D. I.; Haswell, S. J.; Vesselin, N. P. *Analyst* **1999**, *124*, 1273.
- 85 Fletcher, P. D. I.; Haswell, S. J.; Pombo-Villar, E.; Warrington, B. H.; Watts, P.; Wong, S. Z. F.; Yhang, X. *Tetrahedron* **2002**, *58*, 4735.
- 86 Haswell, S. J.; O'Sullivan, B.; Styting, P. *Lab Chip* **2001**, *1*, 126.
- 87 Ueno, K.; Kitagawa, F.; Kitamura, N. *Lab Chip* **2002**, *2*, 231.
- 88 Wilson, N. G.; McCreedy, T. *Chem. Commun.* **2000**, 733.
- 89 McCreedy, T.; Wilson, N. G. *Analyst* **2001**, *128*, 21.
- 90 Yamamoto, T.; Nojima, T.; Fujii, T. *Lab Chip* **2002**, *2*, 197.
- 91 Losey, M. W.; Schmidt, M. A.; Jensen, K. F. *Ind. Eng. Chem. Res.* **2001**, *40*, 2555.
- 92 Lu, H.; Schmidt, M. A.; Jensen, K. F. *Lab Chip* **2001**, *1*, 22.
- 93 Chambers, R. D.; Spink, R. C. H. *Chem. Commun.* **1999**, 883.
- 94 Chambers, R. D.; Holling, D.; Spink, R. C. H.; Standford, G. *Lab Chip* **2001**, *1*, 132.

- 95 Dietzsch, E.; Hönicke, D.; Fichter, M.; Schubert, K. in: Matlos, M.; Ehrfeld, W.; Baselt, J. P. (eds) *Proc. IMRET4*, Springer-Verlag: Berlin, Germany, **2000**, 89.
- 96 Maddou M. J. *Fundamentals of Microfabrication: The Science of Miniaturization*, 2nd ed.; CRC Press: Boca Raton, USA, **2002**.
- 97 Geschke, O.; Klank, H.; Telleman, P. *Microsystem Engineering of Lab-on-a-Chip Devices* 2nd ed.; John Wiley & Sons: New York, USA, **2004**.
- 98 Polson, N. A.; Hayes, M. A. *Anal. Chem.* **2001**, *73*, 312A.
- 99 Greenwood, P. A.; Greenway, G. A. *Trends Anal. Chem.* **2002**, *21*, 726.
- 100 Reyes, D. R.; Iossifidis, D.; Auroux, P.-A.; Manz, A. *Anal. Chem.* **2002**, *74*, 2623.
- 101 Auroux, P.-A.; Iossifidis, D.; Reyes, D. R.; Manz, A. *Anal. Chem.* **2002**, *74*, 2637.
- 102 Vilkner, T.; Janasek, D.; Manz, A. *Anal. Chem.* **2004**, *76*, 3373.
- 103 Oosterbroek, R. E.; Van den Berg, A. *Lab-on-a-Chip: Miniaturized Systems for Bio(chemical) Analysis and Synthesis*, Elsevier Science: Amsterdam, The Netherlands, **2003**.
- 104 For reviews on chip-based separations see: a) Jacobson, S. C.; Ramsey, J. M. in: Landers, J. P. (ed) *Handbook of Capillary Electrophoresis*, CRC Press: Boca Raton, USA, **1997**, 827. b) Fintschenko, Y.; Van den Berg, A. *J. Chromatogr. A* **1998**, *819*, 3. c) Bullard, K. M.; Hietpas, P. B.; Ewing, A. G. *Biomed. Micro-Devices* **1998**, *1*, 27. d) Effenhauser, C. S. in: Manz, A.; Beker, H. (eds) *Topics in Current Chemistry: Microsystem Technology in Chemistry and Life Science*, Springer Verlag: Berlin, Germany, **1998**, *194*, 51. e) Regnier, F. E.; He, B.; Lin, S.; Busse, J. *Trends Biotechnol.* **1999**, *17*, 101. f) Dolnik, V.; Liu, S.; Jovanovich, S. *Electrophoresis* **2000**, *21*, 41. g) Lacher, N. A.; Garrison, K. E.; Martin, R. S.; Lunte, S. M. *Electrophoresis* **2001**, *22*, 2526.
- 105 Fletcher, P. D. I.; Haswell, S. J.; Paunov, V. N. *Analyst* **1999**, *124*, 1273.
- 106 Thorsen, T.; Maerkl, S. J.; Quake, S. R. *Science*, **2002**, *298*, 580.
- 107 Seiler, K.; Fan, Z.; Fluri, K.; Harrison, D. J. *Anal. Chem.* **1994**, *66*, 3485.
- 108 Fluri, K.; Chiem, N.; Fitzpatrick, G.; Harrison, D. J. *Anal. Chem.* **1996**, *68*, 4285.
- 109 Raymond, D. E.; Manz, A.; Widmer, H. M. *Anal. Chem.* **1996**, *68*, 2515.

- 110 Von Heeren, F.; Verpoorte, E.; Manz, A.; Thormann, W. *Anal. Chem.* **1996**, *68*, 2044.
- 111 http://www.csem.ch/detailed/a_621-microfluidics-liquid.
- 112 Grossman, P. D.; Colburn, J. C. (eds) *Capillary Electrophoresis: Theory and Practice*, Academic Press: San Diego, U.S.A., **1992**, 4.
- 113 Oosterbroek, R. E.; Goedbloed, M.; Van den Berg, A. *Proc. (MSM'02) / Nanotech '02*, San Juan, Puerto Rico, **2002**, 72.
- 114 Watts, P.; Wiles, C.; Haswell, S. J.; Pombo-Villar, E. *Tetrahedron.* **2002**, *58*, 5427.
- 115 Watts, P.; Wiles, C.; Haswell, S. J.; Pombo-Villar, E. *Lab Chip* **2002**, *2*, 141.
- 116 Bello, M. S. *J. Chromatogr. A* **1996**, *744*, 81.
- 117 Corstjen, H.; Billiet, H. A.; Frank, J.; Luyben, K. C. A. M. *Electrophoresis* **1996**, *17*, 137.
- 118 Guijt, R. M.; Lichtenberg, J.; Baltussen, E.; Verpoorte, E.; De Rooij, N.; Van Dedem, G. W. K. In: Ramsey, J. M.; Van den Berg, A. (eds) *Proc. μ TAS '01*, Kluwer Academic Publishers: Dordrecht, The Netherlands **2001**, 399.
- 119 Oki, A.; Takamura, Y.; Yoshitaka, I.; Horiike, Y. *Electrophoresis* **2002**, *23*, 2860.
- 120 Taylor, G. *Proc. R. Soc. (London)* **1953**, *A219*, 186.
- 121 Kopf-Sill, A. *Lab Chip* **2002**, *2*, 42N.
- 122 Miyazaki, S.-I.; Kawai, T.; Araragi, M. *IEEE* **1991**, *9*, 283.
- 123 Duffy, D. C.; Gillis, H. L.; Lin, J.; Sheppard, N. F.; Kellog, G. J. *Anal. Chem.* **1999**, *71*, 4669.
- 124 Unger, M. A.; Chou, H.-P.; Thorsen, T.; Scherer, A.; Quake, S. R. *Science* **2000**, *288*, 113.
- 125 Hosokava, K.; Fujii, T.; Endo, I. *Anal. Chem.* **1999**, *71*, 4781.
- 126 Fan, H.; Shakuntala, M.; Granzow, R.; Heaney, P.; Ho, W.; Dong, Q.; Kumar, R. *Anal. Chem.* **1999**, *71*, 4851.
- 127 Fernandez-Suarez, M.; Wong, S. Y. F.; Warrington, B. H. *Lab Chip* **2002**, *2*, 170.
- 128 Kien, R. L.; Parce, J. W. *Fresenius J. Anal. Chem.* **2001**, *371*, 106.
- 129 Shoji, S.; Esashi, M. *J. Micromech. Microeng.* **1994**, *4*, 157.
- 130 Dasgupta, P. K.; Liu, S. *Anal. Chem.* **1994**, *66*, 1792.

- 131 Zengerle, R.; Ulrich, J.; Kluge, S.; Richter, M.; Richter, A. *Sens. Actuators A* **1995**, *50*, 81.
- 132 Wiles, C.; Watts, P.; Haswell, S. J.; Pombo-Villar, E. *Lab Chip* **2004**, *4*, 171.
- 133 Tokeshi, M.; Minagawa, T.; Kitamori, T. *Anal. Chem.* **2002**, *72*, 1711.
- 134 Haswell, S. J.; O'Sullivan, B.; Styring, P. *Lab Chip* **2001**, *1*, 164.
- 135 McBride, S. E.; Moroney, R. M.; Chiang, W. in: Harrison, D. J.; Van den Berg A. (eds) *Proc. μ -TAS '98*, Kluwer Academic Publishers: Dordrecht, The Netherlands, **1998**, 45.
- 136 Gallardo, B. S.; Gupta, V. K.; Eagerton, F. D.; Jong, L. I.; Craig, V. S.; Shah, R. R.; Abbott, N. L. *Science* **1999**, *283*, 57.
- 137 Gau, H.; Herminghaus, S.; Lenz, P.; Lipkowsky, R. *Science* **1999**, *283*, 46.
- 138 Zhao, B.; Viernes, N. O. L.; Moore, J. S.; Beebe, D. J. *J. Am. Chem. Soc.* **2002**, *124*, 5284.
- 139 Bain, C. D. *ChemPhysChem* **2001**, *2*, 580.
- 140 Marmottant, P.; Hilgenfeldt, S. *Nature* **2003**, *423*, 153.
- 141 Herweck, T.; Hardt, S.; Hessel, V.; Löwe, H.; Hofmann, C.; Weise, F.; Dietrich, T.; Freitag, A. *Proc. IMRET 5*, Springer: Berlin, Germany, **2002**, 215.
- 142 Jähnisch, K.; Baerns, M.; Hessel, V.; Ehrfeld, W.; Haverkamp, W.; Löwe, H.; Wile, C.; Guber, A. *J. Fluorine Chem.* **2000**, *105*, 117.
- 143 Antes, J.; Tuercke, T.; Marioth, E.; Lechner, F.; Scholz, M.; Schnürer, F.; Krause, H. H.; Löbbecke, S. in: Matlosz, M.; Ehrfeld, W.; Baselt, J. P. (eds) *Proc. IMRET 5*, Springer: Berlin, Germany, **2002**, 446.
- 144 Burns, J. R.; Ramshaw, C. *Proc. IMRET 4*, AIChE Conference Topical Proceedings: Atlanta, USA, **2000**, 133.
- 145 Surangaliker, H.; Besser, R. S. *Proc. IMRET 6*, AIChE Conference Topical Proceedings: Atlanta USA, **2002**, 285.
- 146 Skelton, V.; Greenway, G. M.; Haswell, S. J.; Styring, P.; Morgan, D. O.; Warrington, B. H.; Wong, S. *Proc. IMRET 4*, AIChE Conference Topical Proceedings: Atlanta, USA, **2000**, 78.
- 147 Wiles, C.; Watts, P.; Haswell, S. J.; Pombo-Villar, E. *Lab Chip* **2002**, *2*, 62.
- 148 Kestenbaum, H.; Lange de Olivera, A.; Schmidt, W.; Schüth, H.; Ehrfeld, W.; Gebauer, K.; Löwe, H.; Richter, T. *Stud. Surf. Sci. Catal.* **2000**, *130*, 2741.

- 149 Bayer, T.; Pysall, D.; Wachsen, O. in: Ehrfeld, W. (ed) *Proc. IMRET 3*, Springer: Berlin, Germany, **2000**, 165.
- 150 Watts, P.; Wiles, C.; Haswell, S. J.; Pombo-Villar, E.; Styring, P. *Chem. Commun.* **2001**, 990.
- 151 Gorge, V.; Watts, P.; Haswell, S. J.; Pombo-Villar, E. *Chem. Commun.* **2003**, 2886.
- 152 Kikutani, Y.; Horiuchi, T.; Uchiyama, K.; Hisamoto, H.; Tokeshi, M.; Kitamori, T. *Lab Chip* **2002**, 2, 188.
- 153 For a recent review on the use of microreactors for combinatorial chemistry see: Watts, P.; Haswell, S. J. *Curr. Opin. Chem. Biol.* **2003**, 7, 380.
- 154 Skelton, V.; Greenway, G. M.; Haswell, S. J.; Styring, P.; Morgan, D. O.; Warrington, B.; Wong, S. Y. F. *Analyst* **2001**, 126, 11.
- 155 Kikutani, Y.; Hibara, A.; Uchiyama, K.; Hisamoto, H.; Tokeshi, M.; Kitamori, T. *Lab Chip* **2002**, 2, 193.
- 156 De Mas, N. *Proc. IMRET 6*, AIChE Conference Proceedings: Atlanta, USA, **2002**, 184.
- 157 De Mas, N.; Jackman, R. J.; Schmidt, M. A.; Jenson, K. F. in: Matlosz, M.; Ehrfeld, W.; Baselt, J. P. (eds) *Proc. IMRET 5*, Springer: Berlin, Germany, **2002**, 60.
- 158 Wießmeir, G.; Hönicke, D. *J. Micromech. Microeng.* **1996**, 6, 285.
- 159 Vesper, G. *Chem. Eng. Sci.* **2001**, 56, 1265.
- 160 Kestenbaum, H.; Lange de Olivera, A.; Schmidt, W.; Schüth, H.; Ehrfeld, W.; Gebauer, K.; Löwe, H.; Richter, T. *Ind. Eng. Chem. Res.* **2000**, 41, 710.
- 161 Chohey, N. P.; Ondrey, G.; Parkinson, G. *Chem. Engin.* **1997**, 104, 30.
- 162 Wießmeir, G.; Hönicke, D. *Ind. Eng. Chem. Res.* **1996**, 35, 4412.
- 163 Rouge, A.; Spoetzl, B.; Gebauer, K.; Schenk, R.; Renken, A. *Chem. Eng. Sci.* **2001**, 56, 1419.
- 164 Steinfeldt, N.; Buyevskaya, O. V.; Wolf, D.; Baerns, M. *Stud. Surf. Sci. Catal.* **2001**, 136, 185.
- 165 Srinivasan, R.; Hsing, I.-M.; Berger, P. E.; Jensen, K. F.; Firebaugh, S. L.; Schmidt, M. A.; Harold, M. P.; Lerou, J. J.; Ryley, J. F. *AIChE J.* **1997**, 43, 3059.

- 166 Rebrov, E. V.; De Croon, M. H. J. M.; Schouten, J. C. *Catal. Today* **2001**, *69*, 183.
- 167 Wörz, O.; Jäkel, P.; Richter, T.; Wolf, A. *Chem. Eng. Technol.* **2001**, *24*, 138.
- 168 Fichtner, M.; Mayer, J.; Wolf, D.; Schubert, K. *Ind. Eng. Chem. Res.* **2001**, *40*, 3475.
- 169 Jensen, K. F. *Chem. Eng. Sci.* **2001**, *56*, 293.
- 170 Schubert, K.; Brandner, J.; Fichtner, M.; Linder, G.; Shygulla, U.; Wenka, A. *Microscale Thermophys. Eng.* **2001**, *5*, 17.
- 171 Schubert, K.; Bier, W.; Brandner, J.; Fichtner, M.; Franz, C.; Linder, G. *Proc. IMRET 2*, AIChE Conference Proceedings: New Orleans, USA, **1998**, 88.
- 172 Alépée, C.; Vulpescu, L.; Cousseau, P.; Renaud, P.; Maurer, R.; Renken, A. *Proc. IMRET 4*, AIChE Topical Conference Proceedings: Atlanta, USA, **2000**, 71.
- 173 For more details see: a) Wörz, O.; Jäkel, P.; Richter, T.; Wolf, A. *Proc. IMRET 2*, AIChE Conference Proceedings: New Orleans, USA, **1998**, 183. b) Wörz, O.; Jäkel, P.; Richter, T.; Wolf, A., *IBC Global Conferences Ltd.*, London, UK, **1998**.
- 174 Hessel, V.; Ehrfeld, W.; Golbig, K.; Hofman, C.; Jungwirth, S.; Löwe, H.; Richter, T.; Storz, M.; Wolf, A. *Proc. IMRET 3*, Springer: Berlin, Germany, **2000**, 151.
- 175 Knight, J. B.; Vishwanath, A.; Brody, J. P.; Austin, R. H. *Phys. Rev. Lett.* **1998**, *80*, 386.
- 176 Löwe, H.; Ehrfeld, W.; Hessel, V.; Richter, T.; Schiewe, J.: *Proc. IMRET 4*, AIChE Conference Topical Proceedings: Atlanta, USA, **2000**, 31.
- 177 Floyd, T. M.; Losey, M. W.; Firebaugh, S. L.; Jensen, K. F.; Schmidt, M. A. *Proc. IMRET 3*, Springer: Berlin, Germany, **2000**, 171.
- 178 Kobayashi, J.; Mori, Y.; Okamoto, K.; Akiyama, R.; Ueno, M.; Kitamori, T.; Kobayashi, S. *Science* **2004**, *304*, 1305.
- 179 Greenway, G. M.; Haswell, S. J.; Morgan, D. O.; Skelton, V.; Styring, P. *Sens. Actuators B* **2000**, *63*, 153.
- 180 Munson, M. S.; Yager, P. *Anal. Chim. Acta* **2004**, *507*, 63.
- 181 For a review on Reynolds numbers in microfluidics devices see: Gravensen, P.; Branebjerg, J.; Jensen, O. S. *J. Micromech. Microeng.* **1993**, *3*, 168.

- 182 Jensen, K. *Nature* **1998**, *393*, 735.
- 183 Knight, J. B.; Vishwanath, A.; Brody, J. P.; Austin, R. H. *Phys. Rev. Lett.* **1998**, *80*, 3863.
- 184 Ueno, M.; Hisamoto, H.; Kitamori, T.; Kobayashi, S. *Chem. Commun.* **2003**, 936.
- 185 Mikami, K.; Yamanaka, M.; Islam, Md. N.; Kudo, K.; Seino, N.; Shinoda, M. *Tetrahedron Lett.* **2003**, *44*, 7545.
- 186 Ehrfeld, W.; Golbig, K.; Hessel, V.; Löwe, H.; Richter, T. *Ind. Eng. Chem. Res.* **1999**, *38*, 1075.
- 187 Skelton, V.; Greenway, G. M.; Haswell, S. J.; Styring, P.; Morgan, D. O.; Warrington, B.; Wong, S. Y. F. *Analyst* **2001**, *126*, 7.
- 188 Garcia-Egido, E.; Wong, S. Y. F.; Warrington, B. H. *Lab Chip* **2002**, *2*, 31.
- 189 Garcia-Egido, E.; Wong, S. Y. F. in: Ramsey, J. M.; Van den Berg, A. (eds) *Micro Total Analysis Systems*, Kluwer Academic Publishers, Dordrecht, **2001**, 517.
- 190 Wiles, C.; Watts, P.; Haswell, S. J.; Pombo-Villar, E. *Lab Chip* **2001**, *1*, 100.
- 191 Wiles, C.; Watts, P.; Haswell, S. J.; Pombo-Villar, E. *Chem. Commun.* **2002**, 1034.
- 192 Mitchell, M. C.; Spikmans, V.; De Mello, A. J. *Analyst* **2001**, *126*, 24.
- 193 Ocvirk, G.; Tang, T.; Harrison, D. J. *Analyst* **1998**, *123*, 1429.
- 194 Jiang, G.; Attiya, S.; Ocvirk, G.; Lee, W. E.; Harrison, D. J. *Biosens. Bioelectron.* **2000**, *14*, 861.
- 195 Chabinye, M. L.; Chiu, D. T.; McDonald, J. C.; Abraham, D. S.; Christian, J. F.; Karger, A. M.; Whitesides, G. M. *Anal. Chem.* **2001**, *73*, 4491.
- 196 Fister, J. C.; Jacobson, S. C.; Davis, L. M.; Ramsey, J. M. *Anal. Chem.* **1998**, *70*, 431.
- 197 Haab, B. B.; Mathies, R. A. *Anal. Chem.* **1999**, *71*, 5137.
- 198 For a review on detection methods for lab-on-a-chip see: a) Schwarz, M.; Hauser, P. *Lab Chip* **2001**, *1*, 1. b) Jakeway, S. C.; De Mello, A. J.; Russel, E. *Fresenius J. Anal. Chem.* **2000**, *366*, 525.
- 199 Rossier, J. S.; Roberts, M. A.; Ferrigno, R.; Girault, H. H. *Anal. Chem.* **1999**, *71*, 4294.
- 200 Martin, R. S.; Gawron, A. J.; Lunte, S. M. *Anal. Chem.* **2000**, *72*, 3196.

- 201 Wang, J.; Chen, G.; Muck, A. *Anal. Chem.* **2003**, *75*, 4475.
- 202 Klett, O.; Nyholm, L. *Anal. Chem.* **2003**, *75*, 1245.
- 203 Garcia, C. D.; Henry, C. S. *Anal. Chem.* **2003**, *75*, 4778.
- 204 Verpoorte, E.; Manz, A.; Lüdi, H.; Bruno, A. E.; Maystre, F.; Krattiger, B.; Widmer, H. M.; Van der Schoot, B. H.; De Rooij, N. F. *Sens. Actuators B* **1992**, *6*, 66.
- 205 Liang, Z.; Chiem, N. H.; Ocvirk, G.; Tang, T.; Fluri, K.; Harrison, D. J. *Anal. Chem.* **1996**, *68*, 1040.
- 206 Salimi-Mosavi, H.; Jiang, Y.; Lester, L.; McKinnon, G.; Harrison, D. J. *Electrophoresis* **2000**, *21*, 1291.
- 207 Swinney, K.; Markov, D.; Bornhop, D. J. *Anal. Chem.* **2000**, *72*, 2690.
- 208 Burggraf, N.; Krattiger, B.; De Mello, A. J.; De Rooij, N. F.; Manz, A. *Analyst* **1998**, *123*, 1443.
- 209 For a review on chip-MS coupling see: De Mello, A. J. *Lab Chip* **2001**, *1*, 7N.
- 210 Wilson, N. G.; McCreedy, T. *Chem. Commun.* **2000**, 733.
- 211 Lu, H.; Schmidt, A.; Jensen, K. F. *Lab Chip* **2001**, *1*, 22.
- 212 Massin, C.; Boero, G.; Eichenberger, P. A.; Besse, P.; Popovic, R. S. *Proc. Transducers '01*, Munich, Germany, **2001**, 784.
- 213 Massin, C.; Vincent, F.; Homsy, A.; Ehrmann, K.; Boero, G.; Besse, P.-A.; Draidon, A.; Verpoorte, E.; De Rooij, N. F.; Popovic, R. S. *J. Magn. Reson.* **2003**, *164*, 242.
- 214 Wensink, H.; Hermes, D.C.; Van den Berg, A., accepted for publication in *J. Magn. Reson.*
- 215 Wensink, H.; Benito-Lopez, F.; Hermes, D. C.; Verboom, W.; Gardeniers, H. J. G. E.; Reinhoudt, D. N.; Van den Berg, A., accepted for publication in *Lab Chip*.

Chapter 3

Rate Enhancement of an Acid-catalyzed Esterification Reaction within a Glass Microreactor[‡]

The acid-catalyzed esterification reaction of 9-pyrenebutyric acid (1) with ethanol, to yield pyrenebutyric acid ethyl ester (2) was studied in a flow-driven glass microreactor. Considerably higher yields of ester 2 were obtained on-chip, indicating a substantial reaction rate enhancement compared to conventional lab-scale procedures. Surface phenomena at the acidic glass wall, which are dominant at the high surface-to-volume ratios typical for microchannels, were demonstrated to play a major role in the observed enhanced reaction efficiency (higher yields and shorter reaction times).

[‡] Part of this work has been published: Brivio, M.; Oosterbroek, R. E.; Verboom, W.; Goedbloed, M. H.; Van den Berg, A.; Reinhoudt, D. N. *Chem. Commun.* **2003**, 1924.

3.1. Introduction

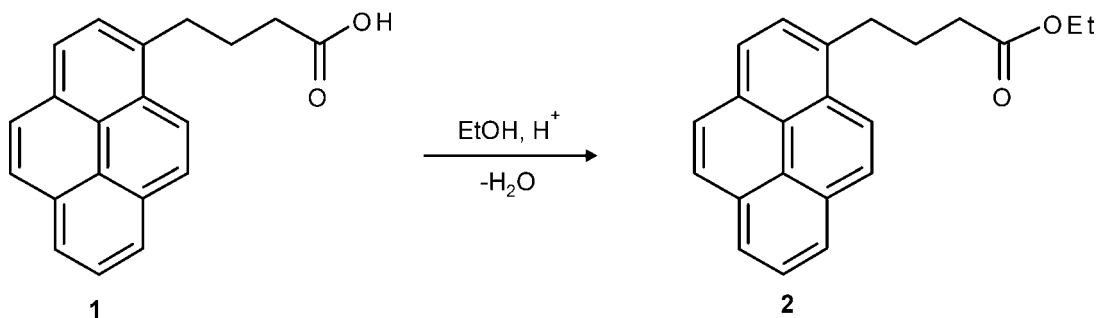
An improved reactivity in terms of product yield and selectivity has been demonstrated for a number of reactions performed in microreactors, as compared to the conventional lab-scale equipment.¹⁻⁵ In most cases the enhanced reaction efficiency has been attributed to the high degree of spatial and temporal reaction control achievable in electrokinetically driven microreaction systems.^{5,6} The electric field associated with the electroosmotic flow (EOF), used to transport solutions within the microchannels, is also assumed to play a significant role.^{7,8} Moreover, fast diffusive mixing under laminar flow conditions, which is inherent to microreactors, is a key feature that enhances reaction rates in microchannels,⁹⁻¹¹ as demonstrated in the derivatization reaction of isocyanates with 4-nitro-piperazino-2,1,3-benzoxadiazole in Chapter 6.

As discussed in Chapter 2, one of the most striking features of microreactors is the high surface-to-volume ratio resulting from downsizing.^{9,12} The large active surface available within microchannels has proven to be beneficial for heterogeneous catalysis, in which a catalyst is either immobilized on the channel surface¹³ or introduced into the channel on a solid support,¹⁴ and for homogeneously catalyzed reactions.¹⁵ A few examples have also shown the positive effect of the large active surface on phase-transfer reactions carried out in microchannels.¹⁶⁻¹⁹ The importance of surface phenomena has also been described in nanochannels.²⁰

The nucleophilic acyl substitution reaction between a carboxylic acid and an alcohol to give the corresponding ester is known as the Fischer esterification.²¹ It is an equilibrium reaction, which proceeds towards the formation of the ester in the presence of large amounts of alcohol. The Fischer esterification is commonly carried out within a few hours under reflux conditions in the presence of a mineral acid as a catalyst.

At large surface-to-volume ratios the catalytic effect of acidic silica-based materials,^{22,23} such as glass, is also expected to be more important in microchannels than in conventional laboratory glassware. In this Chapter the acid-catalyzed esterification reaction of 9-pyrenebutyric acid (**1**) with ethanol to yield the ethyl ester **2** (Scheme 3.1) is carried out in a flow-driven glass microreactor. This reaction was selected because it can easily be monitored by mass spectrometry, in view of the

relatively high molecular weight of acid **1** and ester **2**. A systematic study of the influence of the acidic glass microchannel surface on the esterification of 9-pyrenebutyric acid (**1**) with ethanol demonstrates the important contribution of surface phenomena to the observed enhancement of the reaction rate.



*Scheme 3.1. Acid-catalyzed esterification of 9-pyrenebutyric acid (**1**) in ethanol to give the corresponding ethyl ester **2**.*

3.2. Microreactor and chip holders

3.2.1. Microreactor

All on-chip reactions were carried out in the 197 mm long, 200 μm wide and 100 μm deep borosilicate microchannel (reaction volume = 4 μL) depicted in Figure 3.1a. High precision powderblast micromachining²⁴ was used for the fabrication of inlet and outlet holes in the top wafer. Reaction microchannels were fabricated by standard photolithography and wet chemical HF etching in the bottom wafer.²⁵ Syringes mounted on a microdialysis pump were used to drive solutions through the microchannels in a continuous manner. This simple, well-controllable, and reliable method was chosen to be the most suitable fluidic handling approach to study organic reactions at the microscale (see Chapter 2).

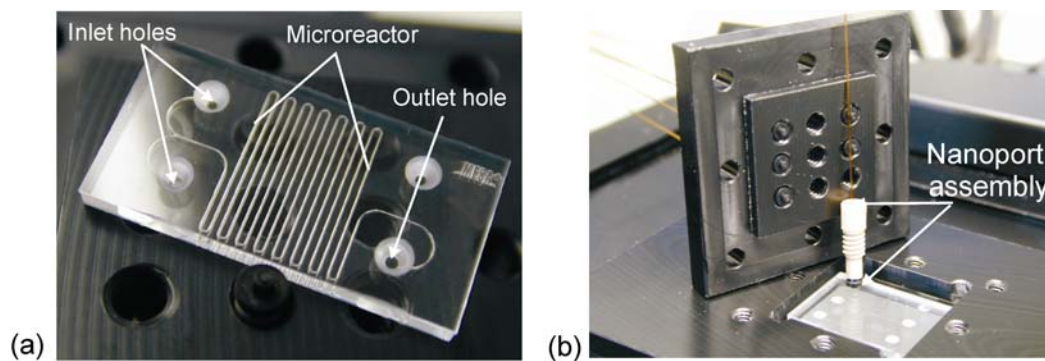


Figure 3.1. (a) Microreactor used for the acid-catalyzed esterification reaction of 9-pyrenebutyric acid (**1**) with ethanol to give ester **2**. (b) Optimized chip holder for fitting fused silica fibers into the inlet and outlet holes by means of low dead volume Nanoport™ assemblies.

3.2.2. Chip holders

During the experiments the glass chips were mounted on two holders and connected to the reactant feeders and to the sample collection / analysis by means of fused silica capillaries. The designs of the holders allow both off- and on-line analyses either by collecting samples in vials or by coupling the outlet fiber to a mass spectrometer *via* an electrospray ion source, respectively. For both types of holder heating of the reactor takes place by heaters or Peltier elements, which can be controlled by temperature sensors.

3.2.2.1. Initial holder

The first holder used in these experiments (Figure 3.2a) consists of two Teflon square blocks. The chip (A) was located between the two blocks (B), which were assembled by means of a screw at each corner. Fused silica capillaries were used to introduce reagent solutions on-chip (C) and to transfer the reaction mixture from the outlet (D) to the mass spectrometer for analysis of the reaction products. Solutions were allowed to flow from the feeding capillaries to the chip inlets and from the chip

outlet to the sample collection / analysis *via* through-holes drilled in the holder. During the experiments the chip was interfaced to a mass spectrometer (Figure 3.2b).

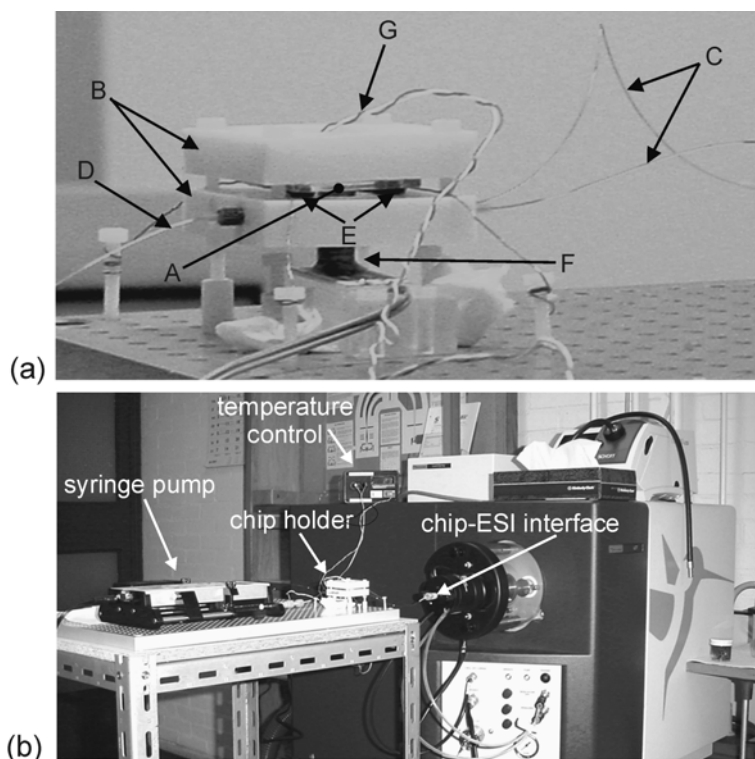


Figure 3.2. (a) Teflon chip holder (B) in which the chip (A) was mounted and connected by capillaries to the reagent feeding (C) and the analysis (D). E are the O-rings at the inlet and outlet holes, F is the heater, and G the temperature sensor. (b) Complete set-up.

Leakage of reagent solutions from the O-rings (E) at the chip inlet and outlet cups was observed at flow rates higher than $1 \mu\text{L min}^{-1}$, revealing the inefficiency of the connection between the chip and the holder (O -rings). The relatively large dead volumes were an even more severe drawback, rendering the set-up not suitable to study reaction dynamics in detail. Each of the three holder through-holes used to transfer solutions to and from the chip introduced a dead volume of $10 \mu\text{L}$ in the fluidic system, which gave a total dead volume of $30 \mu\text{L}$. A very limited flow control due to extremely low flow velocities and bubble trapping, as well as a considerable cross-contamination of reaction mixture with different compositions accumulated in

the dead volumes were the main consequences, which resulted in a very poor spatial and temporal control over the reaction. This means that in general only qualitative information about a reaction can be obtained.

3.2.2.2. Improved chip holder

To improve reaction control a new holder was designed (Figure 3.1b) for fitting fused silica fibers into the inlet and outlet chip reservoirs by means of commercially available Nanoport™ assemblies.²⁶ These connectors allow reagents injection in a continuous flow fashion, eliminating the risk of adhesive contamination and offering the great advantage of adding only a very small dead volume to the flow path. Although designed to seal at the chip surface when using cylindrically drilled holes of 1 mm diameter, perfluoro elastomer (Perlast™) ferrules were fitted into the conically shaped powderblasted holes. The resulting dead volume was calculated to be about 10 nL for each connector, which could be further reduced by using 1.5 mm long ferrules, thinner glass wafers, and an optimized hole shape. The total dead volume introduced by the three Nanoport connectors is 30 nL, which is only 0.75% of the reaction volume (4 μL).

3.3. On-chip esterification reaction

The esterification of 9-pyrenebutyric acid (**1**) in ethanol to yield the corresponding ethyl ester **2** was selected as a model reaction to study the influence of surface phenomena in glass microchannels.²⁷ Having a relatively short reaction time and requiring relatively mild conditions,²⁸ this esterification reaction is expected to show significant conversion levels at the residence times obtained with the microreactor. The reaction was carried out in the glass microreactor of Figure 3.1a, using the optimized holder depicted in Figure 3.1b. For comparison reasons the same reaction was carried out in conventional lab-scale glassware. All experiments were performed under the same conditions; using solutions of 10^{-4} M 9-pyrenebutyric acid (**1**) and 10^{-4} M sulfuric acid, both in ethanol and at room temperature as well as at 50

°C. The on-chip and macroscale reaction were followed off-line by matrix-assisted laser desorption ionization time-of-flight (MALDI-TOF) mass spectrometry (MS). The on-chip formed reaction products were directly transferred from the outlet silica fiber to a MALDI sample plate in a continuous flow fashion by collecting individual droplets, after which the samples on the plate were analyzed batch-wise. After the individual droplets were placed on the plate, the solvent evaporated quickly thus inhibiting further reaction. In this way the reaction-to-analysis delay time, which is inherent to off-line chip analysis, was considerably reduced.²⁹ HPLC was used to determine the conversion of ester **2**.

Table 3.1 Conversion (%) of ester **1** obtained during on-chip and lab-scale experiments carried out at 50 °C.

Residence time (min)	On-chip flow rate ($\mu\text{l min}^{-1}$)	Conversion (%)		
		On-chip	Lab-scale	
			No SiO ₂	SiO ₂ gel
4	1	17	0	8
10	0.4	33	0	9
20	0.2	51	0	10
33	0.12	71	0	n.d. ^a
40	0.1	83	0	15

^a n.d. = not determined

No ester could be detected in aliquots taken from a lab-scale experiment at 4, 10, 20, 30, and 40 min, both at room temperature and 50 °C. However, in the on-chip experiments carried out at room temperature about 15-20% of ester **2** had already formed after 40 min (Figure 3.3). When the on-chip experiments were performed at 50 °C higher yields of ester **2** were obtained. The dependence of the conversion on the residence time is clearly demonstrated in the MALDI-TOF mass spectra (Figure 3.4), while the conversions are summarized in Table 3.1. These results clearly show a considerable increase of the reaction rate of the on-chip reaction compared to the lab-

scale reaction, thus demonstrating the large positive effect of the microchannel environment on the target reaction.

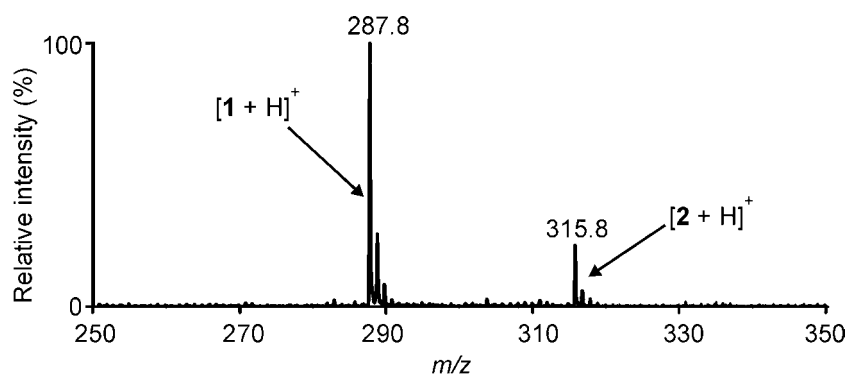


Figure 3.3. MALDI-TOF mass spectrum of ester **2** ($m/z = 315.8$) formed on-chip at room temperature after 40 min and unreacted 9-pyrenebutyric acid (**1**; $m/z = 287.8$)

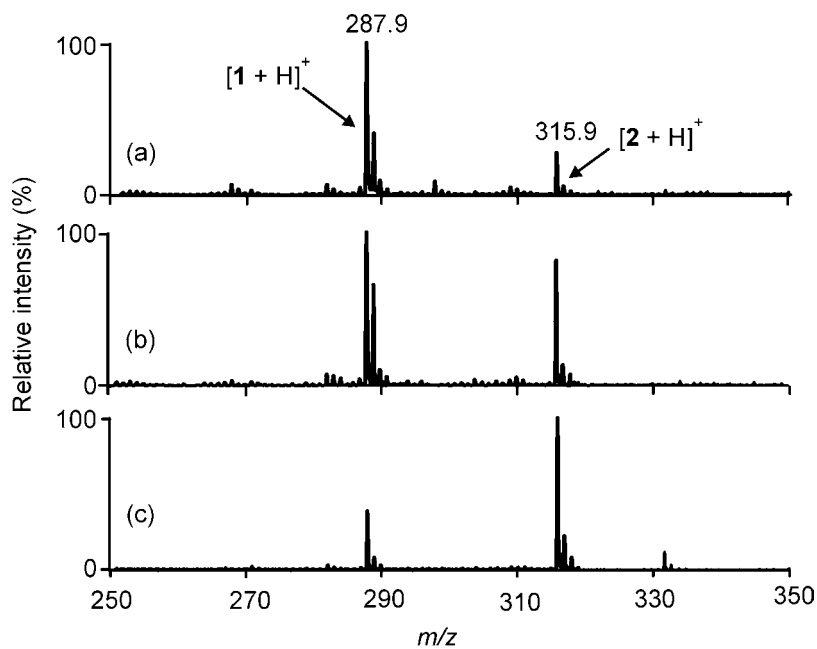


Figure 3.4. MALDI-TOF mass spectra of ester **2** ($m/z = 315.9$) formed on-chip at 50 °C after (a) 4 min, (b) 10 min, and (c) 20 min and unreacted 9-pyrenebutyric acid (**1**; $m/z = 287.9$).

3.4. Influence of surface phenomena

To study the possible influence of the silanol groups at the inner channel surface, the on-chip experiments summarized in Table 3.1 were repeated at room temperature and at 50 °C, without co-injecting sulfuric acid. No ester **2** could be detected in any of the collected samples. However, upon activating the glass surface hydroxyl groups by pretreating the channel with a solution of sulfuric acid and hydrogen peroxide (3:1), 9% of ester **2** was formed in the glass microchannel after 40 min at 50 °C. These results demonstrate the active role of the microchannel glass surface on the formation of ester **2**.

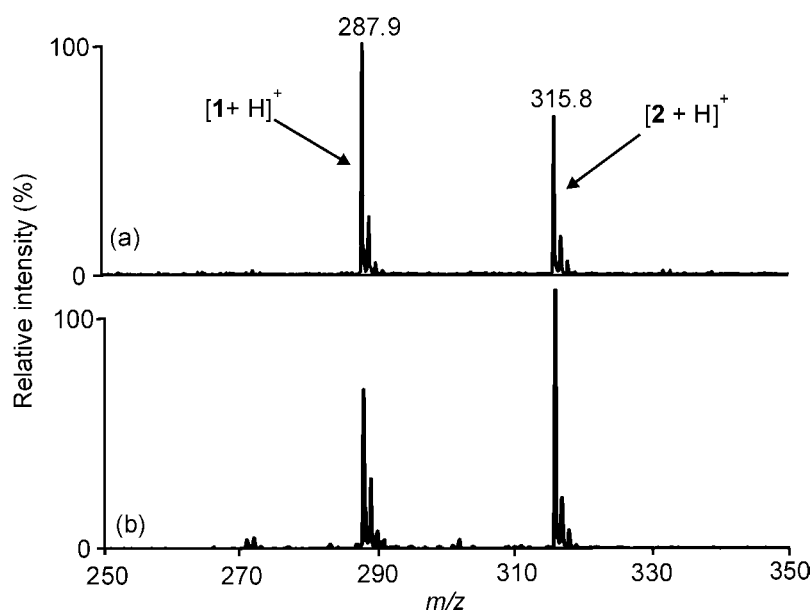
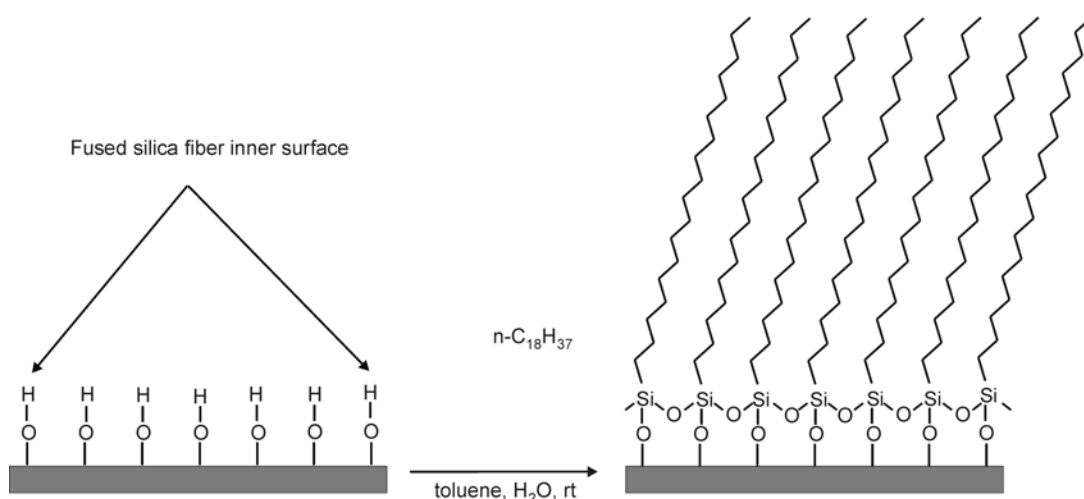


Figure 3.5. MALDI-TOF mass spectra of unreacted 9-pyrenebutyric acid (**1**; $m/z = 287.9$) and ester **2** ($m/z = 315.8$) formed in a fused silica fiber at 50 °C after (a) 10 min and (b) 20 min.

To investigate the possible influence of the mixing dynamics on the observed reaction rate enhancement, the esterification of **2** with ethanol was repeated in a fused silica fiber with an inner diameter (100 μm) comparable with that of the microchannel. The silica fiber was filled with a premixed 1:1 solution of carboxylic acid **1** and sulfuric acid, both in ethanol, and heated at 50 °C for 2, 4, 8, 10, and 20

min, respectively. The MALDI-TOF mass spectra of the samples (Figure 3.5) showed that the conversions at comparable residence times were similar to those obtained in the corresponding on-chip experiments. Subsequently, the experiments were repeated in a glass fiber of which the inner surface had been coated by reaction of the SiOH groups with the lipophilic octadecyltrichlorosilane (Scheme 3.2). No product formation could be detected, again substantiating the effect of the microchannel surface on the esterification reaction. Probably, the large number of acidic hydroxyl groups within the glass microreactor and the uncoated silica fiber activate the ethanol, present in large excess, facilitating esterification.



Scheme 3.2. Schematic illustration of the reaction between the hydroxyl groups at the inner surface of the fused silica fiber and octadecyltrichlorosilane.

Finally, the same reaction was done at lab-scale in the presence of silica gel, imitating the same glass-surface to chemicals-volume ratio ($\sim 1:34$) as in the microchannel. At reaction times of 4, 10, 20, and 40 min conversions of 8%, 9%, 10%, and 15%, respectively, were obtained at 50 °C. The conversions are substantially lower than those obtained at the same residence times in the on-chip experiments (Figure 3.6 and Table 3.1). This clearly indicates a higher efficiency of the micro- over the macroscale reaction. The large difference in the catalytic effect of the silanol groups at the channel surface and in the silica gel may be attributed to a better accessibility of the channel surface to the reagents.

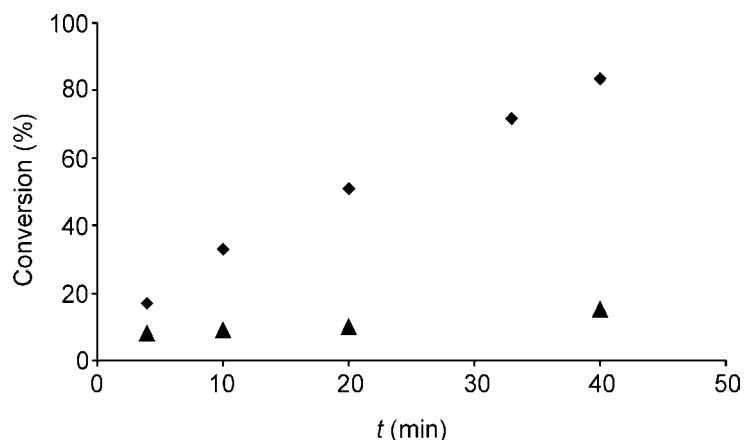


Figure 3.6. Conversion (%) of the (◆) on-chip and (▲) in-flask esterification reaction of 9-pyrenebutyric acid (**1**) with ethanol at a temperature of 50 °C as a function of the reaction time.

3.5. Conclusions

A considerable rate enhancement was observed in the acid-catalyzed esterification of 9-pyrenebutyric acid (**1**) with ethanol carried out in a glass microreactor. Using an optimized chip holder with low dead volume connectors, a satisfactory degree of reaction control was accomplished, allowing quantification of the on-chip reaction conversion. The important contribution of surface phenomena to the on-chip reaction efficiency was demonstrated, giving rise to much shorter reaction times and higher conversions than on conventional laboratory scale.

3.6. Experimental

Chemicals. All reagents and solvents were purchased from Aldrich Chemicals, The Netherlands. Samples were used as supplied commercially without further purification.

Microchips. All glass (Schott Borofloat 33) chips were fabricated by Ir. M. H. Goedbloed at the cleanroom facilities of the MESA⁺ Institute for Nanotechnology at the University of Twente. High precision powderblast micromachining was used for

the fabrication of inlet and outlet holes, while the reaction microchannel was made *via* HF chemical etching.

Fluidic handling. In all experiments sample solutions were mobilized by means of a dual CMA/102 Microdialysis Pump (flow rate range 0.1-20 $\mu\text{L min}^{-1}$ using 1 mL syringes) on which 1 mL and 100 μL flat tip Hamilton syringes were mounted. Syringes were connected to fused silica capillaries (100 μm i.d.) by means of NanoTight™ Unions and Fittings (Upchurch Scientific).

Initial holder. Through-holes with a diameter of 0.9 mm were drilled through the holder to let solutions flow from the feeding capillaries to the chip inlets, and from the chip outlet to the sample collection / analysis device. The fibers, placed into PEEK™ sleeves (i.d. = 360 μm), were connected to the holder by means of Minstack™ type of connectors. Fluoroelastomer Viton® O-rings (E in Figure 3.2a) were used to seal the inlet and outlet holes of the chip to the holder. The outlet capillary was either connected to an electrospray ionization (ESI) interface using Upchurch connectors, or glued into MasCom gold plated ESI-Pipettes (o.d. = 1 mm, tip *ca.* 2 μm).

ESI-TOF MS. A Micromass (Manchester, UK) LCT electrospray time-of-flight mass spectrometer (ESI-TOF MS) operated in the positive and negative ion mode was used in preliminary experiments.

Optimized holder. Upchurch Nanoport™ assemblies for lab-on-a-chip applications were used to directly connect the fibers to the inlet and outlet chip holes in the optimized holder design (Figure 3.1b).

MALDI-TOF MS analysis of 9-pyrenebutyric acid (**1**) esterification with ethanol was performed using a Voyager-DE-RP MALDI-TOF mass spectrometer (Applied Biosystems / PerSeptive Biosystems, Inc., Framingham, USA) equipped with delayed extraction^{30,31} and a 337 nm UV nitrogen laser producing 3 ns pulses. The mass spectra were obtained in the linear positive mode. No matrix was added because of the strong absorption at the laser wavelength ($\lambda = 337$ nm) of 9-pyrenebutyric acid (**1**) and the corresponding ethyl ester **2**.

HPLC analysis. The conversion (%) of the on-chip and in-flask (in the presence of silica) esterification of **1** with ethanol were determined by high pressure liquid chromatography (HPLC), using a apolar LUNA 3 μm C18 (2) column (dimensions: 100 x 4.60 mm). A 60:40 mixture of acetonitrile and an aqueous solution of 2×10^{-2} M NaH_2PO_4 at pH = 4.3 was used as eluent. From $t = 0$ up to $t = 25$ min the mixture composition was changed in a gradient resulting in 100% acetonitrile at $t = 25$ min. The initial composition was finally regenerated to the initial value (60:40) at $t = 30$ min. Samples of the on-chip reaction were collected in HPLC glass vials kept in an ice bath in order to quench the reaction once the mixture was out of the chip.

Fused silica fiber coating. A 100 μm inner diameter fused silica fiber was flushed with a 0.1% v/v solution of octadecyltrichlorosilane in toluene at room temperature for several hours. Prior to coating, the fused silica fiber inner surface was activated using a solution of sulfuric acid and hydrogen peroxide (3:1; *piranha* solution). **Caution:** *piranha* solution is a very strong oxidant and reacts violently with many organic materials. Subsequently, the fiber was rinsed thoroughly with Millipore water to remove the cleaning solution and dried in an oven at 100 $^\circ\text{C}$ overnight.

3.7. References and notes

- 1 Wörz, O.; Jäkel, P.; Richter, T.; Wolf, A. *Chem. Eng. Technol.* **2001**, *24*, 138.
- 2 Sands, M.; Haswell, S. J.; Kelly, S. M.; Skelton, V.; Morgan, D. O.; Styring, P.; Warrington, B. *Lab Chip* **2001**, *1*, 64.
- 3 Wiles, C.; Watts, P.; Haswell, S. J.; Pombo-Villar, E. *Lab Chip* **2004**, *4*, 171.
- 4 Wiles, C.; Watts, P.; Haswell, S. J.; Pombo-Villar, E. *Lab Chip* **2002**, *2*, 62.
- 5 Fletcher, P. D. I.; Haswell, S. J.; Pombo-Villar, E.; Warrington, B. H.; Watts, P.; Wong, S. Z. F.; Yhang, X. *Tetrahedron* **2002**, *58*, 4735.
- 6 Fletcher, P. D. I.; Haswell, S. J.; Paunov, V. N. *Analyst* **1999**, *124*, 1273.
- 7 Watts, P.; Wiles, C.; Haswell, S. J.; Pombo-Villar, E. *Tetrahedron* **2002**, *58*, 5427.
- 8 Watts, P.; Wiles, C.; Haswell, S. J.; Pombo-Villar, E. *Lab Chip* **2002**, *2*, 141.
- 9 Ehrfeld, W.; Hessel, V.; Löwe, H. *Microreactors: New Technology for Modern Chemistry*, Wiley-VCH: Weinheim, Germany, **2000**.
- 10 Suga, S.; Nagaki, A.; Yoshida, J.-I. *Chem. Commun.* **2003**, 354.
- 11 Jensen, K. *Nature* **1998**, *393*, 735.
- 12 Jähnisch, K.; Hessel, V.; Löwe, H.; Baerns, M. *Angew. Chem. Int. Ed.* **2004**, *43*, 406.
- 13 Wilson, N. G.; McCreedy, T. *Chem. Commun.* **2000**, 733.
- 14 Haswell, S. J.; O'Sullivan, B.; Styring, P. *Lab Chip* **2001**, *1*, 164.
- 15 Greenway, G. M.; Haswell, S. J.; Morgan, D. O.; Skelton, V.; Styring, P. *Sens. Actuators B* **2000**, *63*, 153.
- 16 Hisamoto, H.; Saito, T.; Tokeshi, M.; Hibara, A.; Kitamori, T. *Chem. Commun.* **2001**, 2662.
- 17 Ueno, K.; Kitagawa, F.; Kitamura, N. *Lab Chip* **2002**, *2*, 231.
- 18 Ueno, M.; Hisamoto, H.; Kitamori, T.; Kobayashi, S. *Chem. Commun.* **2003**, 936.
- 19 Mikami, K.; Yamanaka, M.; Islam, Md. N.; Kudo, K.; Seino, N.; Shinoda, M. *Tetrahedron Lett.* **2003**, *44*, 7545.
- 20 Jacobson, S. C.; Alarie, J. P.; Ramsey, J. M. *Proc. μ TAS '01*, Monterey CA, USA, **2001**, 57.

- 21 McMurry, J. *Organic Chemistry*, 3rd ed., Brooks/Cole Publishing Company: Pacific Grove, USA, **1992**.
- 22 Mendez, A.; Bosch, E.; Roses, M.; Neue, U. D. *J. Chromatogr. A* **2003**, *986*, 33.
- 23 Adolph, S.; Spange, S.; Zimmermann, Y. *J. Phys. Chem. B* **2000**, *104*, 6429.
- 24 Wensink, H.; Berenschot, J. W.; Jansen, H. V.; Elwenspoek, M. C. *Proc. 13th Int. Workshop on Micro ElectroMechanical Systems (MEMS2000)*, Miyazaki, Japan, **2000**, 769.
- 25 Corman, T.; Enoksson, P.; Stemme, G. J. *J. Micromach. Microeng.* **1998**, *8*, 84.
- 26 Upchurch Scientific, Oak Harbor, USA.
- 27 The acid-catalyzed esterification of 9-anthracenecarboxylic acid with methanol, ethanol, and 2-propanol to give the corresponding esters was also chosen to investigate the surface phenomena in glass microchannels. However, no ester was formed in any of the on-chip and lab-scale esterification reactions. Probably due to the anthracene moiety, methyl, ethyl, and 2-propyl esters of 9-anthracenecarboxylic acid can not be prepared *via* the Fischer esterification reaction. These esters are in fact generally prepared *via* other synthetic routes. For a few examples see: a) Schuster, I., *J. Org. Chem.* **1981**, *46*, 5110. b) Salt, K.; Scott, G. W. *J. Phys. Chem.* **1994**, *98*, 9986. c) Larsen, C.; Harpp, D. N. *J. Org. Chem.* **1980**, *45*, 3713.
- 28 Lehr, R. E.; Taylor, C. W.; Kumar, S.; Duck, Mah H.; Jerina, D. M. *J. Org. Chem.* **1978**, *43*, 3462.
- 29 The esterification reaction of 9-pyrenebutyric acid (**1**) with ethanol could not be followed on-line by ESI-MS because acid **1** and its ethyl ester **2** did not give stable mass spectrometric signals under the same conditions.
- 30 Vestal, M. L.; Juhasz, P.; Martin, S. A. *Rapid Commun. Mass Spectrom.* **1995**, *9*, 1044.
- 31 Juhasz, P.; Vestal, M. L.; Martin, S. A. *J. Am. Soc. Mass Spectrom.* **1997**, *8*, 209.

Chapter 4

Simple Chip-based Interfaces for On-line Nanospray Mass Spectrometry

Two simple interfaces were designed and realized, enabling on-line coupling of microfluidics reactor chips to a nanoflow electrospray (NESI) time-of-flight (TOF) mass spectrometer (MS). The interfaces are based on two different approaches: a monolithically integrated design, in which ionization is assisted by on-chip gas nebulization, and a modular approach implying the use of PicosprayTM tips. Using reserpine as a reference compound in a 1:1 mixture of acetonitrile and water revealed that both interfaces provide a remarkably stable mass spectrometric signal (standard deviations lower than 8% and 1% for the monolithic and modular approaches, respectively). Glass microreactors, containing innovative mixing zones, were coupled to the modular interface to study organic chemical reactions. Investigation of the mixing dynamics showed that complete on-chip reagents mixing is achieved within a few tens of milliseconds.

4.1. Introduction

Mass spectrometry (MS) is one of the most powerful detection techniques used in liquid phase analyses,¹ mainly due to the ease of interfacing with separation techniques such as capillary electrophoresis (CE)^{2,3} and high performance liquid chromatography (HPLC).⁴ Due to its sensitivity and applicability to a wide variety of chemical and biochemical species, MS is also used for the analysis of (bio)chemical molecules processed in microfluidics devices.^{5,6} Electrospray ionization (ESI)⁷⁻¹⁰ is often used to transfer samples from microfluidics chips to a mass spectrometer, involving analyte ionization directly from solutions and operating at flow rates typically used in microfluidics devices.¹¹ Due to its effectiveness, the use of chip-MS coupling has rapidly spread in many research areas with bioanalytical applications,¹² such as the fields of genomics¹³ and proteomics.¹⁴ The first example of the coupling of a microfluidics device with ESI-MS was reported by Xue *et al.*^{15,16} in 1997. They used glass chips as a platform to carry out enzymatic digestions and to deliver standard peptide and protein samples to an ESI-MS. The described lab-on-a-chip (LOC) system relied on hydrodynamic pumping, thus allowing sample infusion at flow rates between 100 and 200 nL min⁻¹. In the same year Ramsey and Ramsey¹⁷ extended this method using electroosmotic flow (EOF) to pump the sample into the mass spectrometer. Figeys *et al.*¹⁸ achieved detection limits in the order of fmol μL^{-1} (*i.e.* 10⁻⁹ M) using a hybrid capillary / micromachined microfluidics device for sequential infusion of peptides into a mass spectrometer, which demonstrates the potential of chip-MS coupling.

Since these first chip-MS-based LOC devices were presented, an intense research activity has started on the development of hyphenated interfaces for coupling microfluidic devices with ESI-MS.^{6,19} As a result, several coupling systems have been exploited,²⁰⁻³¹ based on two main designs. Those that spray liquid samples directly from an exposed channel (Figure 4.1a), as first proposed in 1997 by Xue *et al.*¹⁵ and Ramsey,¹⁷ and those in which a capillary is attached in various ways to the chip (see Figure 4.1b), as first presented by Figeys *et al.*¹⁸ In the early days researchers working on chip-MS coupling were mainly focused on design and microfabrication, aiming to develop a spraying chip able to generate a good quality Taylor cone. More recently, although the optimization of the chip-ESI interface in terms of signal stability is still a

key issue,²⁹⁻³³ more attention is paid to the integration of multiple functions on-chip,^{34,35} aiming to demonstrate the high-throughput potential of the chip-MS coupling.³⁶⁻⁴⁰ However, most of the interfaces reported in the literature have been designed for biochemical applications. This implies a significant limitation in terms of applicability to organic chemical systems, due to the use of glue and polymeric construction materials. Therefore the development of an integrated chip-MS interface that allows rapid on-line study of (bio)chemical reactions without solvent limitations is highly attractive.

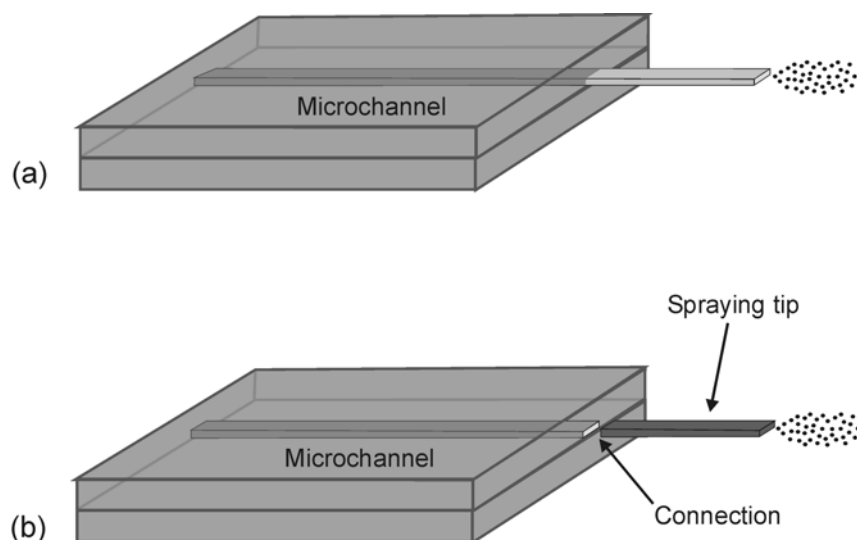


Figure 4.1. Schematic representation of a chip-MS interface in which the spray is generated (a) at the edge of the chip and (b) from a capillary attached to the channel in various ways (e.g. via liquid junction connectors, glue).

In this Chapter a simple and efficient coupling system for on-line MS from glass chips using a nanoflow electrospray ionization (NESI) interface will be described. Two integrating concepts are studied, based on both a monolithic and a modular integration approach. The latter was chosen for the final set-up, making use of glass chips comprising (a) mixer(s) and (a) reactor(s). The mixing capacity of the glass microchip was optimized by exploiting its small dimensions and merging the flows in a unique way.

4.2. Electrospray ionization mechanism

The electrospray ionization process can be divided in three main steps: droplet formation, droplet shrinkage, and vaporization (formation of gas-phase ions).⁴¹ A solution of the analyte flows through a capillary, which is kept at a high potential (Figure 4.2). When the solution approaches the capillary tip a so-called Taylor cone is formed (when surface tension equilibrates electrostatic forces),²⁴ as a result of the high electric field; followed by the formation of a plume of highly charged droplets. The charged droplets fly towards the analyzer because of pressure and potential gradients. While flying to the detector the droplets shrink due to evaporation of the solvent, which causes the charge density on the droplets surface increases to a critical value. When the Coulombic repulsion exceeds the surface tension, the droplets explode into smaller droplets (Coulombic explosion). The continuous solvent evaporation will eventually lead to the formation of fully desolvated ions.⁴²

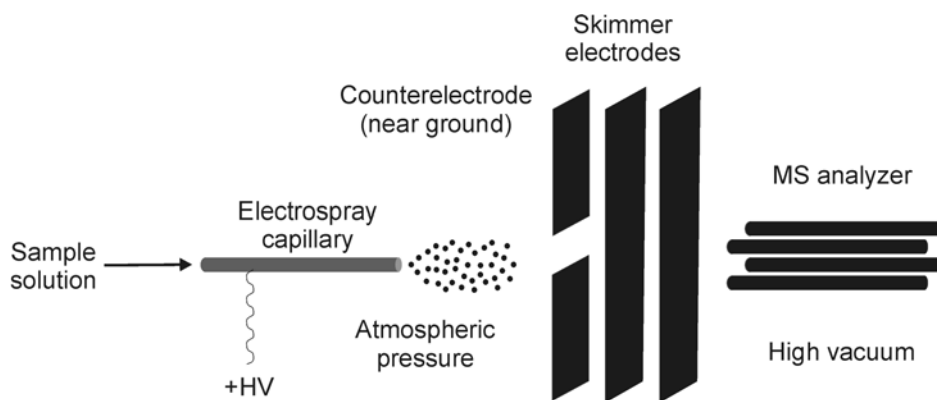


Figure 4.2. Essential features of the electrospray interface.¹

4.3. Nanospray ionization

Nanoflow electrospray (nanospray) has been introduced by Wilm and Mann¹¹ in 1996 in an effort to improve the performances of conventional ESI. The technique employs a spray needle pulled from glass capillaries, having a tip outer diameter in the μm range. Due to the smaller tip diameter, in nanospray the sample solution is infused at a lower flow rate compared to microspray, which has a positive influence

on the sample ionization.^{11,43,44} Nanospray ionization was used to couple glass chips to a mass spectrometer, resulting in a nanoflow electrospray ionization chip (NESIC) interface for coupling to a mass spectrometer (MS).

4.4. Monolithically integrated NESIC-MS interface

In the monolithically integrated NESIC-MS interface (Figure 4.3) the spray is generated directly at the edge of the chip. Although very attractive because of its simplicity, this design is known to suffer from a poor signal stability, which is mainly caused by the formation of large droplets^{16,17} This problem increases at higher flow rates and occurs when the on-chip sample injection speed is higher than the ionization rate. The hydrophilicity of the outlet also contributes to the destabilization of the Taylor cone, due to spreading of the liquid (typically water, alcohols, and acetonitrile) on the chip surface. Attempts to minimize this effect, as reported in the literature, include hydrophobic coating of the chip outlet¹⁷ or pneumatically assisting the spraying process.⁴⁵ In order to avoid this drawback two strategies were followed in the research described here: i) application of a hydrophobic fluoro-containing coating around the channel and ii) the use of a gas flow (nitrogen), which actively nebulizes the liquid into small charged droplets. The interface performances were subsequently evaluated in terms of ionization rate and droplet formation using the set-up depicted in Figure 4.3b. A sample of a phosphate buffer was infused into the glass microchannel (A) through a fused silica fiber (B; i. d. = 100 μm), which was glued into the chip inlet (C). A high potential (up to 1,000 V) was applied to the liquid through sputtered electrodes (D) located in the inlet cup. Sample ionization was assisted by a gas flow introduced on-chip *via* a connection (E) into a side channel (F). Already at the junction where the sample is injected into the gas flow ionization was observed. Interestingly, at high electric fields ($\sim 2,000 \text{ V cm}^{-1}$) stable plasmas could be generated at atmospheric conditions (G), indicating that good and stable ionization rates can be obtained. Furthermore, due to its ability of generating plasmas, the set-up may be employed for optical spectral analysis of liquids.⁴⁶

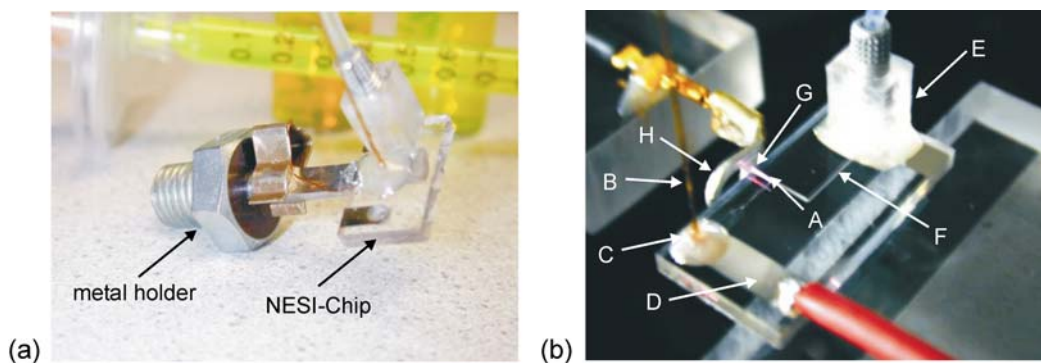


Figure 4.3. Monolithically integrated nanospray chip (a) on the holder used to mount the chip on the Nanospray™ source of the mass spectrometer and (b) on the ionization rate test setup. A = channel for sample infusion, B = fused silica fiber for infusing the sample into the chip, C = fused silica fiber-microchannel inlet connection, D = sputtered electrode, E = gas connection, F = gas flow channel, G = plasma and H = counterelectrode.

In order to test whether the NESIC-MS interface would give a stable m/z mass spectrometric signal, the chip was mounted on the standard Nanospray™ source of the mass spectrometer, using the holder depicted in Figure 4.3a. A standard solution of reserpine was injected through the chip into the mass spectrometer at flow rates varying between a few hundreds of nL min^{-1} and a few tens of $\mu\text{L min}^{-1}$. ESI-TOF mass spectra were acquired at a capillary voltage varying between 1,500 V and 3,500 V. The nebulizing gas (argon) flow turned out to be the most important parameter influencing sample ionization. As a result a stable analyte signal could be obtained at a broad range of sample infusion flow rates, by simply tuning the gas pressure. An example of gas / sample flow rate combination is given by the results reported in Figure 4.4. Values of $10 \mu\text{L min}^{-1}$ flow rate and 6.5 bar of nebulizing argon pressure and 260 L h^{-1} of cone gas flow gave a stable signal with a standard deviation, measured over the total ion current (TIC; Figure 4.4a) during 4 min, lower than 8%. This value is comparable with values for chip-MS devices reported in the literature.^{29,30} In Figure 4.4b the mass spectrum corresponding to the TIC chromatogram integrated over 4 min of acquisition time is shown, which was acquired at a capillary voltage of 3300 V, a cone voltage of 48 V, and an extraction voltage of 15 V.

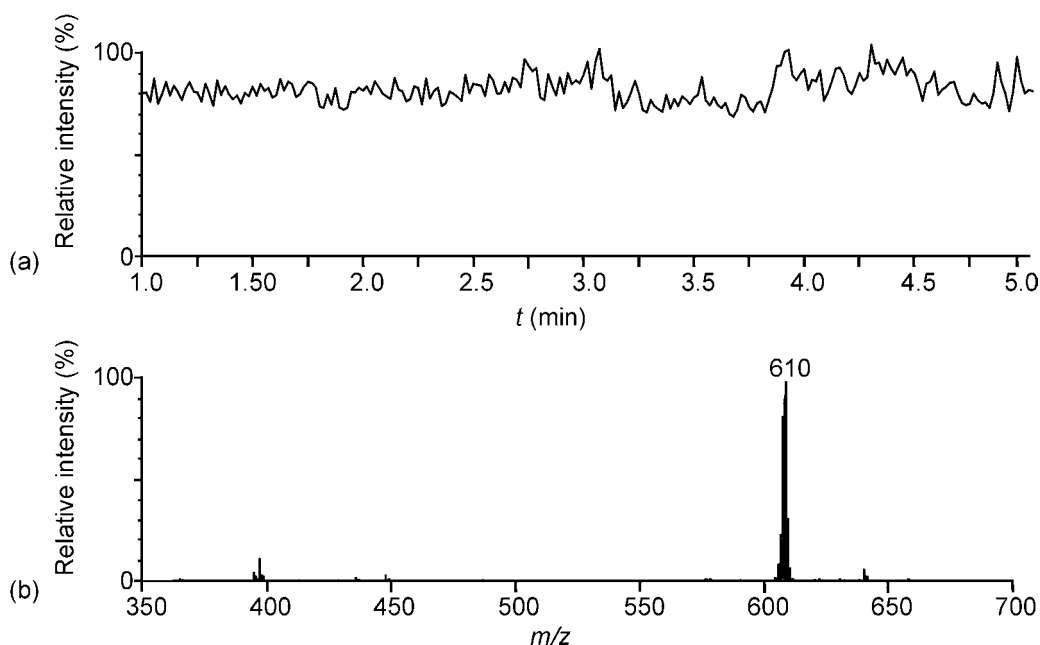


Figure 4.4. (a) Total ion current and (b) mass spectrum of a 1.6×10^{-4} M solution of reserpine in a mixture of acetonitrile and water (1:1 v/v) with 0.1% acetic acid, obtained with the monolithically integrated NESIC-MS interface.

Although the results indicate a good ionization stability, the problem of the unwanted formation of relatively large droplets could not be completely solved. This is possibly due to the formation of a liquid film at the channel wall, which may result from the orientation of the injected liquid flow from one side of the nebulization channel. Further improvement of the spray nozzles is expected to enhance the chip spraying performance. In particular it is expected that by enclosing the liquid in a gas flow at both sides may solve this problem.

4.5. Modular NESIC-MS interface

Modular chip-MS interfaces include micromachined nozzles^{20,29} attached to the chip and conventional needles glued to the microchannel.¹⁹ These designs generally offer several advantages, such as high spray stability and higher sensitivity and resolution of the MS analysis, over the monolithic integration devices. Nevertheless, they often require the use of glue or other materials that, upon prolonged contact with

organic solvents, may pollute the mass spectra of the reaction mixture. Furthermore, the modular integration may introduce large dead volumes between the reactor and the needle or nozzle due to the relatively large wafer-through hole volumes.

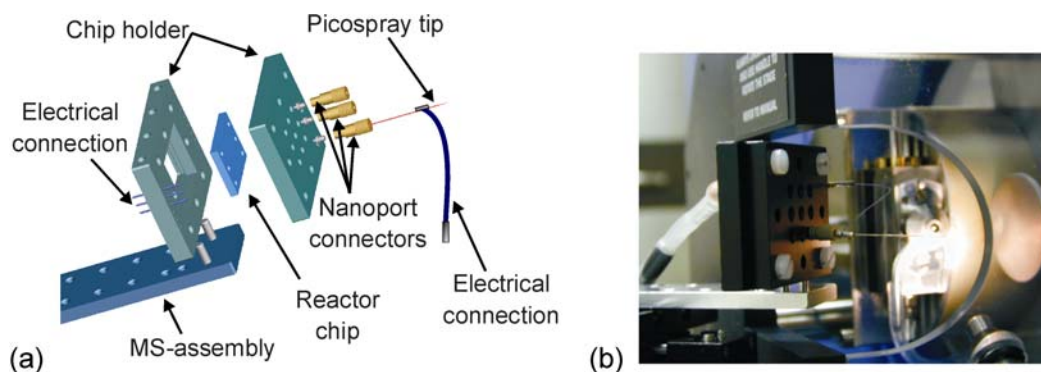


Figure 4.5. (a) Exploded view of the modular approach: the fibers and spray tip are connected to the chip using Nanoport™ connectors and the developed chip holder. (b) Picture of the integrated chip-based system mounted on the Nanospray™ source (turned for a better view).

Commercially available Picospray™ needles with distal coating were used to generate the spray in the modular NESIC-MS interface. Capillaries having tip diameters of 5 and 10 μm were used in order to obtain a stable spray and therefore good MS performances over a broad range of flow rates (between 20 and 100 nL min^{-1} and between 100 and 600 nL min^{-1} , respectively). The capillaries were fitted into the chip inlet and outlet holes by using Upchurch Nanoport™ connectors (see Chapter 4.3). A holder was specially designed in order to accommodate the chip and mount it on the Nanospray™ source of the mass spectrometer. The resulting NESIC-MS modular interface is schematically represented in Figure 4.5a. A picture of the microreactor-spraying tip assembly mounted on the MS ion source is shown in Figure 4.5b. The electrical connection to the fluid was realized *via* a miniature connector attached to the coated tip (Figure 4.5). Nevertheless, on-chip sputtered electrodes, as used for the monolithically integrated solution, could be used as well.

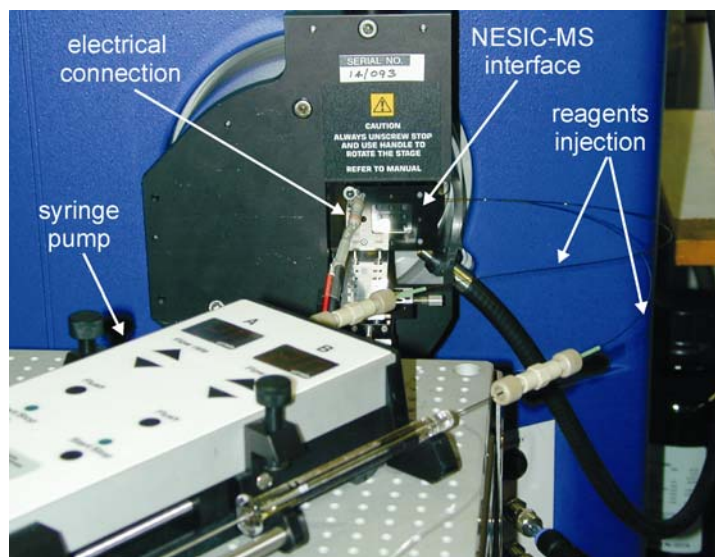


Figure 4.6. Complete flow-driven set-up for the on-line mass spectrometric measurements of samples delivered by the NESIC interface.

Since the modular interface makes use of a commercially available spraying tip, an assessment of the spraying capability was not required. Instead, an evaluation of the NESIC-MS interface performance in delivering samples for mass spectrometric analyses was carried out using the flow-driven system represented in Figure 4.6.

Experiments were carried out by injecting a standard solution of reserpine into the mass spectrometer through the chip-based interface. Various injection speeds were used ranging between 20 and 600 nL min⁻¹. A stable spray was obtained over the whole flow rate range. An example of a chromatogram and the corresponding integrated mass spectrum are shown in Figures 4.7a and 4.7b, respectively. The low standard deviation (1%) of the mass spectrometric signal, calculated over a period of 2 min, indicates a remarkably high ionization stability. The use of specific Picotip™ emitters to generate the spray guarantees a high quality Taylor cone during the ionization process, which certainly leads to an optimal signal. Moreover, the use of Nanoport™ fittings in combination with the fabricated holder and the choice of low-volume connectors and a highly controllable flow-driven pumping method allow the high quality of the ionization process to be maintained even after coupling of the tips with the microreactor unit. Besides the good performance capability, the modular approach offers several advantages. The sprayer can in fact easily be replaced

independently from the chip in case of clogging or rupture. On the other hand, the interface can easily be adapted to study a variety of reactions by simply mounting a suitable microreactor in the holder. Furthermore, the modular interface can be connected to analytical instruments other than a mass spectrometer by simply replacing the needle at the outlet with a fused silica capillary (see Chapter 3).

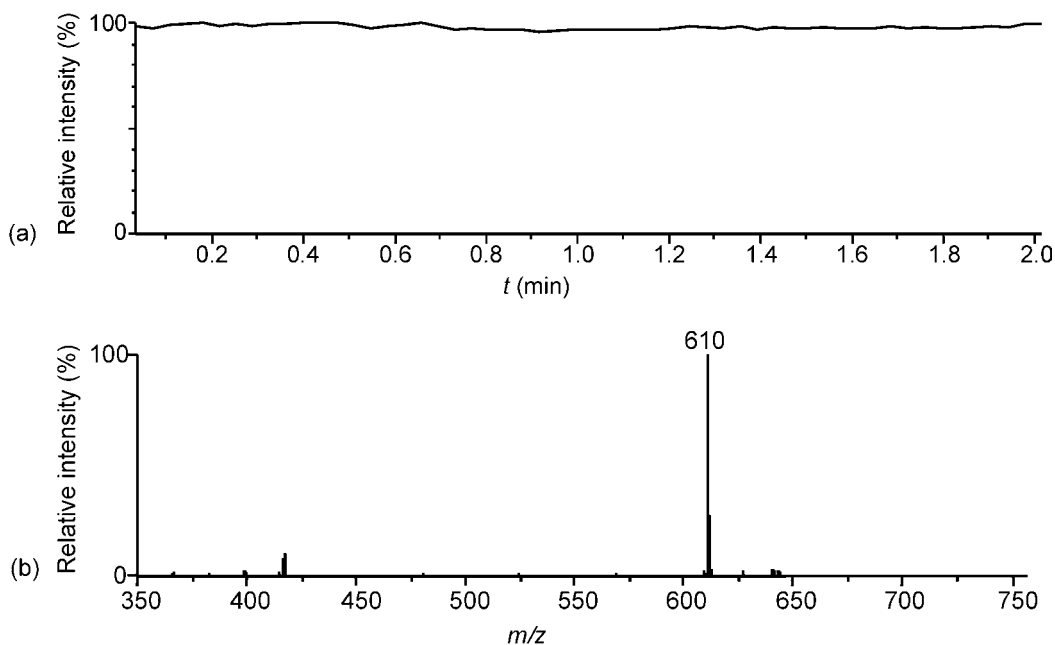


Figure 4.7. (a) Total ion current and (b) mass spectrum of a 1.6×10^{-4} M solution of reserpine in a mixture of acetonitrile and water (1:1 v/v) with 0.1% acetic acid, acquired using the modular NESIC-MS interface.

4.6. Chip design and fabrication

Various types of chips were designed and produced to be used in combination with the NESIC-MS interface. Since the interface was designed for the study of organic reactions, glass was chosen as the fabrication material for the microreactors. Glass is chemically inert, it has good optical properties and it is durable. Glass microreactors are often reused multiple times and efficiently cleaned with a piranha solution (H_2SO_4 and H_2O_2 , 3:1 v/v). Furthermore, the choice of borosilicate glass as a fabrication material has also the practical advantage of being compatible with the

standard glass chip fabrication⁴⁷ at MESA⁺. The process is fairly simple: channels are isotropically etched in one or both glass wafers; inlet and outlet holes for the fluidic connections are powderblasted in the top wafer; after which the wafer pair is fusion-bonded. Two main chip designs were realized having channel cross-sections of $100 \times 50 \mu\text{m}^2$ and $50 \times 20 \mu\text{m}^2$, respectively. A few examples of microreactor chips are shown in Figure 4.8.

4.7. Continuous flow microreactors

Since the ultimate goal of this work was to study organic reactions on-chip by mass spectrometry, flow-driven actuation was chosen as the most suitable mechanism to transport reactant solutions through the microchannels in a continuous flow manner (see Chapter 2). After the reaction has taken place the reaction mixtures (products, intermediates and unreacted reagents) are eventually injected into the mass spectrometer where they are analyzed. Electroosmotically driven flow (EOF) may also be used, in which case platinum electrodes are sputtered through a shadow mask in the inlet and outlet cavities after bonding.⁴⁸ All microreactors consist of a microchannel where reactions proceed for different periods of times, depending on the channel geometry and, of course, the flow rates. Heating or cooling of the microreactor takes place by heaters or Peltier elements and can be controlled by temperature sensors (see Chapter 3).

Due to the small channel dimensions, mixing in microchannels takes place by diffusion. The diffusion time t_d [s] is given by equation 4.1.

$$t_d = \frac{L^2}{D} \quad (4.1)$$

where L [m] is the distance over which diffusion must take place and D [$\text{m}^2 \text{s}^{-1}$] is the diffusion coefficient (see Chapter 2).

Enhancement of mixing in microchannels⁴⁹ is often obtained by integrating micromixer units in the channel design. More simply, complete mixing in microchannels is obtained under laminar flow conditions either by increasing the

residence time or by increasing the diffusion velocity by decreasing the diffusion path. Both types of microreactors designed to be used in combination with the NESIC-MS interface rely on reagents mixing under laminar flow conditions. The channel width / depth aspect ratio in channels etched by isotropic HF chemical etching is higher than 1, which results in rather large diffusion lengths when two channels merge in the wafer plane. In the 100 μm wide by 50 μm deep microreactors (Figure 4.8c) diffusion occurs along the width of the channel (100 μm), resulting in diffusion times in the order of seconds (about 10 s assuming $D = 1 \times 10^{-9} \text{ m}^2 \text{ s}^{-1}$). In order to increase the mixing speed without introducing complex mixer units in the microchannel a new chip design was developed, based on the vertical lamination of the two incoming flows (Figures 4.8a, 4.8b, and 4.8d). To ensure a stable lamination of flows the channels are etched separately in two wafers and merge in a smooth way. After running in parallel for 100 μm , one channel stops such that the channel size is reduced to half the run-in height. Typical cross-section dimensions of the channels for both the mixer and the reactor are 50 μm wide by 20 μm deep, which means that with the chosen vertical lamination, the diffusion time could be reduced 6.25 times compared to conventional merging of two flows in-plane with similar channel dimensions and improved 25 times compared to the old, 100 μm wide channels.⁵⁰ Assuming a diffusion coefficient $D = 1 \times 10^{-9} \text{ m}^2 \text{ s}^{-1}$, based on equation 4.1, a diffusion time $t_d = 400 \text{ ms}$ is calculated in the 20 μm deep channels. This value drops to $t_d = 40 \text{ ms}$ with $D = 1 \times 10^{-8} \text{ m}^2 \text{ s}^{-1}$ for small ions (*i.e.* H^+) in water.⁵¹

4.8. Microreactor mixing evaluation

The performances of the mixer were evaluated by computer simulation using the CFDRC ACE+⁵² programme (Figure 4.9). In the theoretical simulation complete mixing of water molecules in water injected at a total flow rate of 2 $\mu\text{L min}^{-1}$ is achieved within a few tens of milliseconds. Figure 4.11a shows the diffusion and lateral migration during starting-up. Due to the pressure-driven flow the front of the injected flow shows a large parabolic deformation such that not only radial diffusion (wanted) but also lateral convective migration is obtained. Although lateral diffusion

is an unwanted effect (since it gives rise to time-delay effects in the reactor) it is inevitable in Poiseuille flow systems.

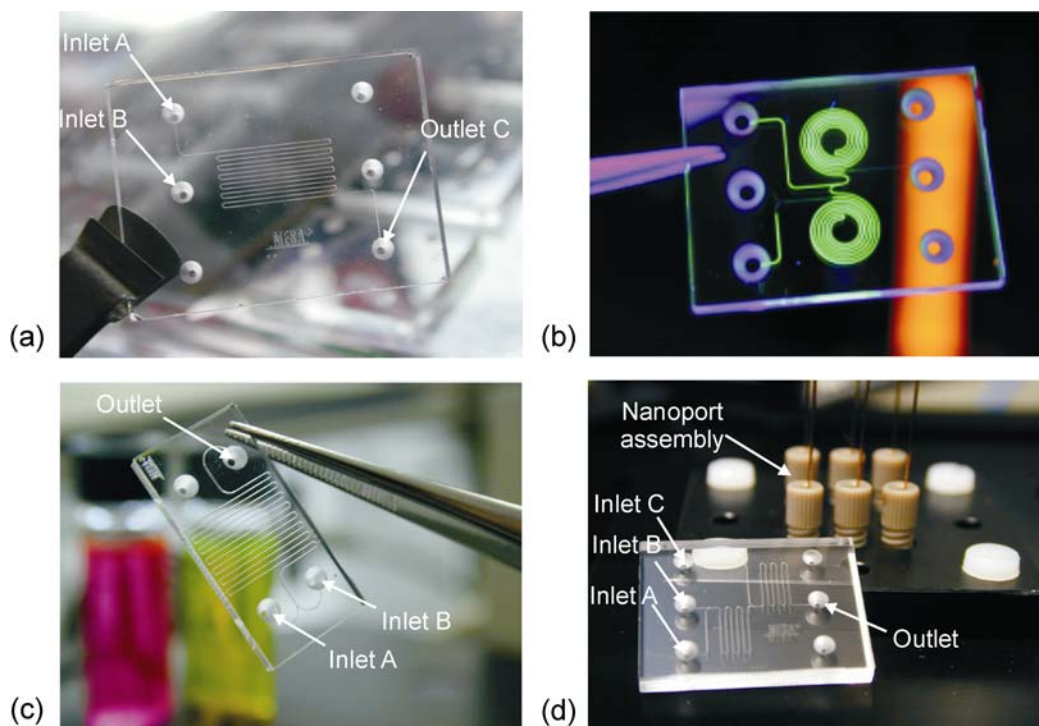


Figure 4.8. Examples of (a) a 50 μm wide by 20 μm deep single microreactor chip, (b) a 50 μm wide by 20 μm deep double microreactor chip, (c) a 100 μm wide by 50 μm deep single microreactor chip, and (d) a 50 μm wide by 20 μm deep double microreactor chip with Nanoport™ assemblies for fitting fibers and capillaries into the powderblasted inlet and outlet cups.

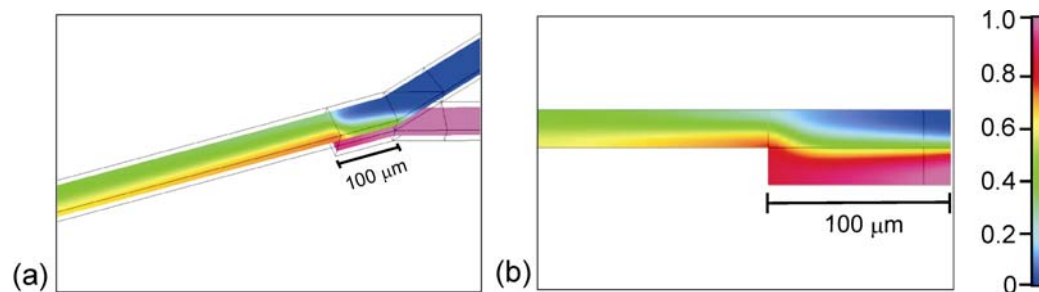


Figure 4.9. (a) Steady-state simulation of the mixing of two laminated flows in the microchannel, top view half-way in the channel. (b) Side view of the mixing profile at the junction of the two channels; because of the channel height reduction diffusion is increased.

A study of the mixing dynamics in both 100 μm wide by 50 μm deep and 50 μm wide by 20 μm deep channels was performed by injecting a solution of fluorescein in water (pH = 8.4) in inlet A and a solution of hydrochloric acid in water (pH = 4) in inlet B of the chip at total flow rates ranging between 0.2 and 2 $\mu\text{L min}^{-1}$. Monitoring the pH-dependent quenching of the fluorescence of solution A, induced by mixing with solution B, allows to study the on-chip mixing dynamics.⁵³

The results of this study in the 50 wide by 20 μm deep channels are reported in Figure 4.10. At a total flow rate of 0.2 $\mu\text{L min}^{-1}$ (Figure 4.10a), complete mixing is within the first 100 μm of the reaction channel, (where the depth is 40 μm), which correspond to a residence time $t_{\text{res}} = 60$ ms, as calculated from equation 4.2.

$$t_{\text{res}} = \frac{l \cdot A}{\phi_v} \quad (4.2)$$

where l [m] is the length of the channel portion with a double depth (100 μm), A [m^2] is the cross-section area, and ϕ_v [$\text{m}^3 \text{s}^{-1}$] is the volumetric flow rate.

At higher flow rates the mixing becomes less efficient, although complete within a few hundred μm channel length. As expected, based on the larger diffusion distance, a much longer mixing time (in the order of seconds) was observed in the 100 wide by 50 μm deep channels. The results of this experiment are in good agreement with the theoretical simulation (*vide supra*). In Figure 4.11 both the simulated and experimental mixing profile at relatively high flow rate (2 $\mu\text{L min}^{-1}$) are shown.

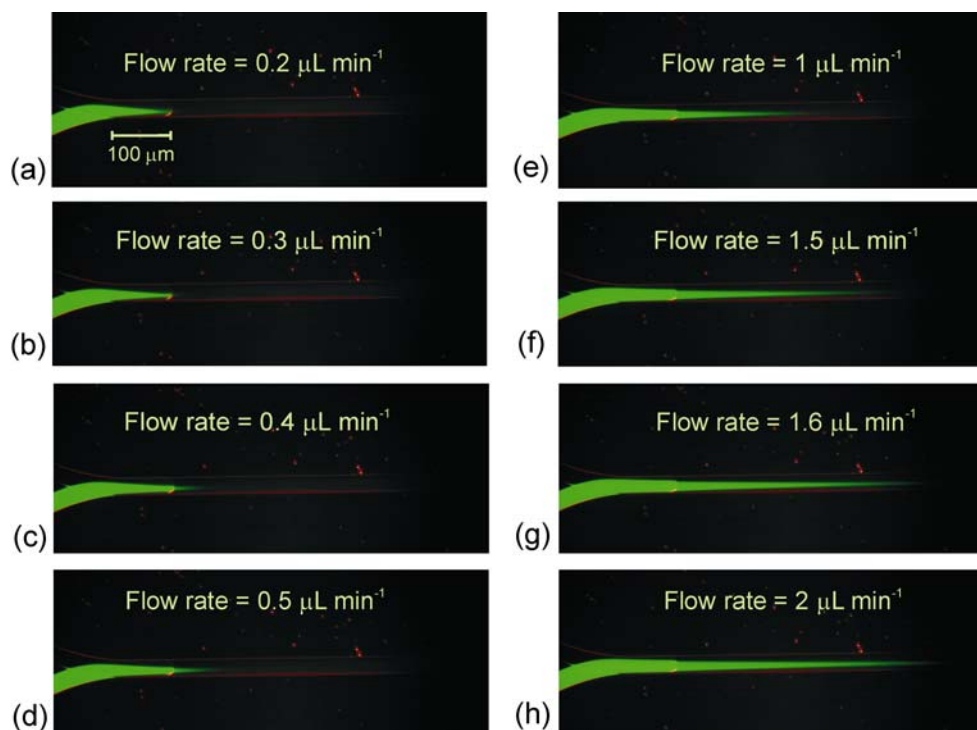


Figure 4.10. Sequence of fluorescence microscope images describing the mixing dynamics in the 50 μm wide by 20 μm deep channels. Quenching of the fluorescence of a solution of fluorescein indicates complete mixing of the reagents injected at total flow rates ranging between 0.2 and 2 $\mu\text{L min}^{-1}$ (from a to h). The double amount of fluorescein in the 40 μm deep channel (first 100 μm) than that in the 20 μm deep channel is clearly visible in the images, due to the higher fluorescence intensity.

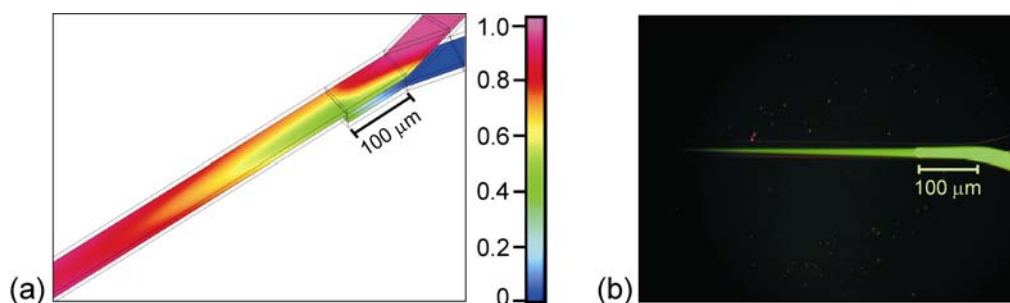


Figure 4.11. (a) Transient simulation result of the diffusion profile during injection of one of the flows resulting in the formation of a parabolic concentration profile. (b) Measured stationary concentration profile, which resembles the result of Figure 4.9a.

4.9. Conclusions

In contrast to many sophisticated interfacing designs reported in the recent literature, two simple microfluidics integrated systems were designed and realized for coupling microreactors to a nanoflow ESI mass spectrometer. A monolithic and a modular integration approach were developed and their mass spectrometric performances were evaluated by infusing a solution of reserpine in a mixture of water and acetonitrile (1:1 v/v) as a standard solution. Sample infusion flow rates and nebulizing gas pressure turned out to be most important parameters determining the ionization efficiency of the modular design. Both interfaces give a high quality Taylor cone and signal stability, as indicated by the standard deviations calculated over the TIC chromatogram ($SD \approx 8\%$ and 1% for the monolithic and modular interfaces, respectively). Due to the better performances and the versatility offered by the design, the modular interface, based on the use of commercially available Picotip™ emitters, was used in the final set-up. The modular integration allows the replacement of the spraying tips, independently from the more expensive chips, as often as required to avoid samples cross-contamination. More importantly, the microreactors can be easily replaced, offering the possibility to study a wide variety of (bio)chemical reactions. The novel mixing concept, integrated in the chip design and enabling complete reagent mixing within a few tens of milliseconds, makes the set-up suitable to study reaction dynamics. The high-throughput potential of the modular NESIC-MS system will be demonstrated in Chapters 5 and 6.

4.10. Experimental

Both monolithic and modular interfaces were realized in cooperation with Dr. E. R. Oosterbroek.

Monolithic interface. The spraying channel (cross-section = $100 \times 50 \mu\text{m}^2$) was obtained by dicing a glass chip perpendicularly to the channel direction. The 3M FC-722/FC-40 fluoro-containing coating was applied around the spraying orifice to change the wettability of the surface. A fused silica capillary for infusing the sample solutions into the channel was fitted into the powderblasted inlet reservoir by using

Araldite Rapid epoxy adhesive (Ciba-Geigy). The nebulizing argon gas was connected to the chip *via* a Teflon tube, screwed into a glued plexiglass piece by means of a Minstack™ (Lee) type of connector.

Ionization rate evaluation set-up. The chip was mounted on the set-up depicted in Figure 4.3b. A 10^{-3} M phosphate buffer of pH 7.4 (Sigma) was dispensed at flow rates in the range of nL min^{-1} to tens of $\mu\text{L min}^{-1}$. Various potentials were applied (up to 1,000 V) *via* a platinum electrode sputtered in the inlet cup. A counterelectrode was located at very close proximity (~ 5 mm) of the exposed channel at the chip's edge. The reciprocal position of electrode (D) and counterelectrode (H) resembles the configuration of the ESI mass spectrometer used in the measurements (z-spray).

ESI-MS process evaluation set-up. The chip glued onto the metal holder depicted in Figure 4.3a was screwed on the Nanospray™ interface of the mass spectrometer. Cone gas (automatically controlled via the ESI-MS software) was set at a value of 260 l h^{-1} . Nebulizing argon gas was dispensed at various pressures up to about 8 bar.

Modular interface. Microreactor chips were mounted on a dedicated holder (Figure 4.5), placed on the Nanospray™ interface of the mass spectrometer using a metal plate. Solutions were introduced on-chip via fused silica capillaries (o.d. = $360 \mu\text{m}$) of 100, 40, or $20 \mu\text{m}$, depending on the microchannel cross-sectional dimension and on the flow rates. New Objective Picotip™ emitters (o.d = $360 \mu\text{m}$; i.d. = 20 and $40 \mu\text{m}$; tip diameter = 5 and $10 \mu\text{m}$) were used to spray the sample into the mass spectrometer. Capillaries and emitters were placed in the inlet and outlet cups, respectively, and kept in place by means of Upchurch Nanoport™ assemblies. The potential, controlled via the ESI-MS software, was applied through an electrical connection attached to the holder (see Figure 4.5).

Fluidic handling. Mobilization of sample solutions was done in all experiments by means of a dual CMA/102 Microdialysis Pump on which $100 \mu\text{L}$ flat tip Hamilton syringes were mounted. Syringes were connected to fused silica capillaries by means of Upchurch™ connectors.

ESI-MS process evaluation experiments. ESI-MS experiments were performed using a Micromass (Manchester, UK) LCT electrospray time-of-flight mass

spectrometer (ESI-TOF-MS). A 1.6×10^{-4} M solution of reserpine in a mixture of acetonitrile and water (1:1 v/v) was used as a standard. Acetic acid (0.1 %) was added to the solution in order to enhance analyte protonation. For both monolithic and modular interfaces, samples were infused at flow rates ranging between a few tens of nL min^{-1} to a few $\mu\text{L min}^{-1}$. Spectra were acquired at various capillary, cone, and extraction voltages and optimized for each of the interfaces (see text).

Microchips. All glass (Schott Borofloat 33) chips were fabricated at the cleanroom facilities of the MESA⁺ Institute for Nanotechnology at the University of Twente by Ing. M. H. Goeldbloed. High precision powderblast micromachining was used for the fabrication of inlet and outlet holes, while the reaction microchannel was made *via* HF chemical etching.

Mixing simulation was carried out by Dr. E.R. Oosterbroek, using the CFDRC ACE+⁵² programme. The mixing time was estimated assuming diffusion of water molecules in water (injected at a total flow rate of $2 \mu\text{L min}^{-1}$) across the microchannel.

Mixers characterization. Studies of the mixing dynamics were carried out in cooperation with Dr. E. R. Oosterbroek according to literature procedures.⁵³ The mixing dynamics in both microchannels was evaluated using an Olympus CK40M inverted microscope with fluorescence kit.

4.11. References

- 1 Gaskell, S. J. *J. Mass Spectrom.* **1997**, *32*, 677.
- 2 Bateman, K. P.; White, R. L.; Thibault, P. *Rapid Commun. Mass Spectrom.* **1997**, *11*, 1253.
- 3 Figeys, D.; Ducret, A.; Abersold, R. *J. Chromatogr. A* **1997**, *763*, 295.
- 4 Davis, M. T.; Stahl, D. C.; Hefta, S. A.; Lee, T. D. *Anal. Chem.* **1995**, *67*, 4549.
- 5 Henry, C. *Anal. Chem.* **1997**, *69*, 359A.
- 6 De Mello, A. J. *Lab Chip* **2001**, *1*, 7N.
- 7 Fenn, J. B. Z.; Mann, M.; Meng, C. K.; Wong S. F.; Whitehouse, C. M. *Science* **1989**, *246*, 64.
- 8 Meng, C. K.; Mann, M.; Fenn, J. B. Z. *Phys. D* **1988**, *10*, 361.
- 9 Fenn, J. B. Z.; Mann, M.; Meng, C. K.; Wong, S. F.; Whitehouse, C. M. *Mass Spectrom. Rev.* **1990**, *9*, 37.
- 10 Smith, R. D.; Loo, J. A.; Edmonds, C. G.; Barinaga, C. J.; Udseth, J. R. *Anal. Chem.* **1990**, *62*, 882.
- 11 Wilm, M.; Mann, M. *Anal. Chem.* **1996**, *68*, 1.
- 12 Khandurina, J.; Guttman, A. *J. Chromatogr. A* **2002**, *943*, 159.
- 13 Figeys, D.; Pinto, D. *Electrophoresis* **2001**, *22*, 208.
- 14 Mouradian, S. *Curr. Opin. Chem. Biol.* **2001**, *6*, 51.
- 15 Xue, Q.; Dunayevskiy, Y. M.; Foret, F.; Karger, B. L. *Rapid Commun. Mass Spectrom.* **1997**, *11*, 1253.
- 16 Xue, Q.; Foret, F.; Dunayevskiy, Y. M.; Zavrachy, P. M.; McGruer, N. E.; Karger, B. L. *Anal. Chem.* **1997**, *69*, 426.
- 17 Ramsey, R. S.; Ramsey, J. M. *Anal. Chem.* **1997**, *69*, 1174.
- 18 Figeys, D.; Ning, Y. B.; Abersold, R. *Anal. Chem.* **1997**, *16*, 3153.
- 19 Oleschuk, R. D.; Harrison, D. J. *Trends Anal. Chem.* **2000**, *19*, 379.
- 20 Desai, A.; Tai, Y.-C.; Davis, M. T.; Lee, T. D. *Proc. Transducers '97*, Chicago, U S A, **1997**, *2*, 927.
- 21 Wen, J.; Lin, Y.; Xiang, F.; Matson, D. W.; Udseth, H. R.; Smith, R. D. *Electrophoresis* **2000**, *21*, 191.
- 22 Yuan, C. H.; Shiea, J. *Anal. Chem.* **2001**, *73*, 1080.
- 23 Kim, J.-S.; Knapp, D. R. *J. Chromatogr. A* **2001**, *924*, 137.
- 24 Rohner, T. C.; Rossier, J. S.; Girault, H. H. *Anal. Chem.* **2001**, *72*, 5353.

- 25 Licklider, L.; Wang, X. Q.; Desai, A.; Tai, Y. C.; Lee, T. D. *Anal. Chem.* **2000**, *72*, 367.
- 26 Lazar, I. M.; Ramsey, R. S.; Jacobson, S. C.; Foote, R. S.; Ramsey, J. M. *J. Chromatogr. A* **2000**, *892*, 195.
- 27 Griss, P.; Melin, J.; Sjö Dahl, J.; Roeraade, J.; Stemme, G. *J. Micromech. Microeng.* **2002**, *12*, 682.
- 28 Chiu, C.-H.; Lee, G. B.; Hsu, H.-T.; Chen, P.-W.; Liao, P.-C. *Sens. Actuators B* **2002**, *86*, 280.
- 29 Schilling, M.; Nigge, W.; Rudzinski, A.; Neyer, A.; Hergenröder, R. *Lab Chip* **2004**, *4*, 220.
- 30 Svedberg, M.; Veszelei, M.; Axelsson, J.; Vangbo, M.; Nikolajeff, F. *Lab Chip* **2004**, *4*, 322.
- 31 Wang, Y.-X.; Cooper, J. W.; Lee, C. S.; De Voe, D. L. *Lab Chip* **2004**, *4*, 363.
- 32 Kameoka, J.; Orth, R.; Ilic, B.; Czaplewski, D.; Wachs, T.; Craighead, H. G. *Anal. Chem.* **2002**, *74*, 5897.
- 33 White, T. P.; Wood, T. D. *Anal. Chem.* **2003**, *75*, 3660.
- 34 Lion, N.; Gellon, J.-O.; Jensen, H.; Girault, H. H. *J. Chromatogr. A* **2003**, *1003*, 11.
- 35 Cavanagh, J.; Benson, L. M.; Thompson, R.; Naylor, S. *Anal. Chem.* **2003**, *75*, 3281.
- 36 Mitchell, M. C.; Spikmans, V.; De Mello, A. J. *Analyst* **2001**, *126*, 24.
- 37 Dethy, J.-M.; Ackerman, B. L.; Delatour, C.; Henion, J. D.; Shultz, G. A. *Anal. Chem.* **2003**, *75*, 805.
- 38 Keetch, C. A.; Hernandez, H.; Sterling, A.; Baumert, M.; Allen, M. H.; Robinson, C. V. *Anal. Chem.* **2003**, *75*, 4937.
- 39 Benetton, S.; Kameoka, J.; Tan, A.; Wachs, T.; Craighead, H.; Henion, J. D. *Anal. Chem.* **2003**, *75*, 6430.
- 40 Zamfir, A.; Vakhrushev, S.; Sterling, A.; Niebel, H. J.; Allen, M.; Peter-Katalinić, J. *Anal. Chem.* **2004**, *76*, 2046.
- 41 Kebarle, P.; Tang, L. *Anal. Chem.* **1993**, *65*, 972 A.
- 42 For reviews on the electrospray ionization mechanism see: a) Kebarle, P.; Peschke, M. *Anal. Chim. Acta* **2000**, *406*, 11. b) Kebarle, P. *J. Mass Spectrom.*

- 2000**, 35, 804. c) Rohner, T. C.; Lion, N.; Girault, H. H. *Phys. Chem. Chem. Phys.* **2004**, 6, 3056.
- 43 Schmidt, A.; Karas, P. *J. Am. Soc. Mass Spectrom.* **2003**, 14, 492.
- 44 Juraschek, R.; Dülcks, T.; Karas, M. *J. Am. Soc. Mass Spectrom.* **1999**, 10, 300.
- 45 Zhang, B.; Liu, H.; Karger, B. L.; Foret, F. *Anal. Chem.* **1999**, 71, 3258.
- 46 Jenkins, G.; Manz, A. *J. Micromech. Microeng.* **2002**, 12, N19.
- 47 Gardeniers, J. G. E.; Oosterbroek, R. E.; Van den Berg, A. in: Oosterbroek R. E.; Van den Berg, A. (eds), *Lab-on-a-Chip, Miniaturized Systems for (Bio) Chemical Analysis and Synthesis*, **2003**, 37.
- 48 Oosterbroek, R. E.; Goedbloed, M. H.; Van den Berg, A. *Proc. μ TAS'01*, Monterey, USA, **2001**, 627.
- 49 Jensen, K. *Nature* **1998**, 393, 735.
- 50 Knight, J. B.; Vishwanath, A.; Brody, J. P.; Austin, R. H. *Phys. Rev. Lett.* **1998**, 80, 3863.
- 51 Atkins, P. W. *Physical Chemistry*, 5th ed., Oxford University Press: Oxford, UK, **1994**.
- 52 CFD Research Corporation, 215 Wynn Drive, Huntsville, Alabama 35805, USA.
- 53 Madhavan-Reese, S.; Lim, D.; Mazumder, J.; Hasselbrink Jr., E. F. *Proc. μ TAS'2002*, **2002**, 900.

Chapter 5

Supramolecular Interactions On-line Studied by Mass Spectrometry in a Nanoflow Electrospray Chip

Metal-ligand interactions of Zn-porphyrin 1 with pyridine (2), 4-ethylpyridine (3), 4-phenylpyridine (4), N-methylimidazole (5), and N-butylimidazole (6) in acetonitrile as well as host-guest complexations of β -cyclodextrin (7) with N-(1-adamantyl)acetamide (8) or 4-tert-butylacetanilide (9) in water were studied in the chip-based nanoflow electrospray (NESIC) interface described in Chapter 4. From mass spectrometric titrations of Zn-porphyrin with pyridine (2) or 4-phenylpyridine (4) in acetonitrile K_a values of $(4.6 \pm 0.4) \times 10^3 M^{-1}$ and $(6.5 \pm 1.2) \times 10^3 M^{-1}$, respectively, were calculated. The K_a values are about four times larger than those obtained with UV/vis spectroscopy in solution, probably due to a higher ionization efficiency of complexed compared to uncomplexed Zn-porphyrin. For the complexation of N-(1-adamantyl)acetamide with β -cyclodextrin a K_a value of $(3.6 \pm 0.3) \times 10^4 M^{-1}$ was obtained, which is comparable to that determined by microcalorimetry.

5.1. Introduction

Supramolecular chemistry,^{1,2} the chemistry beyond the molecule, has rapidly penetrated into many areas. It involves the study of processes based on noncovalent interactions and mimics the role of Nature in controlling biochemical processes by means of weak interactions such as hydrogen-bonding, Van der Waals forces, hydrophobic interactions, and electronic interactions.

Over the past decade, electrospray ionization mass spectrometry (ESI-MS) has been successfully used to study and characterize supramolecular complexes,³⁻⁵ after the detection of non-covalent receptor-ligand complexes by ESI-MS was first reported by Ganem *et al.* in 1991.⁶ A number of methods have been reported in the recent literature for the quantitative determination of non-covalent binding interactions using soft ionization mass spectrometry.^{7,8} However, to the best of our knowledge, supramolecular interactions have not yet been studied in a microreactor interfaced to a mass spectrometer.

In Chapter 4 a pressure-driven simple nanoflow electrospray ionization chip (NESIC) interface has been described, consisting of a glass microreactor mounted on an ESI-TOF-MS nanoflow interface. Monitoring of on-chip reactions was carried out by spraying the reaction mixture directly into the mass spectrometer by means of commercially available Picotip™ capillaries that guarantee a high quality, and a highly stable Taylor cone. The possibility to rapidly control reaction parameters such as reagent concentrations and reaction time makes the NESIC interface suitable for real-time studies of reactions.

The work described in this Chapter will demonstrate that the NESIC system provides a powerful tool to qualitatively as well as quantitatively study supramolecular interactions. It combines the advantages of microfluidics, such as fast low volume sample handling, with the high sensitivity and specificity of nanoflow ESI-MS analysis, and rapid screening offered by on-line detection. Two well-known supramolecular systems were studied, *viz.* Zn-porphyrin complexation with N-containing ligands in acetonitrile and the inclusion of small organic molecules into the cavity of β -cyclodextrin in water.

5.2. Microreactors

The two types of microreactors used are depicted in Figure 5.1. The Zn-porphyrin coordination reactions (Scheme 5.1) were studied in 100 by 50 μm microchannels (Figure 5.1a), while the β -cyclodextrin inclusion interactions (Scheme 5.2) were studied using 50 μm wide by 20 μm deep reaction channels (Figure 5.1b).

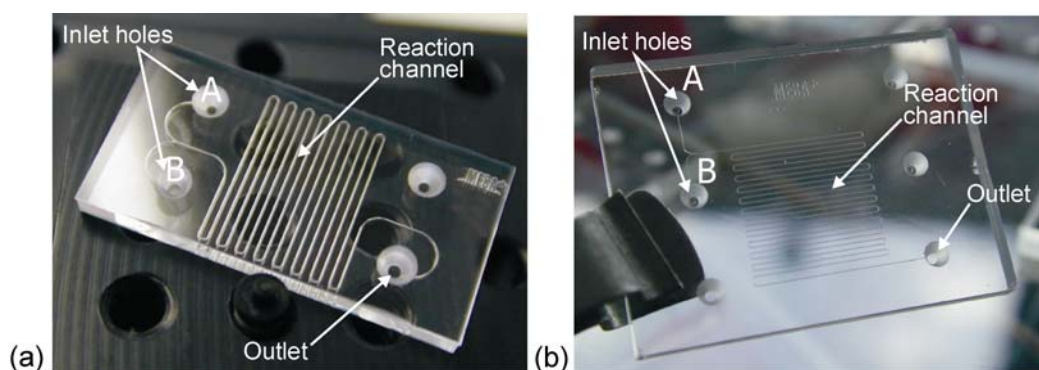
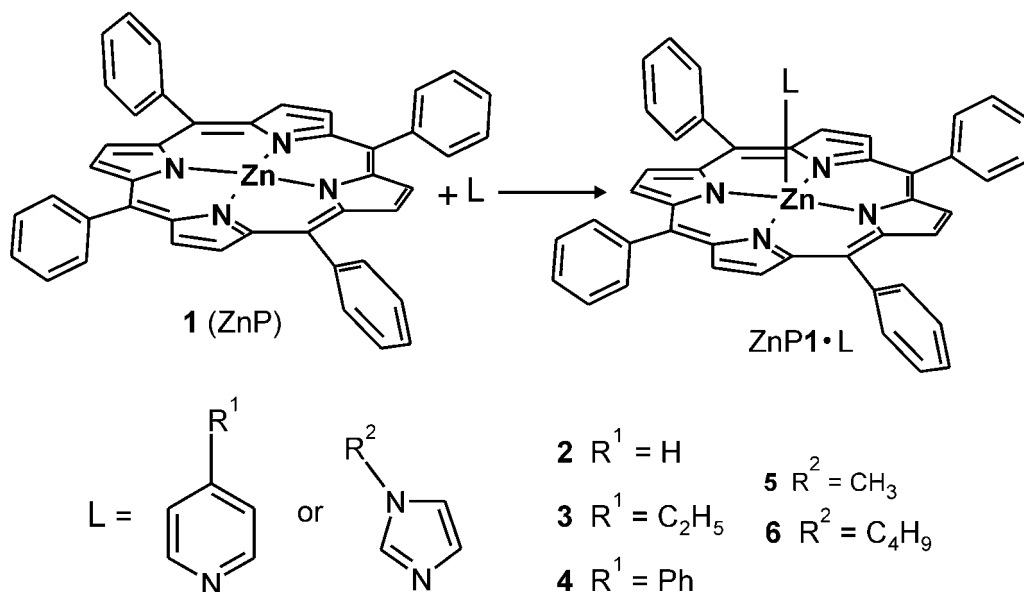


Figure 5.1. Photographs of the glass microreactors used: (a) the larger (100 μm wide by 50 μm deep) channels and (b) the smaller (50 μm wide by 20 μm deep) channels.

5.3. On-chip complexation studies

Metalloporphyrins, which include important complexes as chlorophyll and hemoglobin, represent a vast and unique group of compounds. By varying the metal center, the complexation behavior and characteristics of the metalloporphyrin can be dramatically affected. This great diversity is one of the reasons why metalloporphyrins have found broad application in the production of dyes, semiconductors, and catalysts, as well as in numerous studies spanning the chemical and biological fields.⁹



Scheme 5.1. Coordination of *N*-containing heterocyclic ligands (*L*) to the metal center of Zn-porphyrin **1**.

In Zn-porphyrin **1** the metal center has one binding site available for coordination of a guest molecule such as pyridine (**2**), 4-ethylpyridine (**3**), 4-phenylpyridine (**4**), *N*-methylimidazole (**5**), and butylimidazole (**6**), to yield the corresponding 1:1 complex. Experiments were carried out by injecting solutions of 2×10^{-4} M Zn-porphyrin ($C_{\text{on-chip}} = 1 \times 10^{-4}$ M) and of 1×10^{-3} M pyridine ($C_{\text{on-chip}} = 5 \times 10^{-4}$ M) in acetonitrile into the microreactor at decreasing total flow rates (400, 200, and 100 nL min^{-1}) and keeping constant the ratio between the flow rates at the two inlets (1:1). Figure 5.2 shows the spectra of the mixture after the resulting residence times of (a) 2.5 min, (b) 4.9 min, and (c) 9.9 min. The calculated fractions of Zn-porphyrin-pyridine complex (**1**·**2**) formed on-chip after these residence times are reported in Table 5.1. The fraction of complex formed after 2.5 min is identical to that at the longest residence times, indicating that thermodynamic equilibrium is already reached after 2.5 min. (*i.e.* at a flow rate of 400 nL min^{-1}). This result was confirmed by control experiments performed by analyzing aliquots withdrawn from a mixture of solutions of 1×10^{-4} M Zn-porphyrin **1** and 5×10^{-4} M pyridine at different times.

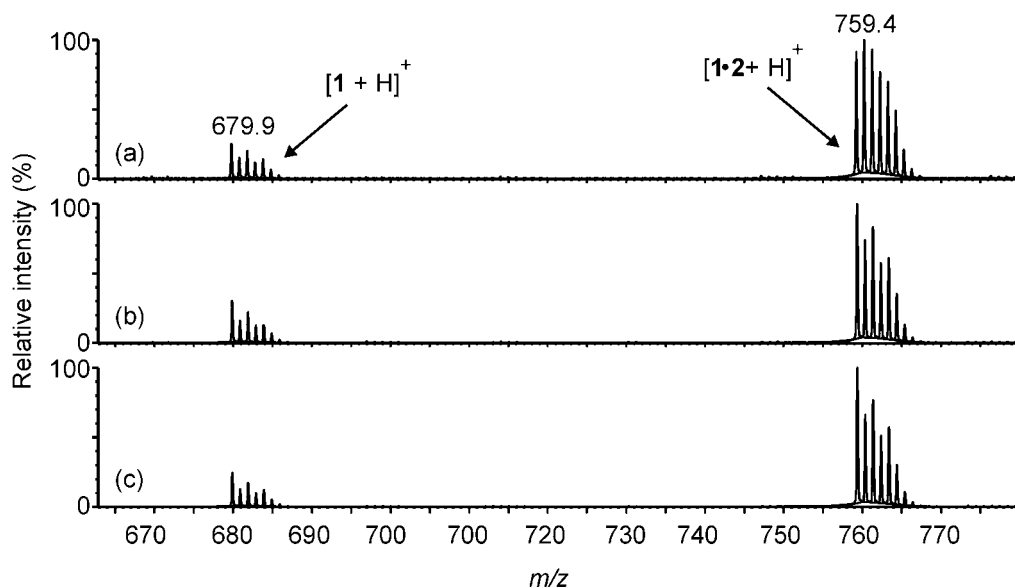


Figure 5.2. ESI-TOF mass spectra showing free Zn-porphyrin **1** ($m/z = 679.9$) and the **1·2** complex ($m/z = 759.4$) formed on-chip by mixing **1** ($C_{on-chip} = 1 \times 10^{-4} M$) and pyridine ($C_{on-chip} = 5 \times 10^{-4} M$) after residence times of (a) 2.5 min, (b) 4.9 min, and (c) 9.9 min.

Table 5.1. Fractions f^a of the Zn-porphyrin-pyridine complex **1·2** formed on-chip varying residence times.

Flow rate	Residence time	f
400 nL min ⁻¹	2.46 min	0.78 ± 0.01
200 nL min ⁻¹	4.93 min	0.77 ± 0.01
100 nL min ⁻¹	9.85 min	0.79 ± 0.01

^a $f = I_{1·2} / (I_{1·2} + I_1)$ where I is the ESI-MS relative signal intensity

It is known¹⁰ that pyridine derivatives, such as **2**, **3**, and **4**, have a comparable binding affinity for Zn-porphyrin **1**, whereas that of imidazoles **5** and **6** is higher. The behavior is evident from the ESI-MS spectra in Figure 5.3 where the relative intensities of the signals of the imidazole complexes **1·5** and **1·6** (Figures 5.3c and 5.3d) are significantly higher than those of the pyridine complexes **1·2** and **1·3** (Figures 5.3a and 5.3b). The four spectra were acquired in a total time of about half an hour, by mixing on-chip a 2×10^{-4} M solution of Zn-porphyrin **1** ($C_{\text{on-chip}} = 1 \times 10^{-4}$ M) injected in inlet A with 4×10^{-4} M solutions of respectively **2**, **3**, **5**, and **6** ($C_{\text{on-chip}} = 2 \times 10^{-4}$ M) injected in inlet B consecutively. Before switching between different guest solutions, solvent was flushed into inlet B. During all the experiments, the flow rate at each inlet was kept constant at 200 nL min^{-1} . These experiments clearly demonstrate the ability of the NESIC interface to provide a very fast screening tool, giving qualitative information about the relative binding strength of different ligands in a high-throughput fashion.

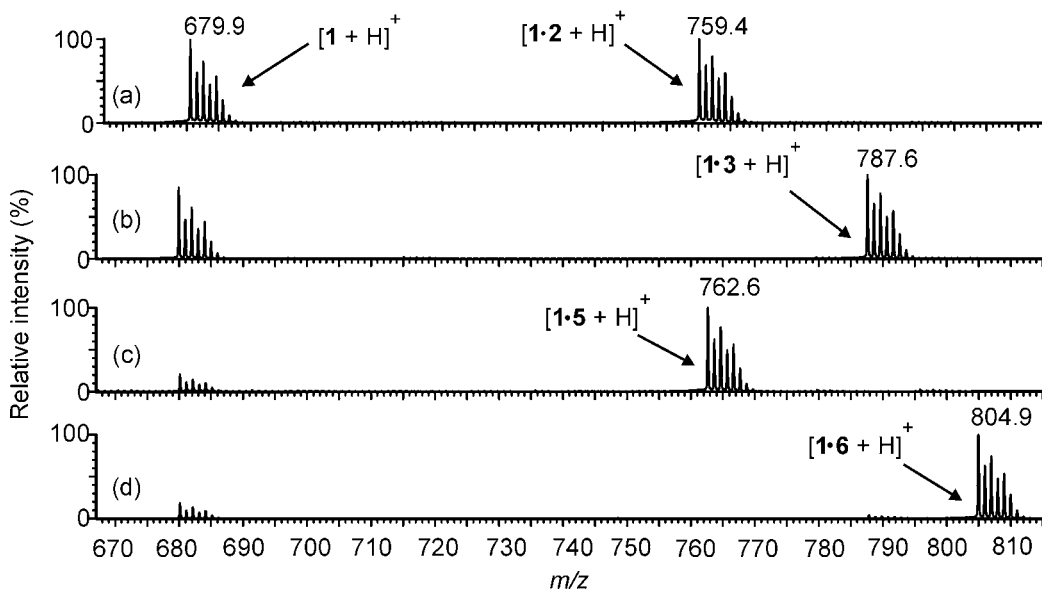


Figure 5.3. ESI-TOF mass spectra showing the free Zn-porphyrin **1** ($m/z = 679.9$) and the complexes formed on-chip when injecting a solution of 2×10^{-4} M of **1** in inlet A and 4×10^{-4} M solutions of (a) pyridine (**2**), (b) 4-ethylpyridine (**3**), (c) N-methylimidazole (**5**), and (d) butylimidazole (**6**), respectively, in inlet B.

A quantitative determination of the binding strength of pyridines **2** and **4** with Zn-porphyrin **1** in acetonitrile was achieved by on-chip titration experiments. Figure 5.4 shows a typical ESI-TOF mass spectra sequence, collected during an on-chip titration experiment performed by varying the ratio between the injection speed of Zn-porphyrin **1** and pyridine **2** stock solutions. Each ESI-TOF mass spectrum was recorded after an equilibration time of about 10 min between two different flow ratios. The experimental titration curves (dots) and the corresponding fits to a 1:1 model (solid lines) for both pyridines **2** and **4** are reported in Figure 5.5. For pyridine **2** and 4-phenylpyridine **4** K_a values of $(4.6 \pm 0.4) \times 10^3 \text{ M}^{-1}$ and $(6.5 \pm 1.2) \times 10^3 \text{ M}^{-1}$, respectively, were calculated.

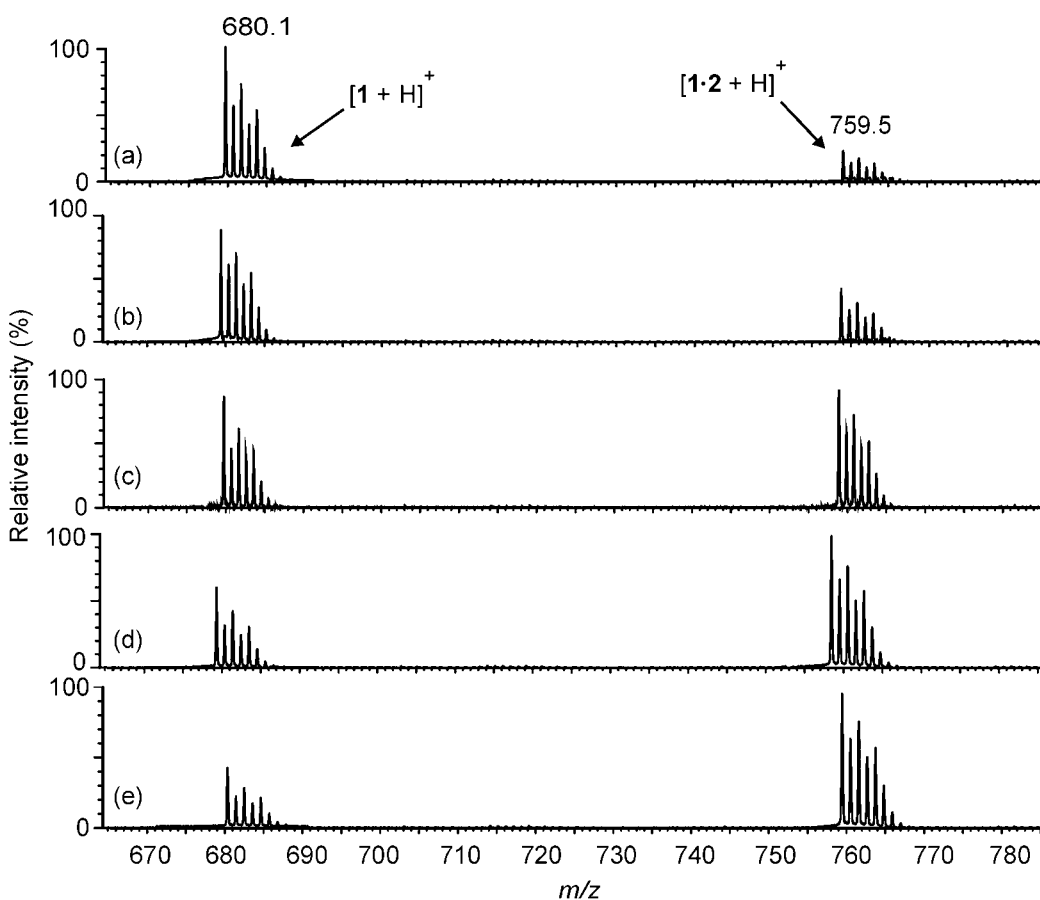


Figure 5.4. On-chip ESI-MS titration of Zn-porphyrin **1** ($1 \times 10^{-3} \text{ M}$) with pyridine (**2**; $1 \times 10^{-3} \text{ M}$) performed at varying reagents injection speed ratios: (a) 9:1, (b) 8:2, (c) 5:5, (d) 3:7, and (e) 1:9.

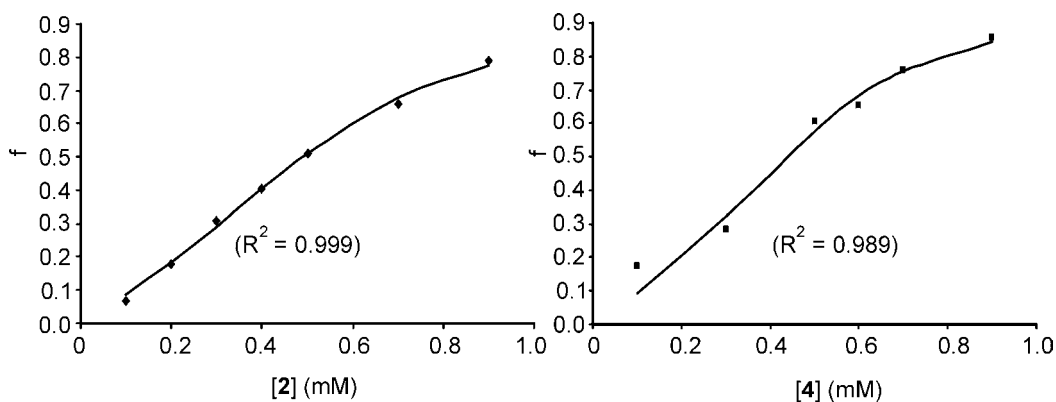


Figure 5.5. Experimental host-guest fractions (markers) as a function of the guest concentration calculated from on-chip ESI-TOF mass spectrometric titrations of Zn-porphyrin **1** with pyridine (**2**; left) and 4-phenylpyridine (**4**; right), and corresponding fit to a 1:1 binding model (solid lines).

For comparison, the same complexations were studied in acetonitrile by UV/vis spectrophotometry (Figure 5.6). Fitting the data to a 1:1 binding model (Figure 5.7), K_a values of $1.1 \times 10^3 \text{ M}^{-1}$ and $1.6 \times 10^3 \text{ M}^{-1}$ were found for pyridines **2** and **4**, respectively.

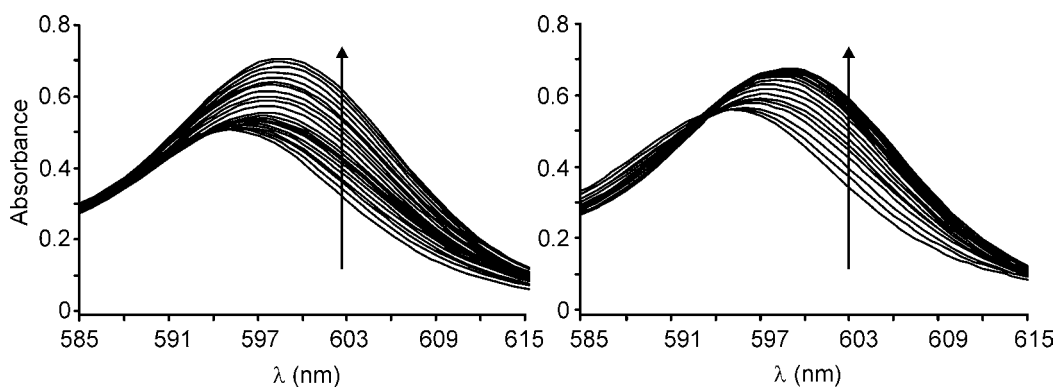


Figure 5.6. UV/vis titration of Zn-porphyrin **1** with (left) pyridine (**2**) and (right) 4-phenylpyridine (**4**) in acetonitrile.

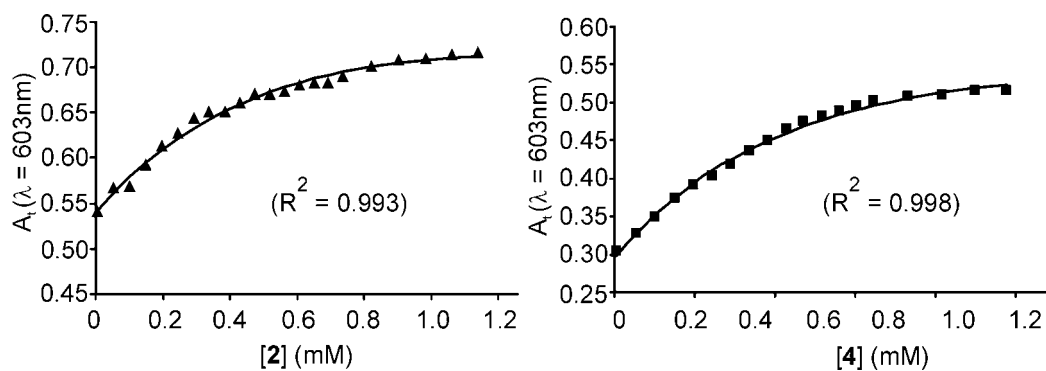


Figure 5.7. Experimental absorbance (markers) at $\lambda = 603 \text{ nm}$ plotted against the concentration of pyridine (**2**) (left) and of 4-phenylpyridine (**4**) (right), and corresponding fit to a 1:1 binding model (solid line).

The K_a values of the complexes of pyridines **2** and **4** with Zn-porphyrin **1** determined using the on-chip ESI-MS method are about four times higher than those determined by UV/vis spectroscopy. This difference indicates that, in the investigated metal-ligand complexation, the ESI-TOF mass spectra do not reflect factually the concentration of the species in solution. Differences in the relative vaporization and ionization efficiencies⁷ of the free and bound Zn-porphyrin **1** are very likely to be responsible for the deviation between solution and gas phase equilibria. In ESI-MS a number of instrumental¹¹ and chemical¹² parameters are known to influence the ionization efficiency and therefore the signal intensity of a given ion. Accounting for all these parameters, a transfer coefficient t_X can be defined for a given compound X, that corrects for the deviations of the ESI-MS signal intensity (I_X) from the real concentration of the species in solution $[X]$ via $I_X = t_X \times [X]$.⁷

Most of the quantitative studies reported in literature assume similar transfer coefficients for free host and host-guest complex, in particular, when the guest is much smaller than the host. However, this assumption is not always correct as demonstrated by a few studies reported in a recent review by Daniel *et al.*⁷ In particular, the difference in solvation energy between free host and host-guest complex in metal-ligand type of interactions has a large influence on the ionization efficiency of the species in solution.¹²

A higher ionization efficiency of the complexed Zn-porphyrins would explain the higher K_a values determined by ESI-MS as compared to those determined by

UV/vis. However, in both cases the relative binding strength of the different ligands remains the same (ESI-MS: $K_a \mathbf{1}\cdot\mathbf{4} / K_a \mathbf{1}\cdot\mathbf{2} = 1.4$; UV/vis: $K_a \mathbf{1}\cdot\mathbf{4} / K_a \mathbf{1}\cdot\mathbf{2} = 1.4$).

Competition experiments were performed by mixing on-chip a 1×10^{-3} M solution of Zn-porphyrin **1** with a mixture of pyridines **2** and **4** (1×10^{-3} M total concentration) at 400 nL min^{-1} , 200 nL min^{-1} , and 100 nL min^{-1} flow rates. In all cases the ratio between the fractions of the **1**·**2** and **1**·**4** complexes is 1.40 ± 0.39 , which is consistent with the ratio found in the independent experiments (*vide supra*).

The experiments described so far have been carried out by diluting reagent solutions on-chip in a continuous flow fashion. Because of the absence of a rinsing step between different flow ratios, a possible limitation of the on-chip titration method might be the contamination between solutions at different concentrations. To verify the reliability of the method titration experiments of Zn-porphyrin **1** with pyridine (**2**) were performed keeping the Zn-porphyrin concentration on-chip constant at 1×10^{-4} M or 2×10^{-4} M (respectively) and injecting solutions of pyridine **2** at different concentrations in the second inlet. The experimental titration curves (dots) and the corresponding fits (solid lines) are given in Figure 5.8. The calculated K_a value of $(5.3 \pm 0.8) \times 10^3 \text{ M}^{-1}$ is in good agreement with that determined *via* the titration performed by varying the reagents flow ratios (*vide supra*). The values of the correlation coefficient between experimental and calculated sets of data ($R^2 = 0.991$ and $R^2 = 0.996$) indicate in both cases a good fitting of the experimental data to the theoretical model. These results clearly show that upon changing the flow ratios within a single on-chip titration experiment no significant contamination takes place, probably due to the very efficient mixing in the microchannel.

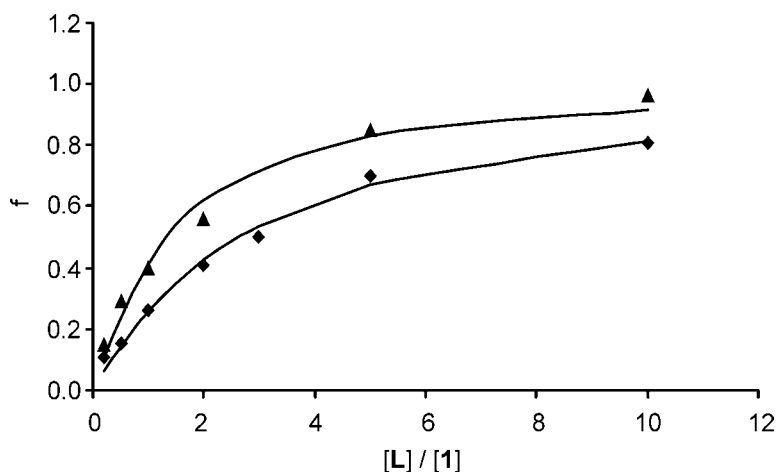
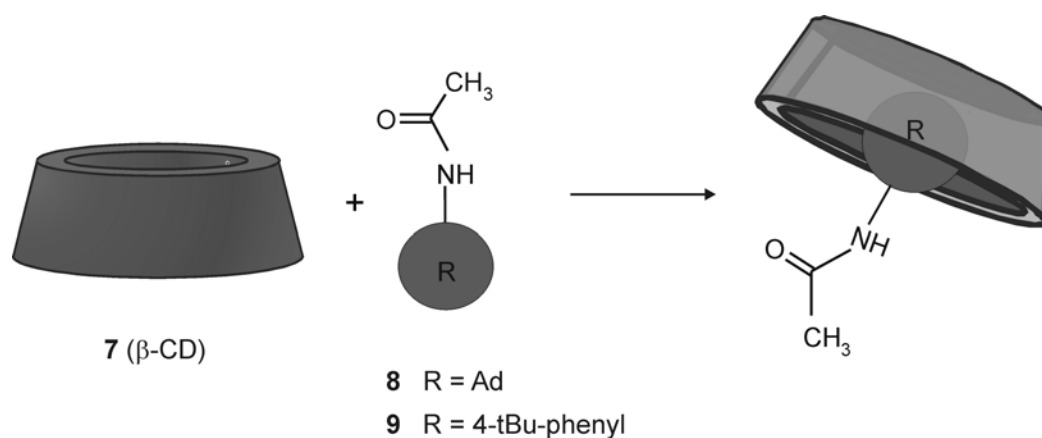


Figure 5.8. Experimental curves (markers) determined by on-chip ESI-TOF mass spectrometric titrations of (▲) $1 \times 10^{-4} M$ and (■) $2 \times 10^{-4} M$ Zn-porphyrin **1** with pyridine (**2**), and corresponding fit to a 1:1 binding model (solid lines).

To study the validity of the method a second type of supramolecular host-guest complex was investigated, namely the encapsulation of small organic molecules into the cavity of β -cyclodextrin (**7**) in aqueous media (Scheme 5.2), driven by the so-called “hydrophobic effect”.¹³ Due to their ability to encapsulate guests in their hydrophobic cavity, cyclodextrins¹⁴ are interesting molecules for applications in drug carrier systems¹⁵, food industry,¹⁶ cosmetics,¹⁶ and various industrial processes¹⁷.



Scheme 5.2. Encapsulation of *N*-(1-adamantyl)acetamide (**8**) and 4-*tert*-butylacetanilide (**9**) in the hydrophobic β -cyclodextrin (**7**) cavity.

p-*tert*-butylphenyl and adamantyl derivatives¹⁸ are well-known guests for β -cyclodextrin in aqueous solution. As guests the neutral *N*-(1-adamantyl)acetamide (**8**) and 4-*tert*-butylacetanilide (**9**) were selected in order to minimize potential differences between the ionization properties of the free neutral host (β -CD) and the host-guest complex.

First, an aqueous solution of 4×10^{-5} M β -cyclodextrin (**7**) was injected in inlet A of the chip. Equimolar solutions of *N*-(1-adamantyl)acetamide (**8**) and, after flushing the channel with solvent, of 4-*tert*-butylacetanilide (**9**), were injected in inlet B (Figure 5.9) at a flow rate equal to that of the β -cyclodextrin solution. Table 5.2 summarizes the host-guest complex fractions f_{7-G} determined by ESI-MS and those calculated based on microcalorimetric experiments.¹⁹ It is evident that the ESI-MS data are in good agreement with those obtained with microcalorimetry.

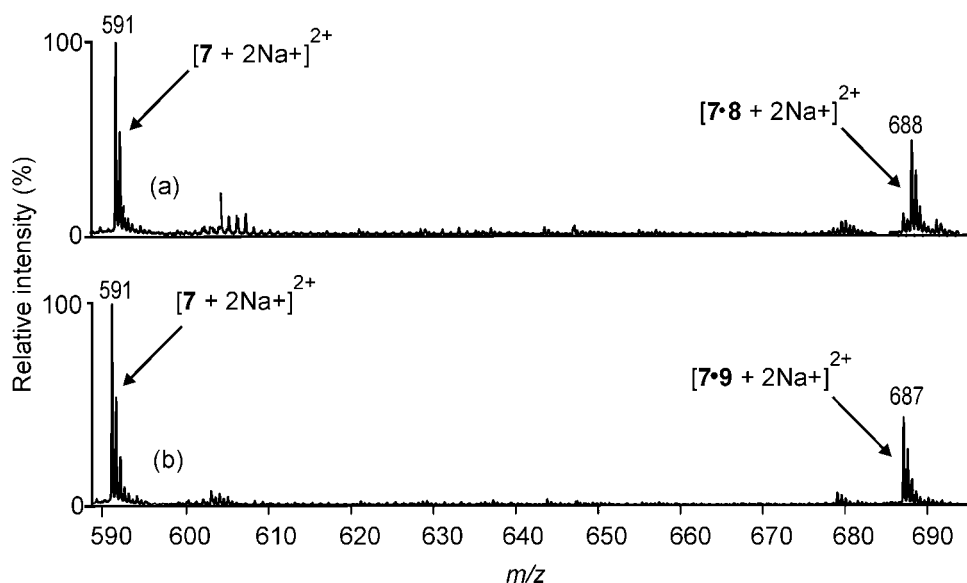


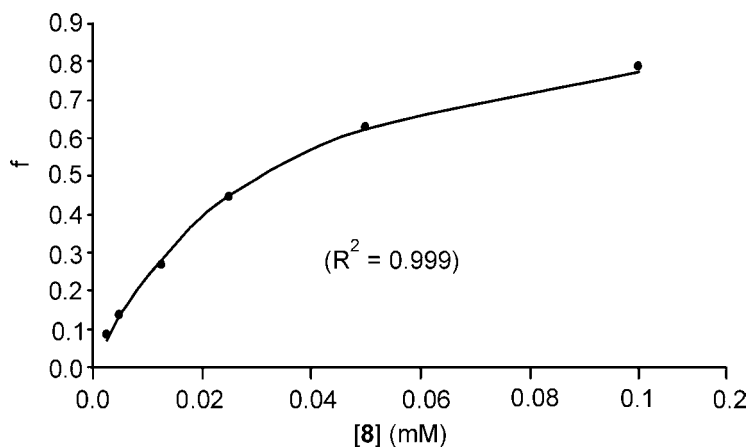
Figure 5.9. ESI-TOF mass spectra of the complexes formed on-chip upon injecting equimolar solutions (4×10^{-5} M) of β -cyclodextrin (**7**) and (a) *N*-(1-adamantyl)acetamide (**8**) or (b) 4-*tert*-butylacetanilide (**9**), respectively, at equal flow rates.

Table 5.2. Molar fractions of the β -cyclodextrin-guest complexes [$f_{(7-G)}$] determined by ESI-MS on-chip experiments and data based on microcalorimetric studies.

On-chip ESI-MS experiments		Microcalorimetric data ¹⁹	
Guest	$f_{(7-G)}$	K_a (M^{-1})	$f_{(7-G)}$
7	0.39 ± 0.02	6.8×10^4	0.43
8	0.31 ± 0.02	3.0×10^4	0.30

^a $f_{(7-G)} = I_{7-G} / (I_{7-G} + I_7)$ where I is the ESI-MS relative signal intensity

Figure 5.10 shows the experimental titration curve (solid dots) and the corresponding fit (solid line) to a 1:1 binding model for the complexation of β -CD with *N*-(1-adamantyl)acetamide. The K_a value of $(3.6 \pm 0.3) \times 10^4 M^{-1}$ is in good agreement with that determined by microcalorimetry (Table 5.2). The somewhat lower K_a value found by on-chip ESI-MS is probably due to the 10% DMSO present in the reaction mixture to enhance the solubility of **8**.

**Figure 5.10.** Experimental (markers) host-guest fractions determined by on-chip mass spectrometric titrations of $5 \times 10^{-6} M$ β -CD with *N*-(1-adamantyl)acetamide, and corresponding fit (solid line) to a 1:1 binding model.

Compared to the extensive studies on cyclodextrin inclusion complexes in solution,¹⁴ corresponding studies in the gas phase are still very limited.^{20,21} During the solution-to-vacuum transfer in the mass spectrometer, the effect of solvent and counterions does not exist any longer. A main consequence is that electrostatic interactions might become dominant, resulting in “unspecific binding” between host and guest, rather than the expected inclusion complex.²² However, ESI-MS studies demonstrated that β -cyclodextrin complexes with amino acids in the gas phase are in fact inclusion complexes.^{23,24} In general, “a peak at the mass of an alleged complex is not a sufficient criterion to prove its specificity”.⁷ Compared to β -cyclodextrin (**7**), the corresponding α -cyclodextrin has one α -D-glucose unit less, resulting in a smaller cavity. In experiments injecting on-chip equimolar (2×10^{-5} M) solutions of α -CD and guests **8** and **9**, no complex could be detected by ESI-MS. This clearly proves the size-selectivity of β -cyclodextrins towards the guests **8** and **9**.

5.4. Conclusions

The modular interface described in Chapter 4 for the coupling of glass microreactors to a nanospray mass spectrometer was successfully used to investigate supramolecular complexations based on the metal-ligand interaction between Zn-porphyrin **1** and the *N*-containing guest molecules **2**, **3**, **4**, **5**, and **6**, and on the encapsulation of guests **8** and **9** in the cavity of β -cyclodextrin (**7**). Fast screening of the relative binding strength of all the selected guests for the corresponding host was possible because the on-line analysis was carried out in a continuous flow manner. The K_a values of the Zn-porphyrin-pyridine and Zn-porphyrin-4-phenylpyridine complexes are about four times higher than those independently determined by UV/vis experiments, which is probably due to the lower ionization efficiency of the free host compared to that of the complexed Zn-porphyrin **1**. However, in the case of the β -cyclodextrin complexation with *N*-(1-adamantyl)acetamide (**8**) and 4-*tert*-butylacetanilide (**9**) the host-guest fractions and the determined K_a value are in good agreement with microcalorimetric data.

The titration method, based on rapidly varying the injection speed of reagent stock solutions into the mass spectrometer *via* a microreactor, offers a valuable

alternative to more conventional lab-scale methodologies, provided that the selected supramolecular system is suitable to be studied by ESI-MS and that mass spectrometric data are validated by control experiments.⁷ The most important advantages of this approach are the limited sample handling, the extremely short delay time between reaction and analysis, and the versatility of the integrated system that combines reaction and analytical unit in a very efficient interface.

The conclusion is that the combination of a microreactor with ESI-MS offers a powerful tool not only to study supramolecular interactions, but also for a variety of (bio)chemical reactions at the microscale.

5.5. Experimental

Microreactors. Both types of microreactors used (Figure 5.1) were fabricated using standard glass microfabrication technologies as described in Chapter 4. In order to provide a broader variety of residence times than those available by adjusting the pump flow rates only, various fluidic path shapes were exploited, resulting in variation of the channel lengths from 100 to 200 mm (corresponding to reaction volumes ranging between 0.5 and 1 μL ; Figure 5.1a) and from 13 to 71 mm (corresponding to reaction volumes ranging between 13 and 71 nL; Figure 5.1b), respectively.

Chemicals. All reagents were purchased from Sigma-Aldrich and used without further purification. Acetonitrile and a mixture of DMSO and water (1:9 v/v) were used as solvents to study the Zn-porphyrin **1** and β -cyclodextrin (**7**) complexation reactions, respectively, due to their suitability for both ESI-MS analysis and for the target complexation reaction.

On-chip experiments were performed by injecting reagent solutions into the microreactor at flow rates ranging between 100 and 400 nL min^{-1} (100 μm wide by 50 μm deep channels), and 20 and 100 nL min^{-1} (50 μm wide by 20 μm deep channels), by means of 100 μL syringes mounted on a CMA/102 Microdialysis Pump.

Qualitative studies of both types of complexation reactions were performed injecting solutions of host and guest molecules in a 1:2 and 1:1 ratio, resulting upon mixing on-chip in a final concentration of 2×10^{-4} M Zn-porphyrin **1**, and of 2×10^{-5} M β -cyclodextrin (**7**), respectively.

Quantitative binding studies were performed in both cases by on-chip mass spectrometric titration experiments.

a) Zn-porphyrin titrations by on-chip dilution. On-chip titrations of Zn-porphyrin **1** with both pyridine (**2**) and 4-phenylpyridine (**4**) were performed by simply varying injection speeds of 1×10^{-3} M solutions of reagents from 100 to 20 nL min⁻¹ and consequently varying the mixture composition.

b) Zn-porphyrin titrations with different titrant solutions. Keeping the total flow rate constant at 400 nL min⁻¹ and the ratio between injection speed at the two inlets at 1:1, two titration experiments were performed by injecting stock solutions of Zn-porphyrin **1** at concentrations of 2×10^{-4} M and 4×10^{-4} M, respectively, in inlet A. Solutions of pyridine (**2**) at concentrations ranging between 4×10^{-5} M and 1×10^{-3} M and between 8×10^{-5} M and 2×10^{-3} M were injected in inlet B. As a result in both titrations the on-chip final [1] / [2] ratios were 5:1, 2:1, 1:1, 1:2, and 1:5.

c) β -CD titrations by on-chip dilution. On-chip titrations of β -CD ($C_{\text{on-chip}} = 5 \times 10^{-6}$ M) were performed by injecting solutions of *N*-(1-adamantyl)acetamide (**8**) at concentrations ranging between 2.5×10^{-6} and 1×10^{-4} M. For all β -cyclodextrin encapsulation reactions formic acid (0.1%) was added to promote protonation of the otherwise neutral molecules.

ESI-MS detection. The complexation behavior was studied by spraying the reaction mixtures directly into the mass spectrometer, allowing real-time reaction monitoring. All complexations were followed by simultaneously monitoring the signal intensities of the singly charged free host (H) and host-guest complex (HG). Spectra were acquired in the positive ion mode at a capillary voltage ranging between 1.2 and 2.0 kV, at a sample cone of 15 V to prevent complex dissociation, and an extraction cone voltage of 2 V. The source temperature was kept constant at 100 °C and the cone gas flow between 80 and 90 L h⁻¹. The fractions of complexes $f_{(\text{HG})}$ were calculated as the

ratio between the complex intensity and the total host the intensities (free and bound) according to equation 5.1.

$$f_{(HG)} = \frac{I(HG)}{I(HG) + I(H)_f} \quad (5.1)$$

Association constants were calculated by fitting the experimental titration curves to a 1:1 binding model based on the K_a equation (equation 5.2) and the mass balances (equations 5.3 and 5.4), by applying a least squares optimization routine.

$$K_a = \frac{[HG]}{[H] \cdot [G]} \quad (5.2)$$

$$[H]_t = [HG] + [H]_f \quad (5.3)$$

$$[G]_t = [HG] + [G]_f \quad (5.4)$$

$[H]_f$ and $[G]_f$ are the concentrations of free host and free guest, respectively, and $[H]_t$ and $[G]_t$ are the total host and guest concentrations.

UV/vis titrations. UV/vis titrations were performed with a Varian Australia Pty Cary 3E UV/Vis spectrophotometer. Titrations of Zn-porphyrin **1** were carried out by adding 5 μ L aliquots (0.5 equivalent) of a 1×10^{-2} M solution of pyridine **2** or **4** to 1 mL of a 1×10^{-4} M Zn-porphyrin **1** solution, up to a maximum of 10 pyridine equivalents. Association constants were calculated by fitting the experimental titration curves to a 1:1 binding model based on the K_a equation (equation 5.2), on the mass balances (equations 5.3 and 5.4), on the Lambert-Beer equation (equation 5.5) and on equation 5.6, by applying a least squares optimization routine.

$$A_i = \varepsilon_i \cdot c_i \cdot \ell_i \quad (5.5)$$

A_i is the absorbance, ϵ_i the extinction coefficient, c_i the concentration of the absorbing species in solution and l_i the path length of the light

$$A_{tot} = A_1 + A_{1\cdot L} \quad (5.6)$$

A_{tot} , A_1 and $A_{1\cdot L}$ are the total absorbance of the sample, the absorbance of Zn-porphyrin **1**, and that of the complex **1**·L (L = **2** or **4**).

5.6. References

- 1 Vögtle, F. *Supramolecular Chemistry*, Wiley: New York, USA, **1993**.
- 2 Lehn, J.-M. *Supramolecular Chemistry*, VCH: Weinheim, Germany, **1995**.
- 3 Vincenti, M. *J. Mass Spectrom.* **1995**, *30*, 925.
- 4 Pramanik, B. N.; Bartner, P. L.; Mirza, U. A.; Liu, Y.-H.; Ganguly, A. K. *J. Mass Spectrom.* **1998**, *33*, 911.
- 5 Schalley, C. A. *Int. J. Mass Spectrom.* **2000**, *194*, 11.
- 6 Ganem, B.; Li, Y. T.; Henion, J. D. *J. Am. Chem. Soc.* **1991**, *113*, 6294.
- 7 For a review see: Daniel, J. M.; Friess, S. D.; Rajagopalan, S.; Wendt, S.; Zenobi, R. *Int. J. Mass Spectrom.* **2002**, *216*, 1.
- 8 Oshovsky, G. V.; Verboom, W.; Fokkens, R. H.; Reinhoudt, D. N. *Chem. Eur. J.* **2004**, *10*, 2739.
- 9 Berezin, B. D. *Coordination Compounds of Porphyrins and Phthalocyanines*, John Wiley and Sons: Chichester, UK, **1981**.
- 10 Rudkevich, D. M.; Verboom W.; Reinhoudt, D. N. *J. Org. Chem.* **1995**, *60*, 6585.
- 11 For a more detailed discussion on the mechanism of ion formation in ESI-MS and the effect of ionization on solution equilibria see: a) Kebarle, P.; Tang, L. *Anal. Chem.* **1993**, *65*, 972A. b) Kebarle, P.; Peschke, M. *Anal. Chim. Acta* **2000**, *406*, 11. c) Kebarle, P. *J. Mass. Spectrom.* **2000**, *35*, 804. d) Cech, N. B.; Enke, G. E. *J. Mass Spectrom. Rev.* **2001**, *20*, 362.
- 12 Leiz, E.; Jaffrezic, A.; Van Dorsselaar, A. *J. Mass Spectrom.* **1996**, *31*, 537.
- 13 Blokzijl, W.; Engberts, J. B. F. N. *Angew. Chem. Int. Ed. Engl.* **1993**, *32*, 1545.
- 14 For reviews on cyclodextrin chemistry see: *Chem. Rev.* **1998**, *98*, Issue 5.
- 15 Uekama, K.; Hirayama, F.; Irie, T. *Chem. Rev.* **1998**, *98*, 2013.
- 16 Szejtli, J. *Chem. Rev.* **1998**, *98*, 1743.
- 17 Hedges, A. *Chem. Rev.* **1998**, *98*, 2035.
- 18 Höfler, Th.; Wenz, G. *J. Incl. Phenom.* **1996**, *25*, 81.
- 19 De Jong, M. R.; Huskens, J.; Reinhoudt, D. N. *Chem. Eur. J.* **2001**, *7*, 4164.
- 20 Lebrilla, C. B. *Acc. Chem. Res.* **2001**, *34*, 653.
- 21 Cay, Y.; Tarr, M. A.; Xu, G.; Yalcin, T.; Cole, R. B. *J. Am. Soc. Mass Spectrom.* **2003**, *14*, 449.

- 22 Cunniff, J. B.; Vouros, P. *J. Am. Soc. Mass Spectrom.* **1995**, *6*, 437.
- 23 Ramirez, J.; Ahn, S.; Grigorean, G.; Lebrilla, C. B. *J. Am. Chem. Soc.* **2000**, *122*, 6884.
- 24 Ahn, S.; Ramirez, J.; Grigorean, G.; Lebrilla, C. B. *J. Am. Soc. Mass Spectrom.* **2001**, *12*, 278.

Chapter 6

Kinetic Study of an On-chip Isocyanate Derivatization Reaction by On-line Picospray Mass Spectrometry

The derivatization reaction of propyl isocyanate (2), benzyl isocyanate (3), and toluene-2,4-diisocyanate (4) with 4-nitro-7-piperazino-2,1,3-benzoxadiazole (NBDPZ) (1) to yield the corresponding urea derivatives (5) was carried out in a continuous flow glass microfluidics chip. Real-time monitoring of the derivatization reactions was done by electrospray ionization mass spectrometry (ESI-MS), making use of the modular chip-MS interface described in Chapter 3. Rate constants of $1.6 \times 10^4 \text{ M}^{-1} \text{ min}^{-1}$, $5.2 \times 10^4 \text{ M}^{-1} \text{ min}^{-1}$, and $2.5 \times 10^4 \text{ M}^{-1} \text{ min}^{-1}$ were determined for propyl isocyanate (2), benzyl isocyanate (3), and toluene-2,4-diisocyanate (4), respectively. Under macroscale batch conditions the rate constants are 3 to 4 times lower. The somewhat faster on-chip kinetics are mainly attributed to the unique conditions under which the continuous flow lab-on-a-chip operates.

6.1. Introduction

To study reaction kinetics real-time analysis of the reaction mixture composition is commonly carried out by quenched-flow^{1,2} and stopped-flow³⁻⁶ methods. Fast kinetic measurements are essential to study processes such as protein folding,⁷ enzymatic kinetics,¹⁻⁶ and chemical reactivity.^{8,9} Both quenched- and stopped-flow methods use turbulence to induce fast mixing by means of very powerful tangential mixers. These methods require high flow rates (mL s^{-1})¹⁰ and suffer from poor reaction control and mixing efficiency due to the large reaction volumes involved. However, it has recently been demonstrated in a number of publications that a turbulent flow is not a requirement.¹¹ The first theoretical model to describe mixing under laminar flow conditions has been proposed by Taylor in 1953.¹² More recently, in a theoretical study of reaction kinetics under laminar flow conditions, Konermann¹³ demonstrated that the distortion of the kinetic data due to the laminar regime is “surprisingly small”.

Microreactors offer a good alternative to conventional lab-scale equipment for the study of reaction kinetics, because they allow low reagent consumption and fast mixing^{14,15} as well as a continuous flow operative mode and real-time analysis.^{16,17} Microfluidics chips have been used to study kinetics of biochemical systems¹⁸⁻²⁰ on various time scales (from seconds to minutes), mainly using optical detection techniques.^{11,21,22} Recently, Song *et al.*²³ presented a microfluidics chip to perform kinetic measurements with millisecond resolution, which relied on chaotic mixing inside moving droplets. Due to the ease of fabrication and their compatibility with aqueous phase biological systems, polymers are the material of choice for the fabrication of microfluidics devices in most of the studies reported in literature. To the best of our knowledge there are no studies in which the use of glass microfluidics devices to study the kinetics of organic reactions and to monitor reactions by mass spectrometry is reported.

In Chapter 4 a flow-driven nanoflow electrospray chip (NESIC), consisting of a glass microreactor mounted on an ESI-MS nanoflow interface is described. Theoretical simulations corroborated by experimental evidence (Chapter 4) have shown complete and efficient mixing of reagents under laminar flow conditions within a few tens of milliseconds at flow rates ranging between 0.2 and 2 $\mu\text{L min}^{-1}$.

Based on flow rates and channel geometry various reaction times, typically in the order of seconds to a few minutes, can be exploited. After on-chip reaction the sample is directly sprayed into the mass spectrometer allowing on-line monitoring.

In this Chapter the use of the integrated NESIC device is described to study the kinetics of the reaction of 4-nitro-piperazino-2,1,3-benzoxadiazole (NBDPZ) with isocyanates (Scheme 1) as a model system. This reaction has been introduced by Karst *et al.*^{24,25} for the derivatization of the extremely reactive isocyanates²⁶ in order to allow their analysis by means of HPLC.

6.2. Continuous flow microreactors

The two types of continuous flow microreactors used are depicted in Figure 6.1. All isocyanate reactions were studied in “two inlet” chips (Figure 6.1a). A list of channel lengths (L), channel volumes (V), and residence times at flow rates ranging between 20 and 100 nL min⁻¹ is given in Table 6.1.

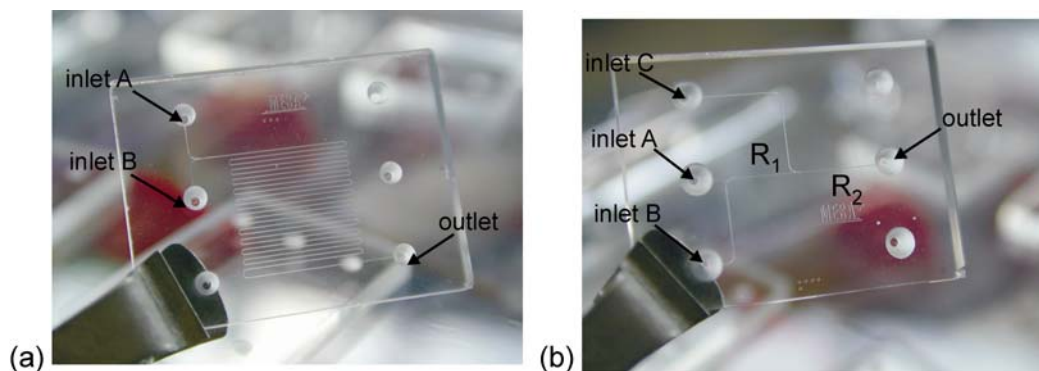


Figure 6.1. Photographs of the (a) “two inlet” and (b) “three inlet” chips used to study reaction kinetics and ion suppression phenomena, respectively.

Two “three inlet” microreactors, having total reaction channel lengths of 28 and 10 mm, respectively, were used to perform control experiments and to study ion suppression phenomena. “Three inlet” chips differ from the “two inlet” ones in that they consist of two distinct mixing zones, R₁ and R₂ (Figure 6.1b), instead of only one. The lengths of the two reaction channels R₁ and R₂ are 13 and 15 mm,

respectively, in the 28 mm long microreactor and 4 and 6 mm, respectively, in the 10 mm long microreactor. Based on the channel length and on the flow rate at which all on-chip control experiments were carried out (200 nL min^{-1}), residence times of 4 and 5 s and 1 and 2 s were calculated, respectively, for the two mixing zones (R_1 and R_2) of the 28 mm and the 10 mm long chip. Since at this time scale no significant conversion is observed for any of the investigated reactions (Figure 6.6; *vide infra*), this type of microreactors is very suitable to perform control experiments.

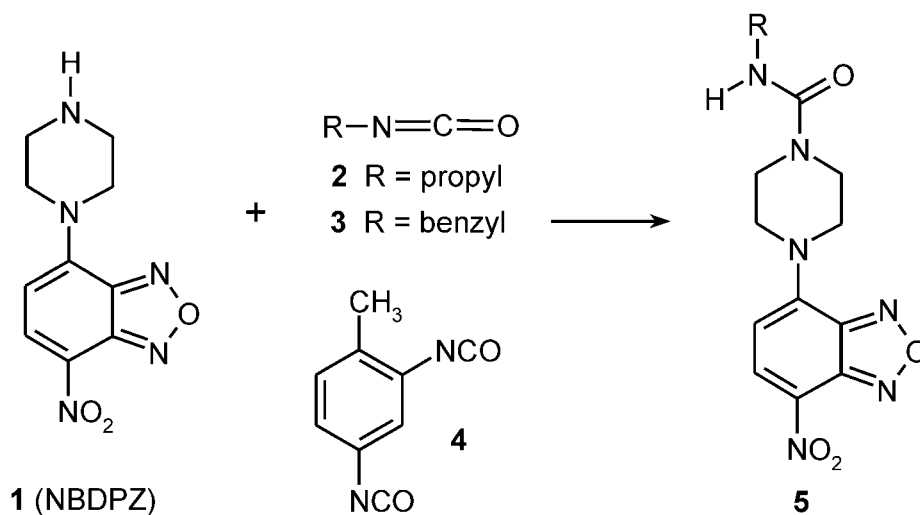
Table 6.1. Lengths (L) and volumes (V) of the microchannel in the “two inlet” devices (Figure 6.1a) and residence times at various flow rates.

Flow rate (nL min^{-1})	$L = 7.1 \text{ cm}$	$L = 10.5 \text{ cm}$	$L = 19.1 \text{ cm}$	$L = 28.4 \text{ cm}$
	$V = 71 \text{ nL}$	$V = 105 \text{ nL}$	$V = 191 \text{ nL}$	$V = 284 \text{ nL}$
100	0.7 min	1 min	1.9 min	2.8 min
80	0.9 min	1.3 min	2.4 min	3.5 min
60	1.2 min	1.8 min	3.2 min	4.7 min
40	1.8 min	2.6 min	4.8 min	7.1 min
20	3.6 min	5.2 min	9.6 min	14.2 min

An additional advantage of the “three inlet” chips over the “two inlet” ones is that reagents can be mixed in different ratios, while keeping the concentration of one of the two reagent solutions and the total flow rate constant. This allows, for example, to study the influence of co-solutes on analyte ionization, by minimizing side effects on the mass spectrometric signal due to changes in flow rates.

6.3. Background of the reaction of NBDPZ with isocyanates

Mono- and diisocyanates are an important class of compounds, being widely used in many industrial processes, such as the production of pesticides, pharmaceuticals, and polyurethanes.²⁷ Due to their high reactivity and toxicity mono- and diisocyanates are relatively difficult to handle and, consequently, to study. Strategies based on the use of various derivatizing agents for the analysis of isocyanates have been widely used in analytical chemistry. Over the past decades amine-based reagents for the analysis of isocyanates have been preferred over other methodologies exploited in the past.²⁸⁻³⁰ The use of 4-nitro-piperazino-2,1,3-benzoxadiazole (NBDPZ) (**1**) as a derivatizing agent to quantify the amount of mono- and diisocyanates in air samples has recently been proposed by Vogel and Karst.^{24,25} The derivatization involves the reaction of NBDPZ (**1**) with (di)isocyanates to give the corresponding urea derivatives (**5**) (Scheme 1). Recently, Henneken *et al.* developed a method using tandem mass spectrometry (MS-MS) to analyze NBDPZ (**1**) and the corresponding methyl urea derivative (**5**) (R = methyl).²⁶



Scheme 6.1. Reaction of NBDPZ (**1**) with propyl isocyanate (**2**), benzyl isocyanate (**3**), and toluene-2,4-diisocyanate (**4**) to give the corresponding NBDPZ-urea derivatives (**5**).

Since NBDPZ (**1**) gives a high intensity, stable, singly charged mass spectrometric signal it is suitable to study its reaction with (di)isocyanates in the chip-based nanoelectrospray interface. In contrast the urea derivatives (**5**) gave a very low intensity and unstable mass spectrometric signal in our experimental set-up. The selected reactions were therefore studied by ESI-MS by monitoring the decrease of **1** upon reaction with the isocyanates.

6.1. On-chip experiments

Mass spectrometric calibration of the NBDPZ (**1**) singly charged signal ($m/z = 251$) revealed a linear relationship between [NBDPZ] and the signal intensity up to [NBDPZ] = 5×10^{-6} M (Figure 6.2). At higher [NBDPZ] a deviation from the linearity was observed, due to suppression phenomena. Reactions of isocyanates **2**, **3**, and **4** with NBDPZ (**1**) were therefore carried out in acetonitrile using equimolar concentration ratios of 5×10^{-6} M of all reagents.

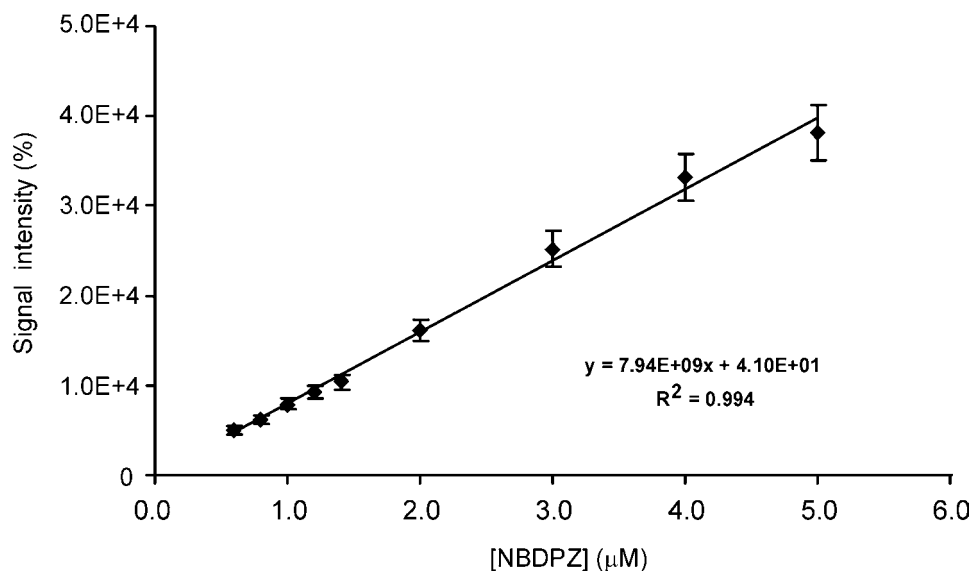


Figure 6.1. ESI-TOF-MS calibration curve of the NBDPZ (**1**) signal intensity (markers) and corresponding linear fit (solid line).

Electrospray mass spectrometry is often used for analyte quantification. However, a good quantification method must take into account all those parameters that may influence the mass spectrometric signal of the analyte under investigation during sample ionization. The nature of the analyte, the solvent, the instrument operative parameters, the capillary tip distance from the mass spectrometer cone, and the sample infusion flow rates are some examples.³¹ A study of the influence that some of those parameters might have on the NBDPZ signal at $m/z = 251$ is therefore required.

6.4.1. Influence of the sample infusion flow rates on the NBDPZ ionization

The flow rate at which the analyte solution is infused into the mass spectrometer through the capillary may influence the efficiency with which ions are formed, transferred to the gas phase, and detected.³² The chip-based interface we use as a tool to study reaction kinetics relies on the quick variation of reagent injection flow rates to allow a range of reaction times. In order to quantify the influence of the decrease of the total flow rate on the NBDPZ (**1**) mass spectrometric signal used to determine the reaction rates, a number of control experiments were carried out by diluting on-chip a solution of 1×10^{-5} M of NBDPZ (**1**) with solvent. The ratio between the flow rates at the two inlets was kept constant (1:1), while the total flow rate was decreased from 100 to 20 nL min^{-1} by steps of 20 nL min^{-1} . As shown in Figure 6.3, no significant changes in the NBDPZ signal at $m/z = 251$ were observed upon decreasing the total flow rate. Standard deviation values of about 1% were calculated for several measurements at each speed, indicating a remarkable stability of the NBDPZ signal. Overall, taking into account the NBDPZ signal intensity at different flow rates, the experimental error is only about 5%.

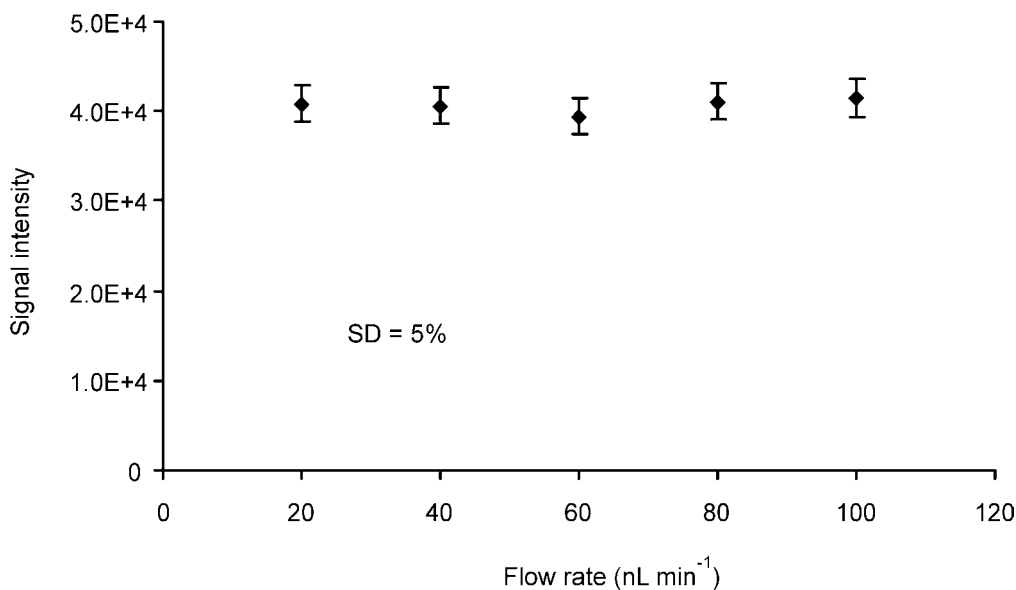


Figure 6.1. Influence of the sample infusion flow rate on the stability of the NBDPZ (1) signal intensity at $m/z = 251$.

6.1.1. Influence of co-solutes on NBDPZ ionization

The composition of the sample and the presence of co-solute in the analyte solution are known to have an influence on analyte ionization.^{31,33} For the reactions of NBDPZ (1) with isocyanates 2, 3, and 4 control experiments were performed in order to study the possible influence of the isocyanates (co-solutes) on the NBDPZ signal intensity at $m/z = 251$. Calibrations of NBDPZ (1) solutions containing the highest concentration of the corresponding isocyanate present in the mixture during the reaction (5×10^{-6} M) were carried out in “three inlet” chips (Figure 6.1b). Due to the short microchannels no significant conversion takes place in the few seconds residence time, at 200 nL min^{-1} total flow rate (*vide supra*). The three experimental calibration curves as well as the linear fits and the corresponding equations are displayed in Figure 6.4. It is evident that the presence of isocyanates in the NBDPZ calibrating solution does not markedly influence the intensity of the NBDPZ signal. This is confirmed by the fact that the averaged value of the slopes of the three calibration curves $[(7.94 \pm 0.24) \times 10^9]$ coincides with the slope of the calibration curve of pure NBDPZ (1) (7.94×10^9) reported in Figure 6.2.

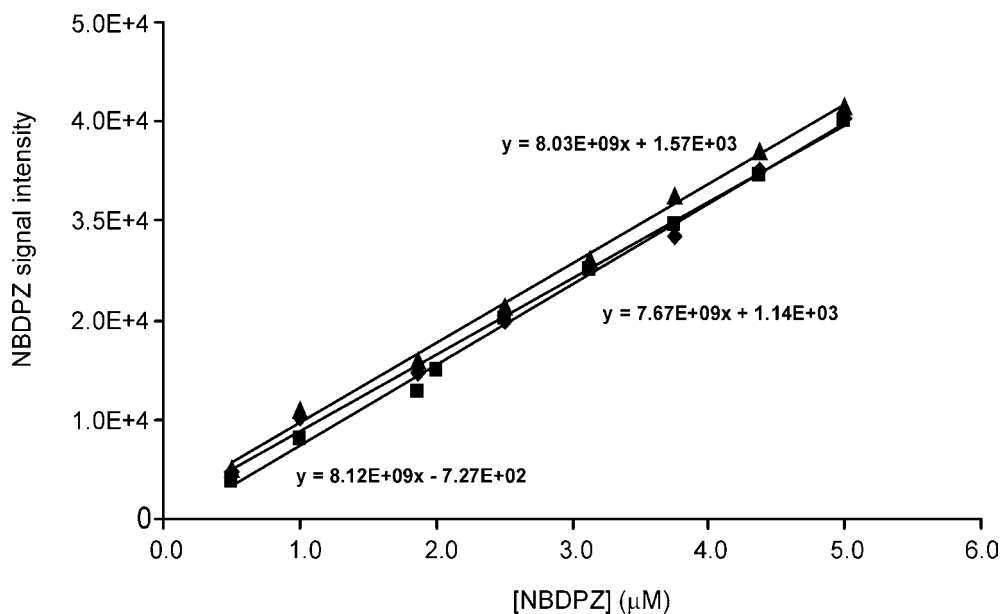


Figure 6.2. Experimental calibration curves (markers) and linear fits (solid lines) of the NBDPZ (1) signal at $m/z = 251$ in the presence of the maximum concentration (5×10^{-6} M) of (◆) propyl isocyanate (2), (■) benzyl isocyanate (3), and (▲) toluene-2,4-diisocyanate (4).

6.1.2. Ion suppression phenomena

Mass spectrometric quantification of analytes in complex samples such as reaction mixtures often suffers from problems related to interference, especially through ion suppression effects.^{34,35} Ion suppression is the result of the presence of a co-solute in the sample that has a different volatility than the analyte, which may significantly affect the ionization efficiency of the analyte. This unwanted, though often observed phenomenon mainly occurs in biological samples rather than in organic systems.³⁴ By using “three inlet” chips on-line coupled with ESI-MS, the possible suppression of the NBDPZ (1) signal at $m/z = 251$ due to the presence of isocyanates in the investigated reaction mixtures was investigated. For each of the isocyanates 2-4 the intensity of the signal of a 5×10^{-6} M NBDPZ solution at $m/z = 251$ was monitored upon mixing with increasing isocyanate concentrations. The very short microreactor (*i.e.* 10 mm) ensures that no reaction takes place in the few seconds on-chip residence time, at 200 nL min⁻¹ total flow rate (*vide supra*). Figure 6.5 does not show significant changes in the intensity of the NBDPZ signal in any of the three

cases, indicating that under the conditions used ion suppression phenomena are negligible.

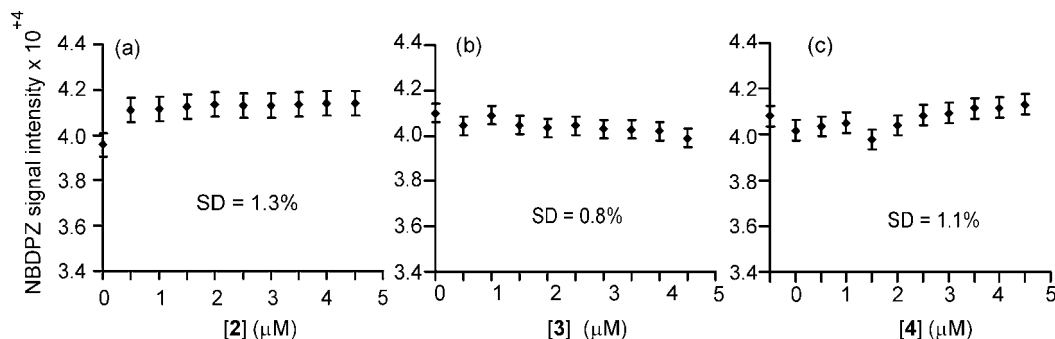


Figure 6.5. Ion suppression study results. The signal intensity of a solution of 5×10^{-6} M of NBDPZ (**1**) at $m/z = 251$ monitored upon addition of increasing concentrations of (a) propyl isocyanate (**2**), (b) benzyl isocyanate (**3**), and (c) toluene-2,4-diisocyanate (**4**).

6.4.4. On-chip reaction kinetics

Figure 6.6 shows the experimental reaction profiles for the on-chip reaction of NBDPZ (**1**) with monoisocyanates **2** and **3** and diisocyanate **4**, determined by ESI-MS by simply varying the total injection speed of the reagent solutions. All reactions were carried out injecting on-chip equimolar (5×10^{-6} M) solutions of reagent **1** and the corresponding isocyanate in acetonitrile. For each reaction, the concentration of NBDPZ (**1**) at different reaction times was calculated from mass spectrometric data, using the equations of the calibration curves (Figure 6.4). Since all reactions were performed under the same conditions, the three decay curves depicted in Figure 6.6 give a quantitative indication of the reactivity of the three reagents. As expected from the nature of their R groups (see Scheme 6.1),²⁷ propyl isocyanate (**2**) shows the lowest reactivity, while benzyl isocyanate (**3**) is the most reactive of the three isocyanates.

Second order kinetics is assumed as most probable mechanism for the investigated reactions, because the concentration of NBDPZ (**1**) is equal to the concentration of the isocyanates (5×10^{-6} M). The same assumption is valid for diisocyanate **4**, since the formation of the monoderivatized product is much faster than

that of the second, as confirmed by ESI-MS data. The experimental data were fitted to a second order kinetic model (Figure 6.6) using equation 6.1. Rate constants (Table 6.2) were determined by applying a least squares optimization routine.

$$\frac{1}{[A]} - \frac{1}{[A]_0} = kt \quad (6.1)$$

$[A]$ is the concentration of NBDPZ (**1**) at a given time, $[A]_0$ is the initial concentration of NBDPZ (**1**), t [min] is the reaction time, and k is the reaction rate constant.

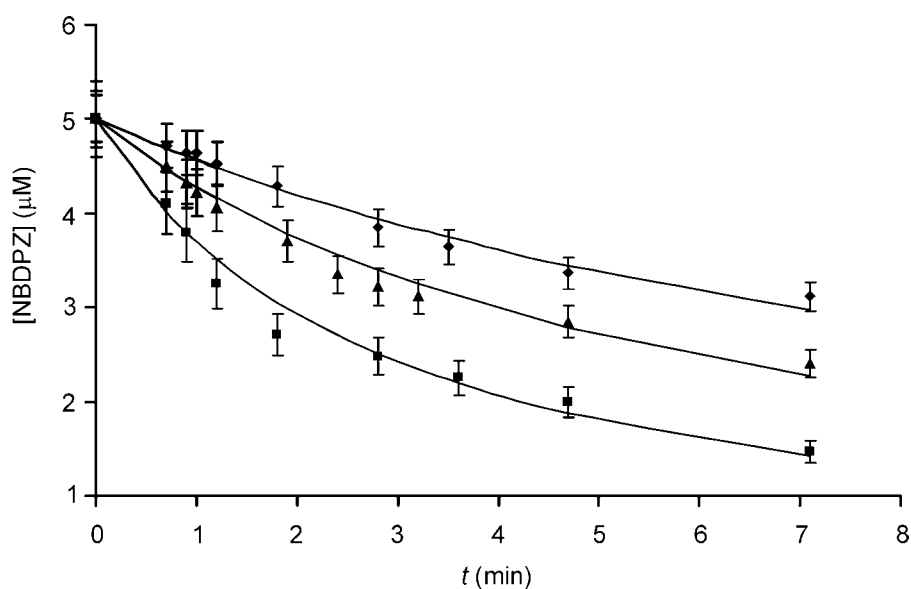


Figure 6.6. Reaction profile of the on-chip derivatization of NBDPZ (**1**) with (◆) propyl isocyanate (**2**), (■) benzyl isocyanate (**3**), and (▲) toluene-2,4-diisocyanate (**4**), and corresponding fits to a second order kinetics model (solid lines).

To verify the assumption that the investigated reactions follow second order kinetics, the initial rate constants (k_0) were also calculated from the slope (a) of the linear initial part of the reaction profiles (Figure 6.7) according to equation 6.2, which is valid when the concentration of NBDPZ (**1**) is equal to that of isocyanates.

$$k_0 = \frac{a}{[NBDPZ]_0^2} \quad (6.2)$$

$[\text{NBDPZ}]_0$ is the initial concentration of NBDPZ (1).

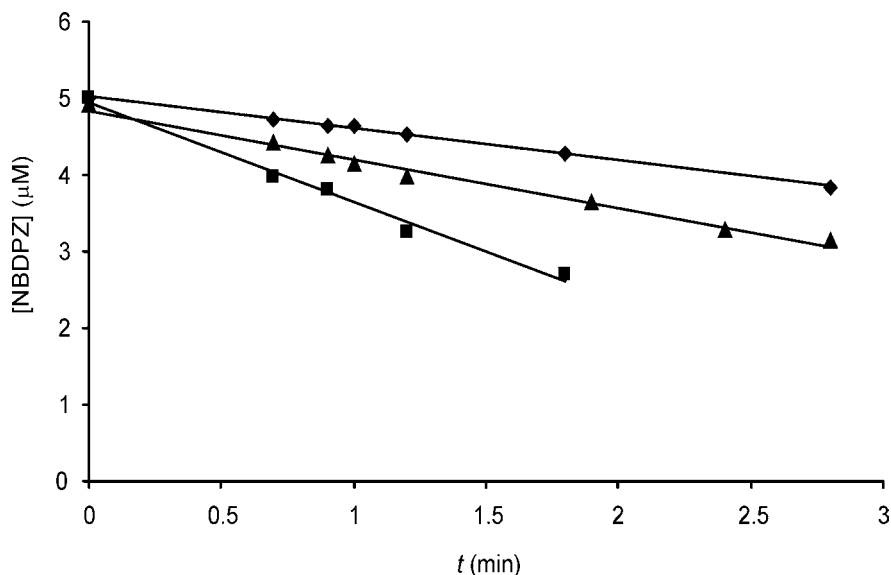


Figure 6.7. Experimental linear part of the reaction profile curves of Figure 6.6 of the on-chip reaction of NBDPZ (1) with (◆) propyl isocyanate (2), (■) benzyl isocyanate (3), and (▲) toluene-2,4-diisocyanate (4), and corresponding linear fits (solid lines).

In Table 6.2 the slopes of the linear part of the reaction profiles (a), the second order kinetic rate constants (k), and the initial rate constants (k_0) are summarized.

Table 6.2. Slope of the first part of the reaction profiles (a) used to calculate the initial rate constant (see equation 6.2), second order rate constant (k), and initial rate constant (k_0) of the reaction of NBDPZ (1) with isocyanates 2-4.

Isocyanate	a (M min^{-1})	k ($\text{M}^{-1} \text{min}^{-1}$)	k_0 ($\text{M}^{-1} \text{min}^{-1}$)
2	4.1×10^{-7}	1.9×10^4	1.6×10^4
3	1.31×10^{-6}	7.0×10^4	5.2×10^4
4	6.36×10^{-7}	3.3×10^4	2.5×10^4

From Table 6.2 it is clear that for the reactions of NBDPZ (**1**) with mono- (**2**, **3**) and diisocyanate (**4**) the rate constants calculated by fitting the data to second order kinetics are in good agreement with those calculated based on initial rates only, supporting the second order kinetics of the reactions. The experimental data were also fitted to a first order kinetics model. From the fits, which are not shown here, and the residual values, it was clear that only the second order reactions kinetics could describe the data well.

6.5. Laboratory-scale reaction kinetics

For comparison reasons, the kinetics of the reaction of NBDPZ (**1**) with isocyanates **2-4** were also studied by Andre Liesner of the Chemical Analysis group of the University of Twente using conventional laboratory-scale procedures. Figure 6.8 shows the reaction profiles determined by ESI-MS. The relative reactivity of the isocyanates **2-4** is in good agreement with that determined on-chip by continuous flow experiments. However, in all cases the lab-scale reactions show slightly slower kinetics compared to the on-chip continuous flow experiments.

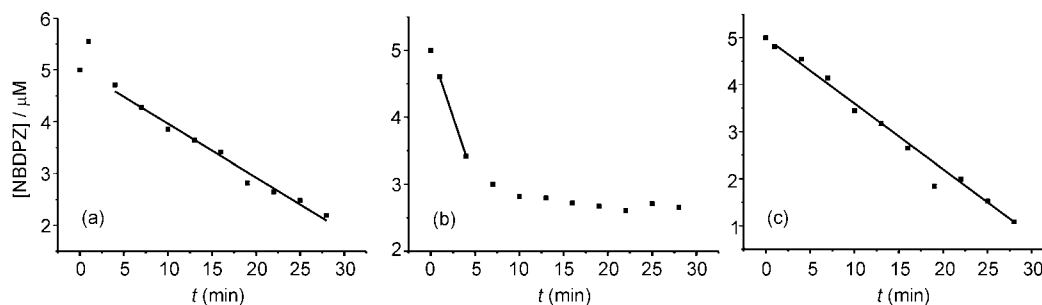


Figure 6.8. Time profiles of the lab-scale reaction of NBDPZ (**1**) with (a) propyl isocyanate (**2**), (b) benzyl isocyanate (**3**), and (c) toluene 2,4-diisocyanate (**4**).

The lab-scale reaction rate constants (k_{lab}) and those determined by on-chip experiments (k_{chip}) are summarized in Table 6.3. From the k_{chip} / k_{lab} ratio it is clear that the on-chip reactions are 3 to 4 times faster than the lab-scale experiments. The somewhat larger on-chip reaction rates may be attributed to the distinctive conditions under which continuous flow microfluidics chips operate, such as fast and efficient

diffusive mixing under laminar flow regime. Operating under continuous flow conditions and allowing on-line analysis, the lab-on-a-chip approach offers a more precise data acquisition, which may result in a higher accuracy of the final result as compared to the lab-scale experiments.

Table 6.3. Reaction rates^a determined by on-chip experiments (k_{chip}) and lab-scale experiments (k_{lab}) and their ratio (k_{chip} / k_{lab}).

Isocyanates	k_{chip} ($M^{-1} \text{ min}^{-1}$)	k_{lab} ($M^{-1} \text{ min}^{-1}$)	k_{chip} / k_{lab}
2	1.6×10^4	4.2×10^3	3.8
3	5.2×10^4	1.6×10^4	3.3
4	2.5×10^4	5.6×10^3	4.3

^aInitial reaction rates calculated according to equation 6.2 (see Experimental).

6.6. Conclusions

The use of a continuous flow microchip-based nanoflow electrospray mass spectrometry interface for the study of reaction kinetics was successfully demonstrated using the reaction of 4-nitro-piperazino-2,1,3-benzoxadiazole (NBDPZ, **1**) with propyl isocyanate (**2**), benzyl isocyanate (**3**), and toluene-2,4-diisocyanate (**4**).

With the NESIC device the reaction rate constants are 3 to 4 times larger compared to that of lab-scale experiments. The somewhat larger rate constants determined by using the lab-on-a-chip may be attributed to the distinctive properties of continuous flow microfluidics devices, leading to overall higher result accuracy. The results reported in this Chapter demonstrate that continuous flow microfluidics systems provide a unique environment to carry out reactions in a very efficient way, using only tiny amount of reagents, increasing process safety, reducing process costs and sample handling. The limited volume of the reaction vessel (only a few nanoliters), which implies reagents mixing under laminar flow conditions at very

short diffusion length scales, offers a high degree of reaction control contrary to macroscale turbulent systems.

A novel type of “three inlet” microreactor offers the possibility to study ion suppression phenomena quickly and systematically as well as the effect of different parameters on the ionization of the analyte, which are all required to study reaction kinetics by ESI mass spectrometry in a justified way.

6.7. Experimental

Microreactors. All microreactors were fabricated by standard glass processing as described in Chapter 3.

Chemicals. NBDPZ (**1**) was synthesized according to Vogel and Karst²⁴. The different isocyanates were purchased from Sigma Aldrich (Steinheim, Germany). 1×10^{-6} M solutions of NBDPZ (**1**) as well as each isocyanate were prepared using dry LC-MS grade acetonitrile (Biosolve, Valkenswaard, The Netherlands) in order to minimize loss of reactants by hydrolysis reactions.

ESI-MS detection. On-chip reactions were studied by directly coupling the microreactor to a Micromass (Manchester, UK) LCT electrospray time-of-flight mass spectrometer (ESI-TOF-MS) (see Chapter 4) and monitoring the decrease of the NBDPZ signal intensity at $m/z = 251$ in time upon reaction of NBDPZ (**1**) with each isocyanate. Spectra were acquired in the positive ion mode at a capillary voltage ranging between 1.8 and 2 kV, at a sample cone voltage of 35 V, and an extraction cone voltage of 2 V. The source temperature was kept constant at 100 °C and the cone gas between 80 and 90 L h⁻¹.

On-chip reaction kinetics studies. All experiments were performed by injecting reagent solutions into the chip by means of 100 μ L flat tip Hamilton syringes mounted on a CMA/102 microdialysis pump. The syringes were connected to fused silica capillaries (inner diameter = 20 μ m) by using Upchurch™ unions. Derivatization reactions of the isocyanates **2**, **3**, and **4** with NBDPZ (**1**) were performed by injecting on-chip equimolar solutions of 10^{-5} M ($C_{\text{on-chip}} = 5 \times 10^{-6}$ M) of both NBDPZ (**1**) and isocyanates **2**, **3**, and **4** in acetonitrile, keeping the ratio (1:1) between the injection

speed of the reagent solutions constant. Various reaction times were exploited by varying the total flow rate from 100 to 40 nL min⁻¹. Longer reaction times were obtained by quickly replacing the chip in the holder during the experiments and thereby varying the reaction volumes between 71 and 284 nL (Table 6.1).

On-chip NBDPZ calibration. Using “two inlet” chips (Figure 6.1a), the calibration of the NBDPZ signal intensity at $m/z = 251$ was carried out by varying the ratio between the injection speeds of a stock solution of NBDPZ (**1**) (1×10^{-5} M) in inlet A of the chip and acetonitrile as a solvent in inlet B. Spectra were recorded at on-chip NBDPZ concentrations ranging between 1×10^{-5} and 1×10^{-7} M. Additional calibrations were done using “three inlet” chips (Figure 6.1b). Equimolar stock solutions (1.25×10^{-5} M) of NBDPZ (**1**) and propyl isocyanate **2** in acetonitrile were injected in inlets A and C, respectively. Solvent was injected in inlet B. The injection speed at inlet C was kept constant at 80 nL min⁻¹, while those of inlets B and A were varied from 40 to 100 nL min⁻¹ and from 100 to 40 nL min⁻¹, respectively. The total flow rate at the chip outlet was kept constant, resulting in a constant on-chip concentration of **2** (5×10^{-6} M) and a concentration of NBDPZ (**1**) varying between 5×10^{-6} M and 1×10^{-6} M. Based on the same principle calibrations were performed by injecting 1.25×10^{-5} M stock solutions of NBDPZ (**1**) in inlet A at flow rates ranging between 80 and 20 nL min⁻¹, 1×10^{-5} M stock solutions of either **3** or **4** in inlet C at a constant flow rate of 100 nL min⁻¹, and solvent in inlet B at flow rates ranging between 20 and 80 nL min⁻¹.

On-chip ion suppression studies were performed for each isocyanate using “three inlet” chips. Experiments were carried out by injecting equimolar stock solutions (1×10^{-5} M) of NBDPZ (**1**) and isocyanates **2** and **3** in inlets A and C, respectively. The injection speed of A was kept constant at a value of 100 nL min⁻¹, resulting in an on-chip NBDPZ concentration of 5×10^{-6} M, while that of inlet C was varied from 10 to 90 nL min⁻¹ (on-chip concentration of isocyanate varying between 4.5×10^{-6} and 5×10^{-7} M). Solvent was injected in inlet B at flow rates ranging between 90 and 10 nL min⁻¹, to compensate for the decrease in injection speed of inlet C, resulting in a constant total flow rate at the chip outlet. Variations of the intensity of the NBDPZ signal at $m/z = 251$ were monitored upon increasing the concentration of isocyanate. In the case of diisocyanate **4** the same method as described for isocyanates **2** and **3**

was used, but by injecting a 1.25×10^{-5} M NBDPZ stock solution in inlet A at a constant flow rate of 80 nL min^{-1} and varying the injection speeds at inlets B and C from 100 to 20 and from 20 to 100 nL min^{-1} , respectively.

Lab-scale control experiments. For the lab-scale experiments a flow injection mass spectrometry (FIA-MS) set-up was used. To this end a G1312a model HPLC pump, which delivered the carrier stream of acetonitrile, and a G1313a model autosampler (both HP1100 series by Agilent, Waldbronn, Germany) for sample introduction were coupled to the mass spectrometric detector. All lab-scale MS experiments were performed on an Esquire 3000+ ion trap mass spectrometer from Bruker Daltonics (Bremen, Germany) equipped with a standard ESI source. For the best possible ionization and detection of the analyte, the conditions were optimized with respect to the intensity of the NBDPZ signal, resulting in the following parameters: nebulizer gas (N_2) pressure: 40 psi; dry gas (N_2) flow: 9.0 L/min; dry gas temperature: $365 \text{ }^\circ\text{C}$; capillary high voltage: 5,000 V; capillary exit: 49.8 V; skimmer: 16.4 V; octopole 1 DC: 13.36 V; octopole 2 DC: 0.00 V; octopole RF: 152.5 Vpp; lens 1: -9.8 V; lens 2: -88.2 V; trap drive level: 35.0. The FIA-MS system was controlled by a PC using Esquire Control 5.1 and HyStar 2.3; data evaluation was done with DataAnalysis 3.1 (all: Bruker Daltonics, Bremen, Germany).

The reaction was started by combining $750 \text{ }\mu\text{L}$ of the NBDPZ solution (1×10^{-5} M) and $750 \text{ }\mu\text{L}$ of the respective isocyanate solution of equimolar concentration in a standard HPLC vial, thus resulting in starting concentrations of 5×10^{-6} M for both reactants. In order to follow the reactions progress $5 \text{ }\mu\text{L}$ aliquots were sampled from the reaction mixture every three minutes and injected into the FIA-MS system, where the decrease of the NBDPZ signal intensity at $m/z = 251$ was monitored.

6.8. References

- 1 Ali, J. A.; Lohman, T. M. *Science* **1997**, *275*, 377.
- 2 Luo, L. S.; Burkart, M. D.; Stachelhaus, D.; Walsh, C. T. *J. Am. Chem. Soc.* **2001**, *123*, 11208.
- 3 Brazeau, B. J.; Austin, R. N.; Tarr, C.; Groves, J. T.; Lipscomb, J. D. *J. Am. Chem. Soc.* **2001**, *123*, 11831.
- 4 Valentine, A. M.; Stahl, S. S.; Lippard, S. J. *J. Am. Chem. Soc.* **1999**, *121*, 3876.
- 5 Krantz, B. A.; Sosnick, T. R. *Biochemistry* **2000**, *39*, 11696.
- 6 Halonen, P.; Baykov, A. A.; Goldman, A.; Lahti, R.; Cooperman, B. S. *Biochemistry* **2002**, *41*, 12025.
- 7 Chan, C. K.; Hu, Y.; Takahashi, S.; Rousseau, D. L.; Eaton, W. A.; Hofrichter, J. *J. Proc. Natl. Acad. Sci. USA.* **1997**, *94*, 1779.
- 8 Nelsen, S. F.; Ramm, M. T.; Ismagilov, R. F.; Nagy, M. A.; Trieber, D. A.; Powell, D. R.; Chen, X.; Gengler, J. J.; Qu, Q. L.; Brandt, J. L.; Pladziewicz, J. R. *J. Am. Chem. Soc.* **1997**, *119*, 5900.
- 9 Cherry, J. P. F.; Johnson, A. R.; Baraldo, L. M.; Tsai, Y. C.; Cummins, C. C.; Kryatov, S. V.; Rybak-Akimova, E. V.; Capps, K. B.; Hoff, C. D.; Haar, C. M.; Nolan, S. P. *J. Am. Chem. Soc.* **2001**, *123*, 7271.
- 10 Bringer, M. R.; Gerdts, C. J.; Song, H.; Tice, J. D.; Ismagilov, R. F. *Phil. Trans. R. Soc. Lond. A* **2004**, *362*, 1087.
- 11 Zhou, X.; Medhekar, R.; Toney, M. D. *Anal. Chem.* **2003**, *75*, 3681.
- 12 Taylor, G. *Proc. R. Soc. (London)* **1953**, *A219*, 186.
- 13 Konermann, L. *J. Phys. Chem.* **1999**, *103*, 7210.
- 14 Jensen, K. *Nature* **1998**, *393*, 735.
- 15 Stroock, A. D.; Dertinger, S. K. W.; Ajdari, A.; Mezi, I.; Stone, H. A.; Whitesides, G. M. *Science* **2002**, *25*, 67.
- 16 Schwarz, M.; Hauser, P. C. *Lab Chip* **2000**, *1*, 1.
- 17 De Mello, A. J. *Lab Chip* **2001**, *1*, 7N.
- 18 Kalkuta, M.; Jayawickrama, D. A.; Wolters, A. M.; Manz, A.; Sweedler, J. V. *Anal. Chem.* **2003**, *75*, 956.
- 19 Mao, H. B.; Yang, T. L.; Cremer, P. S. *Anal. Chem.* **2002**, *74*, 379.
- 20 Kerby, M.; Chien, R. L. *Electrophoresis* **2001**, *22*, 3916.

- 21 Hadd, A. G.; Raymond, D. E.; Halliwell, J. W.; Jacobson, S. C.; Ramsey, J. M. *Anal. Chem.* **1997**, *69*, 3407.
- 22 Seong, G. H.; Heo, J.; Crooks, R. M. *Anal. Chem.* **2003**, *75*, 3161.
- 23 Song, H.; Ismagilov, R. F. *J. Am. Chem. Soc.* **2003**, *125*, 14613.
- 24 Vogel, M.; Karst, U. German Patent *DE 199 26 731* **1999**.
- 25 Vogel, M.; Karst, U. *Anal. Chem.* **2002**, *74*, 6418.
- 26 Henneken, H.; Lindahl, R.; Östin, A.; Vogel, M.; Levin, J.-O.; Karst, U. *J. Environ. Monit.* **2003**, *5*, 100.
- 27 Ulrich, H. *Chemistry and Technology of Isocyanates*; John Wiley & Sons: Chichester, UK, **1996**.
- 28 Dunlap, K. L.; Sandrige, R. L.; Keller, J. *Anal. Chem.* **1976**, *48*, 497.
- 29 Karlsson, D.; Dahlin, J.; Skarping, G.; Dalene, M. *J. Environ. Monit.* **2002**, *4*, 216.
- 30 Nordqvist, Y.; Melin, J.; Nilsson, U.; Johansson, R.; Colmsjö, A. *Fresenius J. Anal. Chem.* **2001**, *371*, 39.
- 31 For a more detailed description of the mechanisms involved in ESI-MS see: a) Gaskel, S. J. *J. Mass Spectrom.* **1997**, *32*, 677. b) Kebarle, P.; Peschael, M. *Anal. Chim. Acta* **2000**, *406*, 11. c) Kebarle, P. *J. Mass. Spectrom.* **2000**, *35*, 804.
- 32 Schmidt, A.; Karas, M. *J. Am. Soc. Mass Spectrom.* **2003**, *14*, 492.
- 33 Tang, L.; Kebarle, P. *Anal. Chem.* **1993**, *65*, 3654.
- 34 Annesley, T. M. *Clin. Chem.* **2003**, *49*, 1041.
- 35 King, R.; Bonfiglio, R.; Fernandez-Metzler, C.; Miller-Stein, C.; Olah, T. *J. Am. Soc. Mass Spectrom.* **2000**, *11*, 942.

Chapter 7

Lab-on-a-chip Device Enabling (Bio)chemical Reactions with On-line MALDI-TOF Mass Spectrometry[‡]

A continuous flow lab-on-a-chip (LOC) consisting of an on-chip microfluidics device connected to a matrix-assisted laser desorption ionization (MALDI) time-of-flight (TOF) mass spectrometer (MS) as an analytical screening device is described. Reaction microchannels and inlet and outlet reservoirs were fabricated by powderblast micromachining of glass wafers that were then bonded to silicon substrates. The LOC was realized by integrating the microdevice with a MALDI-TOF MS standard sample plate, used as carrier to introduce the microfluidics device in the MALDI instrument. A novel pressure-driven pumping mechanism using the vacuum of the instrument as a driving force induces flow in the reaction microchannel in a “self-activating” way. Organic syntheses as well as biochemical reactions can be carried out entirely inside the MALDI MS ionization vacuum chamber and analyzed by MALDI-TOF MS in real-time. The effectiveness of the LOC device has been successfully demonstrated with several examples of (bio)chemical reactions.

[‡] This work has been published: Brivio, M.; Fokkens, R. H.; Verboom, W.; Reinhoudt, D. N.; Tas, N. R.; Goedbloed, M.; Van den Berg, A. *Anal. Chem.* **2002**, *74*, 3972.

7.1. Introduction

The introduction of matrix-assisted laser desorption ionization (MALDI)^{1,2} more than a decade ago has revolutionized not only mass spectrometry but also biomolecular analysis. This soft ionization technique provides a powerful means to ionize a large variety of fragile and non-volatile analytes including peptides and proteins,³⁻⁶ oligonucleotides,⁷ oligosaccharides,⁸ synthetic polymers,^{9,10} and small molecules.¹¹ MALDI sources can be coupled to time-of-flight (TOF) equipment, extending the method capability to the analysis of molecules with molecular masses much higher than those detectable with other MS methods. Using this ionization technique Schriemer and Li¹² have demonstrated the detection of singly charged ions up to 1.5 million Da. MALDI offers the advantage of generating relatively simple spectra because mainly singly charged ions are formed. Other advantages of MALDI MS include the tolerance for buffers and contaminants, a very high sensitivity,¹³ and faster analysis compared to atmospheric pressure ionization techniques.

Several approaches have been reported in the literature to increase the high-throughput capability of MALDI MS. These include off-line analysis of fractions collected from a separation column and deposited on the MALDI target¹⁴ as well as on-line coupling of MALDI with column separations¹⁵⁻¹⁹ or planar separations such as thin layer chromatography (TLC)²⁰⁻²⁴ by means of various types of interfaces. However, on-line chip-MS^{25,26} has mainly been restricted to the electrospray ionization method due to the easy interfacing between the electrospray capillary and microfluidics chips, and because this ionization technique operates at atmospheric pressure. The ionization process in MALDI-TOF MS is mainly carried out in vacuum, which requires special precautions for integration with a microfluidics chip.

In this Chapter the first example of the coupling of a microfluidics device to a MALDI-TOF mass spectrometer by integrating an on-chip microreaction unit with a MALDI-TOF standard sample plate is described. This allows (bio)chemical reactions to take place in the MALDI-TOF instrument. Since it is based on a pressure-driven fluidics handling method, using the vacuum in the ionization chamber of the MALDI-TOF MS, this approach avoids wires and tubes for feed and flow control.

A variety of examples ranging from simple biochemistry to organic and polymer chemistry will illustrate the effectiveness and versatility of this chip-MS device.

7.2. MALDI principle

The basic principle of laser desorption ionization (LDI)²⁷ is schematically depicted in Figure 7.1. A laser light pulse of a specific wavelength strikes the surface of a sample, thus providing the energy that leads to vaporization of ions and neutral molecules from the sample. If the light absorption spectrum of the sample molecules has an absorption peak near the laser emission wavelength, the analyte molecules will absorb energy from the laser and ions as well as neutral molecules will be ablated from the sample. If the analyte does not have an absorption peak at the laser wavelength, the energy will not be absorbed but simply be reflected or scattered. In matrix-assisted LDI (MALDI) the sample is mixed with a matrix, which absorbs energy at the emission wavelength of the laser and subsequently transfers it to the analyte molecules. Both matrix and analyte ions and neutral molecules will then desorb.

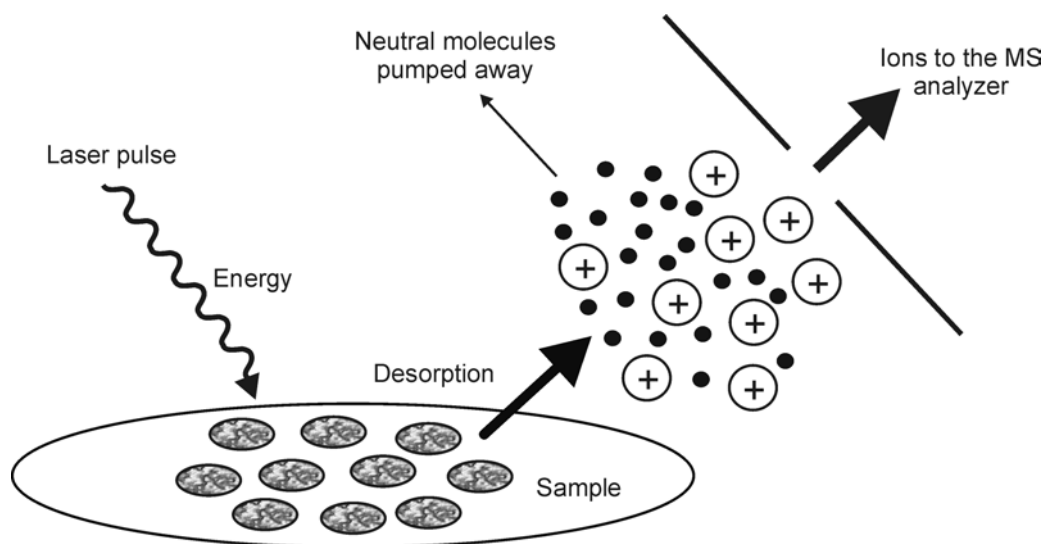


Figure 7.1. Schematic representation of laser desorption ionization: a laser pulse strikes the surface of a sample (only analyte or analyte and matrix) thereby depositing

energy, which is absorbed by the sample molecules, leading to the desorption of ions and neutral molecules. Ions are drawn to the MS analyzer, while neutral molecules will be pumped away.

7.3. MALDI instrument

A schematic drawing of a MALDI-TOF MS instrument is depicted in Figure 7.2. Samples, consisting of a few microliters of analyte solution (with or without matrix), are deposited on a MALDI target (Figure 7.2a). After the solvent has evaporated the sample plate, carrying the solidified samples, is introduced into the MALDI ionization chamber *via* load-lock. The ionization process takes place in a high-vacuum chamber to which the plate is introduced *via* a prechamber kept at a pressure lower than atmospheric. Analyte ions are then accelerated as they are formed and pumped into the TOF analyzer, where they are separated based on their mass-to-charge ratio.

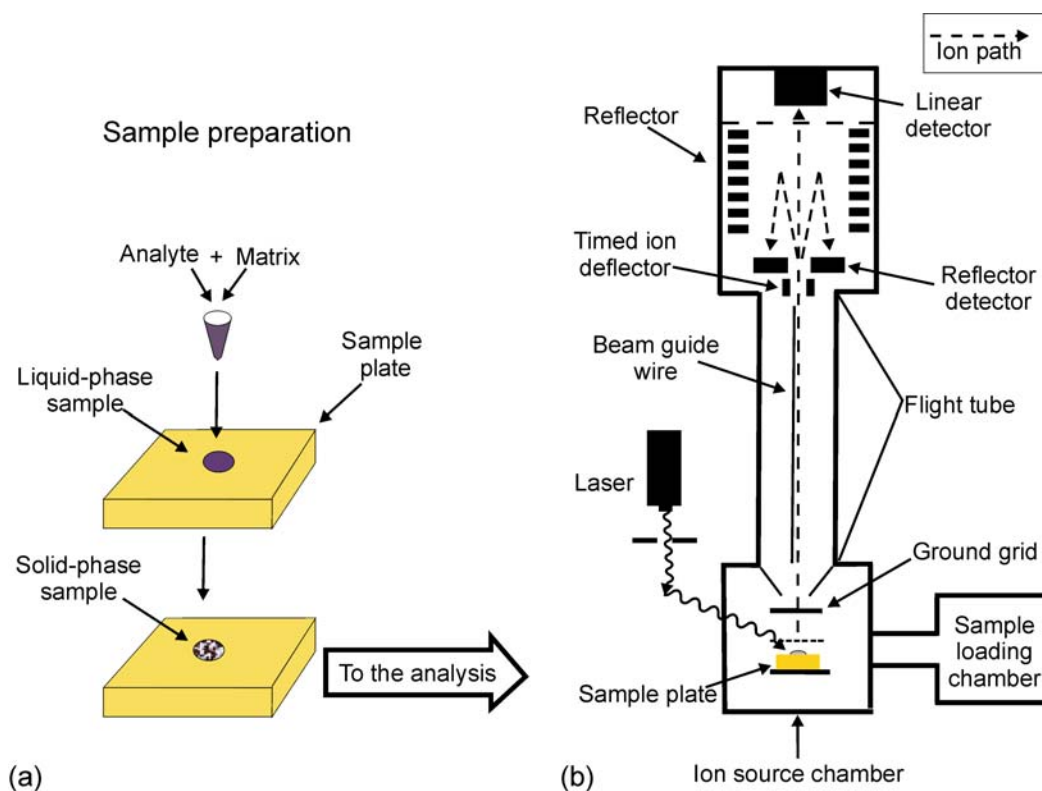


Figure 7.2. Schematic representation of (a) the sample preparation procedure for MALDI MS analysis and (b) the MALDI-TOF MS instrument.

7.4. Microreactor fabrication process and design

The microreactor (Figure 7.3) was designed to study on-line MALDI-TOF MS analyses of products of simple chemical and biochemical reactions ($A+B = C$ type). Therefore, the microreactor consists of two inlet reservoirs (A and B) for the injection of a maximum volume of 5 μL of reagent solutions and a 5 μL outlet pocket (C) where the analyte solution is collected and analyzed. The reaction microchannel in which the reagents react is 80 mm long, 200 μm wide and 100 μm deep. Due to the shape of the powderblasted channel, the cross-section is approximated to a 150 μm wide by 100 μm deep rectangle. The resulting channel volume is 1.2 μL . Microchannels and inlet / outlet holes were realized in a top borofloat wafer (1.1 mm thick) by high-resolution powder-blast micromachining.²⁸ This relatively new microfabrication technique²⁹ is faster but less precise than isotropic HF etching³⁰ and has the advantage of avoiding underetching. Great advantage of this technique is the possibility to realize an unlimited number of vertical feedthroughs in one process step of about 30 min. In order to avoid contact between the chip and the voltage grid of the MALDI instrument (Figure 7.2b), the top borofloat wafer was anodically bonded to a thinner silicon wafer (500 μm thick).

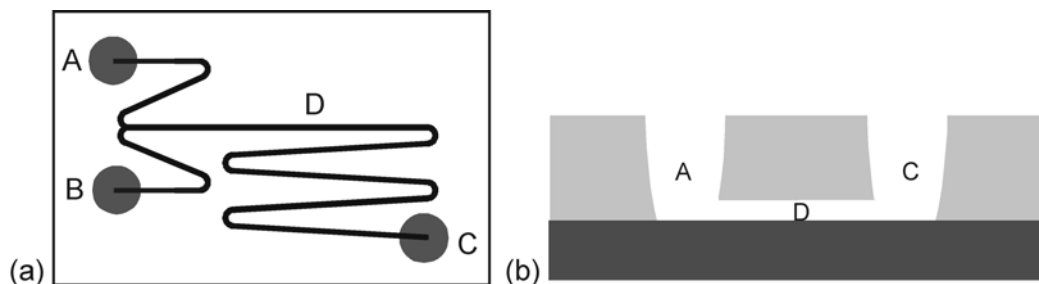


Figure 7.3. (a) Schematic top view of the microfluidics chip with the inlet (A and B) and the outlet (C) cups and the reaction microchannel (D); (b) side view of the micromachined top borofloat wafer (1) with one of the two inlets (A), the outlet (C) and the microchannel (D), anodically bonded with the bottom silicon substrate.

7.5. Inlets filling procedure

The inlet reservoirs were filled one by one using a micropipette and taking care that both the second inlet and the outlet holes were closed. Filling the inlet pockets without carefully following the procedure would cause the capillary force to drive the liquid out from the inlet reservoir into the channel. Closing the outlet and one of the inlet cups while loading the liquid in the other one, causes a counterpressure in the channel that keeps the liquid within the inlet pocket that is being filled. During the filling procedure both the outlet and the inlet holes not being filled were closed by means of adhesive tape. After loading of each inlet was completed, the inlet cups were sealed by applying a piece of glass fixed to the surface of the chip by means of adhesive tape.

7.6. Chip-MALDI sample plate integration

To perform the on-line experiments the glass-silicon chip was integrated in the MALDI-TOF sample plate (Figure 7.4). The integration of the microreaction and detection unit was achieved by placing the chip in a hole (1.35 mm deep) made in the sample plate by milling. Subsequently, the system (chip and sample plate) was introduced into the MALDI-TOF instrument by the standard loading procedure.

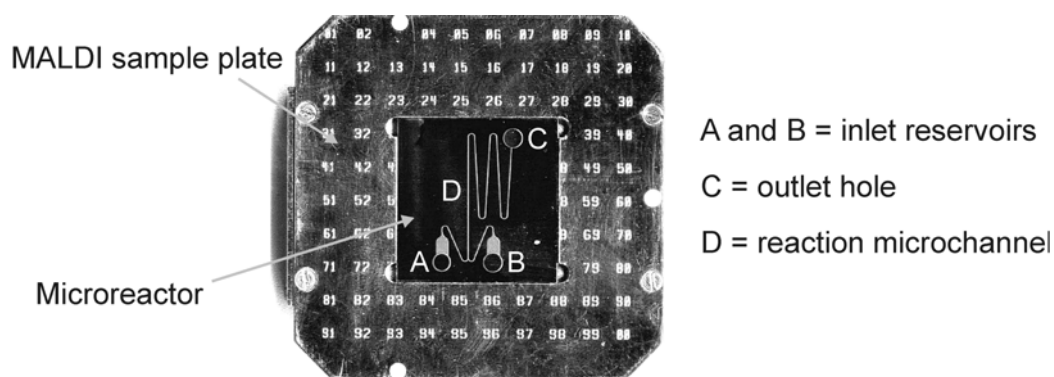


Figure 7.4. Photograph of the microreactor integrated with a standard MALDI-TOF sample plate. Because of the self-activating character of the microfluidics device, the system can be introduced into the MALDI ionization chamber without any wire or tube for the feeding and flow control.

7.7. Activation method

Just before loading the system the tape that closed the outlet pocket was removed. At this stage the liquid is kept in the inlet cups by the atmospheric pressure at the opened outlet (Figure 7.5a). Once the MALDI sample plate with the integrated microchip enters the vacuum ionization chamber, the counterpressure from the outlet disappears and the air in both inlet pockets pushes the liquid through the micro channel towards the outlet pocket (Figure 7.5b).

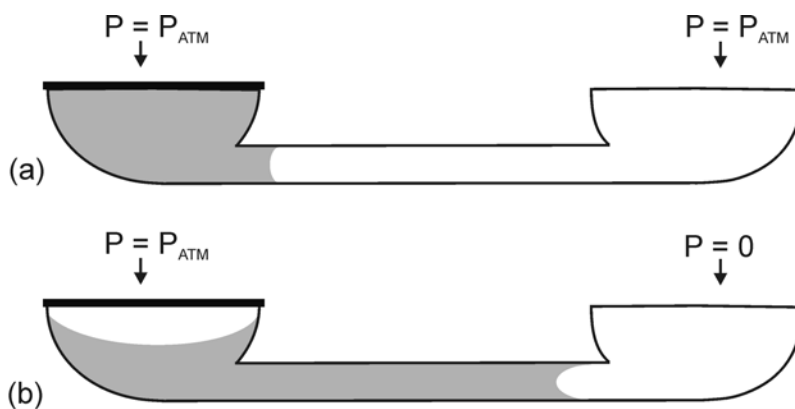


Figure 7.5. Passive pressure-driven mechanism of fluidics handling. (a) The liquid is kept into the inlet reservoirs by air ($p = p_{atm}$) present in the channel. (b) Inside the MS the decrease in pressure at the outlet causes the liquid to flow to the outlet through the microchannel.

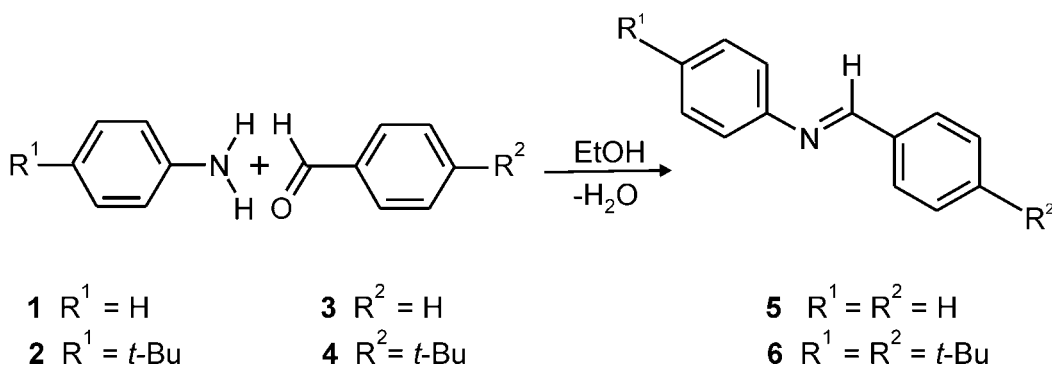
A second driving force that might affect the fluidic flow is the capillary pressure $p_{cap} = 2\gamma/r$ (where r is the radius of the tube and γ is the surface tension of the liquid in the channel).³¹ However, in the current chip, in which the channel diameter is in the order of $100\ \mu\text{m}$, the capillary pressure ($1.44 \times 10^3\ \text{Pa}$ for water) is small compared to the pneumatic driving force ($10^5\ \text{Pa}$).

7.8. On-chip reactions

To demonstrate the effectiveness of the MALDI-based integrated microfluidics device, a few simple chemical and biochemical reactions were carried out in the MALDI-chip and their products analyzed on-line at the chip outlet (*vide supra*).

7.8.1. Schiff base formation

The Schiff base reaction (Scheme 7.1), in which primary amines (**1** and **2**) react with aldehydes (**3** and **4**) to give imines (**5** and **6**), was chosen as a primary study of the microreaction unit and its coupling with MALDI-TOF MS, because it is a straightforward reaction and products are obtained in high yields. The pH control required for the Schiff base formation³² turned out to be not necessary under “lab-on-a-chip” conditions as a consequence of the high surface-to-volume ratio that characterizes microreactors (see Chapter 3).



Scheme 7.1. Schiff base formation reaction.

A first experiment was carried out reacting on-chip equimolar (2×10^{-4} M) solutions of aniline (**1**) and benzaldehyde (**3**) in ethanol. The MALDI mass spectrum (Figure 7.6a) only shows the signal of the reaction product, imine **5** ($m/z = 182$), proving the quantitative reaction of the reagents **1** and **3** in the microchannel. Post source decay experiments³³ were performed on the same sample collected at the chip outlet, in order to confirm the structure of the on-chip formed imine **5**. By *in-situ* fragmentation of the reaction product ions at $m/z = 182$, fragments F_1 ($m/z = 104$) and

F_2 ($m/z = 77$) were generated and detected, validating the structure of imine **5** (Figure 7.6a). Figure 7.6b shows the MALDI mass spectrum of imine **6** ($m/z = 294$) formed on-chip by reacting equimolar (2×10^{-4} M) solutions of reagents **2** and **4** in ethanol. The same reaction was carried out on-chip by reacting two equivalents of aldehyde **4** with one equivalent of amine **2**. In this case signals of both product and excess of reagent were detected by MALDI MS (Figure 7.6c).

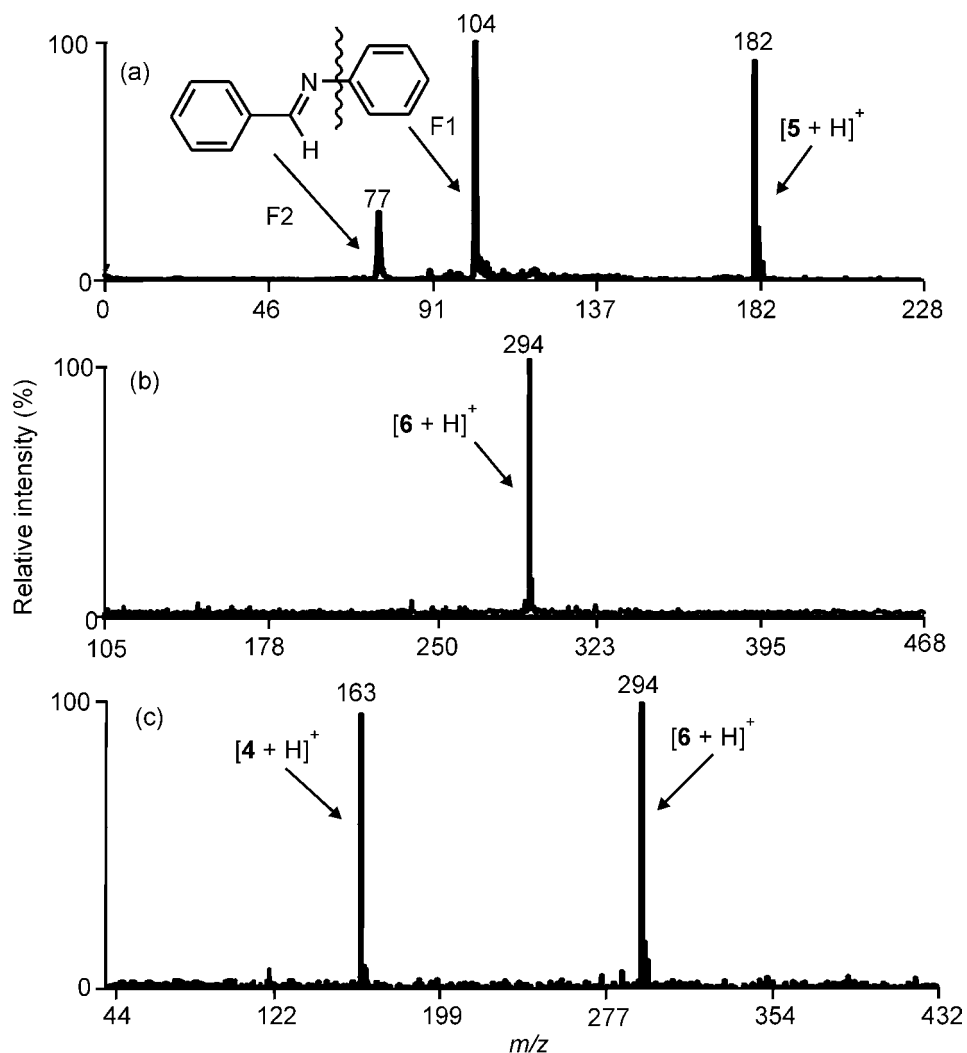


Figure 7.6. MALDI-TOF mass spectra of the Schiff base reaction products: (a) imine **5** at $m/z = 182$ formed in the reaction microchannel in experiment 1 and its MALDI-TOF PSD mass spectrum fragments F1 and F2; (b) imine **6** at $m/z = 294$ formed on-chip during experiment 2; (c) imine **6** at $m/z = 294$ formed on-chip during experiment 3 and the excess of reagent **4** at $m/z = 163$.

7.8.2. Polymers

In order to prove the versatility of the microfluidics system as a platform for different applications, its ability to separate mixtures of polymers was tested. MALDI mass spectra show two different polymer distributions separated in time (Figure 7.7). The two different polymer distributions can be easily assigned to the injected polymers by the peak to peak separation due to the different molecular weight of the monomers. The first pattern recorded in time was assigned to polystyrene (PS; Figure 7.7a) and the second to poly(methyl methacrylate) (PMMA; Figure 7.7b); the difference in mass between adjacent peaks being 104 and 100 mass units, respectively.

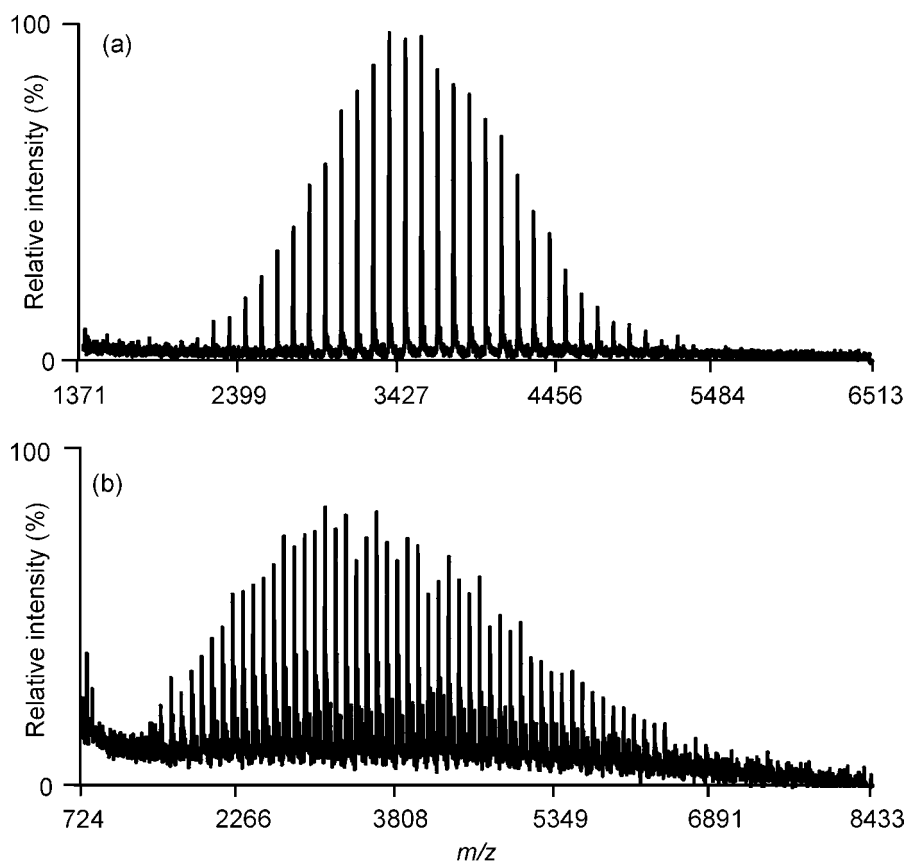


Figure 7.7. MALDI-TOF mass spectra of the two different polymer distributions separated in arrival time at the outlet reservoir and assigned to (a) polystyrene (PS) and (b) poly(methyl methacrylate) (PMMA).

This result shows that the chip is capable of separating the two polymers, on the basis of their different polarities. Due to its polar side chains, PMMA may interact with the channel walls, resulting in longer on-chip residence times than the apolar PS. These results suggest the possible application of the here presented lab-on-a-chip as a separation tool, comparable to gel permeation chromatography.³⁴

7.8.3. Oligonucleotides

Mass spectrometry is an outstanding technique for the characterization and sequence determination of oligonucleotides generated *via* solution-phase chemical reactions.³⁵ The DNA sequence can be determined by the mass difference between the oligonucleotide fragments of (partial) digests from either end of the DNA molecule. Oligonucleotide digestion was performed directly on the microfluidics chip by mixing the oligonucleotide (substrate) with snake venom phosphodiesterase (SVP) that hydrolyzes DNA in the 3' to 5' direction. MALDI MS analysis of the hydrolysis products was performed at the chip outlet where the sample was collected. The mass difference between adjacent pairs of peaks in the MALDI-TOF mass spectrum identifies each nucleotide base in the sequence. In Figure 7.8 the peak of the oligonucleotide (at $m/z = 12586$) and those of the oligonucleotide residues are shown. From the average masses of the individual bases (Table 7.1) the oligonucleotide sequence can be derived (GCTCTAGACT).

Table 7.1. Average masses of the individual nucleotide bases.

Name	Abbreviation	Average mass (Da)
Adenine	A	313.2
Cytosine	C	289.2
Guanine	G	329.2
Thymine	T	304.2

This approach to analyze exonuclease ladders seems to be a particularly promising tool to determine rapidly the sequence of oligonucleotides. Compared to conventional methods, based on the lab-scale preparation of a large number of samples at different enzyme and substrate concentrations followed by MALDI MS analysis, the microfluidics approach offers the advantage of saving time and material. Furthermore, due the limited sample handling, the risks encountered when manipulating biomolecules is also reduced as well as that of sample contamination.

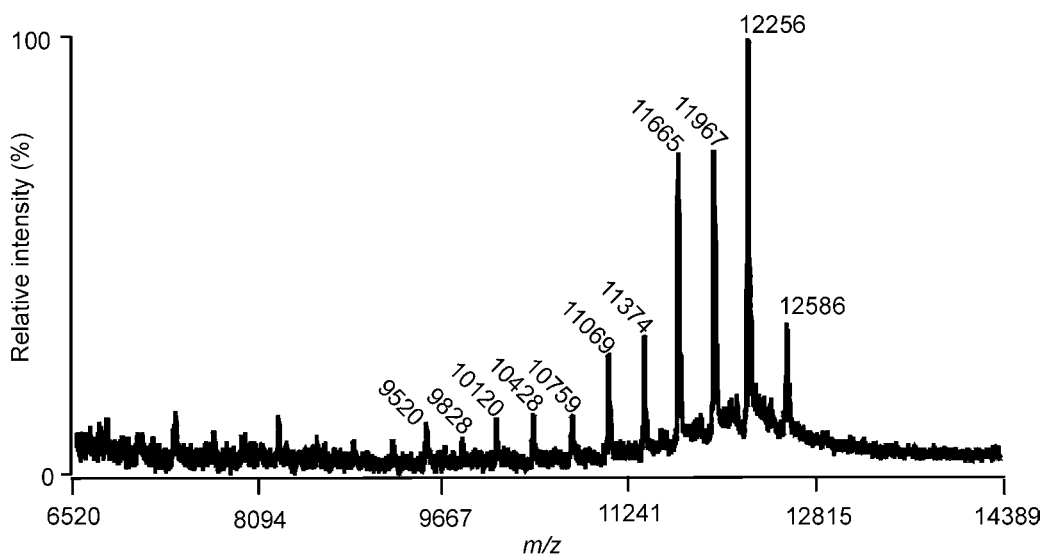


Figure 7.8. MALDI-TOF mass spectrum of the oligonucleotide at $m/z = 12586$ and the oligonucleotide residue average masses after enzymatic digestion carried out on-chip.

7.8.4. Peptide-sequencing

Carboxypeptidase Y (CPY) sequentially hydrolyzes the C-terminal residues of peptides,³⁶ which can be subsequently analyzed directly by mass spectrometry. The sequence of the peptide fragments can be determined from the mass differences between the adjacent peaks in the mass spectrum. In the lab-on-a-chip approach peptide digestion and product analysis are performed directly on the chip, thus minimizing sample handling, sample loss and method development time. In the lab-on-a-chip methods, indeed, only a total of a few picomoles of peptides are required, and the analysis can be made *in-situ* immediately after digestion, thereby avoiding

sample transfer to the mass spectrometer. After data acquisition and mass calculation the mass differences between the adjacent peaks in the ladders were used to determine the C-terminal sequence of the peptide (Figure 7.9).

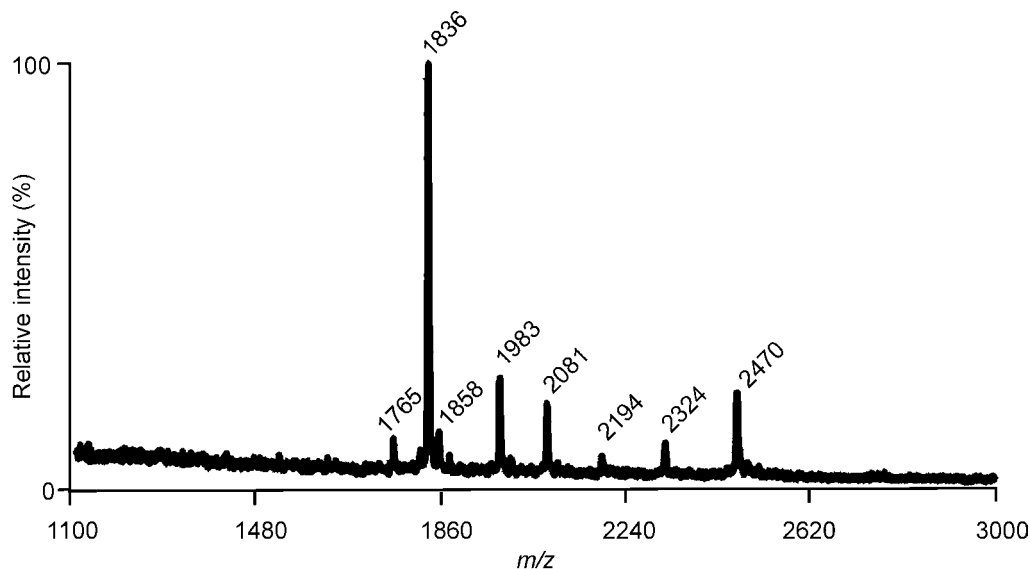


Figure 7.9. MALDI-TOF mass spectrum of the ACTH peptide $m/z = 2470$ and the amino acid residues after enzymatic digestion. The sequence resulting from the partial on-chip digestion is: Phe-Glu-Leu-Pro-Phe-Ala.

7.9. Conclusions

An integrated microfluidics device that allows chemical syntheses, separations, and biochemical processes on a microscale and in real-time monitored by MALDI-TOF MS was developed for the first time. The effectiveness of the lab-on-a-chip device was illustrated for a variety of systems ranging from simple synthetic chemistry to polymer analysis and enzymatic digestion of peptides and oligonucleotides. After the chip is placed in the MALDI-TOF vacuum chamber, and as soon as the reaction mixture (products and unreacted reagents) reaches the outlet, the laser beam ionizes the molecules, which are detected by the TOF analyzer. An important novelty of this approach is the possibility to analyze by MALDI-TOF MS the reaction products *in-situ* as soon as they are formed. Molecules with masses ranging from a few hundred to a few thousand Da were successfully detected, thus

demonstrating the wide range of applicability of the microfluidics system. This result was achieved by realizing a “self-activating” chip, which avoids the need of introducing wires and tubes in to the ionization chamber of the MALDI-TOF instrument.

Main limitation of the integrated microfluidics device is the poor fluidics control. By a proper design of the fluidic circuit and the integration of multiple sampling ports, direct, real-time monitoring of product formation during the reaction will become feasible, thus opening the way to kinetics studies.

7.10. Experimental

The preparation of polymer, nucleotide, and peptide samples was done by Dr. Roel H. Fokkens.

Microreactor. The microfluidics device used in the experiments (Figure 7.3) was fabricated in the cleanroom facilities of the MESA⁺ Institute for Nanotechnology by Ir. M. H. Goedbloed. The fabrication process steps are depicted in Figure 7.10.

Detection. The reaction products formed in the microreactor channel and collected in the chip outlet were, in real-time, identified by MALDI-TOF MS using a Voyager-DE-RP MALDI-TOF mass spectrometer (Applied Biosystems / PerSeptive Biosystems, Inc., Framingham, USA) equipped with delayed extraction^{37,38} and a 337 nm UV nitrogen laser producing 3 ns pulses. The mass spectra were obtained both in the linear and reflectron mode. To avoid fast solidification of the reaction products at the outlet reservoirs of the microchip, the vacuum pressure in the ionization chamber of the mass spectrometer was gradually reduced while introducing the chip-MALDI sample plate. The pressure inside the time-of-flight analyzer was kept at 1×10^{-8} torr (1.33×10^{-6} Pa).

Testing the chip via Schiff base formation. Reagents were obtained from Aldrich Chemicals, The Netherlands. Samples were used as supplied commercially without further purification. No matrix was added for MALDI detection of the aromatic products of these systems, because of their strong absorption at the laser wavelength

($\lambda = 337$ nm). Three Schiff base reactions were performed on-chip and the products were analyzed on-line.

Reaction 1. 3 μL of a solution of 2×10^{-4} M aniline (**1**) in ethanol was placed in inlet A; inlet B was filled with 3 μL of a solution of 2×10^{-4} M benzaldehyde (**3**) in ethanol.

Reaction 2. Inlet A was filled with 3 μL of a solution of 2×10^{-4} M 4-*tert*-butylaniline (**2**) in ethanol and inlet B was filled with 3 μL of a solution of 2×10^{-4} M 4-*tert*-butylbenzaldehyde (**4**) in ethanol.

Reaction 3. Inlet A was filled with 3 μL of a solution of 2×10^{-4} M 4-*tert*-butylaniline (**2**) in ethanol and inlet B was filled with 3 μL of a solution of 4×10^{-4} M 4-*tert*-butylbenzaldehyde (**4**) in ethanol.

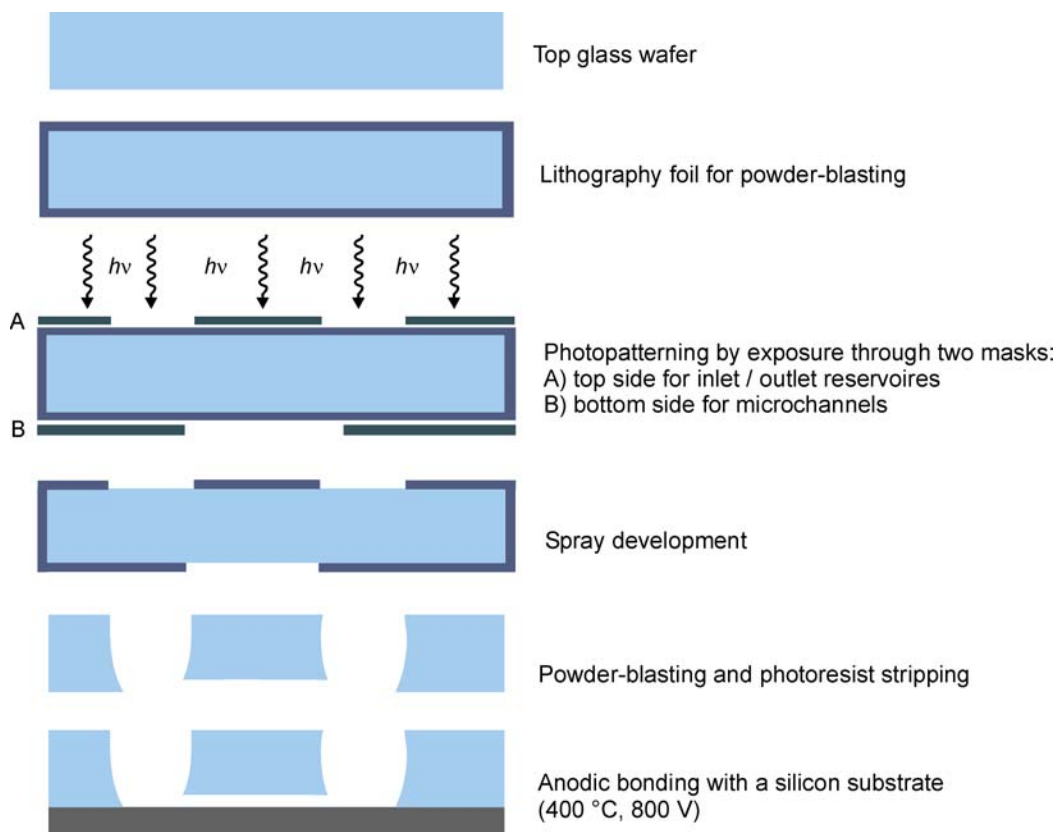


Figure 7.10. Description of the fabrication process of the self-activating chip.

Testing the chip with polymers. Reagents were obtained from Aldrich Chemicals, The Netherlands and were used as supplied commercially without further purification. Dihydroxybenzoic acid (DHB) was used as the matrix. In inlet A 0.3 μL of polystyrene, PS ($MW_{\text{av}} = 3,500$ Da), in THF/water was injected with DHB as the matrix. In inlet B 0.3 μL of poly(methyl methacrylate), PMMA ($MW_{\text{av}} = 3,500$ Da), in THF/water was injected with DHB as matrix.

Testing the chip for oligonucleotide sequencing. The Sequazyme[™] (PerSeptive Biosystems, Framingham, USA) oligonucleotide sequencing kit was used for sequencing synthetic deoxyoligonucleotides by partial exonuclease digestion followed by MALDI-TOF MS. The method was applied to a 41-base oligodeoxynucleotide in which a nucleobase was replaced by a hydrogen atom. Since oligonucleotides strongly bind trace amounts of salts, sample deionization *via* cation exchange is required. To this end the sample was transferred to Parafilm and mixed with the cation exchange beads provided with the kit. Since the investigated oligonucleotide is longer than 10 bases, desalting was performed using spin column purification with a QuickSpin[™] C-25 column (Boehringer, Mannheim, Germany). Inlet A was used for the introduction of 0.3 μL of the oligonucleotide at a concentration of 2×10^{-4} M in HPLC grade-water. The pH optimum for snake venom phosphodiesterase (SVP) digestion experiments is basic and therefore 0.3 μL of ammonium citrate buffer was mixed with 1 μL of SVP dilution (1×10^{-4} M). SVP hydrolyzes in the 3' to 5' direction of the oligonucleotide. A 0.3 μL portion of supernatant SVP was transferred to the inlet position B of the chip device. Additionally, 0.2 μL of a saturated solution of 3-hydroxypicolinic acid (HPA, matrix) in water was injected into inlet B.

Testing the chip for peptide sequencing. The Sequazyme[™] (PerSeptive Biosystems, Framingham, USA) C-peptide sequencing kit enables peptide digestion followed by analysis of sequentially truncated peptides using MALDI-TOF MS. Before digesting and analyzing unknown samples of the peptide (adrenocorticotrophic hormone), the activity of the enzyme carboxypeptidase Y CPY was checked by dilution experiments with citrate buffer (pH = 6.1), CPY dilution and the peptide standard Angiotensin I. The adrenocorticotropin ACTH (18-39) fragment (0.3 μL) was transferred as a solution of 5×10^{-5} M in a 1:1 v/v% mixture of water and acetonitrile to inlet A. Inlet B contained 0.3 μL of a solution of 0.1 mM CPY in HPLC-grade water and

ammonium citrate (pH = 6.1) and 0.2 μL of the matrix α -cyano-4-hydroxycinnamic acid in a 1:1 v/v% mixture of water and acetonitrile and 0.1% trifluoroacetic acid (TFA). Immediately after the introduction of the ACTH 18-39 peptide the CPY dilution including the matrix was transferred to inlet B.

7.11. References

- 1 Karas, M.; Hillenkamp, F. *Anal. Chem.* **1988**, *60*, 2299.
- 2 Overberg, A.; Karas, M.; Bahr, U.; Kaufmann, R.; Hillenkamp, F. *Rapid Commun. Mass Spectrom.* **1990**, *4*, 293.
- 3 Karas, M.; Bahr, U.; Ingendoh, A.; Hillenkamp, F. *Angew. Chem. Int. Ed. Engl.* **1989**, *28*, 760.
- 4 Chan, T.-W. D.; Colburn, A. W.; Derrik, P. *J. Org. Mass Spectrom.* **1992**, *27*, 53.
- 5 Stupat, K.; Karas, M.; Hillenkamp, F. *Int. J. Mass Spectrom. Ion Proc.* **1991**, *111*, 89.
- 6 Karas, M.; Bahr, U.; Ingendoh, A.; Nordhoff, E.; Stahl, B.; Strupat, K.; Hillenkamp, F. *Anal. Chim. Acta* **1990**, *241*, 175.
- 7 Overburg, A.; Hassemburger, A.; Hillenkamp, F. in: Gross, M. L. (ed) *Mass spectrometry in the biological sciences: a tutorial*; Kluwer Academic Publishers: Amsterdam, The Netherlands, **1992**, 181.
- 8 Stahl, B.; Steup, M.; Karas, M.; Hillenkamp, F. *Anal. Chem.* **1991**, *63*, 1463.
- 9 Bahr, U.; Deppe, A.; Karas, M.; Hillenkamp, F.; Giessmann, U. *Anal. Chem.* **1992**, *64*, 2886.
- 10 Danis, P. O.; Karr, D. E.; Mayer, F.; Holle, A.; Watson, C. H. *Org. Mass Spectrom.* **1992**, *27*, 843.
- 11 Cohen, L. H.; Gusev, A. I. *Anal. Bioanal. Chem.* **2002**, *373*, 571.
- 12 Schriemer, D. C.; Li, L. *Anal. Chem.* **1996**, *68*, 2721.
- 13 Keller, B. O.; Li, L. *J. Am. Soc. Mass Spectrom.* **2001**, *12*, 1055.
- 14 For reviews on off-line fraction collection-MALDI analysis see: a) Murray, K. *Mass Spectrom. Rev.* **1997**, *16*, 283. b) Gusev, A. I. *Fresenius J. Anal. Chem.* **2000**, *366*, 691.
- 15 Murray, K. K.; Russel, D. H. *Anal. Chem.* **1993**, *65*, 2534.
- 16 Lawson, S. J.; Murray, K. K. *Rapid Commun. Mass Spectrom.* **2000**, *14*, 129.
- 17 Li, L.; Wang, A. O. L.; Coulson, L. D. *Anal. Chem.* **1993**, *65*, 493.
- 18 Zhan, Q.; Gusev, A. I.; Hercules, D. M. *Rapid Commun. Mass Spectrom.* **1999**, *13*, 2278.
- 19 Ornes, H.; Graf, T.; Degn, H.; Murray, K. K. *Anal. Chem.* **2000**, *72*, 251.
- 20 Chen, Y.-C.; Shiea, J.; Sunner, J. *Rapid Commun. Mass Spectrom.* **2000**, *14*, 86.

- 21 Chen, Y.-C. *Rapid Commun. Mass Spectrom.* **1999**, *13*, 821.
- 22 Gusev, A. I.; Proctor, A.; Rabinovich, Y. I.; Hercules, D. M. *Anal. Chem.* **1995**, *67*, 1805.
- 23 Guittard, J.; Hronowski, X. L.; Costello, C. E. *Rapid Commun. Mass Spectrom.* **1999**, *13*, 1838.
- 24 Mowthorpe, S.; Clench, M. R.; Cricelius, A.; Richards, D. S.; Parr, V.; Tetler, R. W. *Rapid Commun. Mass Spectrom.* **1999**, *13*, 2.
- 25 De Mello, A. J. *Lab Chip* **2001**, *1*, 7N.
- 26 Oleschuk, R. D.; Harrison, D. J. *Trends Anal. Chem.* **2000**, *6*, 379.
- 27 Karas, M.; Bahr, U. *Mass Spectrom. Rev.* **1991**, *10*, 335.
- 28 Wensink, H.; Berenschot, J. W.; Jansen, H. V.; Elwenspoek, M. C., *Proc. 13th Int. Workshop on Micro ElectroMechanical Systems (MEMS2000)*, Miyazaki, Japan, **2000**, 769.
- 29 Slikkerveer P. J.; Bouten, P. C. P.; De Haas, F. C. M. *Sens. Actuators* **2000**, *85*, 296.
- 30 Corman, T.; Enoksson, P.; Stemme, G. J. *J. Micromach. Microeng.* **1998**, *8*, 84.
- 31 Atkins, P. W. *Physical Chemistry*, 5th ed.; Oxford University Press: Oxford, UK, **1994**; Chapter 28.
- 32 Solomons, T. W. G., *Fundamentals of Organic Chemistry*, 5th ed.; John Willey & Sons: New York, USA, **1998**; Chapter 8.
- 33 Stahl-Zeng, J.; Hillenkamp, F.; Karas, M. *Eur. J. Mass Spectrom.* **1996**, *2*, 23.
- 34 Nielen, M. W. F. *Mass Spectrom. Rev.* **1999**, *18*, 309.
- 35 Limbach, P. A. *Mass Spectrom. Rev.* **1996**, *15*, 297.
- 36 Patterson, D. H.; Tarr, G. E.; Martin S. A. *Anal. Chem.* **1995**, *67*, 3971.
- 37 Vestal, M. L.; Juhasz, P.; Martin, S. A. *Rapid Commun. Mass Spectrom.* **1995**, *9*, 1044.
- 38 Juhasz, P.; Vestal, M. L.; Martin, S. A. *J. Am. Soc. Mass Spectrom.* **1997**, *8*, 209.

Chapter 8

Towards a MALDI-Chip Integrated Device for the Study of Reaction Kinetics

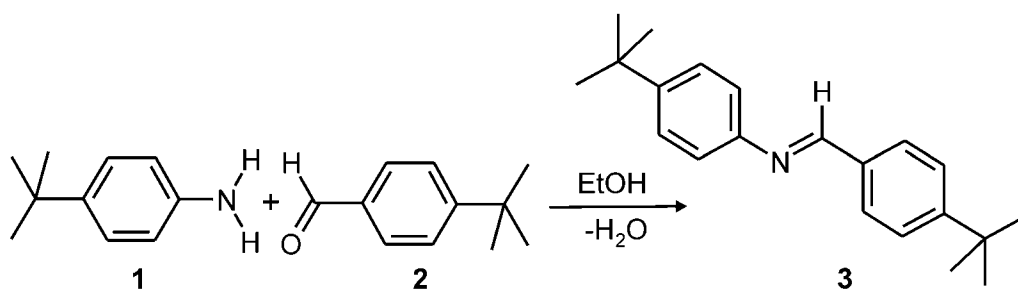
*This Chapter deals with the optimization of the integrated MALDI-chip device described in Chapter 7. A new microchip is fabricated, allowing longer reaction and measuring times. A new concept is introduced consisting of the integration of a monitoring port along the microfluidics path into the chip design, for real-time reaction monitoring. The Schiff base reaction between 4-tert-butylaniline (**1**) and 4-tert-butylbenzaldehyde (**2**) in ethanol was carried out on-chip in the MALDI ionization chamber and the formed imine **3** was detected in situ, demonstrating the feasibility of the “monitoring window” approach. This preliminary result opens the way to on-chip kinetic studies by MALDI MS, which will become feasible by opening multiple monitoring windows along the microchannel.*

8.1. Introduction

In Chapter 7 a MALDI-chip integrated device was described. Reactions were initiated by using the vacuum of a mass spectrometer to move solutions within the microreactor. An important novelty of such an integrated microfluidics system is the possibility to analyze “on the spot” the reaction mixture by matrix-assisted laser desorption ionization (MALDI)^{1,2} time-of-flight (TOF) mass spectrometry (MS), immediately after the reaction has taken place. The chip is placed in the MALDI-TOF vacuum chamber and as soon as the reaction product reaches the outlet the MALDI laser beam ionizes the molecules, which are subsequently detected by the TOF analyzer.

Based on the channel geometry very high flow rates can be generated using the vacuum-driven actuation, which results in very short residence times. Furthermore, the reaction mixture can only be analyzed at one sampling spot (the outlet) where the reaction mixture is collected. As a consequence no time-dependent experiments can be done. A proper design of the fluidic circuit and the integration of multiple outlet ports would allow a *quasi*-continuous monitoring of the reaction mixture in time, thus extending the use of the MALDI-chip to kinetic studies.

This Chapter deals with the fabrication of a microreactor, which allows longer reactions and measurements times. In addition, a novel concept is described, consisting of the integration of a “monitoring window” into the chip design for monitoring reactions by using the MALDI-chip set-up. As a model reaction the Schiff base reaction³ between 4-*tert*-butylaniline (**1**) and 4-*tert*-butylbenzaldehyde (**2**) in ethanol to give the corresponding imine **3** (Scheme 1) was carried out in the MALDI-chip and the reaction mixture was analyzed through the “monitoring window”.



Scheme 8.1. Schiff base formation reaction.

8.2. Fluid dynamics

In the MALDI-chip of Chapter 7 the fluid is transported through the microchannels due to a pressure difference between the inlet, where a small air bubble is present (atmospheric pressure), and the outlet (vacuum). The relation between the generated flow rate and the applied vacuum pressure is defined by equation 8.1.^{4,5}

$$\Delta p = R \cdot \phi_v \quad (8.1)$$

where Δp [N m⁻²] is the pressure drop across the channel and ϕ_v [m³ s⁻¹] is the volumetric flow through the channel. The hydraulic resistance R [N s m⁻⁵], which is dependent on the channel geometry and the viscosity of the fluid μ [N s m⁻²], is calculated by integrating the velocity profile over the cross-section area. Based on the channel geometry a number of design formulas for the calculation of the hydraulic resistance have been derived.⁶ For rectangular channels (Figure 8.1), such as that of the MALDI-chip, the resistance R can be calculated according to equation 8.2.

$$R = \frac{4 \cdot \mu \cdot l}{a \cdot b^3} \left\{ \frac{16}{3} - 3.36 \cdot \frac{b}{a} \cdot \left(1 - \frac{b^4}{12 \cdot a^4} \right) \right\}^{-1} \quad (8.2)$$

where l [m] is the channel length, $2a$ and $2b$ the channel width and depth, respectively, and μ [Nsm⁻²] the liquid viscosity. Equation 8.2 is valid for low Reynold numbers (*i.e.* laminar flow regimes) and long channels, implying that entrance effects can be neglected. Using equation 8.1 and knowing the channel length l of the MALDI-chip the residence time $t_{(r)}$ [s] can be calculated according to equation 8.3.

$$t_{res} = \frac{l \cdot A \cdot R}{\Delta p} \quad (8.3)$$

where A [m²] is the channel cross-sectional surface area. In the MALDI-chip microchannel ($2a = 1.5 \times 10^{-4}$ m; $2b = 1 \times 10^{-4}$ m; $l = 8 \times 10^{-2}$ m) the calculated resistance is $R = 1.55 \times 10^{13}$ N s m⁻⁵ (for water; $\mu = 1 \times 10^{-3}$ N s m⁻²). The residence time for an applied pressure difference of 1 bar (10⁵ Nm⁻²) is $t_{(r)} = 1.9 \times 10^{-1}$ s.

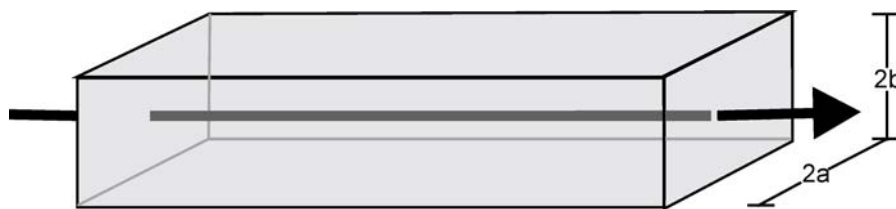


Figure 8.1. Schematic representation of a rectangular channel where $2a$ and $2b$ define the cross section dimensions.

It is evident that no time-dependent experiments are possible using the microfluidics device of Chapter 7, since the residence times are in the order of two hundred milliseconds. Even when opening multiple sampling ports along the channel, the time necessary to move the ionizing laser from one window to the next would be much too long compared to the on-chip residence times. Channels that have a higher hydraulic resistance are a possible solution to the short on-chip residence times. A new microfluidics system was therefore designed to allow a longer residence time (in the order of a few tens of seconds).

8.3. Microreactor optimization

8.3.1. Microreactor design and fluid dynamics

A microreactor was designed (Figure 8.2) having $30\ \mu\text{m}$ wide, $10\ \mu\text{m}$ deep and $125\ \text{mm}$ long channels, fabricated in a glass substrate by wet chemical etching using HF. The hydraulic resistance as well as the residence time in this new channel design were calculated using equations 8.2 and 8.3 to give values of $R = 6.3 \times 10^{16}\ \text{N s m}^{-5}$ and $t_{(r)} = 24\ \text{s}$.

Due to downscaling of the microchannel the surface free energy^{7,8} (“surface tension”) becomes considerable. As a consequence the contribution of capillary pressure to the MALDI-chip pumping mechanism will be significant. For a flat rectangular channel the capillary pressure P_c [Pa] is given by equation 8.4.^{9,10}

$$P_c = \frac{2 \cdot \gamma \cdot \cos \theta_c}{h} \quad (8.4)$$

where γ [N m^{-1}] is the surface tension of the liquid in the channel, θ_c is the contact angle between the meniscus and the channel wall (which for water in hydrophilic channels is assumed to be between 0° and 30°), and h [m] is the channel depth. However, the capillary pressure P_c ($1.3 \times 10^4 \text{ N m}^{-2}$) estimated for water ($\gamma = 0.07 \text{ N m}^{-1}$; $\cos\theta_c \sim 0.9$ with $\theta_c = 25^\circ$) is only about 10% of the pneumatic pressure used to drive the flow in the channel (10^5 N m^{-2}). Therefore it can be concluded that the hydraulic resistance and residence times calculated according to equations 8.2 and 8.3, without taking into account the contribution of the capillary pressure, are a good estimation of the fluid dynamics in the microchannel depicted in Figure 8.2.

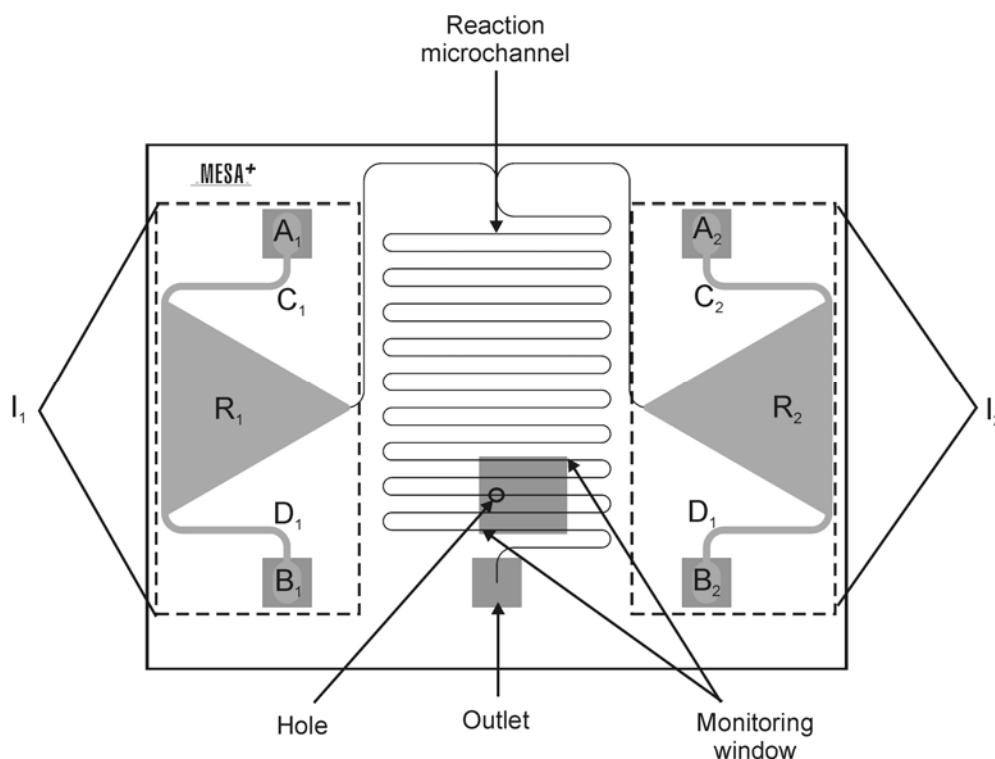


Figure 8.2. Schematic overview of the chip used to prove the “monitoring window” principle. Each inlet loading system (I_x and I_x) consists of two inlet holes (A_x and B_x) connected to a reservoir (R_x) through channels C_x and D_x (with $x = 1$ and 2).

Although the estimated residence times in the new microchannel are about 2 orders of magnitude higher than those in the previous MALDI-chip design, they are still too short to study reaction kinetics by MALDI MS. However, a considerably longer total measurement time (~ 75 min) can be obtained by the introduction of

relatively large reservoirs for the reagent solutions (*vide infra*). Due to the long measurement time obtainable, this chip was used to demonstrate the “monitoring window” principle.

8.3.2. “Monitoring window” description

The key element of the new microreactor (Figure 8.2) is the “monitoring window”. This consists of a freestanding $\sim 2\ \mu\text{m}$ thick silicon membrane doped with boron, positioned above the channel (Figure 8.3a). Ions can be extracted from the flowing reaction mixture through holes within the silicon membrane. Holes (250 and 500 by 500 nm), which could be visualized by scanning electron microscopy (SEM), were made by means of a focused ion beam (FIB). A SEM micrograph of the 250 by 250 nm holes is given in Figure 8.3b. The hole dimensions are important, since a pressure drop along the channel may arise from too large holes in the membrane, thereby affecting the microfluidics actuation mechanism.

The position and the dimensions of the “monitoring window” are also important factors. The dimensions of the window in the top silicon wafer must be large enough to let the laser beam, which hits the chip surface under an angle of about 30° , reach the small holes fabricated in the boron-doped silicon membrane on the bottom side of the same wafer.

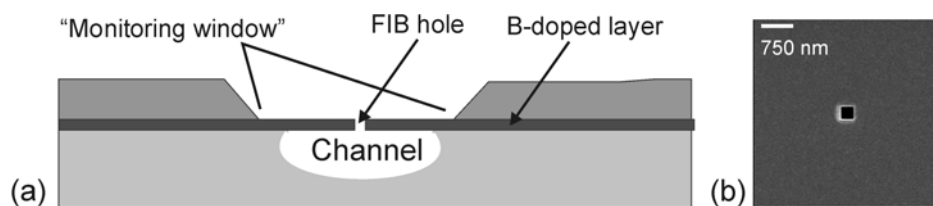


Figure 8.3. (a) Cross section of the silicon / glass hybrid chip with a KOH-etched “monitoring window” and a sampling hole above the HF-etched microchannel. (b) SEM image of a 250 by 250 nm sampling hole made by FIB in the doped silicon layer.

8.3.3. Inlet loading system

In the first version of the MALDI-chip reagent solutions were loaded in inlet cups fabricated in the top wafer by powderblast micromachining. The inlets were then sealed with adhesive tape. A drawback of this inlet system is that the solutions can easily become contaminated by coming into contact with the adhesive tape. A new reagents loading scheme was developed (Figure 8.2) consisting of two inlet systems (I_1 and I_2). Each system comprises two *via*-holes etched in the top silicon wafer (A_1 , B_1 and A_2 , B_2 , respectively), a triangular reservoir (R_1 and R_2) and two 200 by 100 μm powderblasted channels (C_1 , D_1 and C_2 , D_2) that connect each inlet hole with the corresponding reservoir. Flap valves (Figure 8.4a) were fabricated in the doped silicon layer at the bottom of the inlet holes (Figure 8.4b). These valves keep the loaded solutions in the bottom wafer, thereby eliminating the risk of contamination. The triangular reservoirs (5.4 mm high, 6.2 mm wide and 100 μm deep) were powderblasted in the bottom glass wafer.

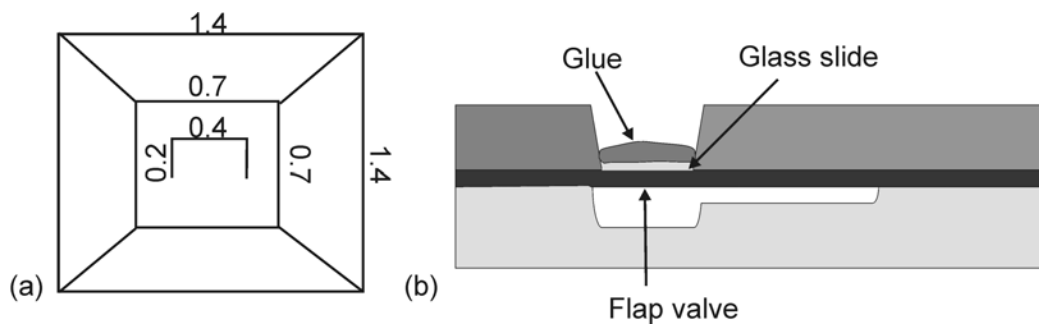


Figure 8.4. (a) Top view of the flap valve at the bottom side of each inlet hole (the dimensions are given in mm) and (b) cross-section of the inlet hole.

The microreactor was used to test the feasibility of monitoring on-chip reactions by ionizing liquid-phase samples through the “monitoring window”.

8.4. “Monitoring window” testing

8.4.1. Inlet filling procedure

The reservoirs were filled by suction of reagent solutions using a syringe. About 3 μL of reagent solutions were placed in holes A_1 and A_2 , while the syringe was placed on holes B_1 and B_2 . During the filling procedure the chip was placed in a suitable holder. In order to prevent the liquid from filling the reaction channel before entering the MALDI chamber, all other openings (outlet, monitoring window and second inlet) were sealed with adhesive tape during the filling procedure of each inlet. Furthermore, due to the triangular shape of the reservoirs an air bubble was entrapped during the filling procedure (at the reservoir corner where the small channel starts). This prevents filling of the small channel due to capillary forces. After both reagents were placed in the reservoirs, the four inlet holes were closed using a UV-curable glue. A glass slide (700 by 700 μm) was placed in the inlet holes to prevent the glue from entering the inlet channels, thereby polluting the reactants.

8.4.2. On-chip reaction and analysis

To prove the principle of the “monitoring window” the Schiff base formation reaction between 4-*tert*-butylaniline (**1**) and 4-*tert*-butylbenzaldehyde (**2**) in ethanol (Scheme 1) was carried out using the MALDI-chip device equipped with the chip of Figure 8.3. The chip on the MALDI sample plate was introduced into the vacuum chamber by load-lock. The first MALDI-TOF mass spectrum was acquired as soon as the plate reached the right spot in the chamber. The analysis was started after about 1 min. Ions were extracted from the channel through the hole, by hitting the “monitoring window” with the laser. The reaction product, imine **3**, was clearly visible in the mass spectrum at $m/z = 295$ (Figure 8.5). Even after about 1 h imine **3** could still be detected, indicating that reagent solutions were still available for the reaction, as predicted by theoretical calculations.

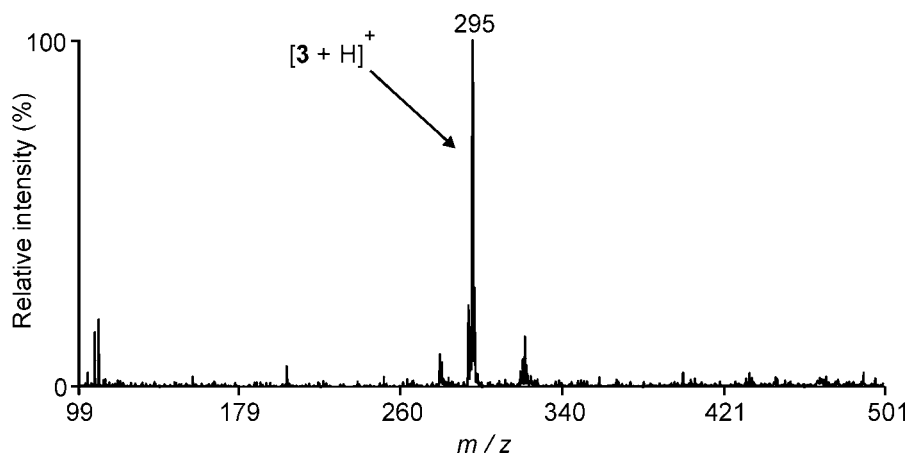


Figure 8.5. MALDI-TOF mass spectrum of the imine **3** ($m/z = 295$) formed on-chip within the ionization chamber of the MALDI instrument. The product was detected by extracting ions from the reaction mixture through the “monitoring window”.

After the last mass spectrum was recorded (~1 h), the chip was examined by an optical microscope. The air bubble in the reservoirs expanded into the channel, while liquid was still present in the portion of the channel close to the outlet.

8.5. Conclusions

Modelling of the fluid dynamics in the MALDI-chip device described in Chapter 7 revealed the need for the optimization of the microfluidics circuit. A new chip was fabricated, allowing longer reaction and measuring times. As foremost improvement a “monitoring window” was integrated in the chip design. This window consists of a freestanding silicon membrane doped with boron, which allows analyte ions to fly from the channel to the MALDI detector *via* holes of a few hundred of nanometer. The effectiveness of the window design has been demonstrated by detecting the product (imine **3**) of the on-chip Schiff base reaction of 4-*tert*-butylaniline (**1**) and 4-*tert*-butylbenzaldehyde (**2**) in ethanol within the MALDI chamber. Though very preliminary, these results clearly demonstrate the possibility of extracting ions from a flowing solution for analysis of the composition of the reaction mixture.

8.6. Outlook

Although improvements in residence and measuring times were achieved by resizing the microfluidics circuit, a poor flow control resulting from the passive fluidics actuation remains the main limitation of the MALDI-chip device. An accurate control of the liquid flow is a prerequisite for the realization of a fully functioning MALDI-based lab-on-a-chip device for the study of reaction kinetics. This can be achieved either by an optimal channel design or by the use of an active pumping mechanism. In particular, when increasing the hydraulic resistance by resizing the reaction channel, contributions to the pumping as a result of surface forces as well as pressure drops due to the integration of multiple openings along the channel must be taken into account. Also the delay time between the beginning of the vacuum pumping and the first possible analysis contributes to the loss of flow control and, consequently, of the reaction. This limitation might be avoided by closing the chip outlet with a membrane, which would prevent the liquid to start flowing. The membrane may be opened only when the set-up is ready for the first analysis.

8.7. Experimental

Microreactors were fabricated by Ir. M. H. Goedbloed in the cleanroom facility of the MESA⁺ Institute for Nanotechnology at the University of Twente. Inlet and outlet holes as well as the “monitoring window” were fabricated in the top silicon wafer by KOH chemical etching. The reaction microchannel was fabricated in the bottom borofloat wafer by HF etching, whereas the triangular reservoirs as well as the bigger inlet channels (going from the inlet holes to the reservoirs) were fabricated by powderblast micromachining. Square-shaped holes in the monitoring window were fabricated by a focused ion beam (FIB). Various combinations of dimensions and number of holes were tested. The preliminary experiment reported in this Chapter was carried out using a monitoring window with only one sampling hole of 500 by 500 nm.

Reagent solutions. Reagents were obtained from Aldrich Chemicals, The Netherlands, and were used as supplied commercially without further purification. No matrix was added for MALDI detection of imine **3**, because of its strong absorption at

the laser wavelength ($\lambda = 337$ nm). Reservoir A was filled with a solution of 1×10^{-4} M 4-*tert*-butylaniline (**1**) and reservoir B was filled with a solution of 1×10^{-4} M 4-*tert*-butylbenzaldehyde (**2**), both in ethanol.

Filling procedure. The reservoir filling procedure was monitored by mounting the chip, placed on a suitable holder, on an Olympus CK40M inverted microscope.

MALDI-TOF. The reaction product formed in the microreactor channel was identified in real-time *via* a “monitoring window” by MALDI-TOF MS using a Voyager-DE-RP MALDI-TOF mass spectrometer (Applied Biosystems / PerSeptive Biosystems, Inc., Framingham, USA) equipped with delayed extraction^{11,12} and a 337 nm UV nitrogen laser producing 3 ns pulses. The mass spectra were obtained in the reflectron mode.

Focused ion beam (FIB). Holes in the doped silicon membranes (250 by 250 nm and 500 by 500 nm) were made using a FEI 200 Focused Ion Beam System operated by Dr. Vishwas Gadgil. The resulting holes were imaged in situ using a Scanning Electron Microscope (SEM).

8.8. References

- 1 Karas, M.; Hillenkamp, F. *Anal. Chem.* **1988**, *60*, 2299.
- 2 Overberg, A.; Karas, M.; Bahr, U.; Kaufmann, R.; Hillenkamp, F. *Rapid Commun. Mass Spectrom.* **1990**, *4*, 293.
- 3 Solomons, T. W. G., *Fundamentals of Organic Chemistry*, 5th ed., John Wiley & Sons: New York, **1998**; Chapter 8.
- 4 White, F. W. *Fluid Mechanics*, 3rd ed, McGraw-Hill: New York, **1994**.
- 5 Lammerink, T. S. J.; Tas, N. R.; Berenschot, J. W.; Elwenspoek M. C.; Fluitman, J. H. J. *8th Int. Workshop on MicroMechanical Systems (MEMS 2000)*, Amsterdam, The Netherlands, **1995**, 13.
- 6 Oosterbroek, R. E., *PhD Thesis*, University of Twente, Enschede, The Netherlands, **1999**.
- 7 Adamson, A. W.; Gast, A. P. *Physical chemistry of surfaces*, 6th ed., John Wiley & Sons: New York, **1997**.
- 8 Probstein, R. F. *Physiochemical hydrodynamics, an introduction*, 2nd ed., John Wiley & Sons: New York, **1994**.
- 9 Atkins, P. W. *Physical Chemistry*, 5th ed.; Oxford University Press: Oxford, **1994**; Chapter 28.
- 10 Tas, N. R.; Berenschot, J. W.; Lammerink, T. S. J.; Elwenspoek, M. C.; Van den Berg, A. *Anal. Chem.*, **2002**, *74*, 2224.
- 11 Vestal, M. L.; Juhasz, P.; Martin, S. A. *Rapid Commun. Mass Spectrom.* **1995**, *9*, 1044.
- 12 Juhasz, P.; Vestal, M. L.; Martin, S. A. *J. Am. Soc. Mass Spectrom.* **1997**, *8*, 209.

Summary

The realization of a lab-on-a-chip system in which chemical reactions are carried out in a continuous flow mode and monitored on-line by a suitable analytical technique is the main topic of this thesis. Two types of a lab-on-a-chip were realized, both using mass spectrometry (MS) as the on-line detection technique, *viz.* electrospray ionization (ESI) and matrix-assisted laser desorption ionization (MALDI) MS. Microreactors were fabricated in glass or a combination of glass and silicon. Syringes mounted on a microdialysis pump were used to transport reagent solutions and reaction mixtures through the microchannels in a controlled manner. This simple, well controllable, and reliable method was chosen to be the most suitable fluidic handling approach to study organic reactions at the microscale. A novel passive pressure-driven pumping mechanism, using the vacuum of the MALDI instrument, was used to activate the MALDI MS integrated microchip (Chapters 7 and 8).

The basic concepts of microfluidics as well as the application of microfluidics devices to the field of analytical chemistry are described in the first part of Chapter 2. Subsequently a literature overview is given, covering the application of microreactors to organic chemistry. Particular attention is given to the effects of downscaling of the reaction vessel on the physical parameters of a reaction, as well as to practical issues in lab-on-a-chip technology, such as fluidics handling and reaction monitoring.

Chapter 3 deals with the acid-catalyzed esterification reaction of 9-pyrenebutyric acid with ethanol to yield the corresponding ethyl ester, carried out in a flow-driven glass microreactor. A higher efficiency in terms of product yields and reaction times was observed on-chip compared to the conventional laboratory procedure. In a systematic investigation of the influence of acidic silanol groups at the microchannel wall on the acid-catalyzed reaction it was demonstrated that surface phenomena play a key role in the observed reaction enhancement.

Two interfacing approaches for coupling glass microchips to a nanoflow ESI (NESI) mass spectrometer are described in Chapter 4. The microfluidics-based interfaces are based on two different integration designs. The first is a monolithic

approach, in which the sample solution is sprayed out from the end of the microchannel at the edge of the chip. The second is a modular approach, using commercially available Picotip™ emitters attached to the chip outlet by means of low dead volume connectors. Both interfaces showed good ionization stability properties, giving a deviation of the total ion current over a few minutes acquisition time of about 8% and 1%, respectively. Offering a high versatility, the modular design was chosen for further applications and its high-throughput potential was demonstrated in Chapters 5 and 6. A microreactor design based on a novel mixing concept by laminating the incoming flows was developed and its mixing dynamics was investigated by computational and experimental methods. At flow rates in the order of a few tens to a few hundreds of nL min^{-1} , complete reagents mixing is achieved in the microchannel within a few tens of milliseconds.

Chapter 5 deals with an on-chip qualitative and quantitative study of the binding strength of supramolecular interactions of different nature. Metal-ligand interactions of Zn-porphyrin with pyridine, 4-ethylpyridine, 4-phenylpyridine, *N*-methylimidazole, and *N*-butylimidazole in acetonitrile as well as host-guest complexations of β -cyclodextrin with *N*-(1-adamantyl)acetamide and 4-*tert*-butylacetanilide in water were studied by mass spectrometry using the NESI-chip interface. K_a values of $(4.6 \pm 0.4) \times 10^3 \text{ M}^{-1}$ and $(6.5 \pm 1.2) \times 10^3 \text{ M}^{-1}$ were determined for the complexation of Zn-porphyrin with pyridine and 4-phenylpyridine, respectively. These K_a values are about four times larger than those obtained with UV/vis spectrophotometry, probably due to a higher ionization efficiency of the complexed compared to the uncomplexed Zn-porphyrin. A K_a value of $(3.6 \pm 0.3) \times 10^4 \text{ M}^{-1}$ was calculated for the complexation of *N*-(1-adamantyl)acetamide with β -cyclodextrin, which is in good agreement with that independently determined by microcalorimetry.

In Chapter 6 the NESI-chip interface is used for a kinetic study of the derivatization reaction of propyl and benzyl isocyanates, and toluene-2,4-diisocyanate with 4-nitro-7-piperazino-2,1,3-benzoxadiazole (NBDPZ) to yield the corresponding urea derivatives. Rate constants of $1.6 \times 10^4 \text{ M}^{-1} \text{ min}^{-1}$, $5.2 \times 10^4 \text{ M}^{-1} \text{ min}^{-1}$, and $2.5 \times 10^4 \text{ M}^{-1} \text{ min}^{-1}$ were determined for propyl isocyanate, benzyl isocyanate, and toluene-2,4-diisocyanate, respectively. The on-chip rate constants are 3 to 4 times higher than those determined using batch macroscale conditions, probably due to the properties of

the NESI-chip device such as fast diffusive mixing, continuous flow operative mode, and on-line reaction mixture analysis. The results reported in this Chapter demonstrate that continuous flow microfluidics devices, where only nanoliter reagent volumes are mixed and react very quickly and efficiently under laminar flow conditions, and with a very limited sample handling offer a valuable alternative to conventional lab-scale equipment for the study of reaction kinetics.

In Chapter 7 a lab-on-a-chip is described consisting of a glass / silicon hybrid microreactor integrated with a MALDI mass spectrometer. The integrated system enables (bio)chemical reactions to be carried out on-chip, inside the MALDI ionization chamber, and the reaction products to be analyzed *in-situ* by mass spectrometry. The effectiveness of the MALDI-chip integrated system was demonstrated for a number of reactions ranging from simple organic syntheses to polymer separation as well as peptide and oligonucleotide enzymatic digestion.

Chapter 8 focuses on the optimization of the MALDI-chip system described in Chapter 7, aiming to realize a lab-on-a-chip for kinetic studies. Monitoring windows, consisting of freestanding doped silicon membranes, were opened in the top wafer along the fluidics path, allowing sampling of the reaction mixture flowing through the channel. As a proof of principle the simple reaction of 4-*tert*-butylaniline with 4-*tert*-butylbenzaldehyde in ethanol to yield the corresponding Schiff base was carried out on-chip in the MALDI ionization chamber. The product was detected not only at the microchannel outlet, but also within the channel through a sampling window.

The results presented in this thesis demonstrate that lab-on-a-chip systems are valuable tools to study (bio)chemical reactions. Microreactors offer a unique environment where reactions are carried out in micro- to nanoliter reaction volumes, thereby profiting from the large surface-to-volume ratio available and the fast diffusive mixing under laminar flow regimes. The continuous flow operative mode and the on-line monitoring offer high-throughput possibilities, which make lab-on-a-chip systems unique compared to lab-scale equipment.

Samenvatting

De realisatie van een “laboratorium op een chip” (lab-on-a-chip) waarin chemische reacties worden uitgevoerd via een “continue-doorstroom wijze” en die “on-line” worden gevolgd met behulp van een geschikte analysetechniek, is het hoofdthema van dit proefschrift. Twee soorten “lab-on-a-chips” zijn gerealiseerd, die beide massaspectrometrie (MS) als on-line analysetechniek gebruiken, namelijk electrospray ionisatie (ESI) en matrix-geassisteerde laser-desorptie-ionisatie (MALDI). De microreactoren zijn gemaakt van glas of van een combinatie van glas en silicium. Om de reagentia en reactiemengsels op een gecontroleerde manier door de microkanaaltjes te sturen wordt een microdialysepomp gebruikt. Om de vloeistoffen in de MALDI-MS chip te transporteren wordt het vacuüm in het MALDI instrument gebruikt.

De basisprincipes en de toepassingen van microfluidica op het gebied van de analytische chemie worden beschreven in het eerste gedeelte van Hoofdstuk 2. Vervolgens wordt er een literatuuroverzicht gegeven van het gebruik van microreactoren in de organische chemie. De nadruk ligt op de relatie van de reductie van het reactorvolume en de fysische parameters van reacties, alsmede op enkele essentiële praktische onderwerpen in de “laboratorium-op-een-chip”-technologie, zoals behandeling van vloeistofstromen en de beheersing van reacties.

Hoofdstuk 3 beschrijft de zuurgekatalyseerde verestering van 9-pyreenboterzuur met ethanol tot de overeenkomstige ethylester, uitgevoerd in een flowgestuurde microreactor. In termen van opbrengst en reactietijden, vergeleken met conventionele laboratoriumprocedures, werd een hogere efficiëntie waargenomen. In een systematisch onderzoek naar de invloed van de zure silanolgroepen op de wanden van de microkanaaltjes op de zuurgekatalyseerde reactie, is aangetoond dat oppervlakte-verschijnselen een belangrijke rol spelen in de waargenomen reactieversnelling.

In Hoofdstuk 4 worden twee strategieën beschreven om glazen microchips aan een nanoflow ESI MS te koppelen. De microfluidische koppelingen zijn gebaseerd op

twee verschillende ontwerpen. De eerste is een monolithische aanpak, waarbij de oplossing op de chip wordt verneveld door deze te injecteren in een gasstroom. De tweede is een modulaire aanpak, waarbij gebruik wordt gemaakt van een commercieel verkrijgbare PicotipTM uitlaat, die direct aan de uitgang van de chip is gekoppeld waardoor het dood volume klein is. Beide interfaces tonen stabiele ionisatie-eigenschappen, waarbij de variatie in de totale ionenstroom, gemeten over enkele minuten, slechts respectievelijk 8% en 1% is. Vanwege de veelzijdigheid is het modulaire ontwerp gekozen voor verdere toepassingen. Het high-throughput potentieel van dit chipsysteem wordt gedemonstreerd in Hoofdstuk 5 en 6. In het microreactorontwerp werd een nieuw en eenvoudig mengconcept geïmplementeerd waarbij de inkomende vloeistofstromen niet in het horizontale vlak, maar vertikaal gelamineerd worden om, in combinatie met ondiepe kanalen, de diffusie te versnellen. De dynamica van het mengen werd experimenteel en met behulp van computersimulaties onderzocht. Bij stroomsnelheden in de orde van enkele tientallen tot honderden nanoliters per minuut wordt er in de mixer een volledige menging van de reagentia gerealiseerd in enkele tientallen milliseconden.

Hoofdstuk 5 behandelt een kwalitatieve en kwantitatieve studie naar de bindingssterkte van verschillende supramoleculaire interacties in een chip. Metaal-ligand interacties van Zn-porfyrine met pyridine, 4-ethylpyridine, 4-fenylpyridine, *N*-methylimidazool en butylimidazool in acetonitril en ook de gastheer-gast complexaties van β -cyclodextrine met *N*-(1-adamantyl)aceetamide en 4-*t*-butylacetanilide in water, werden bestudeerd met behulp van massaspectrometrie met de NESI-chip interface. Voor de complexatie van Zn-porfirine met pyridine en 4-fenylpyridine werden K_a -waarden gevonden van respectievelijk $4.6 \pm 0.4 \times 10^3 \text{ M}^{-1}$ en $6.5 \pm 1.2 \times 10^3 \text{ M}^{-1}$. Deze K_a -waarden zijn ongeveer 4 keer groter dan de waarden die bepaald werden met UV/vis spectrofotometrie, hetgeen waarschijnlijk wordt veroorzaakt door de hogere ionisatie-efficiëntie van de gecomplexeerde Zn-porfyrine vergeleken met de ongecomplexeerde variant. Voor de complexering van *N*-(1-adamantyl)aceetamide met β -cyclodextrine werd een K_a -waarde van $3.6 \pm 0.3 \times 10^4 \text{ M}^{-1}$ berekend, wat in goede overeenstemming is met de waarde die onafhankelijk bepaald is met microcalorimetrie.

In Hoofdstuk 6 wordt de NESI-chip interface gebruikt voor de bestudering van de kinetiek van de derivatiseringsreactie van propyl- en benzyloxyanaat, en toluen-

2,4-diisocynaat met 4-nitro-7-piperazino-2,1,3-benzoxadiazol (NBDPZ) tot de overeenkomstige ureumderivaten. Reactie-constanten van $1.6 \times 10^4 \text{ M}^{-1} \text{ min}^{-1}$, $5.2 \times 10^4 \text{ min}^{-1}$, en $2.5 \times 10^4 \text{ M}^{-1} \text{ min}^{-1}$ werden bepaald voor respectievelijk propylisocynaat, benzylisocynaat, en toluen-2,4-diisocynaat. De on-chip reactieconstanten zijn 3 tot 4 maal groter dan welke bepaald zijn onder batchcondities. Dit is waarschijnlijk het gevolg van de eigenschappen van de NESI-chip, zoals de zeer snelle massadiffusie, eliminatie van tijdsvertragingen door de on-line analyse en de betere reagentia- en producthandling. De resultaten laten duidelijk zien dat de continue-doorstroom microreactoren, waarin volumes van slechts nanoliters eenvoudig gemengd worden en vervolgens zeer snel en efficiënt reageren onder laminaire stromings condities, een waardevol alternatief bieden voor de studie van de reactiekinetiek met conventionele methodes op laboratorium schaal.

In Hoofdstuk 7 wordt een “laboratorium-op-een-chip” beschreven, bestaand uit een hybride glas/silicium microreactor geïntegreerd met een MALDI massaspectrometer. Het geïntegreerde systeem maakt het mogelijk om (bio)chemische reacties op een chip uit te voeren in de MALDI ionisatiekamer, en de reactieproducten *in situ* te analyseren. De effectiviteit van het MALDI-chip geïntegreerd systeem werd gedemonstreerd voor een aantal reacties, variërend van simpele organische reacties tot polymeerscheiding en de enzymatische afbraak van peptiden en oligonucleotiden.

Hoofdstuk 8 richt zich op de optimalizatie van de MALDI-chip, beschreven in Hoofdstuk 7, tot een “laboratorium-op-een-chip” om reactiekinetiek mee te kunnen bestuderen. Vensters, bestaande uit 250 nm and 500 nm openingen in vrijstaande doped siliciummembranen, werden aangebracht in de bovenste wafer boven het kanaal om de analyse van het reactiemengsel terwijl het door het kanaal stroomt op verschillende posities mogelijk te maken. Met behulp van de reactie van 4-*t*-butylaniline met 4-*t*-butylbenzaldehyde uitgevoerd in ethanol in de MALDI ionisatie kamer werd de werking aangetoond. Het gevormde imine werd niet alleen in het uiteinde van het kanaal gedetecteerd maar ook door het “monitoring” venster.

De in dit proefschrift beschreven resultaten laten zien dat “laboratorium-op-een-chip” systemen belangrijke nieuwe instrumenten zijn om (bio)chemische reacties te bestuderen. Microreactoren vormen een unieke omgeving voor de uitvoering van reacties in micro- tot nanoliter volumes, vanwege de grote oppervlakte-volume

verhouding en de snelle, diffusieve, menging onder laminaire stromings condities. Het gebruiken van de reactoren onder continue doorstromings condities en de mogelijkheid tot on-line analyse, resulteren in een zeer hoge analyseproductie die “laboratorium-op-een-chip” systemen uniek maakt ten opzichte van conventionele laboratoriummethodes.

Acknowledgments

During my stay in Tukkerland I was very often asked why I left my beautiful country to come to Enschede and do my Ph.D. Well, for those who are interested in how it happened...

...it was about five years ago when I first came to Twente to carry out my master thesis final project at the Membrane Technology Group. A few days before going back to Italy I met Mercedes in a corridor. I told her that I was thinking about becoming a Ph.D student in Twente and (for those who still think we, people from the south, are not efficient) by the end of the day she arranged a meeting with David for me. A few days later I had not only a Ph.D position, but even a project suitable for my “non-chemical” background. Merce, thank you for setting me up with the SMCT.

The results of years of exciting research carried out within the multidisciplinary working environment at MESA⁺ are collected in this thesis. Each chapter is the result of the joint effort and enthusiasm of a number of people that, at different stages and in various ways, have been either guiding or following me through this journey.

My deepest appreciation is certainly addressed to my promotor, Prof. Reinhoudt, who gave me the opportunity to work in his group. Dear David, I will always remember how my interview with you started. First, you wanted to know for which reason I (a “non-chemist”) was looking for a position in an organic chemistry group. Then, to avoid misunderstandings, you told me that “...well, I’m not going to give you a synthetic project.” Terrified by the image of myself struggling with smelly compounds that never give the wanted result, I replied to you: “Four years in front of a fume hood? I don’t want such a project myself!” Well, as a result of the interview, you offered me a position on the first “chemistry on a chip” project of the University of Twente. This project required a lot of energy and also considerable social skills (otherwise known as “a big mouth”), which I turned out to have. David, thank you for all the freedom, trust and support you constantly gave me during the past four years, especially when choices had to be made. During our work-meetings you often

reminded me that a Ph.D should not only produce scientific results but also learn how to overcome obstacles. That was a truth and a very useful advice.

I would like to thank my co-promotor, Dr. Verboom, with which I shared troubles and joys of a very young and intriguing project. Dear Wim, thank you for the fruitful yet endless discussions we had during the past four years. I remember a few weeks ago after I agreed a few times in a row with you, first you looked at me skeptically, than proudly and you said: “you see, finally we start thinking in the same way.” I honestly believe that our often different opinions and attitudes have been very helpful to my professional growth. I would like to thank you for teaching me how to write scientific papers and for the meticulously correcting my thesis.

If I look back to the past four years and I consider the good and bad aspects of dealing with a multidisciplinary project, I can’t deny that what I have mostly enjoyed is the opportunity and pleasure to cooperate and interact with many people. Prof. van den Berg has played a key role in my research, first as director of the MiCS scientific program of the MESA⁺ and afterwards as head of the BIOS group. Dear Albert, you never made me feel like I was a guest in your group, instead, you always considered me as one of your own Ph.D students. I truly enjoyed the scientific discussions and feedback during both our monthly meetings and the periodic MiCS meetings as well as the BIOS social events.

The first thing I did when I started my Ph.D project was trying to set-up a sort of working group. Having no experience at all I decided to use my “communicative skills”. I went to the engineering department (EL-building) and I started talking about my project almost to any person belonging either to the MiCS or to the Mic-Mec group. To be honest, I still don’t know whether I triggered their scientific curiosity or rather a desperate need to keep me quite, what anyway happened is that I ended up with many people discussing problems with me and helping me to find the right solution.

I am grateful to Niels van der Veen for introducing me to a number of EL people that have helped me during my project. Dear Niels, I would also like to thank you for explaining me that “a Ph.D student is like a juggler and the balls he throws in the air are ideas, part of his project. The juggler has to catch each ball at the right time, develop it and throw it back in the air.”

One of the first balls I threw in the air during my Ph.D was a very lucky one, which resulted in my first publication (Chapter 7) Niels Tas, at that time post-doc at the Mic-Mec group, has meticulously been supporting me with enlightening scientific discussions, practical suggestions and a lot of calculations (which, I afterwards learned, he likes very much). Allora Niels, thank you for supervising the engineering part of the MALDI-chip project, for always showing a great interest in my work even when, in my last year of Ph.D research, I embarked on a tricky business: the “monitoring window”(Chapter 8).

Chapters 5 and 6 are the results of many experiments carried out using an interface (described in Chapter 4), which was realized and characterized in cooperation with Edwin Oosterbroek. Dear EdwinO, it was a great pleasure to work with you. I can honestly say that I have learned many things from our very long discussions. You have always been eager to help me, to give me advices and suggestions, to explain me those terrible formulas you have in your thesis and to listen to my complains. I know, sometimes I made you feel like you were a social worker rather than a scientist; you complained about that sometimes. When I was in the full-stress writing stage, I remember a couple of times a doubt coming to my mind. My Italian temperament would then prevail: stop thinking, start panicking and sending SOS e-mail to EdwinO. And of course if I did not get a reply for a few minutes, I would move to the “emergency plan”: call EdwinO.

Chapter 6 is the result of a rewarding cooperation with the Chemical Analysis Group of Prof. Uwe Karst. I am grateful to Andre Liesener for the fruitful discussions and for carrying out the lab-scale kinetic experiments.

I would like to thank the master of glass micromachining, Martijn Goedbloed, for the discussions on chip design, resulting in functional chips, and for the technical support on the MALDI-chip work. Resourceful Remco Sanders, otherwise known as Pino, thank you for helping me to break down the MALDI instruments: we did a great job, didn't we. Han Gardeniers, nowadays responsible for the “microreactor” projects at the BIOS group, thank you for reading a few Chapters of my concept thesis. I am deeply grateful to Jurriaan Huskens, who, despite being always very busy with his numerous Ph.D students, never refused me his help whenever I knocked on his door wondering whether a data fit was correct. Dear Jurriaan, thank you for checking

carefully all the data reported in Chapters 5 and 6, and for the enlightening discussions we had.

Jeroen Bode, you have been my only student during the whole Ph.D research and I even had to share you with Emiel. Thank you for keeping me away from the fume hood by synthesising the esters for me.

I must not forget to thank Roberto Fiammengo for the chemical support during my first year at the SMCT lab. Issimo, I will never forget how simple chemistry sounds when you explain it!

I would also like to thank Jurriaan Huskens, Barbara Dordi (however, nevertheless...) and Dennis Lensveld for correcting my concept thesis, as well as for providing me with valuable suggestions.

Thank you to my SMCT lab-on-a-chip team-mates Fernando and Menglin for the constructive scientific interaction and the amusing less scientific discussions. It was an honour to share with you the annual MESA⁺ poster price. Good luck for the future of your Ph.D research! A kind word of thank also goes to my lab-mates Olga, Amela, Menglin, Miguel, Gena, Richard, Fernando, Christian, Alart, Mattijs, Jessica, Paolo, Jurien, David.

Although not directly related to my work, there are many persons who I would like to thank for making my stay in Twente very pleasant. First of all the secretaries of both SMCT and BIOS: Carla, Izabel, Hermine, and Ida. I would also like to thank Richard for solving computer-related problems, Marcel, Nancy and Ben for always finding a solution for each technical problem, Fijs for trying very hard to improve my artistic skills, Tieme and Bianca for making my stay in the mass spectrometry lab very enjoyable, Gena for the discussions on mass spectrometry, and all the SMCT, Bios and Mic-Mec younger and older group members who I have not mentioned.

Sometimes I wonder what would have my life in Enschede been without the Beiaard?

A very special word of gratitude goes to the Beiaard-mates with whom I have spent every single Thursday night eating vegaburgers and drinking wit bier, bok bier, or gewoon bier. Emiel, Barbara, Bas, Ale, Olga, Fer, Lourdes, Miguel, Marina, Mattijs, Tommaso, thank you for the great time we had together. A word of thank also

goes to Barty, Ziggy, Azita, Sander, Steffen, Cornelia, Francesca, Marta, Soco, Mirko, Wojtek, Domenik, Beata, Maria, Pascale, Henkino, Marloes, Chris Mrinal, and Paolo for coming around from time to time and sharing with us a burgermenu, a dagschotel or a bakje patat. Well, I hope we will not lose this good habit. Thank you also to my Wednesday evening squash-mates (Aldrik I will beat you sooner or later)

Cari paranimfen, I am glad you will be there with me the day of my promotion, I will certainly feel more comfortable on the podium with the two of you around (and not only because of the bad name Italians have). Dino, we met a long time ago when you arrived in Twente, ready to start your Ph.D project. You arrived on a Thursday when we (Macandra people) were ready to go to a Norwegian party. You jumped on the back of my bike and started your “Macandra party season”. We spend a long time together cooking, drinking wine, going to the pubs and dancing all night long at the Atak or at some AKI party. Thank you for all the fun we had together and for being such a good friend. Sbabbara, especially during the past three years we spent a lot of time together. No matter what, every Thursday again we were at the Beiaard, every Saturday we went shopping, and every Tuesday (was it on Tuesday?) we had Dutch lesson...and of course every Sunday we would call each other to decide which Dutch oefening to skip. I truly enjoyed the time we spent together, particularly the Saturday afternoons drinking wit bier on the terrace, as well as the dinners we cooked either at your or at our place. Thank you for your affectionate friendship and for being my matron of honour as well as my paranimf. Bassy, sharing with you those boring moments in which Barbara and Emiel start discussing about AFM, XPS, surface science and bla bla bla makes me feel a little relieved. Thank you for amusing me with your mania of taking notes on the properties of anything you drink (do you also do it with water?).

More than five years away from Italy is quite a long time and those few days per year I spend in Monza are certainly not enough to see all the friends I grew up with and those with whom I shared the great time of my studies in Milano. Rosa, Mea, Paola, Ivan, Fabio, Laura, Andrea, Dona, Scatto, Cla, Villetta, Fede, Fante, Fillo, Funesto, Janny, AnnaSvaria, Markino, Lisa Giovanna, Stefy, Massi, Silvia, Beppe, Markino, Lele, Guido, Frizzi, Marzia ...to all of you I give a big hug and thank you for trying to see me every time I am back and to make me feel a little closer with your emails.

Emiel, since we met about four years ago you have always been there, ready to give me your help and support. Thank you for always being present, for always trying to help me out with my problems (when an experiment or a measurement went wrong), even when I started complaining and being annoying (and you know I can be). If I look back at the time I was writing my thesis (and you were as well, by the way) I feel ashamed of all the hours I spent doing nothing else than writing. Although you were probably pushed by a survival instinct yourself, thank you for cooking every evening, preventing me from certain starvation.

Mamma, I still wonder where you found the strength to support me for all these years, encouraging me when I was supposed to hearten you. Thank you for pushing me to finish my Ph.D when we lost our daddy, because he would have wanted me to do so. Thank you for always reminding me how many times he told you he was glad and proud for what his daughter was doing. One evening I told you that the day of my promotion without my father would have not been as I have imagined it many times. Probably, it will not be, but I am glad you will be there to share it with Emiel and me. Uncle Renato and Marzietta, thank you for coming all the way to the north for my promotion and... to have some good beer.

Mamma, non riesco ad immaginare dove tu abbia trovato la forza di sostenermi per tutti questi anni, dandomi coraggio quando ne avrei dovuto dare io a te. Grazie per avermi spinto a continuare il dottorato dopo la perdita del papa', perche' lui avrebbe voluto cosi'. Grazie per avermi sempre ricordato quante volte lui ti abbia detto di essere felice ed orgoglioso di quello che "la sua tusa" stava facendo. Una sera ti ho confidato che il giorno della mia promozione senza il papa' non sarebbe mai stato come me lo ero immaginato tante volte. Probabilmente non lo sara' ma in ogni caso sara' un giorno speciale e sono felice che tu sarai qui a dividerlo con me ed Emiel. Un grazie speciale allo zio Rena e a Marzietta per essere venuti nel profondo nord ad assistere alla mia promozione e... a bere della buona birra. Un abbraccio a tutti quelli che avrebbero voluto ma non sono potuti venire.



Curriculum Vitae

Monica Brivio was born in Monza (Mi), Italy on June 8th, 1973. In July 1992 she received her diploma from the "Liceo Scientifico" P. Frisi (Monza). She studied Food Science and Technology at the University of Milano, Italy, where she received her degree in March 2000. During her undergraduate training period she worked on the chemical and physical chemical characterization of non-ionic and active surfactants and their role in emulsification processes. The work, that was carried out at the Membrane Technology Group of Prof. M. Wessling at the University of Twente, The Netherlands, resulted in the thesis "Realization of encapsulated liquid membrane: stabilization of micro- and macroemulsion by using functionalized surfactant molecules ". From May 1st, 2000 till June 30th, 2000 she worked at the University of Twente in the group of Prof. M. Wessling on liquid membranes for the transport of oxygen. Since December 2000 she joined the Supramolecular Chemistry and Technology Group of Prof. Reinhoudt at the University of Twente, The Netherlands, as Ph.D candidate. The results of her research are described in this thesis. From February 1st, 2005 she will work as a post-doc in the Biomedical and Environmental Sensorsystems Group of Prof. A. van den Berg at the University of Twente, The Netherlands.

